8-1995

Elastic-Plastic Fracture Toughness Determination Under Some Difficult Conditions

Kang Lee
University of Tennessee - Knoxville

To the Graduate Council:

I am submitting herewith a dissertation written by Kang Lee entitled "Elastic-Plastic Fracture Toughness Determination Under Some Difficult Conditions." I have examined the final electronic copy of this dissertation for form and content and recommend that it be accepted in partial fulfillment of the requirements for the degree of Doctor of Philosophy, with a major in Engineering Science.

John D. Landes, Major Professor

We have read this dissertation and recommend its acceptance:

T. G. Carley, J. A. M. Boulet, R. S. Benson

Accepted for the Council:

Carolyn R. Hodges

Vice Provost and Dean of the Graduate School

(Original signatures are on file with official student records.)

To the Graduate Council:

I am submitting herewith a dissertation written by Kang Lee entitled "Elastic-Plastic Fracture Toughness Determination under Some Difficult Conditions". I have examined the final copy of this dissertation for form and content and recommend that it be accepted in partial fulfillment of the requirements for the degree of Doctor of Philosophy, with a major in Engineering Science.

John D. Landes

Dr. John D. Landes, Major Professor

We have read this dissertation
and recommend its acceptance:

Accept for the Council:

C. W. Minkel

Associate Vice Chancellor and
Dean of The Graduate School

ELASTIC-PLASTIC FRACTURE TOUGHNESS DETERMINATION UNDER SOME DIFFICULT CONDITIONS

A Dissertation Presented
for
the Doctor of Philosophy degree

The University of Tennessee, Knoxville

Kang Lee

August, 1995

DEDICATION

To my uncle, C. W. Lee, my aunt Jean Lee
and my wife Yuying Yang

Without your love, support and encouragement
this degree would not have been achieved.

ACKNOWLEDGMENTS

In the course of this dissertation research, a number of scholars have assisted me generously. I would like to thank them for their advice, support and encouragement.

In particular, I am most indebted to Dr. John D. Landes for his invaluable direction, support and friendship. As my major professor, Dr. Landes suggested all the subjects in this research and supplied a number of experimental data to support the research. Each step in progress of the research was full of his painstaking effort. His consistent advice, criticism and encouragement were the guide leading me toward the completion of the research. After the first draft of this dissertation was finished, Dr. Landes reviewed the whole manuscript for several times and suggested a lot of corrections and improvements.

I would like also to express my appreciation to Dr. T. G. Carley, Head of the department, Dr. J. A. M. Boulet and Dr. R. S. Benson, Who served as my doctoral committee members and reviewed the manuscript of this dissertation, for their consultation, criticism and encouragement.

Finally, I would like to thank my uncle Dr. C. W. Lee, My aunt Jean Lee and my wife Yuying Yang. I am most fortunate to have such a wonderful uncle aunt and wife. Their continued love, support and encouragement, especially my uncle's advice were always the source of the power in my progress.

With their help I was able to complete this dissertation research otherwise impossible. Whatever errors remained in my work, however, are solely my responsibility.

ABSTRACT

The J_{Ic} value and J-R curve have been widely used to characterize elastic-plastic fracture behavior in modern engineering practice. Their determination has been standardized. To determine the J_{Ic} value and the J-R curve using the ASTM standard test methods, three measurements, load, displacement and crack length, must be obtained simultaneously from the test. This may sometimes be difficult or even impossible due to the restrictions of test equipment, adverse environments, test conditions or test arrangements.

Recently, a method of normalization has been introduced by Landes and his group as a convenient way for J-R curve determination. This method uses the principle of load separation to relate the three variables, load, displacement and crack length, during the fracture process. A functional form, named the LMN function, has been successfully used to relate the normalized load to the plastic deformation. It gives an unique relationship between load, displacement and crack length. The method of normalization provides an analytical basis to predict any one of the three variables from the other two.

In this study the method of normalization was further developed for J-R curve determination under some difficult conditions. Four subjects were included. They are:

- J-R curve determination from load versus displacement records without crack length measurements.

- J-R curve determination from load versus crack length records without displacement measurements.

- J-R curve determination under the conditions when load is difficult to measure.

- J-R curve determination under dynamic loading conditions.

For each subject, the new features and problems needed to be solved were described. A major problem solved for all the subjects was how to determine the LMN function accurately and efficiently under the different conditions. A large number of experimental data sets were collected to support this study. Based on the analysis results of these test data, new approaches were developed for each subject. Each approach was examined under the condition assumed for corresponding application. Results of the analysis were presented to show its adequacy on each subject.

It has been demonstrated that the approaches developed in this study could greatly simplify the J-R curve test procedure, and improve the resulting J-R curve accuracy. The results are more reliable, especially under the specific difficult test conditions. These methods will likely have extensive applicability in engineering practice.

TABLE OF CONTENTS

LIST OF TABLES

LIST OF FIGURES

Chapter 1

Introduction and Background

1.1 Introduction

The essential task of engineering design is to determine the load level, the geometry and dimensions of structural elements and to select materials in such a way that the elements perform their operating functions in an efficient, safe and economic manner. The determination of a safe load level is usually based on some appropriate failure criteria. When a structural component contains some crack-like flaws, it could fail at a stress level which is considerably lower than the ultimate strength of the material. The traditional failure criteria cannot adequately account for flaws in developing a safe design. Since the existence of crack-like flaws cannot be precluded in any engineering structure, methods to deal with them must be incorporated into the failure criteria. Defects can appear in a structure in the following different ways: first, they can exist in a material due to its composition, as second-phase particles, debonds in composites, etc.; second, they can be introduced into a structure during fabrication, as in welding, forging, casting and machining; and, third, they can be created during the service life of a structural component due to the conditions that include fatigue loading, severe environment, and creep behavior. Some extreme conditions like environmental conditions, fluctuating loads, and accidental overload, can accelerate the initiation and growth of the cracks. To deal with the

determination of design loads in structure components, fracture mechanics technology has been developed. Today, it is playing an increasingly important role in modern engineering practice.

Fracture mechanics is an engineering discipline that quantifies the conditions under which a load-bearing structural component can fail due to the enlargement of a dominant crack contained in that component. Fracture mechanics research develops parameters which characterize the propensity of a crack to extend and ultimately cause failure. Such parameters should be able to relate laboratory test results to structural performance, so that the response of a structure with cracks can be predicted from laboratory test data. These parameters are determined as a function of material behavior, crack size, structure geometry and load conditions. The critical value of such fracture parameters is known as fracture toughness. Fracture toughness is assumed to be a property of a material which can be determined from laboratory tests. Fracture toughness expresses the ability of a material to carry load or deform plastically and resist fracture in the presence of cracks. It can be used to rank a material's ability to resist fracture within the framework of fracture mechanics, in the same way that the yield or ultimate strength can be used to rank a material's resistance to yielding in the conventional engineering design. By equating a fracture parameter to its critical value a relation is obtained between applied load, crack size and structural geometry that gives the necessary information for structural design.

During the 20th century, but mostly in the last four decades, many significant research efforts have been devoted to the study of fracture mechanics technology. The first analysis of fracture behavior of components that contained crack-like flaws was developed by Griffith in 1921 [1]. The

analysis was based on the assumption that a crack will begin to propagate if the elastic energy released by its growth is equal to or greater than the energy required to create the fracture surface. The basic content of modern fracture mechanics — or more strictly, the linear elastic fracture mechanics (LEFM) — was developed in the 1946 to 1966 period. After many year growth, LEFM has matured and become popular. The stress intensity factor, K, and energy release rate, $\mathcal{G}$, have been widely employed in engineering design as fracture toughness parameters for characterizing the crack tip conditions to prevent sudden fracture and optimize material selection. It is generally accepted that LEFM is applicable only when the plastic zone developed at the crack tip is very small during the fracture process compared with other planar dimensions of the structure. This is usually the case in materials where fracture occurs appreciably below the yield stress. With the increasing progress in the technology and materials, modern structural components are constructed of materials which exhibit considerable plasticity before failure occurs. At the same time, the world-wide demands for energy and material conservation are dictating that structures be designed with smaller safety margins. The limits of LEFM preclude the use of this technology for most modern structural materials. Thus since the 1960's, several attempts have been made to develop new approaches that are not limited to linear behavior but can be applied to the elastic-plastic behavior, now known as the elastic-plastic fracture mechanics (EPFM). Among them methods based on the J-integral and the crack tip opening displacement (CTOD) have been the two most successful.

1.2 Elastic-Plastic Fracture Mechanics (EPFM) and the J-Integral Method

The J-integral method was introduced by Rice [2] in 1968. By idealizing elastic-plastic deformation as nonlinear elastic, Rice provided the theoretical basis for extending fracture mechanics methodology well beyond the validity limits of LEFM. In the same year, Hutchinson [3-4] and Rice et al. [5] related the J-integral to crack tip stress fields in nonlinear materials and showed that J can be regarded as a nonlinear stress intensity parameter as well as an energy release rate. This method has been viewed as a direct extension of linear elastic fracture mechanics into the elastic-plastic regime. Its physical and analytical basis are as powerful as LEFM. The significance, the role and the application of J-Integral can be summarized as follows.

(1). The value of J is the numerical result of a line integral from the lower to the upper surface of a crack, independent of the particular path of integration.

Consider an arbitrary counter-clockwise path Γ, as illustrated in Fig. 1.1*, surrounding the crack tip and lying completely inside a body which is homogeneous and presents an elastic (linear or nonlinear) behavior. The J-integral is defined by

$$J = \int_{\Gamma} \left(W dy - T_i \frac{\partial u_i}{\partial x} ds \right) \tag{1.1}$$

---

* All figures may be found in the Appendix

where

W = loading work per unit volume or, for elastic bodies, strain energy density,

ds = increment of the contour path,

T_i = outward traction vector on the contour path,

u_i = displacement vector on the contour path,

$T_i \frac{\partial u_i}{\partial x} ds$ = the rate of work input from the stress field into the area enclosed by Γ.

Rice has shown [2] that the value of the J-integral is independent of the path of integration around the crack, hence the integral taken along any path Γ gives a unique value. The only restriction in the definition of J is that W be the strain energy density for linear or nonlinear elastic behavior. However, when plasticity is treated by deformation theory, there is no difference between an elastic-plastic behavior and a purely nonlinear elastic behavior. Incremental plasticity can be treated in a similar manner, provided no unloading occurs. In other words, assume that both the nonlinear elastic and the elastic-plastic stress-strain curves are identical for monotonically increasing load, the only difference between them is their response to unloading, as illustrated in Fig. 1.2. Thus an analysis that assumes nonlinear elastic behavior could be applied to an elastic-plastic material, provided no unloading occurs.

The path-independence of the integral implies that J can be a crack tip characterizing parameter for elastic-plastic materials. That is, the crack tip is the only point enclosed by all Γ contours, and thus J is related to the stress state at or near the crack tip, and to the intensity of the stress-strain

singularity. At the same time, its value can be determined on a large contour from conditions far from the crack tip.

(2). J can be interpreted as the potential energy release rate per unit crack extension for the nonlinear elastic counterpart of an elastic-plastic material.

A more physical meaning of J can be obtained from the J-integral definition of Eq. (1.1) by considering Fig. 1.3, where let Γ be an arbitrary contour around the crack tip and assume crack grows by da carrying the contour with it to new position Γ^*. Then:

$$J\,da = \int_{\Gamma} \left(W\,dy\,da - T_i \frac{\partial u_i}{\partial x}\,ds\,da \right) \tag{1.2}$$

The first term on right-hand side is the strain energy gained by moving the contour with the crack tip, and the second term is the work done by traction in moving. Thus $J\,da$ is the total energy coming across the contour for a cracked area da (per unit thickness).

$$J = -\frac{dU}{da} \tag{1.3}$$

This provides an alternative interpretation: J can be interpreted as the potential energy release rate per unit crack extension for an elastic-plastic material, which was also suggested by Rice [6].

On a load versus load-line displacement P-v plot of two identical specimens with slightly different crack lengths, Fig. 1.4, the area between two P-v curves is $J\,da$. The value of $J\,da$ can be evaluated in load control (load is

held constant) or in displacement control (displacement is held constant). There is a difference of a small triangular area between two methods. This small area is a second order term and may then be neglected. Therefore, an alternative, equally valid definition of J can be

$$J = -\frac{dU}{da} = -\int_0^v \left.\frac{\partial P}{\partial a}\right|_v dv = \int_0^P \left.\frac{\partial v}{\partial a}\right|_P dP \tag{1.4}$$

This result allowed Begley and Landes to do the first experimental evaluation of J [7-8]. After their critical experiments, significant effort was devoted to evaluate J as a function of applied load, displacement and crack length. From this, various approaches for J determination were developed.

(3). J is the strength of the crack tip elastic-plastic stress-strain field singularity, thus J could be the governing parameter of that field.

Work done by Hutchinson [3-4] and Rice and Rosengren [5] showed that the crack tip elastic-plastic stress-strain field can be related to J by

$$\sigma_{ij}(r,\theta) = \sigma_0 \left(\frac{J}{\sigma_0 \varepsilon_0 r}\right)^{\frac{1}{n+1}} \tilde{\sigma}_{ij}(n,\theta) \tag{1.5a}$$

$$\varepsilon_{ij}(r,\theta) = \varepsilon_0 \left(\frac{J}{\sigma_0 \varepsilon_0 r}\right)^{\frac{1}{n+1}} \tilde{\varepsilon}_{ij}(n,\theta) \tag{1.5b}$$

where

σ_0 = reference stress, is usually equal to the yield stress,

ε_0 = σ_0 / E,

n = the strain hardening exponent

r, θ = the position coordinates of a point ahead of the crack tip with the origin at the crack tip,

$\tilde{\sigma}_{ij}$, $\tilde{\varepsilon}_{ij}$ = dimensionless functions of n and θ.

The Eqs. (1.5a) and (1.5b) are called the HRR (Hutchinson, Rice and Rosengren) singularity. J defines the amplitude of the HRR singularity, just as the stress intensity factor, K, characterizes the amplitude of the linear elastic singularity. Therefore, J completely describes the conditions within the plastic field.

(4). J can be used as a fracture initiation criterion, defined as J_{Ic}.

It is clearly implied by Eqs. (1.5a) and (1.5b) that for a given material, equal J values mean equal intensities of geometrically identical surrounding crack-tip stress-strain fields. Thus, crack growth begins when a critical value of the strength of that field is attained.

Eq. (1.4) relates the J to the load versus displacement diagrams. Begley and Landes [7-8] used this concept to evaluate J at the point of initiation of crack growth (J_{Ic}) for different materials and geometries, as well as specimen sizes. They found that the value of J_{Ic} obtained from small specimens, where large amounts of yielding had occurred, was the same (for the same material) as that for big specimens where the plastic zone was very small compared with other planar dimensions. That is

$$J_{Ic}(plastic\ tests) = J_{Ic}(elastic\ tests) = \frac{K_{Ic}^2}{E} \tag{1.6}$$

This result provided the possibility of using J as a more general fracture toughness parameter than $\mathcal{G}$ or K. Indeed J coincides with $\mathcal{G}$ for LEFM and it has been proven to be an adequate characterizing parameter for EPFM too.

(5). J can be used for constructing the material property J-R curve to characterize the resistance response of materials to stable crack growth, as an extension of the $\mathcal{G}$-R curve of LEFM.

The J-R curve can be used as an index of material toughness for engineering design, material selection, and quality assurance. It applies even for significant amounts of crack growth under certain restrictions [9-11]. The J-R curve can also be used to analyze conditions for ductile instability [12-13].

(6). J can be uniquely relate to CTOD

An analysis provided by Shih [14] demonstrated that there is a unique linear relationship between J and CTOD for a given material

$$J = \sigma_{ys}\,\delta \tag{1.7}$$

where

σ_{ys} = yield stress,

δ = CTOD.

Thus, both parameters are equally valid for characterizing elastic-plastic fracture. This gives an analytical basis to use CTOD as an elastic-plastic fracture parameter and leads to the J-based material testing and structural design approach developed in the U. S. and the British CTOD methodology

begin to merge, with advantages of each approach combined to yield improved analysis.

Up to this point it has been clearly seen that J is a powerful characterizing parameter and can be used to construct a complete picture of EPFM.

1.3 Elastic-Plastic Fracture Toughness Determination

Elastic-plastic fracture behavior has been well characterized. The J_{Ic} and J-R curve have been widely used to measure the fracture toughness for ductile materials, and their determination has been standardized. When a ductile fracture occurs, structural components do not fail by sudden unstable crack propagation. The complete failure usually occurs after some stable crack growth. J_{Ic} measures only the initiation of the stable crack growth process. Therefore, it may represent a very conservative fracture criterion. A more complete elastic-plastic fracture analysis will characterize the entire stable crack growth by a J-R curve.

1.3.1 J_{Ic} Value and J-R Curve Determination Using ASTM Standard Methods

The first experimental evaluation of J was done by Begley and Landes in 1972 [7-8], based on the potential energy release rate definition of J, Eq. (1.4). After that, many other significant evaluations of J and J-R curves were done

by Bucci et al. [15], Rice et al. [16], Landes and Begley [9], Clarke et al. [17], McCabe and Heyer [10-11], Ernst et al. [18], Hudak and Saxena [19] and others [20]. Based on these works, two ASTM standard test methods, E813 and E1152 [21-22], have been developed and published for J testing. Both produce a J-R curve, a plot of J versus crack extension. The E1152-87 standard determines the entire J-R curve, while E813-87 is concerned only with J_{Ic}, a single point near the initiation of slow stable crack growth on the R curve. A given fracture toughness test could be analyzed in terms of either or both standards. Due to the similarities between these two test methods, a new combined J testing standard has been developed which combines the testing and analysis procedures of E813 and E1152.

The determination of J_{Ic} values and J-R curves using the ASTM standard test methods requires three simultaneous measurements, that of load, P, load-line displacement, v and crack length, a. They are obtained by testing a fatigue precracked fracture toughness specimen. The suggested specimen is the standard compact specimen [C(T)], which is pin-loaded in tension with an initial normalized crack length, a_0/W of 0.5 to 0.7. An alternate specimen is the three-point bend specimen [SE(B)], which is a single edge-cracked beam and also has an initial normalized crack length, a_0/W, of 0.5 to 0.7. In general, load versus load-line displacement can be recorded directly either digitally for processing by a computer or autographically with an "x-y" plotter via the load transducer and displacement gage. Crack length, on the other hand, cannot usually be measured directly during the test. Either a multiple specimen or a single specimen technique can be used to determine the crack length measurements. The single specimen technique is preferred (only the single specimen technique is allowed by the E1152 standard test method for the J-R

curve determination). With the multiple specimen technique, a series of nominally identical specimens are loaded to various levels and then unloaded. Some stable crack growth occurs in most specimens. This crack growth is marked by heat tinting or fatigue cracking after the test. Each specimen is then broken open and the crack extension is measured on the crack surface. When the single specimen technique is used, the crack length is measured during the test through an indirect method. The most common single specimen technique is the elastic unloading compliance method, which is illustrated in Fig. 1.5. It monitors the crack extension through the change in test specimen compliance. As the crack grows, the specimen becomes more compliant (less stiff). The compliance measurements are taken on a series of partially unloading-reloading segments spaced along the load versus displacement record [17, 23]. The crack length is then determined from these elastic compliance measurements. For C(T) specimens, they are related by [19]

$$C_i = \frac{1}{E B_e}\left(\frac{W + a_i}{W - a_i}\right)^2 [2.1630 + 12.219\,(a_i / W) - 20.065(a_i / W)^2 - 0.9925(a_i / W)^3 + 20.609(a_i / W)^4 - 9.9314(a_i / W)^5] \quad (1.8)$$

where

E = the modulus of elasticity,

W = the specimen width,

B = the specimen thickness,

B_e = $B - (B - B_N)^2 / B$, the effective specimen thickness,

B_N = the net thickness of side grooved specimen,

C_i = $\Delta v_i / \Delta P_i$, the specimen elastic compliance on an unloading/ reloading sequence.

For the SE(B) specimens, they are related by [24]

$$C_i = \frac{1}{E B_e}\left(\frac{S}{W-a_i}\right)^2 [1.193 - 1.980\,(a_i / W) + 4.478(a_i / W)^2 - 4.443(a_i / W)^3 + 1.739(a_i / W)^4] \quad (1.9)$$

where

S = specimen span, the distance between specimen supports.

An alternative single specimen technique is the electrical potential drop method in which the crack growth is monitored through the difference in electrical resistance that accompanies a loss in cross-sectional area. It has become more popular as the electronic equipment used has been improved. After many years of development, these two methods are now used routinely and with very good success in many laboratories. However, both techniques are practical only when used in conjunction with a computer data acquisition and analysis system. Some advanced testing skills are also required to make them work successfully.

Once the measurements of applied load, load-line displacement and crack length are obtained, the J value can be evaluated at any point by using the method provided by Ernst et al. [18]. That is

$$J_i = J_{el(i)} + J_{pl(i)} \quad (1.10)$$

where

$J_{el(i)}$ = the elastic component of J,

$J_{pl(i)}$ = the plastic component of J.

The $J_{el(i)}$ is determined from

$$J_{el(i)} = \frac{K_i^2(1-\nu^2)}{E} \tag{1.11}$$

where

ν = the Poisson ratio.

The K_i is the crack tip stress intensity factor. It can be determined from ASTM standard test method E399. For C(T) specimens it is given by

$$K_i = \frac{P_i}{(BB_N W)^{1/2}} f(a_i / W) \tag{1.12}$$

with

$$f(a_i / W) = \frac{2 + a_i / W}{(1 - a_i / W)^{3/2}} [0.886 + 4.64(a_i / W) - 13.32(a_i / W)^2 + 14.72(a_i / W)^3 - 5.6(a_i / W)^4]$$

For SE(B) specimens

$$K_i = \frac{P_i S}{(B B_N)^{1/2} W^{3/2}} f(a_i / W) \tag{1.13}$$

with

$$f(a_i / W) = \frac{3(a_i / W)^{1/2}\{1.99 - (a_i / W)(1 - a_i / W)[2.15 - 3.93(a_i / W) + 2.7(a_i / W)^2]\}}{2(1 + 2a_i / W)(1 - a_i / W)^{3/2}}$$

On the other hand, the $J_{pl(i)}$ is determined by

$$J_{pl(i)} = [J_{pl(i-1)} + (\frac{\eta_i}{b_i})\frac{A_{pl(i)} - A_{pl(i-1)}}{B_N}] [1 - \gamma_i \frac{(a_i - a_{i-1})}{b_i}] \qquad (1.14)$$

where

b_i = $W - a_i$, the remaining uncracked ligament,

for the C(T) specimens

η_i = $2.0 + 0.522 b_i / W$,

γ_i = $1.0 + 0.76\, b_i / W$,

for the SE(B) specimens

η_i = 2.0,

γ_i = 1.0,

$A_{pl(i)}$ can be calculate from the equation

$$A_{pl(i)} = A_{pl(i-1)} + [P_i + P_{i-1}][v_{pl(i)} + v_{pl(i-1)}] / 2 \qquad (1.15)$$

where

$v_{pl(i)}$ = $v_i - P_i C_i$, the plastic part of the load-line displacement

The J-R curve can be plotted from the J-integral values and the corresponding crack extension values, provided the validity requirements of ASTM standard test method E1152 are satisfied. A typical J-R curve from the compliance method is given in Fig. 1.6. According to the ASTM standard test method E813, the J_{Ic} value can be determined from a J-R curve by using at least four qualifying data points which lie within two specified exclusion lines. These data reflect the material resistance to crack growth. The J versus crack growth behavior is approximated with a best-fit power law relationship. A blunting line is drawn, approximating crack tip stretch effects. The blunting line is calculated from material flow properties, using the expression

$$J_B = 2\sigma_y \Delta a \tag{1.16}$$

where

σ_y = $(\sigma_{YS} + \sigma_{UTS})/2$, the flow stress

J_B = the J value from blunting line

An offset line parallel to the blunting line but offset by 0.2 mm (0.008 in) is drawn. The intersection of this line and the power law fit defines J_{Ic}, provided the validity requirement of ASTM standard test method, E813, are satisfied.

1.3.2 Potential Problems for J_{Ic} and J-R Curve Determination

There may exist some special cases for which the simultaneous measurements of load, load-line displacement and crack length are extremely difficult or impossible to obtain. Then the determination of J_{Ic} or the J-R curve using ASTM standard methods under such conditions may be a problem. Some examples of these difficult cases are described below.

(1). Difficulty in measuring crack length

The crack length may be difficult to measure due to equipment or material restrictions. It has been mentioned in last section that the preferred single specimen techniques require sophisticated equipment and advanced test skills to monitor the crack extension. Not all laboratories have the required equipment and skills. Moreover, it has been found that the elastic unloading compliance method does not work well for the materials such as most plastics, that

show viscoelastic behavior. Each unloading-reloading cycle for these materials results in a hysteresis loop instead of a straight elastic line. It is difficult to estimate the compliance and hence the crack length from such a curved loop. It has also been found that the elastic unloading compliance method works well to monitor the crack extension only when the specimen is side-grooved. Sometimes the side-grooving technique is not applicable such as for thin sheet metals or other materials. For most plastics side-grooving may cause crazing and trigger unexpected brittle fracture.

(2). Difficulty in measuring displacement

For some fracture toughness test situations, displacement may be difficult to measure. Examples of this could be for high-temperature testing where a conventional strain gauged displacement transducer cannot operate or a test in a hot cell where the mounting of a gage may be difficult. For the latter case, this may be especially true for nuclear surveillance specimens that are small and do not have the correct design to accommodate the load-line displacement gage suggested by the standard test method.

(3). Difficulty in measuring load

For testing a crack-line-wedge-loaded specimen C(W), the loading arrangement does not permit load measurement; but the displacement can be measured easily. Also the crack length cannot be measured by using the elastic unloading compliance technique without load measurement. However, it could be measured by an electrical potential drop system. If the J-R curves can be developed from displacement versus crack length with no load measurement, this could provide a convenient way to test fracture toughness for ductile materials.

(4). Dynamic tests

The Charpy impact test has been widely used for assessing the brittle-ductile fracture characteristics of structural materials under dynamic loading conditions. The advantage of this test method is that it is simple and inexpensive, easy to conduct and backed by a wealth of interpretive experience on conventional materials. Previously the Charpy impact test was used to determine the energy absorbed to fracture a specimen, which provides

only a qualitative indication of material toughness. By using some empirical correlations the static fracture toughness, K_{Ic}, and the dynamic fracture toughness, K_{Id}, could be estimated from impact test results. When the striker of a Charpy machine is instrumented a load versus time record can be obtained from the test. This load-time curve is not difficult to convert into a load-displacement curve. It has been found that considerable plastic deformation is involved in Charpy impact fracture except at very low temperatures [25]. This situation would require the use of an elastic-plastic fracture parameter like J for better characterizing the fracture behavior under impact test conditions. If the on-line crack length measurements can be predicted from the load versus displacement records, J-R curve can then be developed from a Charpy impact test. It would provide a useful method for elastic-plastic fracture toughness determination under dynamic loading conditions.

Recently, a method of normalization has been introduced by Landes et al. [26-29] as a convenient way to determine the J-R curves when the crack length measurement or the displacement measurement is difficult to obtain from the test. It employs the principle of load separation, which was originally suggested by Ernst et al. [18, 30] and developed by Sharobeam and Landes [31], to functionally relate three variables: load, displacement and crack length. If a suitable functional form is determined, it can be used to predict any one of the three variables given the other two. The most successful version of the method of normalization uses a three-parameter LMN function to relate the three variables. With this function the J-R curves can be successfully developed from load versus displacement without crack length [28] and from

the load versus crack length without displacement measurement [29]. However, the method suggested seems too complicated to be used widely by the engineering public. A further improvement is needed. Also some new applications of the method of normalization could be developed to determine J-R curves under some other of the difficult conditions mentioned above.

1.4 Objectives

As the title states, the goal of this work is to develop some approaches that can be used to determine the elastic-plastic fracture toughness under some difficult conditions. Four primary objectives are included in this work.

(1). Improve the current approach for J-R curve determination from load versus displacement records without crack length measurements using the method of normalization.

(2). Improve the current approach for J-R curve determination from load versus crack length records without displacement measurements using the method of normalization.

(3). Develop two new approaches for J-R curve determination from displacement versus crack length records without load measurements and from only displacement data by predicting both load and crack length measurements using the method of normalization.

(4). Develop a new approach for J-R curve determination under dynamic loading conditions using Charpy impact tests.

Obviously, these topics are important in development of elastic-plastic fracture mechanics and in the determination of fracture toughness. The methods to be developed here will likely have extensive applicability to engineering practice.

Chapter 2

Review of Method of Normalization

2.1 The Principle of Load Separation

The principle of load separation is an important concept in elastic-plastic fracture mechanics. This concept was first used by Rice et al. [34] to evaluate J from a single load-displacement record for a deeply cracked bend type specimen. Later, it was used by Merkle and Corten [35] to develop another single specimen J determination approach for the compact type specimen. More recently, a method of normalization was developed by Landes et al. [26-29]; based on this principle J-R curve can be determined when crack length or displacement measurements are difficult to obtain from the test. The following is a brief introduction of the principle of load separation.

During the loading of a cracked body, the load, displacement and crack length can change continuously. Since these are the only interacting variables for the fracture procedure, they could be related by an arbitrary function F with an arbitrary constant factor k

$$P = k F(a / W, v / W) \tag{2.1}$$

where the crack length, a, and displacement, v, are normalized with the specimen width, W. An important development in study of the relationship between the load, displacement and crack length was made by Ernst et al.

[18, 30], who showed analytically that the load can be separated into two multiplicative functions, one of crack length, a, and the other of plastic displacement, v_p, when the total displacement is represented as a sum of its elastic and plastic components. That is

$$P = G(a/W)\, H(v_p/W) \tag{2.2}$$

and

$$v = v_e + v_p \tag{2.3}$$

where both variables, a and v_p, are normalized by the specimen width dimension, W. The elastic component of displacement, v_e, is given by the load and a compliance function $C(a/W)$

$$v_e = P\, C(a/W) \tag{2.4}$$

The principle of separation has been experimentally confirmed and demonstrated to work for all types of specimen geometry by Sharobeam and Landes [31-33]. If both functions, G and H, in Eq. (2.2) are known, a unique relationship between the load, displacement and crack length is determined.

The function $G(a/W)$ is dependent upon the particular specimen geometry. It has been suggested [32, 33] that for the specimen geometries used commonly $G(a/W)$ could be expressed as

$$G(a/W) = W\, B\, (b/W)^{\eta_{pi}} \tag{2.5}$$

where

B = specimen thickness

b = uncracked ligament, $W - a$

η_{pl} is a constant for a specific specimen configuration for example

η_{pl} = 2.15 for a compact specimen

η_{pl} = 2 for a three-point bend specimen.

The determination of the function $H(v_p / W)$, the deformation function, will be given in next section.

2.2 The Method of Normalization

The method of normalization was developed using the principle of load separation described in last section. When the load is divided by the geometry function $G(a / W)$, a normalized load P_N is defined.

$$P_N = P / G(a / W) = H(v_p / W) \tag{2.6}$$

$H(v_p / W)$ represents the plastic flow character of the material and specimen geometry. If P_N is plotted versus (v_p / W) a graphical form of $H(v_p / W)$ function is defined. The deformation function $H(v_p / W)$ should be material dependent. It depends on flow strength, hardening character and other material features. The method of normalization assumes that a functional form could be inferred for $H(v_p / W)$ that is general for many materials. The functional form would have unknown constants that could be determined

from calibration points for which the load, displacement and crack length are known simultaneously.

In studying most test records it was found that the deformation behavior showed a power law character at the early range of plastic displacement and changed to a straight line character later [27-28]. Fig. 2.1 shows a typical plastic deformation curve for an A508 steel. The latest version of the method of normalization uses a three-parameter LMN function modeled after a functional form originally suggested by Orange [36]. It is given by

$$P_N = H(v_p / W) = \frac{(L + M\, v_p / W)\,(v_p / W)}{N + v_p / W} \tag{2.7}$$

where L, M and N are the unknown fitting constants. This function resembles a power law (or polynomial) when (v_p / W) is the order of N and a straight line when $(v_p / W) >> N$. It gives the best representation of the material deformation behavior observed from the tests of commonly used materials.

The determination of three constants L, M and N in equation (2.7) requires at least three calibration points. The previous application of normalization used three types of point as the LMN function fitting calibration points [28, 29]. They are illustrated in Fig. 2.2 and briefly described as follows.

(1). Point A is taken at final load, displacement and crack length where the final crack length is measured on the fracture surface of a broken specimen half after the test is completed. When the J-R curve is developed from load,

P, versus crack extension, Δa, a final plastic displacement can be measured from the permanent plastic deformation at the end of the test. The corresponding final displacement can be found from

$$v_f = P\,C(a_f / W) + v_{pf} \tag{2.8}$$

(2). Points B are a set of points taken at the initial part of the test record before the maximum load is reached or before measurable crack extension occurs.

For the case where the J-R curve is developed from the P versus v record, a forced blunting assumption is used for evaluating the crack lengths for points B [28]

$$\Delta a = J / 2\sigma_Y \tag{2.9}$$

where σ_Y is the flow stress. If the J-R curve is developed from the P versus Δa record, a power law fit works well for estimating plastic displacements in this range [29].

$$P_N = \mu\,(v_p / W)^{\kappa} \tag{2.10}$$

where the exponent κ is taken to be a constant equal to 0.13. The factor μ is related to flow stress by

$$\mu = 107.37 - 2.176\,\sigma_Y + 0.0197\,\sigma_Y^2 \tag{2.11}$$

(3). Points C are an intermediate set of points taken at

$$v_p = v_{p(\max)} + [v_{pf} - v_{p(\max)}] / 3 \qquad (2.12)$$

where the subscript (max) refers to the maximum load point and "f" to the final point. The values of P_N vary between $P_{N(\max)}$ and P_{Nf}, and are used to optimize the fit of the LMN function.

Each set of points A, B_i and C_j could determine a set of L, M and N constants. For the first fitting step points B_i (i=1,2,...I_{max}) are taken with point A and point C_1, which is usually chosen at the lowest value of P_N on points C, to determine a set of L, M and N fitting constants. The standard deviation for L, M and N in this sequence is then computed. In the second step a new point of C, C_2, is chosen by slightly increasing the P_N value from C_1. The procedure in the first step is repeated for points A, B_i and C_2 and L, M and N are again determined along with their standard deviations. This process is repeated until the fitting is complete; that is when the minimum standard deviation sum of L, M, N is reached. The optimum fitting constants in equation (2.7) are found from the average values of L, M and N at the point C_i which gives the smallest standard deviation for L, M, N and also satisfies the criterion that the average value of N is greater than 0.0005.

Once the L, M and N are determined, equation (2.7) can be combined with equations (2.3-2.6) to predict any one of the three parameters, load, displacement and crack length, knowing the other two. These can then be used to determine the J-R curves using the ASTM standard E1152 formula.

Chapter 3

Application I of Method of Normalization: J-R Curve Determination from Load versus Displacement Records without Crack Length Measurements

3.1 Introduction

Originally, the method of normalization was introduced as an alternative way to determine J-R curves from the experimental load versus displacement data by predicting crack length analytically from the plastic character of the material. It has been demonstrated [28, 37] that with a three-parameter LMN function to relate load, displacement and crack length, Eq. (2.7), the crack length can be predicted and the J-R curve can be developed accurately. The accuracy of the prediction is as good as or even better than the traditional elastic unloading compliance method. Obviously, this technique has many advantages compared with the compliance method and other techniques.

- It can eliminate the need for an on-line crack length monitoring system, and therefore simplify the test procedure for J-R curve determination significantly.

- It is more reliable. This is particularly clear when the compliance method fails to measure the crack length for some reason, such as when the side-grooving technique cannot be used.

- The normalization method works well for a wide range of materials, including polymeric materials, whereas the elastic unloading compliance method and electrical potential drop technique only work for most metals.

However, in applying the normalization method the LMN function needs to be determined individually for each specimen. The LMN function has three constants which need to be determined using at least three calibration points. The previous approach uses three kinds of calibration point, the final calibration point, the initial calibration points from a forced blunting line and the intermediate calibration points, to fit the three constants, as illustrated in chapter 2. The first and second calibration points have been defined definitely, while the third calibration points are not defined so clearly. They are adjustable and used to optimize the fitting result. The determination of the LMN function then involves a complicated fitting procedure that is not easy to understand, nor convenient to use. Therefore, a new approach is developed here to improve the previous approach and simplify the procedure.

3.2 An Improved Approach for J-R Curve Determination from Load versus Displacement Records

As has been mentioned before, the LMN function has a power law character at the initial range of plastic displacement and changes to a straight line character later. The constant N is usually a very small number (around 0.001). When the $(v_p/W) >> N$, Eq. 2.7 reduces to a straight line

$$P_N = L + M\ v_p / W \tag{3.1}$$

where, graphically L is the y-intercept and M is the slope. When the load is normalized with the initial crack length a_0, the normalized load value at maximum load point, labeled L_0, appears to be approximately equal to L.

$$L \approx L_0 = \frac{P_{\max}}{WB\left(\frac{W-a_0}{W}\right)^{\eta_{pl}}} \tag{3.2}$$

This concept is illustrated schematically in Fig. 3.1. A more accurate relationship between L and L_0 could be given by introducing a factor into Eq. (3.2). That is

$$L = k L_0 = k \frac{P_{\max}}{WB\left(\frac{W-a_0}{W}\right)^{\eta_{pl}}} \tag{3.3}$$

This relationship can be used to determine the constant L first. The remaining two constants, M and N, can be then determined using only first and second calibration points. In this way the third type of calibration point, the intermediate calibration points C, are not needed anymore. Discarding them eliminates the complicated part of the fitting procedure. Meanwhile, since the L is determined from the test information itself, it is more reliable than the previous approach and could improve the accuracy of the whole LMN function.

To find an optimum way to determine the LMN function using the maximum load point, a deformation behavior study has been conducted on a large experimental data base. This data base contains a total of two hundred and twenty-two test specimens in eighteen material groups including two

polymeric materials. They were tested under different conditions and measurements of all three parameters, load, displacement and crack length, were taken for J-R curve determination (for the specimens of polymeric materials, only load versus displacement were measured). All these data sets were collected from the literature [38-45] and no new tests were conducted in this work. Tables 3.1 summarizes the relative information about this data base. These data sets represent a wide range of materials, different specimen sizes and various specimen geometries. Therefore, conclusions from the analysis of this data base could be reasonably general. The LMN function has been used to fit all the specimen deformation curves included in this data base. It has been found that the successful fitting values of the constant L for all specimens studied distribute within a range of (1.0 L_0) to (1.12 L_0), depending on the material used. It has also been found that the value of the constant N controls the location on the deformation curve where there is a significant slope change (i. e. where the deformation curve changes from the power law character into the straight line character) and the curvature around this location. This can be seen from the Fig. 3.2. The study showed that the value of the constant N could be used to help determine a suitable constant L during the fitting procedure. The procedure is first to assume that the constant L has a value of $L = L_0$. Using this with calibration point A, the final calibration point, and the calibration points B, the initial calibration points from the forced blunting line, the remaining constants M and N are determined. If the resulting constant $N \geq 0.0006$ (the N is taken at the average value of all the N_i determined), this value of L is suitable to give an accurate LMN function fit. On the other hand if the resulting $N < 0.0006$, the assumed value of $L = L_0$ is lower than a suitable one. By increasing the L

Table 3.1 A Summary of the J-R Curve Data Base Used in This Study

Materials	σ_{ys} Mpa (ksi)	σ_{UTS} Mpa (ksi)	Number of Specimens	Notes	Sources
Metallic Materials:					
2024 Aluminum	315.1 (45.7)	462.0 (67.0)	3	All CT without side-grooving	[38]
A106 Steel	324.1 (47.0)	558.5 (81.0)	3	All CT with side-grooving	[39]
A508 Steel	386.1 (56.0)	544.7 (79.0)	34	CT in 1/2T, 1T, 2T, 4T, 10T w. side-grooving	[40]
HSST Weld	426.1 (61.8)	512.3 (74.3)	8	All CT with side-grooving	[41]
A533B Steel	441.3 (64.0)	599.8 (87.0)	20	CT, CCT, DEN, SEN are included	[39]
HSLA-80 Steel	482.6 (70.0)	572.3 (83.0)	16	CT with/without side-grooving	[42]
HSLA-710 Steel-Heat 1	510.2 (74.0)	599.8 (87.0)	4	All CT with side-grooving	[39]
HSLA-710 Steel-Heat 2	570.8 (82.8)	675.0 (97.9)	3	All CT with side-grooving	[43]
HSLA-710 Steel-Heat 3	551.6 (80.0)	620.5 (90)	5	All 3-PB without side-grooving	[43]
7075 Steel	530.9 (77.0)	586.1 (85.0)	3	All CT without side-grooving	[38]
HY80-Ni Steel	613.6 (89.0)	730.8 (106.0)	3	All CT with side-grooving	[39]
HY130 Steel	930.8 (135.0)	1034.2 (150.0)	22	CT in 1T, 2T, 4T	[42]
4340 Steel	1041.1 (151.0)	1123.9 (163.0)	27	All CT without side-grooving	
A304 Stainless Steel	293.7 (42.6)	610.9 (88.6)	6	CT with/without side-grooving	[44]
1-1/4 Cr Steel at 1000°C	140.0 (20.3)	250.3 (36.3)	5	All CT with side-grooving	
2-1/4 Cr Steel at 1100°C	104.8 (15.2)	188.9 (27.4)	6	All CT with side-grooving	
Polymeric Materials:					
ST801 Nylon	50.1 (7.3)		29	All 3-PB without side-grooving	[45]
ST901 Nylon	68.7 (9.96)		25	All 3-PB without side-grooving	[45]

value slightly and using it to determine the constants M and N again, the constant N will increase with L. By repeating this procedure, the suitable value of L can be found when $N \geq 0.0006$ or $L = 1.12\ L_0$ is reached, whichever comes first (when the case of $L = 1.12\ L_0$ occurs, the N may be smaller than 0.0006 for some materials).

The new approach for J-R curve determination from load versus displacement can be summarized in two flow charts. For convenience the equations used are repeated here [Same equations are given by Eq. (1.10), (1.11), (1.14), (2.3) through (2.7) and (2.9)].

$$v_i = v_{e(i)} + v_{p(i)} \tag{3.4}$$

$$v_{e(i)} = P_i\, C(a_i / W) \tag{3.5}$$

$$P_{N(i)} = \frac{P_i}{WB(b_i / W)^{\eta_{pl}}} \tag{3.6}$$

$$P_{N(i)} = H(v_{p(i)} / W) = \frac{(L + M\, v_{p(i)} / W)\,(v_{p(i)} / W)}{N + (v_{p(i)} / W)} \tag{3.7}$$

$$J_{Bi} = 2\sigma_Y \Delta a_i \tag{3.8}$$

$$J_i = \frac{K_i^2 (1 - \nu^2)}{E} + J_{pl(i)} \tag{3.9}$$

$$J_{pl(i)} = [J_{pl(i-1)} + (\frac{\eta_{pl}}{b_i B_N}) \frac{(P_i + P_{i-1})(v_{p(i)} - v_{p(i-1)})}{2}]\ [1 - \gamma \frac{(a_i - a_{i-1})}{b_i}] \tag{3.10}$$

The flow chart given by Fig. 3.3 illustrates the LMN function determination procedures using the new approach while the flow chart given by Fig. 3.4 describes the crack length prediction procedure using the LMN function

determined. A computer code in FORTRAN language has been developed for determining the J-R curve automatically using the new approach. It is given in Appendix B of this dissertation.

3.3 Results from the Application of the New Approach

To evaluate the proposed approach, it has been applied to all of the J-R curve test specimens collected in the data base. Because most of these specimens were tested previously using elastic compliance method, load, displacement and crack length for the J-R curve determination were all recorded. When the new method was applied, the crack length was assumed to be missing and J-R curves were determined from only load and displacement measurements with the crack length being predicted from the new method. A total of thirty-one examples are reported here and compared with the corresponding J-R curve results determined from the compliance method as well as the previous three-point fitting normalization method. They could be divided into five groups to see how well the new method works for five areas of concern including different metallic materials, different specimen sizes, specimens without side-grooving, different specimen geometries and polymeric materials. The results for these five areas of concern are discussed separately below.

(1). J-R curve results for different metallic materials

The first group of results includes fifteen compact specimen J-R curves from fifteen different metallic materials, one for each type of metallic material listed in Table 3.1. The results are shown in Fig. 3.5 through Fig. 3.19

in terms of J versus crack extension, Δa. The materials involved have very different properties, from low strength, low toughness materials like 2024 aluminum to high strength, high toughness materials like HSLA-710 steel, and from high strength, low toughness materials like HY130 steel to low strength, high toughness materials like 1-1/4 Cr at high temperature. Also a very ductile material, A304 stainless steel, is included. Therefore, these results represent a wide range of materials. It can be seen from these results that the new approach worked very well for all the materials studied. When compared with the traditional elastic compliance method and the previous three-point fitting approach, the new approach showed the following features.

- When the final physical crack length was correctly or near correctly estimated by the elastic compliance method, the J-R curves determined from three methods are almost identical, especially for the side-grooved specimens. This could be seen from the Fig. 3.6 through Fig. 3.11 for A106 steel, A508 steel, HSST weld, A533B steel, HSLA-80 steel and HSLA-710 steel-heat 1 respectively and the Fig. 3.14 for HY80-Ni steel, the Fig 3.15 for HY130 steel.

- When the elastic compliance method sometimes cannot estimate the final physical crack length correctly for some reason, the method of normalization (including both previous three-point fitting approach and the new approach) always gives better J-R curve results. This can be seen from the Fig. 3.16 for 4340 steel, Fig. 3.17 for A304 stainless steel, Fig. 3.18 and Fig. 3.19 for 1-1/4 Cr steel and 2-1/4 Cr Steel at high temperature. For all of these cases the final physical crack lengths were underestimated by the elastic compliance method. The main reasons for the underestimation of the final

physical crack length could be that the specimens were not side-grooved, the cases in the Fig. 3.16 and Fig. 3.17, and the tests were conducted at high temperature, the cases in the Fig. 3.18 and Fig. 3.19. However, for all these cases the normalization method corrected the crack length values to fit the final physical crack lengths. The final physical crack length is measured on the fracture surface after the test is completed by breaking the specimen into two. It should be viewed as the actual physical crack length. The J-R curve determined from method of normalization is based on the final physical crack length and fits it exactly. Therefore, it more correctly represents the actual crack extension.

Note that the A304 stainless steel is a difficult material case for applying the method of normalization. Since it is a very ductile material, its plastic displacement component is much larger than its elastic component. A little error in the plastic displacement component prediction will lead to a large error in the elastic displacement component prediction in terms of percentage, and therefore cause a large error in the prediction of crack length. Reference [44] suggests that the blunting line for this material should be $J = 4\sigma_y \Delta a$. This was used in this study when the normalization method was applied. The result shown in Fig. 3.17 looks good.

• Sometimes the elastic compliance method could accidentally estimate the crack length incorrectly. An example of this can be seen from Fig. 3.12 for HSLA-710 steel-heat 2. In this case the compliance method predicted the crack length incorrectly at the initial part of the crack growth but worked very well at the later part. Again, however, the normalization method predicted the crack length correctly and gave a much better J-R curve result.

• The results in this group show that the new approach worked as well as or even better than the previous three-point fitting approach. The cases where it works better can be seen in Fig. 3.5, Fig. 3.8 and Fig. 3.14. This is expected for the case where the constant L is determined from the test information itself.

(2). J-R curve results for different specimen sizes

The second group of J-R curve results consists of Fig. 3.7 and Fig. 3.20 through Fig. 3.25. They are presented to show how well the new approach works for different specimen sizes. Seven specimens of different sizes are included in this group. Among them, five are standard compact specimens in sizes from 10T to 1/2T and two are non-standard compact specimens, one is in a very small thickness and the other is in very deep initial crack length. All specimens were made from A508 steel with 20% side grooving. The specimen information included in this group is listed in Table 3.2.

Table 3.2 A Group of A508 Steel Specimens in Different Sizes Used in this Study

Figs.	Size Name	W in, (mm)	B in, (mm)	a_0 in, (mm)	Notes
Fig. 3.20	10T	20, (508)	10, (254)	11.77, (299.0)	Standard
Fig. 3.21	4T	8, (203.2)	4, (101.6)	4.08, (103.6)	Standard
Fig. 3.22	2T	4, (101.6)	2, (50.8)	2.114, (53.7)	Standard
Fig. 3.7	1T	2, (50.8)	1, (25.4)	1.031, (26.2)	Standard
Fig. 3.23	1/2T	1, (25.4)	1/2 (12.7)	0.525, (13.3)	Standard
Fig. 3.24	10T	20, (508)	1, (25.4)	11.054, (280.8)	Small Thickness
Fig. 3.25	4T	8, (203.2)	2, (50.8)	7.074, (179.7)	Deep a_0

The size range covered by this group of specimens is large and general enough for size effect evaluation. It is obvious that the new approach worked quite well for all specimen sizes included in this group. For three out of seven cases including the 2T specimen in Fig. 3.22, the 1T specimen in Fig. 3.7 and the 10T small thickness specimen in Fig. 3.24, where the compliance method estimated the final physical crack length accurately, the new approach gave the almost same results as the compliance method did. For other four cases, where the compliance method underestimated the final physical crack length, the new approach improved the results to fit the final physical crack length.

(3). J-R curve results for different specimen geometries

The new approach not only worked very well for compact specimen as shown above, but also work very well for other specimen geometries. This can be seen from the third group of J-R curve results. Four specimen geometries are included in this group. These results are shown in Fig. 3.26 for three point bend specimens (3PB/SE(B)), in Fig. 3.27 for single edge notched tension specimens (SENT), in Fig. 3.28 for double edge notched tension specimens (DENT) and in Fig. 3.29 for center cracked tension (CCT) specimens. Each figure contains two J-R curve results determined by the new approach for each specimen type, these results were compared with the results from the elastic compliance method. The information for the specimens used in this group is given in Table 3.3.

Table 3.3 The Information of Specimens in Different Geometries Used in this Study

Figures and Materials	Specimens	Specimen Geometry	W in, (mm)	B in, (mm)	a_0 in, (mm)
Fig. 3.26, HSLA-710	Specimen #1	3PB	2, (50.8)	0.96, (24.384)	1.106, (28.09)
Steel-Heat 3	Specimen #2	3PB	2, (50.8)	0.96, (24.384)	1.0775, (27.37)
Fig. 3.27	Specimen #1	SENT	20, (508)	0.1, (2.54)	6 , (152.4)
A533B Steel	Specimen #2	SENT	20, (508)	0.1, (2.54)	8, (203.2)
Fig. 3.28	Specimen #1	DENT	16, (406.4)	0.1, (2.54)	3.97, (100.84)
A533B Steel	Specimen #2	DENT	8, (203.2)	0.1, (2.54)	1.945, (49.403)
Fig. 3.29	Specimen #1	CCT	16, (406.4)	0.1, (2.54)	4, (101.6)
A533B Steel	Specimen #2	CCT	8, (203.2)	0.1, (2.54)	2, (50.8)

The new approach to the method of normalization showed its superiority here again for all geometries studied.

- For most specimens reported in this group, the elastic compliance method worked quite well. Each J-R curve from the new approach was very close to the corresponding one from the compliance method for these specimens.

- For the cases where the compliance method did not measure the crack length correctly, the new approach can predict the crack length more accurately and give the better J-R curve results. This can be clearly seen from the result for the 3PB specimen #2, Fig. 3.26, for which the compliance underestimated the final physical crack length considerably and from the result for the CCT specimen #2, Fig. 3.29, for which the

incorrect crack length measurements and unexpected crack jumps were found at some points from compliance method. All these problems were corrected by the new approach.

- Therefore, all the cases in this group showed that the J-R curve results from the new approach were more consistent for each specimen geometry.

- For the specimen geometries studied in this group, only the 3PB/SE(B) specimen is a standard specimen type used in ASTM test methods. The results reported here show that J-R curve tests can be conducted successfully for non-standard specimen types, especially when the new method is used.

(4). J-R curve results for specimens without side-grooving

Experience from previous practice showed that difficulty often occurred when the elastic compliance method was used to measure the crack length for specimens without side-grooving during the J-R curve tests. An important advantage for the method of normalization is that it can be used to determine J-R curves without any difficulty for non-side-grooved specimens. The fourth group of J-R curve results contains 7 specimens without side-grooving, Fig. 3.5 for 2024 aluminum, Fig. 3.13 for 7075 steel, Fig. 3.15 for HY130 steel, Fig. 3.16 for 4340 steel, Fig. 3.17 for A304 stainless steel and Fig. 3.30 and 3.31 for two identical specimens of a HSLA-80 steel. They are used to evaluate how well the new approach works for J-R curve determination when non-side-grooved specimens are used.

Results from this group showed that the new approach worked as well as or even better than the previous three point-fitting approach for the specimens without side-grooving. The same features discussed above were found here again under the condition of non-side-grooving. That is, for the three cases of low toughness materials, 2024 aluminum in Fig. 3.5, 7075 steel in Fig. 3.13 and HY130 steel in Fig. 3.15, the compliance method measured the final physical crack length correctly, but some incorrect crack length measurements were found for the case of the 7075 steel. The results from the new approach were very close to those from compliance method and the incorrect points were improved for the case of 7075 steel. For other two cases, 4340 steel in Fig. 3.16 and A304 stainless steel in Fig. 3.17, the final crack lengths were underestimated by the compliance method. The new approach fitted the final physical crack length. The results shown in Fig. 3.30 and Fig. 3.31 were the cases for which the elastic compliance method failed to work. They were from two identical compact 2T specimens in a HSLA-80 steel. The J-R curves determined should be the same for both of them. However, each of the resulting J-R curves from the compliance method appeared to be a set of scattered points, that were totally different from each other. This is clearer when they were plotted together, Fig. 3.32. In contrast, the new approach determined the J-R curves for these two specimens successfully. The two resulting J-R curves were almost the same, Fig. 3.32, as was expected for the two identical specimens.

(5). The J-R curve results for polymeric materials

It has been mentioned before that the standard test method for J-R curve determination cannot be applied to polymeric materials. This is because the

traditional elastic compliance method and electrical potential drop method do not work for these materials. With the development of the method of normalization, the J-R curves could be determined using the single specimen technique. The polymeric material test data collected for this study were originally developed for determining J-R curves using the multiple specimen method [45]. Four multiple specimen sets were included. Their specimen information was listed in Table 3.4.

Table 3.4 The Specimen Information of the Polymeric Materials Used in this Study

Material and Specimen Sets	Number of Mult-Specimens	Specimen Geometry	W in, (mm)	B in, (mm)	a_0 in, (mm)
ST801 Nylon, Set 1	18	3-Point Bend	0.25, (6.35)	0.125, (3.175)	0.125, (3.175)
ST801 Nylon, Set 2	11	3-Point Bend	1, (25.4)	0.5, (12.7)	0.5, (12.7)
ST901 Nylon, Set 1	15	3-Point Bend	0.25, (6.35)	0.125, (3.175)	0.125, (3.175)
ST901 Nylon, Set 2	10	3-Point Bend	1, (25.4)	0.5, (12.7)	0.5, (12.7)

Only load versus displacement measurements as well as the final physical crack length were determined for each specimen. The traditional multiple specimen test method can use the data from each specimen to determine only one point on J-R curve. However, with the method of normalization, the whole J-R curve could be determined from the same data for each specimen, if the specimen had stable crack growth.

The fifth group of results reports the J-R curves developed by the new approach from the above multiple specimen data for polymeric materials. They were shown in Fig. 3.33 and Fig. 3.34 for a ST801 nylon and in Fig. 3.35

and Fig. 3.36 for a ST901 nylon. Each figure reports three J-R curves from three identical specimens in each multiple specimen set. Results were compared with the corresponding J-R curve determined from multiple specimen method. All results showed that the J-R curves determined by the new approach agreed very well with the results from the multiple specimen method when the crack extension was small, but showed the increased difference in J values when the crack length was greater. This is because the multiple specimen method does not include the crack extension correction for the J calculation. As the crack extension gets larger, more error is introduced into J. Therefore, the J-R curves from new approach are more accurate.

3.4 Summary

A new approach to the method of normalization has been suggested in this chapter for J-R curve determination from load versus displacement without crack length measurements. It uses the maximum load point to determine the constant L in the LMN function. Therefore, the LMN function determination procedure can be greatly simplified. A large J-R curve test data base was collected and evaluated for this study. The new approach has been demonstrated to work for a wide range of materials including polymeric materials, different specimen sizes, various specimen geometries and non-side-grooved specimens. Actually, the new approach has all the advantages of the previous three-point fitting approach, and the following additional advantages.

- The new approach is simpler, easier to understand and more convenient to apply when compared to the previous three-point approach.

- The new approach can improve the J-R curve determination accuracy. This is because the new approach determines the constant L from the test data itself and the accuracy of LMN function is improved.

Therefore, the method of normalization with the new approach suggested here can be used as an alternative method for J-R curve determination, especially under conditions when the crack length is difficult to determine during the test.

Chapter 4

Application II of Method of Normalization: J-R Curve Determination From Load versus Crack Length Records without Displacement Measurements

4.1 Introduction

Another important application of the method of normalization is the J-R curve determination from test records which contain only load versus crack length values with no measure of displacement. This technique could be useful when the test conditions are such that it is difficult to measure the displacement. In modern engineering practice this could happen as described in Chapter 1. The method of normalization uses the principle of load separation to relate the three variables load displacement and crack length in fracture problems. Therefore, it provides a theoretical basis to predict displacement from load versus crack length measurements. Then, the J-R curve could be determined from such a data set. An approach has already been developed with good success for this application [29]. It used the LMN function to relate the normalized load and plastic displacement. The same three types of calibration points and three-point fitting procedure were used as used in the previous approach for application I to construct the LMN functions, but a power law fit, Eq. (2.10), was used to give the initial calibration points. The advantage of the three point fitting technique is it can determine the LMN function correctly for each test specimen. Therefore, the

displacement values can be predicted with good accuracy from the LMN function determined. The disadvantage is that the fitting procedure is too complicated since an adjustable intermediate calibration point is used. This has been pointed out in chapter 3 and it is the same here. A new approach which results in an easier procedure is then developed in this chapter.

4.2 A New Approach for J-R Curve Determination from Only Load versus Crack Length Pairs Using the Method of Normalization

It has been shown in last chapter that the maximum load point can be used to determine the constant L in LMN function when the method of normalization is used to determine the J-R curves from load versus displacement records without crack length measurements. In this way the LMN function determination procedure is considerably simplified and the prediction accuracy from the method of normalization is improved. For the case considered here this idea could also be adopted to eliminate the complicated fitting procedure in the previous approach.

A study has been conducted to use the maximum load point to determine the constant L when the J-R curve is determined from the load versus crack length without displacement measurements. The specimens made from nine metallic materials were included in this study. They were 1-1/4 Cr steel at 1000 °C, 2-1/4 Cr steel at 1100 °C, A106 steel, A508 steel, A533 steel, HSLA-80 steel, HSLA-710 steel, HY80 steel and HY130 steel. Also the specimen sizes from 1/2 T (W=1, B=0.5 in) to 10T (W=20, B=10 in) were covered. The relevant material property and specimen size information have been

reported in the Table 3.1 and 3.2. It was found that the LMN function could be determined successfully by using the maximum load point combined with final calibration point as well as the initial calibration points estimated from the power law fit given by Eq. (2.10). The evaluation procedure is almost the same as the one developed in last chapter.

The new approach then can be described clearly by two flow charts, Fig. 4.1 for the LMN function determination and Fig. 4.2 for the plastic displacement prediction, with the equations involved listed below.

$$v_i = v_{e(i)} + v_{p(i)} \tag{4.1}$$

$$v_{e(i)} = P_i\, C(a_i / W) \tag{4.2}$$

$$P_{N(i)} = \frac{P_i}{WB(b_i / W)^{\eta_{pl}}} \tag{4.3}$$

$$P_{N(i)} = H(v_{p(i)} / W) = \frac{(L + M\, v_{p(i)} / W)\,(v_{p(i)} / W)}{N + (v_{p(i)} / W)} \tag{4.4}$$

$$P_N = \mu\, (v_p / W)^{\kappa} \tag{4.5}$$

$$J_i = \frac{K_i^2 (1 - \nu^2)}{E} + J_{pl(i)} \tag{4.6}$$

$$J_{pl(i)} = [J_{pl(i-1)} + (\frac{\eta_{pl}}{b_i B_N}) \frac{(P_i + P_{i-1})(v_{p(i)} - v_{p(i-1)})}{2}]\, [1 - \gamma \frac{(a_i - a_{i-1})}{b_i}] \tag{4.7}$$

$$L_0 = \frac{P_{\max}}{WB\left(\frac{W-a_0}{W}\right)^{\eta_{pl}}} \tag{4.8}$$

$$L = kL_0 = k\frac{P_{\max}}{WB\left(\frac{W-a_0}{W}\right)^{\eta_{pl}}} \tag{4.9}$$

Note that in the new approach the exponent constant κ for the Eq. (4.5) is taken to be the value of 0.25 and the factor μ is determined from the material flow stress using the following equation.

$$\mu = 24.836 - 0.382\sigma_Y + 2.773\times10^{-2}\sigma_Y^2 - 1.0652\times10^{-4}\sigma_Y^3 \tag{4.10}$$

They are different from those used in previous approach. The study conducted showed that these changes could better relate the factor μ to the material flow property and extend the range of application for the new approach to more materials.

4.3 J-R Curve Results Determined from Load versus Crack Length Pairs by Applying the New Approach

To demonstrate the new approach, it was used to analyze the J-R curve test data for two groups of specimens. The first group of specimens originally had the full load, displacement and crack length measurements available. The assumption was made that the displacement was missing when the new approach was applied. The second group of specimen test data was supplied

by Dr. Randy Nanstad of Oak Ridge National Laboratory for an A533B nuclear grade pressure vessel steel in the form of only load versus crack length pairs. Also the initial and final crack lengths as measured on the fracture surface and the final plastic displacement were provided. The analysis was done as described in the flow charts of Fig. 4.1 and 4.2. The final load, final plastic displacement and final physical measured crack length were first used to get the calibration point A and Eq. (4.5) was used to determine the calibration points B at the initial part of the load versus displacement curve up to maximum load point. Then the maximum load point was used to determine the constant L_0. It was found in last chapter that a suitable value of the constant L is between $(1.0\,L_0)$ and $(1.12\,L_0)$. The constant N was used to help determine the actual value of constant L. Namely, a value of constant L between $(1.0\,L_0)$ and $(1.12\,L_0)$ was assumed, then starting from $L = L_0$ and the value of L was increased slightly in increments (in the flow chart 4.1 the increment of L is suggested as $0.02\,L_0$ each increment), using calibration point A and each of the calibration points B, a set of constants of M and N was determined for each increment of L. Then the average values of constants M and N in each set were calculated. The suitable values of constants L, M and N were found when $N \geq 0.0005$ or $L = 1.12\,L_0$ was reached, whatever which one came first. The load versus crack length pairs were then subjected to the method of normalization using the LMN function determined so that the plastic displacements could be predicted for each load and crack length pair. Also, the elastic displacement values could be found from the load and crack length pairs using the compliance formula, Eq. 4.2, and then the full displacement could be determined. Once displacement was known, the

values of J could be calculated at each data point and J-R curves could then be plotted.

(1). Results for first group of specimens

Some example results from the first group of specimens are reported here to illustrate how well the new approach works. Fig. 4.3a through Fig. 4.13a report the P-v curves predicted from the new approach; these are compared with the test results in each figure. Fig. 4.3b through Fig. 4.13b report the corresponding J-R curve results determined form the load versus crack length pairs with the predicted displacement values. These are also compared with the J-R curves developed from the test data. The specimen information for each case is listed in Table 4.1.

Table 4.1 A Summary of Specimens Reported in Fig. 4.3 through Fig. 4.13

Figs.	Materials	Specimen Geometry Type	W in, (mm)	B in, (mm)	a_0 in, (mm)
Fig. 4.3a, b	A106 Steel	Compact	2, (50.8)	1, (25.4)	1.228, (31.19)
Fig. 4.4a, b	A508 Steel	Compact	2, (50.8)	1, (25.4)	1.031, (26.2)
Fig. 4.5a, b	A508 Steel	Compact	20, (508)	10, (254)	11.77, (299.0)
Fig. 4.6a, b	A508 Steel	Compact	8, (203.2)	4, (101.6)	4.08, (103.6)
Fig. 4.7a, b	A508 Steel	Compact	4, (101.6)	2, (50.8)	3.628, (92.15)
Fig. 4.8a, b	A508 Steel	Compact	1, (25.4)	1/2 (12.7)	0.525, (13.3)
Fig. 4.9a, b	A533 Steel	Compact	2, (50.8)	1, (25.4)	1.214, (30.84)
Fig. 4.10a, b	HSLA-80 Steel	Compact	1.99, (50.55)	0.99, (25.15)	1.322, (33.58)
Fig. 4.11a, b	HSLA-710 Steel	Compact	2, (50.8)	1, (25.4)	1.245, (31.62)
Fig. 4.12a, b	HY80 Steel	Compact	2, (50.8)	1, (25.4)	1.21, (30.73)
Fig. 4.13a, b	HY130 Steel	Compact	1.99, (50.55)	1, (25.4)	1.434, (36.42)

The materials represented by these examples have very different properties. Also a large enough size range is covered. It can be clearly seen from these results that the new approach worked very well for all the cases reported. All the P-v curves reported show that the displacement values were accurately predicted by the new approach. All the J-R curves determined from the new approach agree very well with the J-R curves determined from the test data. This could be expected since the displacement values were predicted accurately by this method.

(2). Results for second group of specimens

The second group contains eight specimens. They are all 1T size compact specimens with 20% side grooves. Two example of raw data, as supplied originally by Dr. Nanstad, are given in Fig. 4.14 and 4.15, where the solid dots are the points of the final load versus final physical crack extension measurements. Four examples of the resulting J-R curves determined by the new approach are reported here. They are shown in Fig. 4.16 through Fig 4.19. The J-R curves were first determined from the original test data. They are show in each figure by the square symbol. The first two cases , Fig. 4.16 and 4.17, the J-R curve results look correct. For these two cases the final physical crack extensions were accurately estimated by the elastic compliance measurements. The errors were within 2.5%. However, for the last two cases, Fig. 4.18 and 19, the J-R curves look incorrect near the end. This is probably caused by the greater mismatch between the final physical crack extension measurement and the final compliance crack extension prediction. The errors for the mismatch were larger than 5%. A correction scheme has

been suggested to change the J-R curve trend near the end when the mismatch happens [29]. That is

$$(v_p / W)_i = (v_p / W)_{\max} + [(v_p / W)_f - (v_p / W)_{\max}] \left(\frac{\Delta a_i - \Delta a_{\max}}{\Delta a_f - \Delta a_{\max}}\right) \qquad (4.11)$$

This correction scheme was used to adjust the predicted plastic displacement values to fit the final physical crack length measurement. It was based on an empirical relationship between crack extension and normalized plastic displacement which was observed to be nearly linear after the maximum load point was passed. In this study it was used to correct the plastic displacement and crack length values simultaneously for the points after the maximum load was passed and the J-R curves were determined again. They are also given in the same figures, Fig. 4.16 though Fig. 4.19, by the triangle symbol to compare with the unadjusted J-R curves. Results show that the incorrect part was removed for all the J-R curves reported.

Chapter 5

Application III of Method of Normalization: J-R Curve Determination under the Conditions When the Load Is Difficult to Measure

5.1 Introduction

An additional new application of the method of normalization is to determine the J-R curves from displacement versus crack length data sets by predicting the load values. In practice this could be used to provide a convenient method for J-R determination by testing the crack-line-wedge-loaded compact specimens, C(W). Fig. 5.1 illustrates a scheme of a C(W) specimen test. Such a test arrangement does not allow direct measurement of the opening loads applied to the specimen. However, the load-line displacement can be easily measured. Since the elastic unloading compliance technique can not be applied without the load measurement, an electrical potential drop system can be used to monitor the crack length during the test. Currently the C(W) specimen is only used to determine the elastic fracture toughness parameter K [46-47], because the technique used to evaluate the load applied to the specimen is from the combined measurements of displacement and crack length, and is limited to the elastic range of loading behavior. The method of normalization uses the principle of load separation to functionally relate the three variables, load, displacement and crack length in the elastic-plastic fracture range. The LMN function has been successfully

used to represent this functional relationship. It can be used to predict any one of the three variables when the other two are known. This includes predicting the load when displacement and crack length are known.

In this chapter the method of normalization was studied to predict the load values for J-R curve determination when load was not measured from the test. The study was performed by analyzing the test data from the pin loaded compact specimens, but the methods developed could be applied to analyze the wedge loaded specimen, C(W), test data. It was conducted in two steps. First, a new approach was developed so that the method of normalization could be used to evaluate J-R curves from displacement versus crack length data by predicting the load values. In the second step an approach for J-R curve determination from only displacement data without load and crack length measurements was investigated. The study concentrated on the second step since this approach could further eliminate the need of an on-line crack length monitoring system for the J-R curve test. Details for the two new approaches are described in the following sections.

5.2 A New Approach for J-R Curve Determination from Displacement versus Crack Length Data without Load Measurements

Theoretically, the method of normalization can be used to predict the load values from load-line displacement versus crack length data for elastic-plastic fracture problems, provided the LMN function can be correctly determined. Since it has been assumed that the load cannot be measured during the test for this application, the technique using the maximum load to determine the

constant L cannot be used for LMN function determination. The three calibration point fitting technique described in Chapter 2 is adopted here to determine LMN function. It has been proven to be an effective technique for the LMN function determination [28-29], although the fitting procedure used is more complicated. When it is used in this application, the three types of calibration points are defined as before in Fig. 2.2. However, since the load is not measured, the final calibration point can not be obtained directly from the test. In the new approach the final calibration point is determined by measuring the final plastic displacement after the test is completed. Then the following relationship could be used to determine the final load value.

$$v_{ef} = v_f - v_{pf} = P_f C(a_f / W) \tag{5.1}$$

In this way, the final calibration point could be defined. It has been found that the power law fit given by equation (2.10) works well for determining calibration points B for this application. In this case the load P is embedded in the following equations and cannot be solved for explicitly.

$$v_i = v_{e(i)} + v_{p(i)} \tag{5.2}$$

$$v_{e(i)} = P_i C(a_i / W) \tag{5.3}$$

$$P_{N(i)} = \frac{P_i}{WB(b_i / W)^{\eta_{pl}}} \tag{5.4}$$

$$P_N = \mu (v_p / W)^{\kappa} \tag{5.5}$$

An iterative method was used for solving the value of load P at each point. This is illustrated by a flow chart given in Fig 5.2. The calibration points C work in the same way as before and are used to optimize the fit. The three constants were then determined from three types of calibration points, A, B and C by using the same fitting procedure described in Chapter 2. Once the LMN function is determined, it can be used to predict load P from the displacement versus crack length pairs so that the J-R curve could be developed.

To evaluate this new approach it was used to determine J-R curves for the five steels, A106, A508, A533B, HSLA-80 and HY80-Ni steels. Fourteen test specimens were included. These are all compact specimens with 50.8 mm width and 25.4 mm thickness and 20% side grooves. These data were obtained from previous tests and had been used to determine J-R curves with the elastic unloading compliance method and regular normalization method for measuring crack length. For more details refer to the Table 3.1. When the new approach was applied, the test records were assumed to have only displacement and crack length measurements; the load was predicted by the new approach and J-R curves were then developed from measured displacement versus crack length and predicted load. Results are given in both load versus displacement and J-R curve formats. Five examples are reported here, one for each steel. In Figs. 5.3a through 5.7a plots of predicted load versus measured displacement are compared with corresponding test data. All the cases show the loads were predicted fairly accurately. The error between the predicted load and test data is less than 5% for all the cases. Figs. 5.3b through 5.7b show the J-R curves determined by the new approach using the predicted load values, which are compared with both corresponding J-R

curves developed from load versus displacement test data with the compliance measured crack length and the crack length predicted from regular normalization. A good agreement was found for all cases shown. The difference between three corresponding sets of J-R curves is also within 5%.

5.3 A Further Development of Method of Normalization - J-R Curve Determination from Only Displacement without Both Load and Crack Length Measurements

The method introduced in the previous section provides a way to develop J-R curves by testing specimens like the C(W) geometry where the need for measuring the load is eliminated but the crack length must be measured during the test. To measure the crack length during a C(W) specimen test, a sophisticated electrical potential drop system or other advanced system is required. This could be a problem for some laboratories. A method which can be used to predict both load and crack length values is desirable. This would provide a very easy test method for J-R curve determination where only the displacement would have to be measured from the C(W) specimen test. A further development of method of normalization is investigated in this section for J-R curve determination from only displacement by predicting the load and crack length values.

To determine the J-R curves from only displacement, two variables, load, P, and crack length, a, must be predicted. Therefore more functional relationships between load, displacement and crack length must be established. An idea for developing such relationships can be taken from the

normalized load definition in equation (2.6) and the evaluation of the elastic component of displacement in equation (2.4). The equations (2.4) and (2.6) give both the elastic component of displacement and normalized load as a function of load and crack length. A certain functional relationship should exist between normalized load and the elastic component of displacement. After conducting a careful study on the five steels mentioned in the last section, a good linear relationship was found between the normalized load and the elastic component of front face displacement. Two examples are given in Fig. 5.8 for an A508 steel and Fig. 5.9 for an HSLA-80 steel; both show this linear relationship. An additional idea can also be developed from the normalized load definition. The normalized load is defined as load divided by the geometry function $G(a/W)$. It actually is a combined function of load and crack length as well as plastic displacement. Since crack extension is a function of plastic displacement, the normalized load P_N versus crack extension, $\Delta a/W$, can be plotted and it shows a relationship similar to the one for normalized load P_N versus plastic displacement v_p/W. This can be seen from Fig. 5.10 for an A508 steel and Fig. 5.11 for an HSLA-80 steel. It can also be fit best by the LMN type of function form with the constants not necessary being related to the ones for normalized load versus plastic displacement. The analysis to predict load and crack length from only displacement is based on these two relationships, one where normalized load is related to the elastic component of front face displacement and the other where the LMN function is used to relate the normalized load versus crack extension.

By combining these two relationships with four additional ones used in the previous normalization method the load and crack length could be predicted. The six relationships used are given in the following six equations.

$$v = v_e + v_p \tag{5.6}$$

$$v_e = P\,C(a/W) \tag{5.7}$$

$$v_{0e} = P\,C_0(a/W) \tag{5.8}$$

$$P_N = \frac{P}{WB(b/W)^{\eta_{pl}}} = \frac{(L_1 + M_1 v_p/W)(v_p/W)}{N_1 + (v_p/W)} \tag{5.9}$$

$$P_N = \frac{P}{WB(b/W)^{\eta_{pl}}} = \frac{(L_2 + M_2 \Delta a/W)(\Delta a/W)}{N_2 + (\Delta a/W)} \tag{5.10}$$

$$P_N = K_1 (v_{0e}/W) + K_2 \tag{5.11}$$

Where v, v_e, v_p are the load line displacement and its elastic and plastic components; v_{0e} is the elastic component of front face displacement; C and C_0 are the load line and front face compliance respectively, the relationships between C, C_0 and a/W can be found in reference [48]; L_1, M_1, N_1, L_2, M_2, N_2 and K_1, K_2 are fitting constants. Six unknowns, P, Δa, v_e, v_p, v_{0e} and P_N, are contained in six equations (5.6) through (5.11) and therefore could be uniquely determined. By introducing a relationship between v_{0e}, the component of front face displacement, and P_N a new relationship can be established to

determine these six unknowns that would not be available from only the load line displacement relationships.

Equations (5.6) through (5.11) constitute the basis of the new approach. To use these equations to predict load and crack length and then to develop J-R curves, some information from the test is first needed. This includes the load line displacement measured during the test and the initial and final crack length measured physically from the fracture surface as well as the final plastic displacement measured from the permanent plastic deformation after the test is complete. It is easy to get all this information by testing a C(W) specimen. The next step is to determine the eight fitting constants in equations (5.6-11). Because there are not enough calibration points, the new approach uses some material properties and the information obtained from the test to determine all the fitting constants. The steps involved are described as follows.

(1) A calibration point could be defined at the final crack length. This is by solving equations (5.6) and (5.7) for elastic displacement and the load using final displacement and its plastic component as well as the final crack length measured from the fracture surface.

(2) In studying the relationships between the constants in the equations it was found the constant L_1 in equation (5.9) and constant L_2 in equation (5.10) depend up on material flow stress and material toughness. A study based on the same five steels mentioned in the previous section showed that the values of L_1 and L_2 could be related to the normalized limit load through a

factor determined from a material toughness parameter, TP, defined later. They are given by

$$L_1 = \begin{cases} P_{LN} & for\ TP > 0.6 \\ 1.08 P_{LN} & for\ TP \leq 0.6 \end{cases} \tag{5.12}$$

and

$$L_2 = \begin{cases} [1.06 + (TP-1)/20] P_{LN} & for\ TP > 1.0 \\ 1.06 P_{LN} & for\ TP \leq 1.0 \end{cases} \tag{5.13}$$

with

$$P_{LN} = \frac{P_L}{G(a_0/W)} = \frac{P_L}{WB(b_0/W)^{\eta_{pl}}} \tag{5.14}$$

Where P_{LN} is the limit load normalized by the $G(a/W)$ function evaluated at initial crack length a_0. For a compact or C(W) specimen the limit load solution in the GE-EPRI Handbook [49] can be used to find P_L. It has the following form

$$P_L = \alpha \beta b \sigma_Y B_N \tag{5.15}$$

where

$$\beta = \left[(2a_0/b_0)^2 + 4(a_0/b_0) + 2\right]^{1/2} - 2(a_0/b_0) - 1 \tag{5.16}$$

$$\alpha = \begin{cases} 1.455 & \textit{for plane strain} \\ 1.071 & \textit{for plane stress} \end{cases}$$

and

$\sigma_Y = (\sigma_{YS} + \sigma_{UTS}) / 2$, the flow stress

a_0 = the initial crack length

$b_0 = W - a_0$

B_N = the net thickness of the specimen

The term TP is a material toughness parameter. It is defined as follows

$$TP = \frac{P_{Nf} - P_{LN}}{\sigma_Y (\Delta a_f / W)} \tag{5.17}$$

where

P_{Nf} = normalized final load from the calibration point

Δa_f = final crack extension.

The high toughness materials such as HSLA-80 steel have $TP \geq 2.0$ and the low toughness, high strength materials such as HY80 steel have $TP \leq 0.6$. The relationships in equations 5.12 through 5.17 were all derived empirically from the results of this study.

(3) The values of N_1 and N_2 are found to be approximately constant for all of the metals studied. The following N_1, N_2 were used in this study.

$$N_1 = 0.0006$$

$$N_2 = 0.0004$$

(4) The values of M_1 and M_2 are then determined from equations (5.9) and (5.10) respectively by using the final calibration point, P_f, Δa_f, v_f and v_{pf}.

(5) The values of constants K_1 and K_2 could be determined by taking some points in the initial elastic range of the deformation and combining these with the final calibration point. The points in the initial elastic range of the deformation could be assumed to have zero plastic displacement and zero crack extension. This gives

$$v_e \cong v$$

$$a \cong a_0$$

Then the load, P, and front face elastic displacement, v_{0e}, can be determined by using equations (5.7) and (5.8) for these points. Each initial elastic point combined with the final calibration point can determine a set of K_1 and K_2. An average of K_1's and K_2's gives the fitting constants in equation (5.11).

Once all fitting constants are known, equations (5.6) through (5.11) can be used to predict the load and crack length from the displacement. The J-R curve is then developed from the predicted load and crack length values with the displacement measurement from the test by following the procedures of

ASTM standard method E1152. A flow chart is given in Fig. 5.12 to illustrate the procedures of applying the new approach.

To illustrate how well this new approach works, it was applied to the same fourteen specimens from the five steels used in the last section. When the new approach was applied, the test records were assumed to have only displacement measurements. Five examples, from analyzing the same test specimens used before, are reported here. Fig. 13a through Fig. 17a show the predicted load P versus v curves compared with the actual test data. Results show the predicted values of load, P, are within 10% of the test data. Fig. 13b through Fig. 17b show the J-R curves determined from the new approach compared with the ones from standard test method (crack length was measured by the compliance method) and from the regular normalized method (crack length was predicted from P-v). A good agreement was found between the three methods. It is interesting to note that the errors in this method introduced into the P-v curves are not as great as in the J-R curves. This is probably due to offsetting errors in predicted load and crack length.

The method just described can be used to develop J-R curves from only a calibration point defined at the final crack length, because the determination of the eight fitting constants only involves the final calibration point and some material properties. The displacement can be chosen arbitrarily at increments based on the final displacement. Two examples are given in Fig. 18a, b for an A508 steel and Fig. 19a, b for an A533 steel to show the results of the P-v curves and J-R curves determined from only a final calibration point. The displacement was divided into fifty equal steps between zero and the

final point. The result was found to be as good as the one developed by using the displacement measurement from the test.

5.4 Summary

(1). The method of normalization can be used to develop J-R curves from the test where only displacement and crack length measurements are made and from tests where the displacement alone is measured.

(2). When the method of normalization is used to develop J-R curves from the displacement versus crack length without the load measurement, a power law fit worked well to give some calibration points which are needed for the LMN function determination. The detailed procedure has been developed for this application of the method of normalization. Results are in good agreement with the test data which had the full measurements of load, displacement and crack length.

(3). When the J-R curves are determined from only displacement without the load and crack length measurement by using the method of normalization, some further functional relationships between load, displacement and crack length need to be developed. Two new equations, one relating the normalized load and front face elastic displacement and another relating the normalized load and crack length, are used in this study. These two new equations taken together with the other equations from the method of normalization work well for predicting load and crack length from

only displacement, and then for developing J-R curves. The error in all predictions is within ±10%.

(4). The latter method could be used to determine J-R curves from only a displacement measured at final crack length. The result is as good as the one developed by using the displacement measured during the test.

(5). The development of the methods to predict J-R curves from displacement and crack length measurements and from displacement measurements alone was done here for five steels that are ferritic and generally in the same strength range. The relationships developed to generate the six basic equations used in the method were shown to work only for this limited range of steels. It remains to be shown that the same equations can be used for other metals and that the method applies to a larger range of metals. This is suggested as a topic for future work.

Chapter 6

Application IV of Method of Normalization: J-R Curve Determination under Dynamic Loading Conditions Using Charpy Impact Tests

6.1 Introduction

In modern engineering practice, structural components are often dynamically loaded well into the plastic range. The components serving under such circumstances demand that their design be based on dynamic material properties which are valid in the elastic-plastic range. However, so far there is no standard test method for elastic-plastic fracture toughness determination under dynamic loading conditions. This is due to the fact that the crack length cannot be measured simultaneously with load and displacement under dynamic loading conditions during the test. To fill in this gap, a new approach is investigated in this chapter for J-R curve determination under dynamic loading conditions. The new approach will use the method of normalization to predict crack length from the experimental data obtained in an instrumented Charpy impact test.

The Charpy impact test is essentially a high rate loading, three-point bend test of a notched specimen. It has been widely accepted as a useful tool for evaluating the dynamic response of a wide range of materials. When the striker of a Charpy machine is instrumented, a load versus time curve (P-t curve) can be measured from a Charpy impact test. This P-t curve cannot be

used to determine the J-R curve directly. It must be converted to a load versus displacement curve first. This could be done by applying an incremental calculation method based on the conventional dynamics theory [50]. The load versus displacement record can then be analyzed to determine the J-R curve by first predicting the crack length using the method of normalization.

The method of normalization has been successfully applied to the standard fracture toughness test data where only load and displacement pairs are measured for J-R curve determination. This has been demonstrated in Chapter 3. For the standard test case an initial and final value of crack length can be measured physically on the fracture surface corresponding to an initial and final set of load and displacement pairs in the test record. They are necessary information to define the final calibration point for the LMN function determination. However, for the Charpy impact test case there is no point similar to the final point in the standard test case where the crack length can be measured physically after test is complete, since the test is run to full separation of the specimen. This leaves the analysis of the test results without an important parameter. An empirical scheme will be invented to predict a provisional final crack length at an arbitrarily defined value of displacement after the maximum load is passed.

In the following sections the new approach will be described in detail for the J-R curve determination from Charpy impact load versus time record.

6.2 The Charpy Impact Test Record Conversion from Load versus Time to Load versus Displacement

During a Charpy impact test, the energy lost by the hammer can be expressed as

$$\Delta E = E_I + E_{SD} + E_B + E_{MV} + E_{ME} \tag{6.1}$$

where

ΔE = the energy lost by the hammer,

E_I = the increment of energy required to accelerate the specimen from rest to the velocity of the hammer,

E_{SD} = the energy absorbed to fracture the specimen,

E_B = the energy consumed by Brinell-type deformation at the specimen load point,

E_{MV} = the energy absorbed by the test machine through vibrations after initial contact with the specimen,

E_{ME} = stored elastic energy absorbed by the test machine system as a result of the interactions at the specimen load point,

E_{MV} is usually quite small compared with ΔE and can be ignored. For elastic-plastic fracture E_I and E_B are usually negligible contributions to the ΔE. Therefore, the energy absorbed to fracture the specimen can be estimated by

$$E_{SD} = \Delta E - E_{ME} = \bar{\rho}\int_0^t P dt - \frac{1}{2} P^2 C_M \tag{6.2}$$

where

$\bar{\rho}$ = the average speed of the hammer,

C_M = the test machine system elastic compliance.

At any specified time t_i after the initial contact of the tup and specimen, the reduction in hammer energy can be represented by the change in kinetic energy

$$\Delta E_i = E_0 - E_i = \frac{1}{2} m(\rho_0^2 - \rho_i^2) \tag{6.3}$$

where

E_0 = the initial hammer energy,

E_0 = the hammer energy at time t_i,

ρ_0 = the initial hammer speed,

ρ_i = the instantaneous hammer speed at the time t_i,

m = the mass of the hammer.

Also the load versus time record can be related to the hammer speed by the statement of the equivalence between linear impulse and change in linear momentum

$$\int_0^{t_i} P dt = m(\rho_0 - \rho_i) \tag{6.4}$$

By combining Eq. (6.3) and (6.4), it can be shown that the ΔE at the time t_i can be estimated by

$$\Delta E_i = E_0 - E_i = E_{a(i)}\left[1 - \frac{E_{a(i)}}{4E_0}\right] \tag{6.5}$$

where the $E_{a(i)}$ is defined as

$$E_{a(i)} = \rho_0 \int_0^{t_i} P dt \tag{6.6}$$

Then ΔE_i is used to determine the instantaneous hammer speed at the time t_i

$$\rho_i = \rho_0 \left(1 - \frac{\Delta E_i}{E_0}\right)^{1/2} \tag{6.7}$$

The load-line displacement then can be determined from

$$v_i\big|_{total} = v_{i-1} + \frac{\rho_i + \rho_{i-1}}{2}(t_i - t_{i-1}) \tag{6.8}$$

$$v_i\big|_{specimen} = v_i\big|_{total} - v_i\big|_{machine} \tag{6.9}$$

To accurately convert a load versus time curve to a load versus load-line displacement curve, the compliance of the test machine must be determined. This is known as the test machine compliance correction. A test machine compliance correction curve can be obtained by conducting a low-blow test. Then the $v_i\big|_{machine}$ can be determined from the test machine correction curve at any specified load P_i. Fig. 6.1a, b and Fig. 6.2a, b show two examples of P-t curves obtained from the instrumented Charpy impact test for an A533B steel and their corresponding P-v curves converted using above approach.

6.3 A New Approach for a Provisional Final Calibration Point Prediction

After the load versus time record from a Charpy impact test is converted to load versus displacement data, the problem for the J-R curve determination under dynamic loading conditions is reduced to a J-R curve determination from load versus displacement pairs using the method of normalization. A successful approach for crack length prediction has been developed in Chapter 3. There the required data is obtained from the standard J-R curve test procedure. This approach uses the three-parameter LMN function to relate three variables, load displacement and crack length, therefore, the crack length values can be predicted from load versus displacement pairs. However, in applying the approach suggested the three constants in the LMN function need to be determined first individually for each specimen. The approach uses the maximum load point in the load versus displacement record to determine the constant L first. The remaining constants M and N are then determined using two types of calibration points, the final calibration point obtained from the test and the initial calibration points obtained from a forced blunting assumption. When the method of normalization is applied to determine the J-R curve from the Charpy impact test data, the maximum load point and the initial calibration points are available, but the final calibration point cannot be obtained. This is because the specimen is completely broken in two in a Charpy impact test. For this type of test, there is actually no a point similar to the final point in the standard J-R curve test. The technique used before by measuring the final crack length or the final permanent plastic deformation at the end of the test to define the final calibration point cannot be used here. To make the

method of normalization work for the J-R curve determination from Charpy impact test data, a new approach must be developed to predict a provisional final calibration point.

In a study of the relationship between load, displacement and crack length, it was found that the displacement v versus its elastic component v_e show a linear relation after maximum load point was passed. This can be seen from two examples given in Fig. 6.3 and Fig. 6.4 for a compact specimen of an A508 steel and a three-point bend specimen of an HSLA-710 steel respectively. Once this linear relationship is known, it can be used to predict a provisional final calibration point at any specific value of displacement after maximum load point is passed. It has been found that an empirical scheme can be used to determine this linear relationship between the v and v_e. It was derived based on the analysis of eight specimen test data groups. The materials involved were A106, A508, HSST weld, A533, HSLA-80, HSLA-710 and HY80-Ni steels. Compact specimens with sizes of 1/2T, 1T, 4T and three-point bend specimens with a size of W = 2, B = 1 inch were included. These specimen test data sets have been used in the studies reported in previous sections. More information on these specimens can be found from the Table 3.1. The suggested scheme for computation can be summarized by the following equations

$$(P_{N0})_{i\max} = \frac{P_{i\max}}{WB\left(\frac{W-a_0}{W}\right)^{\eta_{pl}}} \tag{6.10}$$

$$(P_N)_{i\max} = \frac{P_{i\max}}{WB\left(\frac{W-a_{i\max}}{W}\right)^{\eta_{pl}}} \tag{6.11}$$

$$(P_N)_{i\max} = 1.0612(P_{N0})_{i\max} + 0.25236 \tag{6.12}$$

$$v_{e(i\max)} = P_{i\max} C(a_{i\max}) \tag{6.13}$$

$$[v_{e(f)} - v_{e(i\max)}] = 0.51(v_f - v_{i\max}) + 0.0003W \tag{6.14a}$$

for the compact specimens,

$$[v_{e(f)} - v_{e(i\max)}] = 0.51(v_f - v_{i\max}) - 0.0025W \tag{6.14b}$$

for three-point bend specimens,

$$v_{e(f)} = P_f C(a_f) \tag{6.15}$$

where the subscript "imax" refers to the value at the maximum load point and "f" refers to the value at the (provisional) final point. The empirical relationship given by Eq. (6.12) is used first to determine the normalized load at the maximum load point. The crack length at the maximum load point can then be determined from this value using the normalized load definition. Up to this step a calibration point has been defined at the maximum load value. This point can then be used to determine the linear relationship between the displacement, v, and its elastic component, v_e, for each specimen using Eq. (6.14a) for the compact specimens and Eq. (6.14b) for the three-point bend specimens. The (provisional) final crack length can then be determined from the compliance relationship, Eq. (6.15), by first finding the final elastic component of displacement from Eq. (6.14a) or (6.14b) at any specific value of displacement after the maximum load point is passed.

Once the (provisional) final calibration point is defined, the method of normalization can be applied to the load versus displacement data converted from the Charpy impact test record to determine the J-R curve using the new approach suggested in Chapter 3.

6.4 J-R Results by Applying the New Approach

In previous sections of this chapter a new approach has been fully developed for J-R curve determination from an instrumented Charpy impact test record. In this section the new approach is applied to the experimental data to examine the suggested method. The examination is performed in two steps. In the first step, data from standard elastic unloading compliance tests are used. These data have the standard set of measurements: load, displacement and crack length. When the new approach is applied, the data sets are assumed to have only load and displacement measurements. Also the final calibration point is assumed to be not available. After the analysis is completed, J-R curves determined from the complete test data (where the crack length was measured by the elastic compliance method) and from the regular normalization method (where the J-R curve was determined from only P-v by predicting the crack length with the known final calibration point) are used for comparison. In this way the success of the new approach could be evaluated. This step is mainly used to examine the suggested scheme for the final calibration point prediction, since the approach developed in Chapter 3 is used. It has been demonstrated to be reliable for J-R curve determination from only a P-v record when the final calibration point

is known and measured correctly. In the second step the new approach is applied to the real data obtained from the instrumented Charpy impact tests. The J-R curve results could not be compared with any other results, since the J-R curve could not be determined previously under dynamic loading conditions. However, their reliability could be illustrated indirectly by the results obtained in the first step.

6.4.1 J-R Curve Results by Applying the New Approach to the Standard J-R Curve Test Data

The first step in examining the new approach was to apply the method to the eight groups of standard J-R curve test data which has been used in the previous sections. The analysis was done by inputting only load versus displacement pairs from the test record (all other information was assumed to be not available). The final calibration point was predicted first from the empirical scheme using the P-v values at the maximum load point. Once it was known, the approach developed in Chapter 3 could be applied to determine the LMN function. That is, the constant L was determined first from the maximum load point and the remaining constants M and N were then determined using the calibration point A and calibration points B, Fig. 2.2. For the case considered here, the predicted final calibration point was used as the calibration point A and the forced blunting assumption was used to obtain the calibration points B as before. More detail about LMN function determination procedure can be found in Chapter 3. The LMN function determined was then used to predict the crack length at each load versus displacement pair. Up to this point, the information for J calculation was

completely determined. The values of J can be can be calculated at each measured point by following the ASTM standard E1152 procedures, and then the J-R curve can be plotted.

Twelve examples of J-R curve predictions are reported here. They are shown in Fig. 6.5 through Fig. 6.16. The specimens used are summarized in Table 6.1 with their material, size and geometry information.

Table 6.1 A Summary of Specimen Information Reported in Fig. 6.5 through Fig. 6.16

Figs.	Materials	Specimen Geometry	W in, (mm)	B in, (mm)	Notes
Fig. 6.5	A106 Steel	Compact	2, (50.8)	1, (25.4)	
Fig. 6.6	A508 Steel	Compact	2, (50.8)	1, (25.4)	
Fig. 6.7	HSST Weld	Compact	2, (50.8)	1, (25.4)	
Fig. 6.8	A533 Steel	Compact	2, (50.8)	1, (25.4)	
Fig. 6.9	HSLA-80 Steel	Compact	1.99, (50.55)	0.99, (25.15)	
Fig. 6.10	HSLA-710 Steel-Heat 1	Compact	2, (50.8)	1, (25.4)	
Fig. 6.11	HY80-Ni Steel	Compact	2, (50.8)	1, (25.4)	
Fig. 6.12	A508 Steel	Compact	1, (25.4)	1/2 (12.7)	
Fig. 6.13	A508 Steel	Compact	8, (203.2)	4, (101.6)	
Fig. 6.14	HSLA-80 Steel	Compact	9.99, (253.75)	5, (127)	
Fig. 6.15	HSLA-710 Steel-Heat 3	3-Point Bend	2, (50.8)	0.96, (24.38)	Span = 8 in
Fig. 6.16	HSLA-710 Steel-Heat 3	3-Point Bend	2, (50.8)	0.96, (24.38)	Span = 15.9 in

These examples represent eight metal material groups analyzed. Compact specimens in 1/2 T, 1T, 4T, 5T sizes and three-point bend specimens with different spans are included. For each specimen reported, J-R curves are compared between three methods, namely the new method, the standard J-R

curve test method with the elastic compliance technique and the regular normalization method with the physically measured final calibration point. From these results it can be seen that:

- The empirical scheme suggested worked quite well for the provisional final calibration point prediction. For eight out of twelve cases, the final calibration point prediction was as good as the final physical measurement. For other four cases, A508 steel 1T compact specimen in Fig. 6.6, A533 steel 1T compact specimen in Fig. 6.8, A508 steel 4T compact specimen in Fig. 6.13 and HSLA-710 steel-heat 3 three-point bend specimen with large span in Fig. 6.16, the predicted values had some error when compared with the physical measurements, but the accuracy of the prediction was still comparable with elastic compliance measurements. Based on these predicted provisional final calibration points, the J-R curves were then successfully developed.

- Results showed that the new method worked for different materials, specimen sizes and both compact and three-point bend geometries.

- In the new approach the information from the test data (the maximum load point) is used for both the final calibration point prediction and the LMN function determination. This is the main reason why the new approach can work so well for J-R curve determination without crack length measurements and missing a final calibration point. For the same reason, it should work when it is applied to the Chary impact test data.

Based on above, it could be concluded that the suggested approach could be applied to the Charpy impact test data for J-R curve determination.

6.4.2 The J-R Results Developed from Charpy Impact Test Data

In last section the new approach has been successfully applied to the standard J-R curve test data for J-R curve determination by assuming the crack length measurements and the final calibration point were not available. It has been concluded that the new approach could work for J-R curve determination from the Charpy impact test data since the provisional final calibration point and the LMN function are determined from the test information itself.

The next step in the examination of the new approach is to analyze the actual Charpy impact test data. The data used were supplied by Dr. Randy Nanstad of Oak Ridge National Laboratory. The original data were supplied in the form of voltage versus time traces with the maximum load measurements and the time measurements from the impact to the maximum load. They were obtained from instrumented Charpy impact tests. Five three-point bend specimens in W = 10, B = 10 mm were included. The specimens were only notched as in a standard Charpy impact test and were not precracked. They were made from an A533B nuclear grade pressure vessel steel. These specimens could be divided into two groups, since the A533B steel used had two different sets of material properties. The first group had three specimens, specimen J103, J104, and K106. The material for this

group had a yield stress of 76.3 ksi and an ultimate strength of 99.12 ksi. The second group included specimen J109 and K107 with a material yield stress of 60 ksi and an ultimate strength of 80 ksi. The original voltage versus time traces were first converted to the load versus time data by using the proportional relationship between the load and voltage. Two examples of such P-t curves have been given in Fig. 6.1a and 6.2a. The analysis was begun by converting the P-t data to P-v data using the approach described in Section 6.2. After P-v pairs were obtained, the empirical scheme was applied to predict the provisional final calibration point for each specimen. Typically, the standard J-R curve test is conducted until the final load drops to 40-50% of the maximum load obtained. For this reason the provisional final calibration point was picked at the point where the maximum load dropped by 50% ($P_f \geq 0.5P_{max}$) for each specimen analyzed here. Also, for comparison, the point where maximum load dropped only by 40% was used for some specimens. The remaining analysis was conducted using the procedures described in last section.

The analysis results for the five specimens are reported here in both P-v curve and J-R curve forms. They are given in Fig. 6.17a through Fig 6.21a for P-v curves and Fig. 6.17b through Fig. 6.21b for J-R curves. Results show that J-R curves were successfully developed for all the specimens studied. Also in Fig. 6.17b, the J-R curves for specimen J103 determined from two different provisional final calibration points are reported, one is at the point where the load has dropped by 50% from the maximum load and the other by 40%. Results show that the two J-R curves are almost identical. This demonstrates that the location of the provisional final calibration point has little effect on the J-R curve determination for the new approach. It should be mentioned

that the value of J in the R curves reported here is relatively high when compared with other A533B steel results. The reason for this is that the impact specimens were not fatigue precracked, they were only notched as in a standard Charpy impact test. The notched specimens usually exhibit a much higher initiation value of J than the precracked specimens.

6.5 Summary

An approach has been developed in this chapter for J-R curve determination under dynamic loading conditions using the method of normalization. The test data are obtained from a Charpy impact test. In these tests load versus time can be measured as an instrumented hammer strikes a standard Charpy specimen. An incremental calculation approach has been suggested in this study to convert the load versus time, P-t, pairs to the load versus displacement, P-v, pairs. The load versus displacement record can be analyzed to determine a J-R curve using the method of normalization. This has been done with good success for J-R curve determination from standard fracture toughness test data where the crack length values are not measured. However, when it is applied to the Charpy impact test data, a problem arises. That is, the final calibration point, which is important for the LMN function determination, cannot be obtained from a Charpy impact test since the test is run to complete separation of the specimen. An empirical scheme was then developed for predicting a provisional final calibration point using the maximum load point of the P-v pairs. After the final calibration point is

known, the approach developed in Chapter 3 could be applied to determine the J-R curve from the P-v pairs.

To examine the new method, it was applied to the standard J-R curve test data by assuming the crack length measurements and the final calibration point were not available. Results showed that the final calibration point was predicted fairly accurately from the empirical scheme for each specimen studied. The prediction of a final crack length value was found to be close to the final physical crack length measurement and comparable with the elastic compliance measurement. Also, the new method was found to work quite well for different materials, a large range of specimen sizes and for both compact and three-point bend specimen geometries. Since the method uses the maximum load point from the test data for the provisional final calibration point determination and the LMN function determination, these features could be applied in the same way to the Charpy impact test data for the J-R curve determination. The new method was then applied to the actual Charpy impact test data. Results showed that the J-R curve was developed for all the specimen analyzed.

This method then provides a way to easily determine the J-R curve under dynamic loading conditions.

Chapter 7

Summary and Discussion

As the title states, the overall objective of this study is to further develop the method of normalization for elastic-plastic fracture toughness determination under some difficult conditions. Currently, the determination of a material's elastic-plastic fracture toughness, J_{Ic} value and J-R curve, in the laboratory using the ASTM standard test methods requires a simultaneous measure of the load, displacement and crack length from the test. The current standard test methods have many limitations, such as the need for a sophisticated equipment and advanced test skills to monitor the crack extension, application only to metallic materials and working well only when the specimen is side-grooved, etc. Also, it can be difficult to measure the load or displacement during the test for some special cases.

The method of normalization uses the principle of load separation to relate the three variables, load, displacement and crack length, during the fracture process. This relationship is expressed by an LMN functional form which could be determined from some calibration points, material properties or other test information. It provides an analytical basis for predicting any one of the three variables from the other two.

The following four different applications of method of normalization have been investigated in this study.

- Application I: J-R curve determination from load versus displacement records without crack length measurements.

- Application II: J-R curve determination from load versus crack length records without displacement measurements.

- Application III: J-R curve determination under conditions where load is difficult to measure.

- Application IV: J-R curve determination under dynamic loading conditions.

Theoretically speaking, the method of normalization can be applied to all the cases studied to accomplish the required predictions. However, before the method of normalization can be applied, the LMN function need to be determined for each specimen. This is an important step in applying the method of normalization, since the success of the method and the prediction accuracy are mainly dependent on the LMN function determined. Different problems arise in attempting a determination of the LMN function for each specific subject. Four approaches have been then developed for each application.

A large number of specimen test data were collected to support this study. Based on the analysis results of these experimental data sets the four new approaches could then be developed. Also these test data sets have been used to examine the new approach developed for each application.

The summary and discussion for each area are given in the following sections.

7.1 J-R Curve Determination without Crack Length Measurements

The method developed to predict the J-R curve without a crack length measurement is very useful in engineering practice. It can eliminate the need for a sophisticated on-line crack length monitoring system, and therefore, greatly simplify the J-R curve test procedure. Also, It has been demonstrated that this method can work for both metallic and non-metallic materials, for both side-grooved and non-side-grooves specimens.

Several attempts have been made and several versions of the method of normalization have been developed on this subject. Among them, the LMN function approach with the three-point fitting procedure is a most successful version of the method. However, this approach was found to be too complicated, not easy to understand, nor convenient to use.

A new approach has been developed in this study to improve the previous approach. In the suggested approach, a new concept was developed which relates the maximum load point to the constant L for the LMN function determination. It has been found that this value of L taken with the calibration point A from the final point and the calibration points B from the forced blunting assumption can determine the LMN function accurately. This improvement can remove the complicated part in the LMN function determination procedure. The LMN function determination is then completely based on the test information and the material properties.

The new approach has been examined with a large experimental data base, taken from the literature, which contains in total two hundred and twenty-two test specimens in eighteen material groups including polymeric materials. These test data represent a wide range of materials, different

specimen geometries, a large range of specimen sizes and both side-grooved and non-side-grooved specimens. Results demonstrate that the new approach worked successfully for both crack length prediction and J-R curve determination. The overall prediction accuracy has been found to be as good as or even better than the standard J-R curve test method and the best previous version of the method of the normalization.

Based on these results, it could be concluded that the new version of the method of normalization developed in this work has reached a mature level. It could be offered as a candidate for incorporating into the present standard test methods to provide an alternative method for J-R curve determination, especially under the conditions when the crack length is difficult to measure during the test.

7.2 J-R Curve Determination without Displacement Measurements

The technique developed for predicting J-R curves without displacement measurement has an advantage for determining J-R curve tests in adverse environments such as a test at high temperature or in a hot cell. Previously, an approach has been developed for this subject. It also uses the LMN function approach with the three-point fitting procedure in the method, but a power law fitting assumption was used to obtain the calibration points B at the early range the deformation. The same problem, that is the complicated nature of the LMN function fitting procedure, was found to be a deterrent to use of this approach.

A new improved approach has been developed for this case. The idea of relating the maximum load point to the constant L is also adopted here to eliminate the complicated part of the LMN function fitting procedure. In the new approach this concept is suggested to be used with the final calibration point (used as the calibration point A) and the calibration points determined from the power law fitting at the early range of the deformation (used as the calibration points B) to determine the LMN function.

The new method has been evaluated by using two groups of experimental data. The first group of test data actually had the complete measurements of load, displacement and crack length for each specimen. When the new approach was applied, only the load and crack length measurements were used. J-R curves were developed by predicting the displacement values from the new approach. Results could be then compared with the test data. The second group of the test data were used to simulate the actual conditions assumed for this subject. Only load and crack length measurements were available for each specimen in this group. Results showed that the displacement values were predicted accurately and then the J-R curves were determined successfully by the new approach for each case analyzed. It has been found that a correction should be placed on values of the input crack length and the predicted plastic displacement when the mismatch error between the compliance measurement and the final physical measurement of crack length is larger than the 5%. A correction scheme has been suggested with the new approach.

The method suggested here provides a easy way to determine J-R curves when the displacement is difficult to measure from the test. However, since an empirical formula is used to determine the constant in the power law

fitting which is for obtaining the calibration points B in the LMN function determination, and this empirical formula is based only on the analysis results of the nine metallic materials studied in this work, its range of application may be limited to metallic materials in the similar range. It remains to be shown that the same formula is applicable to a large range of materials or needs to be further developed for other materials. This is suggested as a topic for future study.

7.3 J-R Curve Determination without the Load Measurements

The techniques developed for the J-R curve determination without load measurement could provide a convenient way to determine the J-R curves by testing crack-line-wedge-loaded compact specimens. The study on this subject was performed in two steps.

(1). In the first step, the method of normalization was studied so that it could be applied for J-R curve determination from displacement and crack length pairs without load measurements. A new approach has been developed for this using the LMN function and the three-point fitting procedure.

The new approach has been successfully applied to five metallic materials for load prediction and J-R curve determination. Results were found in good agreement with the test data. The prediction error was found within 5% for both load and J-R curve.

(2). In the second step, an attempt has been made on this subject to further eliminate the need of monitoring of the crack length from the test. An additional approach has been developed for J-R curve determination from only displacement without both load and crack length measurements. Two new functional relationships were suggested in this study to work with the method of normalization for both load and crack length prediction.

The evaluation based on five metallic material groups of specimens showed that the new approach worked well to predict the load and crack length from only displacement measurements for all the specimens studied. The prediction was found within 10% for both load and crack length when compared with the test data. The J-R curve could be then determined using only the displacement data from the test where the load and crack length values were predicted for each specimen. Results were found to be in good agreement with the ones determined from the full test data.

It has been found that the approach developed in second step could be used to determine the J-R curve from only a calibration point defined at the final crack length. Results were found to be as good as the ones determined using the actual displacement test data.

The later method introduced in this study has great significance in engineering practice. It provides a very simple and convenient way for J-R curve determination. Only displacement or even only a calibration point needs to be measured from the test. This would greatly simplify the J-R curve test procedure and the test equipment. However, this technique is in the early stage of development. The two new functional relationships suggested

in this study were derived based on empirical observations of the test data. Their theoretical basis should be further studied. Also, since only five metallic materials and 1T size specimens were covered in this study, further study is suggested for a larger range of materials and specimen sizes to see if the method has a wider range of applicability.

7.4 J-R Curve Determination under Dynamic Loading Conditions

The method of normalization has been further developed in this study for J-R curve determination under dynamic loading conditions using the Charpy impact test. In the new approach, load versus time, P-t, measurements are first converted to load versus displacement, P-v, values. Before the method of normalization can be applied to the dynamic P-v data, a final calibration point needs to be determined. An empirical scheme has been developed to predict a provisional final calibration point using the maximum load point of the P-v data. The method suggested in Chapter 3 is then used to determine the J-R curve from the dynamic P-v data with the provisional final calibration point.

The new approach was examined first using the experimental data from the standard J-R curve test. To simulate the dynamic test data, the crack length measurements and the final calibration points were assumed to be unavailable for these test data. The analysis was done by inputting only P-v pairs for each specimen studied. It has been demonstrated that the new method worked well to determine the J-R curves for different materials, a large range of specimen sizes, and both compact and three-point bend

specimen geometries. The prediction accuracy for the provisional final calibration points was found to be close to the final physical measurements or comparable with the compliance measurements.

The new method was then applied to the real dynamic test data obtained from the Charpy impact tests to determine the J-R curves. The J-R curve results were found to be reasonable for the material used.

The method suggested here provides a convenient way to determine the J-R curves under dynamic loading conditions. It is only the first step toward this goal. More details should be further evaluated for this method of evaluating dynamic loading J-R curves. These include the following:

- Some formulas, such as the compliance relationship to relate the elastic displacement and the crack length, were developed originally for use under standard test conditions. These formulas have been used in the new method. It remains to be shown whether these formulas could be used under dynamic loading conditions or should be modified.

- Further study could be done based on a larger range of materials, including the metallic and non-metallic materials.

- Further study could be needed to assess the accuracy of the J-R curves determined from the real dynamic test data. For this some alternate method of developing the dynamic loading J-R curve would be needed for comparison.

REFERENCES

1 Griffith, A. A., "The Phenomena of Rupture and Flow in Solids," Philosophical Transactions of the Royal Society of London, A221, 1921, pp. 163-197.

2 Rice, J. R., "A Path Independent Integral and the Approximate Analysis of Strain Concentration by Notches and Cracks," Journal of Applied Mechanics, Vol. 35, 1968, pp. 379-386.

3 Hutchinson, J. W., "Singular Behavior at the End of a Tensile Crack Tip in a Hardening Material," Journal of the Mechanics and Physics of Solids, Vol. 16, 1968, pp. 13-31.

4 Hutchinson, J. W., "Plastic Stress and Strain Fields at a Crack Tip," Journal of the Mechanics and Physics of Solids, Vol. 16, 1968, pp. 337-347.

5 Rice, J. R. and Rosengren, G. F., "Plane Strain Deformation Near a Crack Tip in a Power-Law Hardening Material," Journal of the Mechanics and Physics of Solids, Vol. 16, 1968, pp. 1-12.

6 Rice, J. R., "Mathematical Analysis in the Mechanics of Fracture," Fracture Vol. II, H. Liebowitz , Ed., Academic Press, pp. 191-311.

7 Begley, J. A. and Landes, J. D., "The J Integral as a Fracture Criterion", Proceedings of the 1971 National Symposium on Fracture, Part II, Fracture Toughness, ASTM STP 514, American Society for Testing and Materials, Philadelphia, 1972, pp. 1-20.

8 Landes, J. D. and Begley, J. A., "The Effect of Specimen Geometry on J_{Ic}," Proceedings of the 1971 National Symposium on Fracture, Part II, Fracture Toughness, ASTM STP 514, American Society for Testing and Materials, Philadelphia, 1972, pp. 24-39.

9 Landes, J. D. and Begley, J. A., "Test Results from J-Integral Studies: An Attempt to Establish a J_{Ic} Testing Procedures," Fracture Analysis, ASTM STP 560, American Society for Testing and Materials, 1974, pp. 170-186.

10 Heyer, R. M. and McCabe, D. E., "Crack Growth Resistance in Plane Stress Fracture Testing," Engineering Fracture Mechanics 4, 1972, pp. 413-430.

11 McCabe, D. E. and Heyer, R. H., "R Curve Determination Using a Crack-line Wedge Loaded (CLWL) Specimen," Fracture Toughness Evaluation by R Curve Methods, ASTM STP 527, American Society for Testing and Materials, 1973, pp. 17-35.

12 Paris, P. C., Tada, H., Zahoor, A. and Ernst, H., "Instability of the Tearing Mode of Elastic-Plastic Crack Growth," Elastic-Plastic Fracture, ASTM STP 668, J. D Landes, J. A. Begley and G. A. Clarke, Eds., American Society for Testing and Materials, 1979, pp. 5-36.

13 Paris, P. C., Tada, H., Ernst, H. and Zahoor, A., "An Initial Experimental Investigation of the Tearing Instability Theory," Elastic-Plastic Fracture, ASTM STP 668, J. D Landes, J. A. Begley and G. A. Clarke, Eds., American Society for Testing and Materials, 1979, pp. 251-265.

14 Shih, C. F., "Relationship between the J-Integral and the Crack Opening Displacement for Stationary and Extending Cracks," Journal of the Mechanics and Physics of Solids, Vol. 29, 1981, pp. 305-326.

15 Bucci, R. J., Paris, P. C., Landes, J. D. and Rice, J. R., "J Integral Estimation Procedures," Proceedings of the 1971 National Symposium on Fracture, Part II, Fracture Toughness, ASTM STP 514, American Society for Testing and Materials, 1972, pp. 40-70.

16 Rice, J. R., Paris, P. C. and Merkle, J. G., "Some Further Results of J-Integral Analysis and Estimates," Progress in Flaw Growth and Fracture Toughness, ASTM STP 536, American Society for Testing and Materials, 1973, pp. 231-245.

17 Clarke, G. A., Andrews, W. R., Paris, P. C. and Schmidt, D. W., "Single Specimen Tests for J_{Ic} Determination," Mechanics of Crack Growth, ASTM STP 590, American Society for Testing and Materials, 1976, pp. 27-42.

18 Ernst, H. A., Paris, P. C. and Landes, J. D., "Estimation on J-Integral and Tearing Modules T from a Single Specimen Test Record," Fracture Mechanics: Thirteenth Conference, ASTM STP 743, American Society for Testing and Materials, 1981, pp. 476-502.

19 Hudak, S. J. and Saxena, A., "Review and Extension of Compliance Information for Common Crack Growth Specimens," International Journal of Fracture, Vol. 14, No. 5, Oct. 1978, pp. 453-468.

20 "Recommended Practice for R Curve Determinations," ASTM Annual Book of Standard Part 10, American Society for Testing and Materials, Philadelphia, 1975.

21 "Standard Test Method for J_{Ic}, A Measure of Fracture Toughness," ASTM Designation: E 813-87, 1987 Annual Book of ASTM Standards, Vol. 03. 01.

22 "Standard Test Method for Determining J-R Curve," ASTM Designation: E1152-87, 1987 ASTM Annual Book of ASTM Standard, Vol. 03. 01.

23 Joyce, J. A. and Gudas, J. P., "Computer Interactive J_{Ic} Testing of Navy Alloys," Elastic-Plastic Fracture, ASTM STP 668 American Society for Testing and Materials, 1979, pp. 451-468.

24 Baratta, F. I., Kapp, J. A., and Underwood, J. H., "More on Compliance of the Three-Point Bend Specimen," International Journal of Fracture, Vol. 28, 1985, pp. R41-R45.

25 Turner, C. E., "Measurement of Fracture Toughness by Instrumented Impact Test," Impact Testing of Metals, ASTM STP 466, American Society for Testing and Materials, Philadelphia, 1970, pp. 93-114.

26 Herrera, R. and Landes, J. D., "Direct J-R Curve Analysis of Fracture Toughness Test," Journal of Testing and Evaluation, JTEVA, Vol. 16, No. 5, Sep. 1988, pp. 427-449.

27 Herrera, R. and Landes, J. D., "Direct J-R Curve Analysis: A Guide to the Methodology," Fracture Mechanics: Twenty-first Symposium, ASTM STP 1074 J. P. Gudas, J. A, Joyce and E. M. Hackett, Eds., ASTM 1990, pp. 24-43.

28 Landes, J. D., Zhou, Z., Lee, K., and Herrera, R., "Normalization Method for Developing J-R Curves with the LMN function," Journal of Testing and Evaluation, JTEVA. Vol. 19 No. 4, July 1991, pp. 305-311.

29 Lee, K. and Landes, J. D., "Developing J-R Curves Without Displacement Measurement Using Normalization," Fracture Mechanics: Twenty-Third Symposium, ASTM STP 1189, Ravinder Chona, Eds., American Society for Testing and Materials, Philadelphia, 1993, pp. 133-167.

30 Ernst, M. A., Paris, P. C., Rossow, M. and Hutchinson, J. W., "Analysis of Load-Displacement Relationships to Determine J-R Curve and Tearing Instability Material Properties," Fracture Mechanics, ASTM STP 677, C. W. Smith, Ed., American Society for Testing and Materials, 1979, pp. 581-599.

31 Sharobeam, M. H. and Landes, J. D., "The Separation Criterion and Methodology in Ductile Fracture Mechanics," International Journal of Fracture, Vol. 47 1991, pp. 81-104.

32 Sharobeam, M. H. and Landes, J. D., "Development of Eta Factors in Elastic-Plastic Fracture Testing Using a Load Separation Technique," Elastic-Plastic Fracture Test Methods: The User's Experience (Second Volume), ASTM STP 1114, J. A. Joyce, Ed., ASTM 1991, pp. 114-132.

33 Sharobeam, M. H. and Landes, J. D., "The Load Separation and η_{pl} Development in Precracked Specimen Test Records", International Journal of Fracture, Vol. 59, 1993, pp. 213-226.

34 Rice, J. R., Paris, P. C. and Merkle, J. G., "Some Further Results of J-Integral Analysis and Estimates," Progress in Flaw Growth and Fracture Toughness Testing, ASTM STP 536, American Society for Testing and Materials, 1973, pp. 231-245.

35 Merkle, J. G. and Corten, H. T., "A J-Integral analysis for the Compact Specimen, Considering Axial Force as Well as Bending Effects," Journal of Pressure Vessel Technology, Transactions, American Society of Mechanical Engineers, 1974, pp. 286-292.

36 Orange, T. W., "Methods and Models for R-Curve Instability Calculations," Fracture Mechanics: Twenty-First Symposium, ASTM STP 1074, J. P. Gudas, J. A. Joyce, and E. M. Hackett Eds., ASTM 1990, pp. 42-56.

37 Zhou, Z., "Development and Application of an Advanced Ductile Fracture Mechanics Methodology," Ph.D. Dissertation, University of Tennessee, Knoxville, April, 1992.

38 McCabe, D. E. and Newman, J. C., "Data Development for ASTM E24.06.02 Round Robin Program on Instability Prediction," Final Report.

39 Joyce, J. A., Davis, D. A., Hackett, R. A. and Hayes, R. A., "Application of the J-Integral and the Modified J-Integral to Cases of Large Crack Extensions," NUREG CR-5143, Feb. 1989.

40 Landes, J. D., McCabe, D. E. and Ernst, H. A., "Fracture Testing of Ductile Steels," Electric Power Research Institute, MP-5014, Final Report of Research Project 1238-2, Jan. 1987. And Landes, J. D., McCabe, D. E. and Ernst, H. A., "Elastic-Plastic Methodology to Establish R-Curves and Instability Criteria," Electric Power Research Institute, RP-1238-2, Final Report, March 1983.

41 Van Der Sluys, Private Communications.

42 Link, R. E., Private Communications.

43 Westinghouse Private Communications.

44 Landes, J. D. and McCabe, D. E., "Toughness of Austenitic Stainless Steel Pipe Welds," Electric Power Research Institute, NP-4768, Topical Report on Research Project 1238-2, Oct. 1986.

45 Huang, D. D., "A Comparison of Multispecimen J-Integral Methods as Applied to Toughened Polymers," in Advances in Fracture Research, Vol. 4, Seventh International Conference on Fracture, University of Houston, 1989, pp. 2725-2732.

46 E 561-86, "Standard Practice for R-Curve Determination," American Society for Testing and Materials, Philadelphia, 1988.

47 E 1221-88, "Standard Test Method for Determining Plane-Strain Crack-Arrest Fracture Toughness, K_{Ia}, of Ferritic Steels," American Society for Testing and Materials, Philadelphia, 1988.

48 Hudak, S. J. and Saxena, A., "Review and Extension of Compliance Information for Common Crack Growth Specimens," International Journal of Fracture, Vol. 14, No. 5, October 1978, pp. 453-468.

49 Kumar, V., German, M. D. and Shih, C. F., "An Engineering Approach for Elastic-Plastic Fracture Analysis," Electric Power Research Institute NP 1983, Topical Report, July 1991.

50 Ireland, D. R., "Procedures and Problems Associated with Reliable Control of the Instrumented Impact Test," Instrumented Impact Testing, ASTM STP 563, American Society for Testing and Materials, 1974, pp. 3-29.

APPENDIX

APPENDIX A

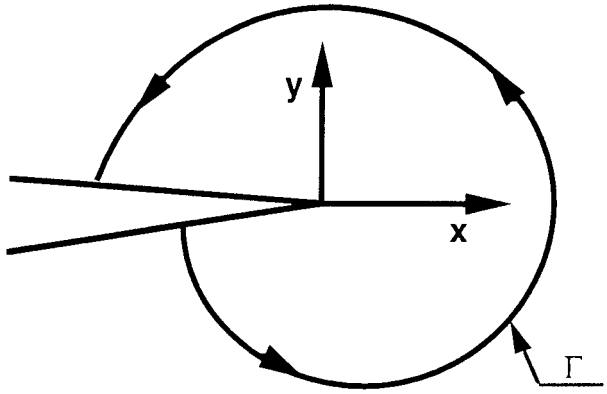

Fig. 1.1 Arbitrary J-Integral Contour around the Crack Tip

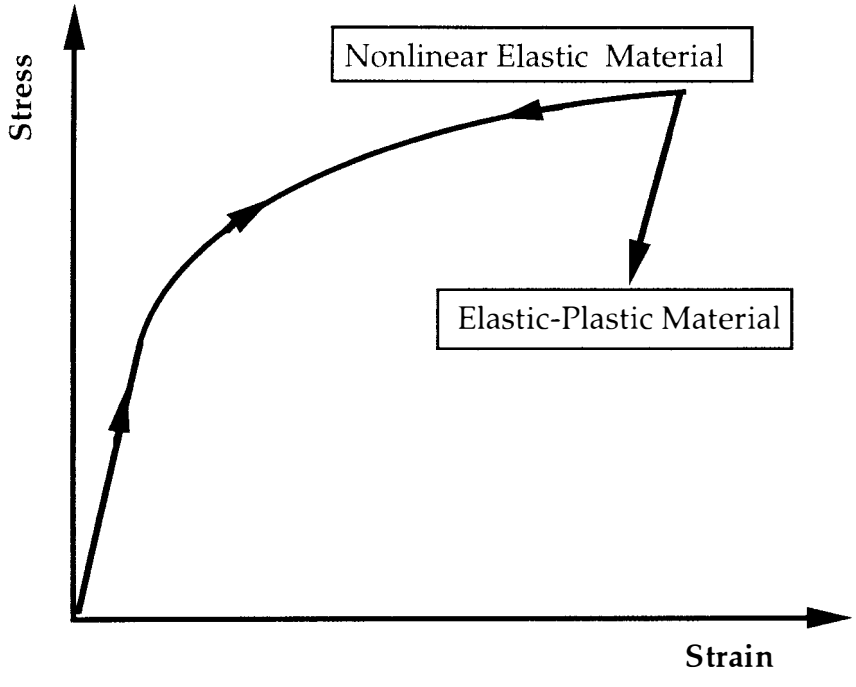

Fig. 1.2 Schematic Comparison of the Stress-Strain Behaviors of Elastic-Plastic and Nolinear Elastic Materials

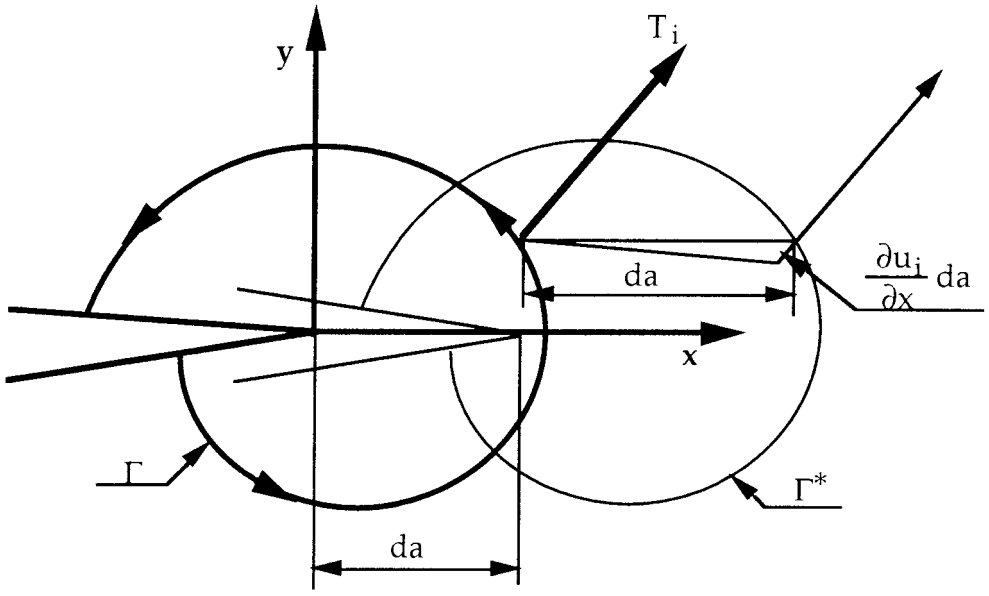

Fig. 1.3 Schematic of J-Integral Countor Around Crack Tip with Crack Extension Showing Physical Meaning of J-Integral

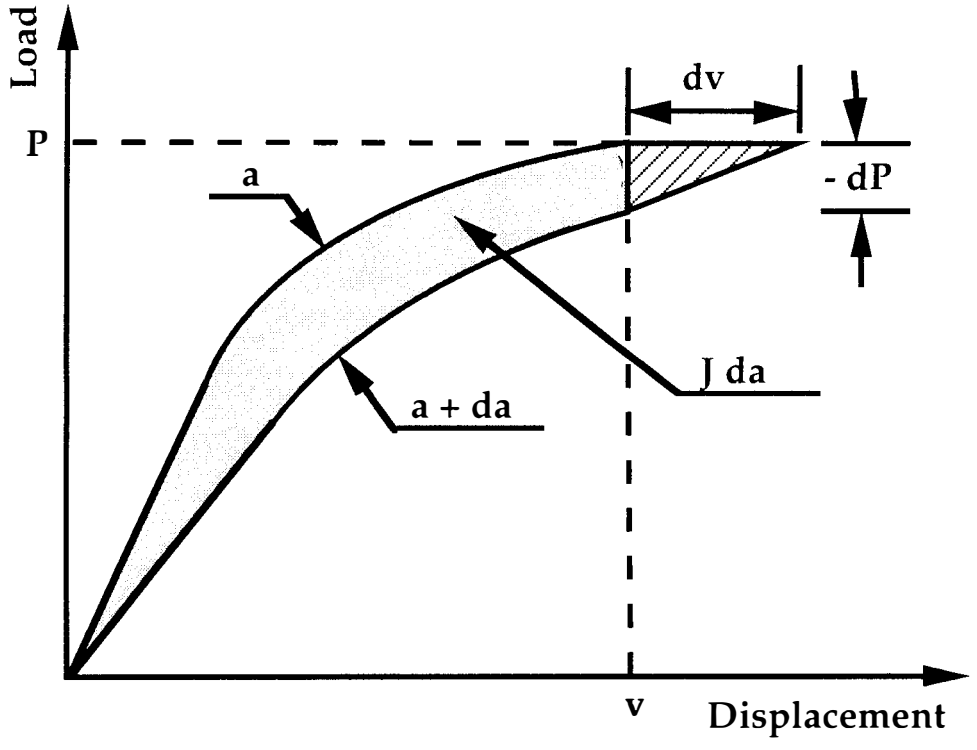

Fig 1.4 Schematic of Graphical Measurement of J

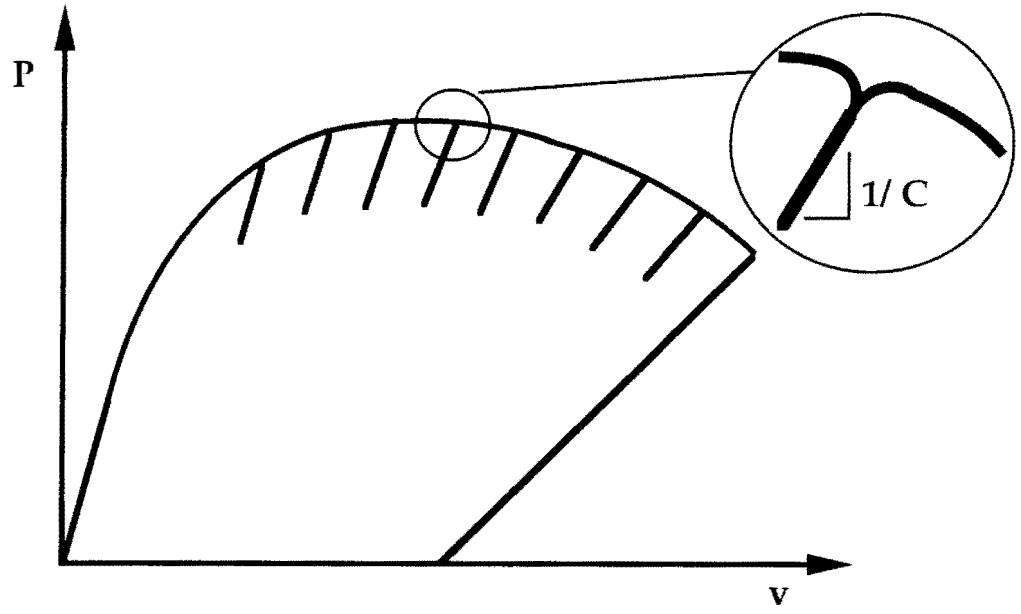

Fig. 1.5 The Elastic Unloading-Reloading Compliance Method for Mornitoring Crack Growth

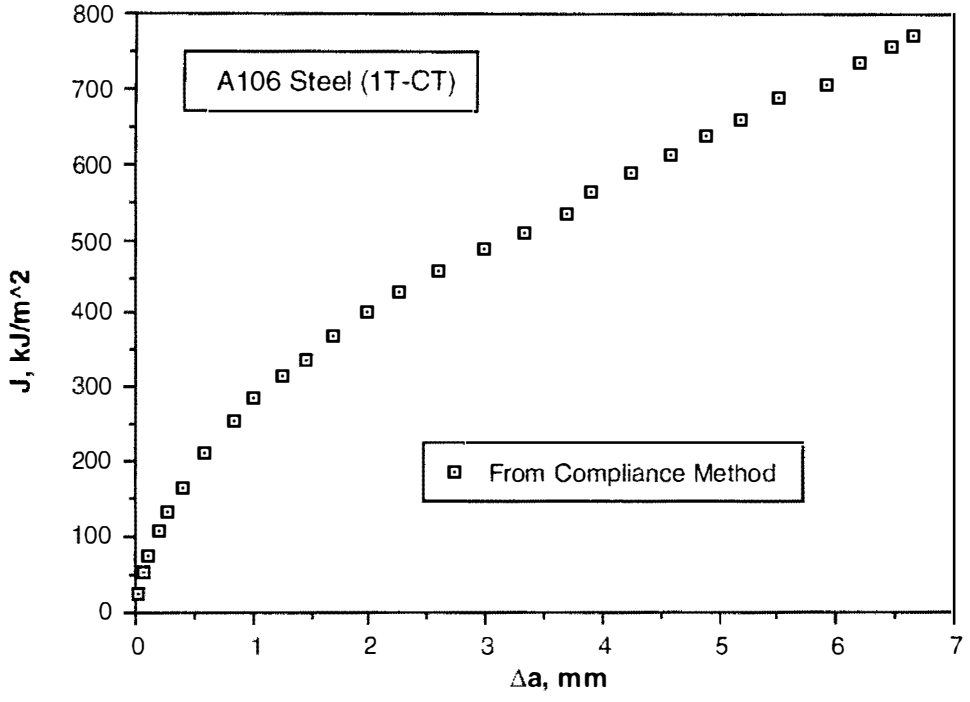

Fig. 1.6 A Typical J-R Curve from Compliance Method

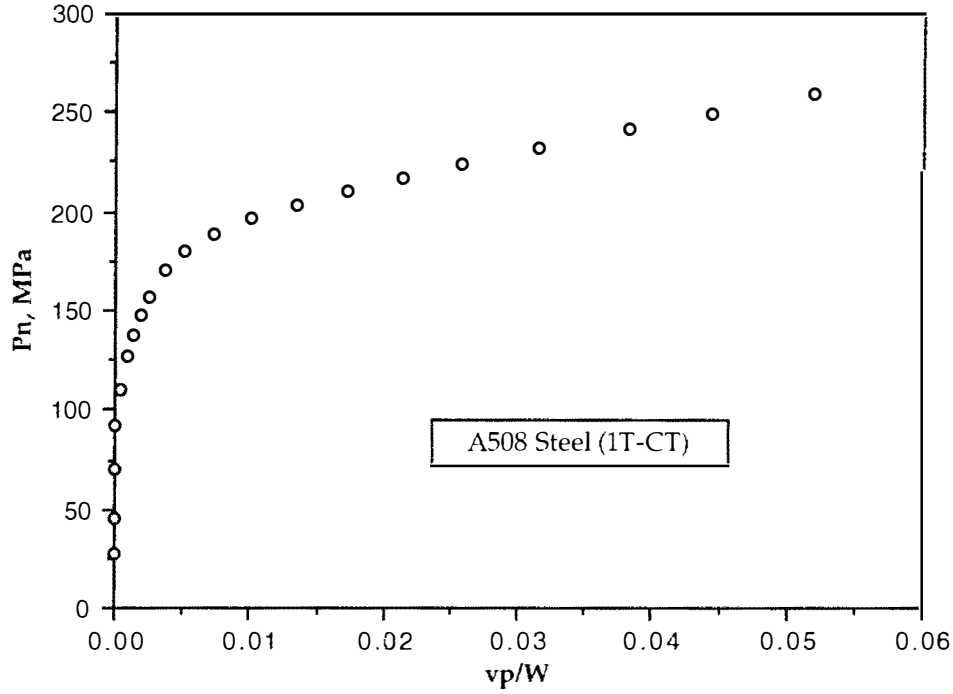

Fig. 2.1 - A Typical Normalized Load versus Plastic Displacement, A508 Steel, Compact Specimen

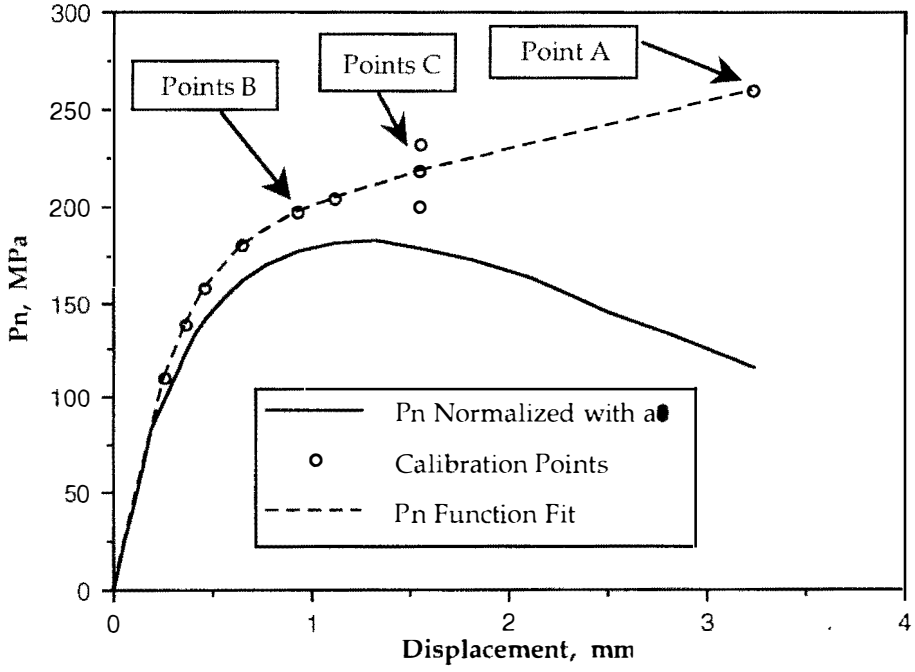

Fig. 2.2 - Normalized Load versus Displacement Showing All Calibration Points

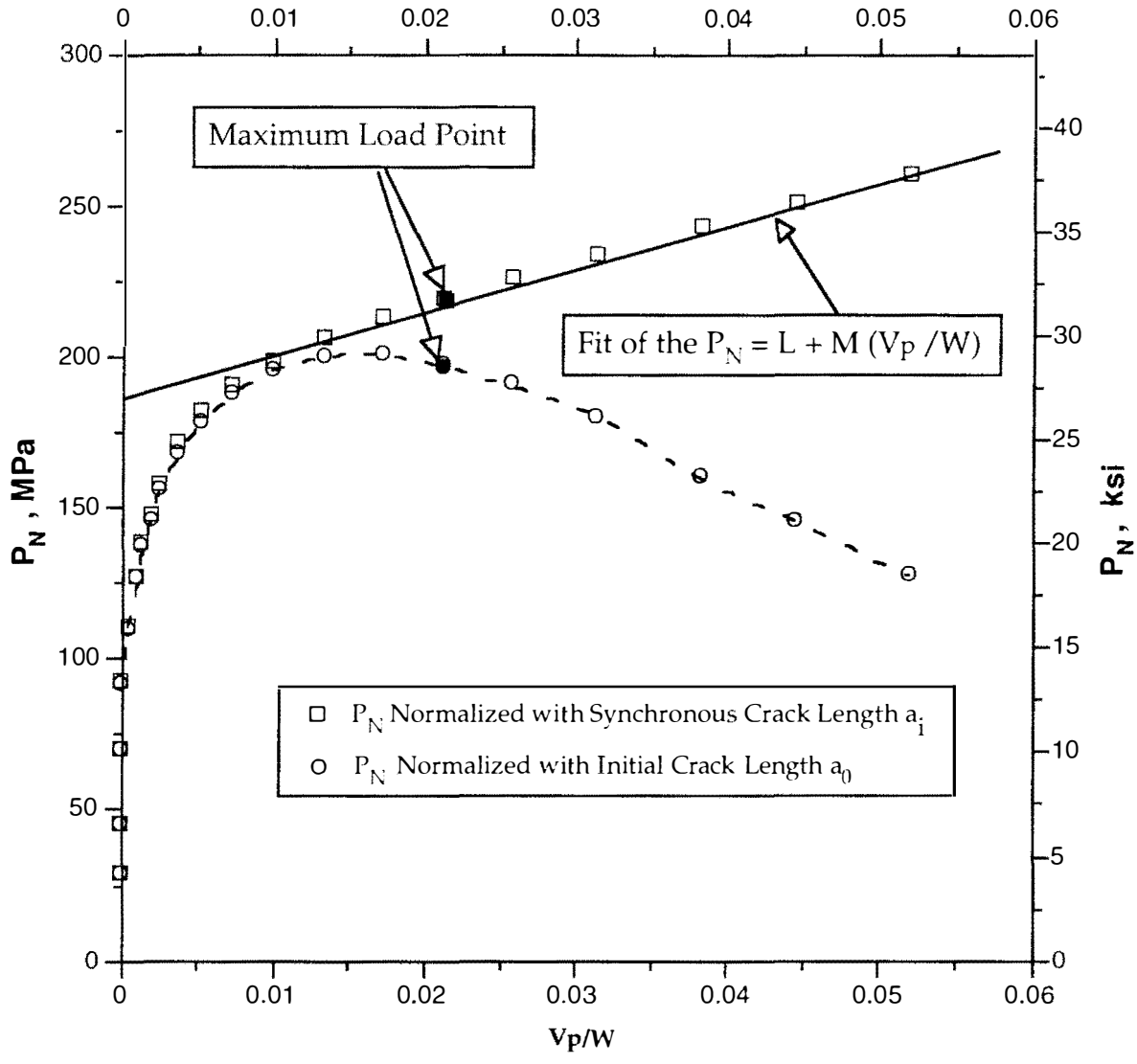

Fig 3.1 - Schematic of Maximum Load Point Normalized at a_0 Could Be Used to Determine Constant L

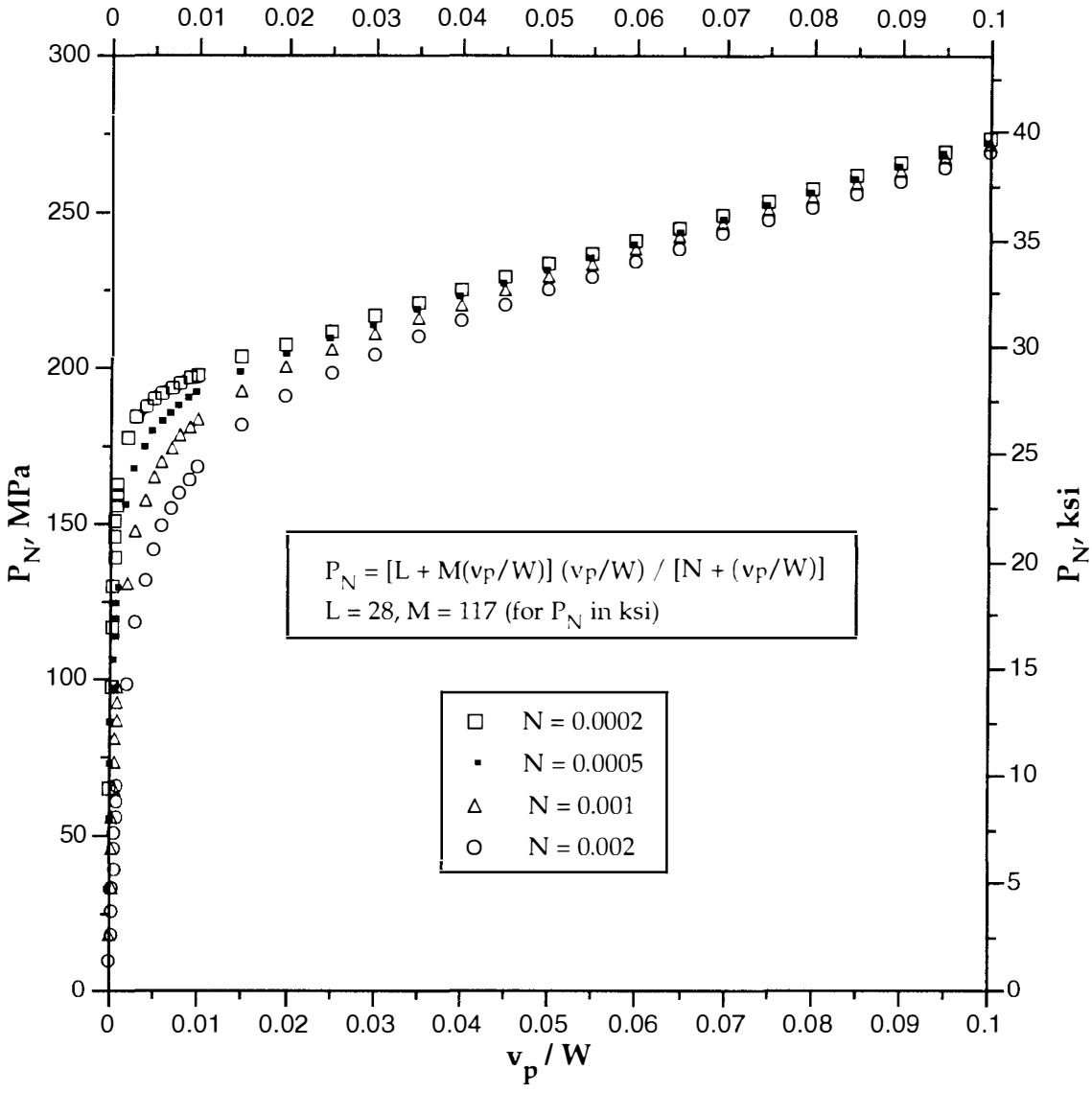

Fig 3.2 - Comparison of LMN Function at Different Values of Constant N when Constants L and M Are Held Constant

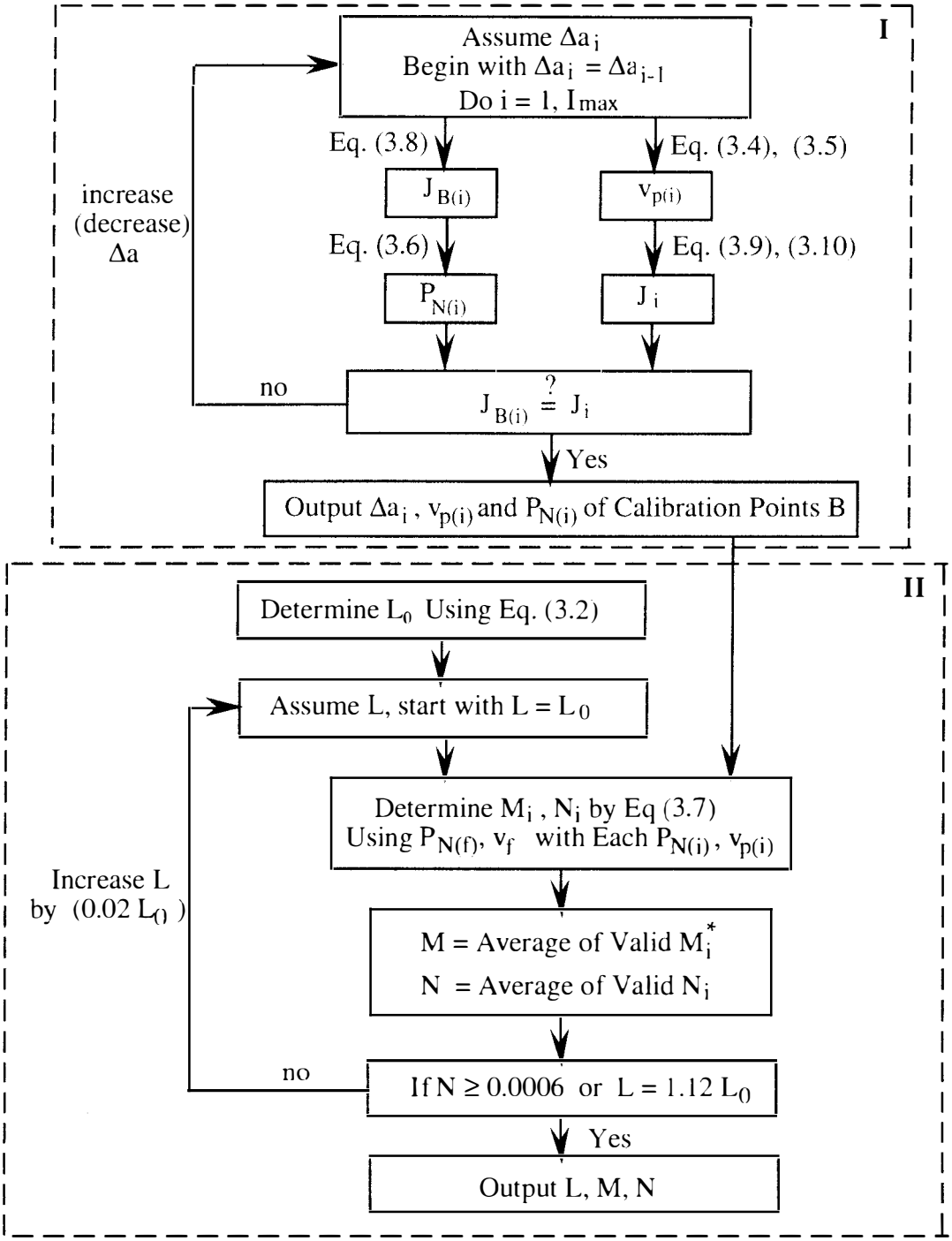

Note:

Part I: Calibration points B determination from blunting assumption.

Part II: Constants L, M, N dtermination.

* : M_i and N_i determined are valid when $N_i > 0$

Fig. 3.3 - A Flow Chart for LMN Function Determination from Maximum Load Point and Blunting Assumption

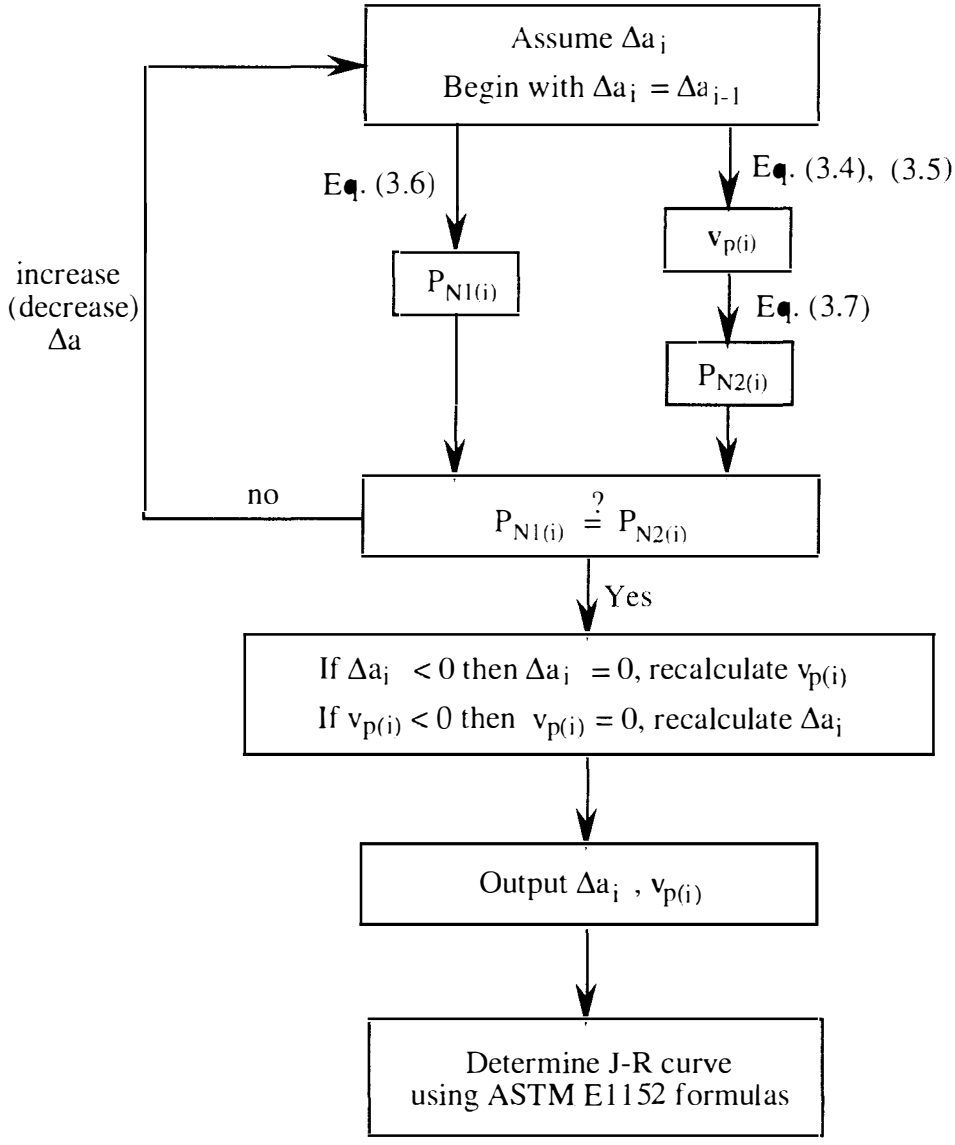

Fig. 3.4 - A Flow Chart for J-R Curve Determination by Predicting Crack Length Using Method of Normalization with LMN Function

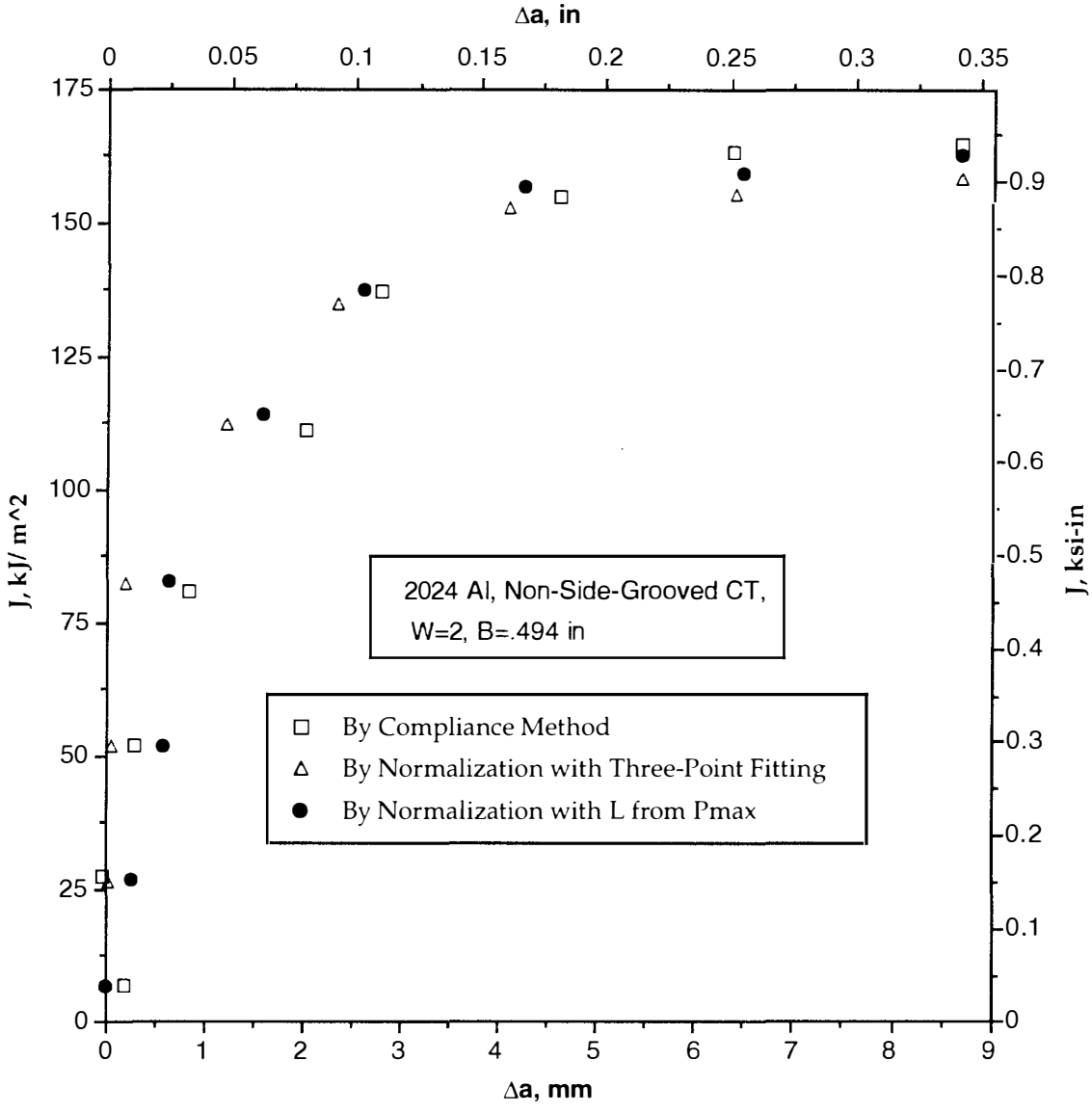

Fig. 3.5 - J-R Curve Developed by Method of Normalization Using L from P_{max} Compared with Results from Three-Point Fitting and Compliance Method, 2024 Aluminum, Compact Specimen without Side-Grooving

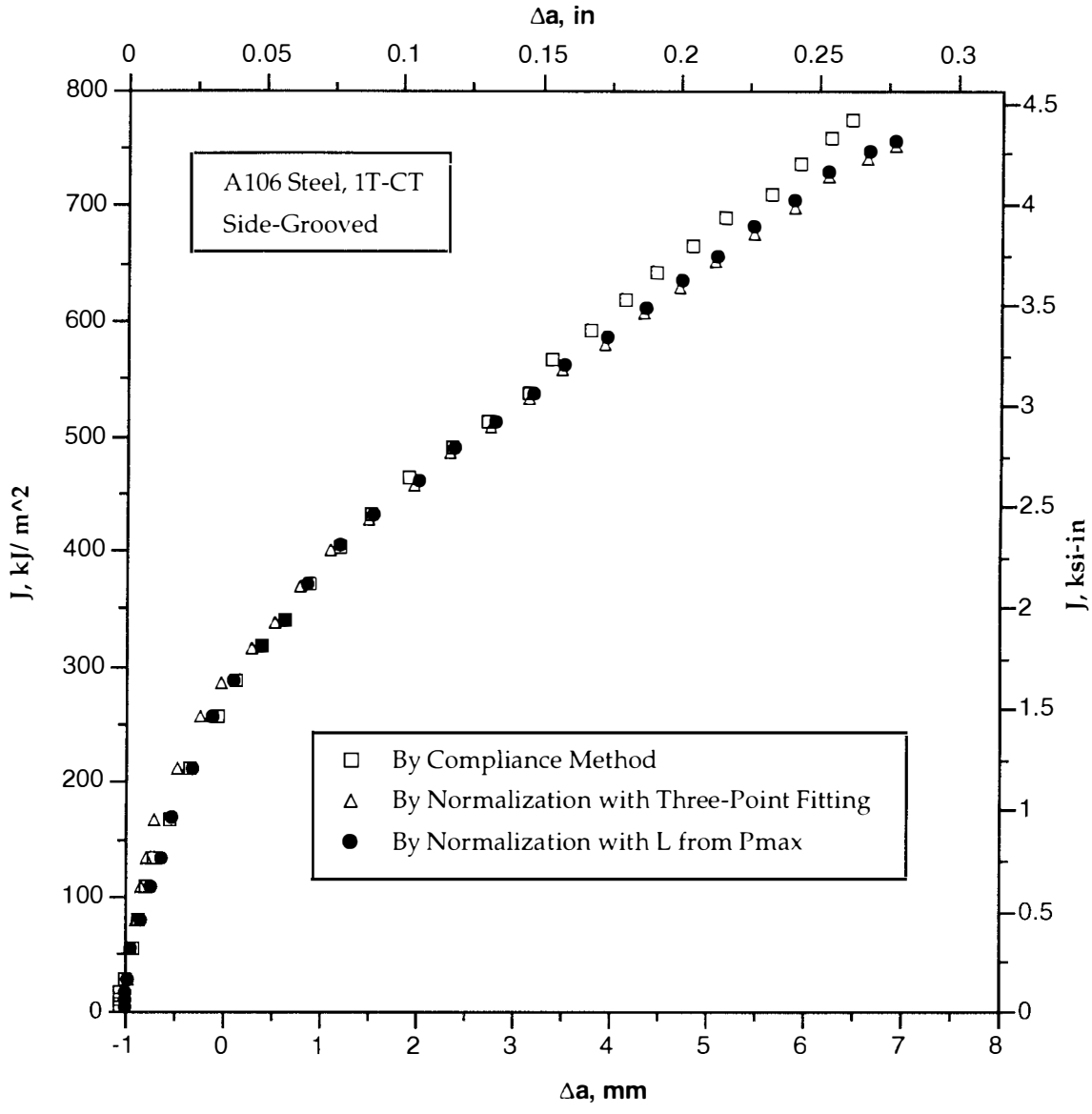

Fig. 3.6 - J-R Curve Developed by Method of Normalization Using L from P_{max} Compared with Results from Three-Point Fitting and Compliance Method, A106 Steel, Compact Specimen with Side-Grooving

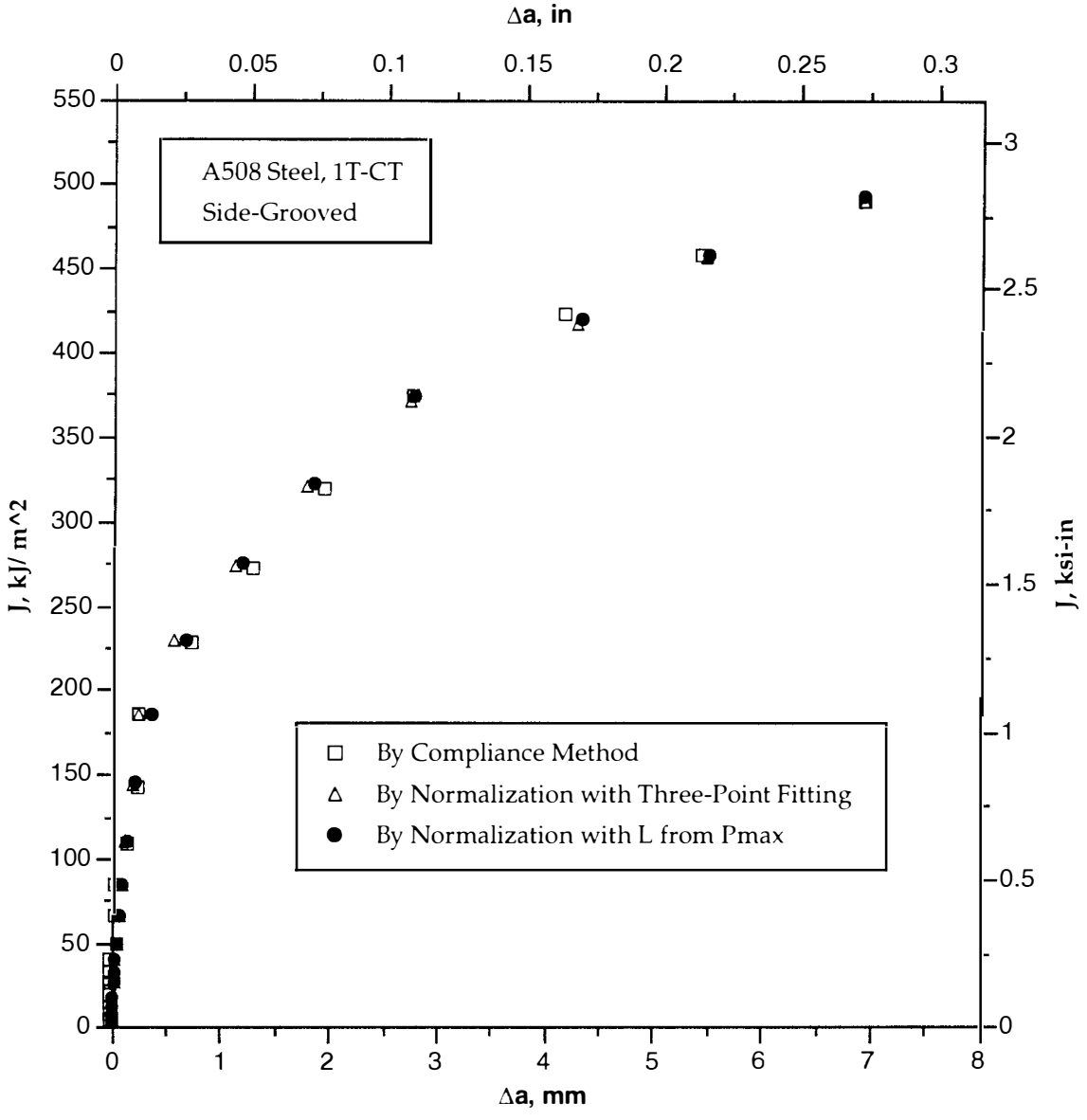

Fig. 3.7 - J-R Curve Developed by Method of Normalization Using L from P_{max} Compared with Results from Three-Point Fitting and Compliance Method, A508 Steel, Compact Specimen with Side-Grooving

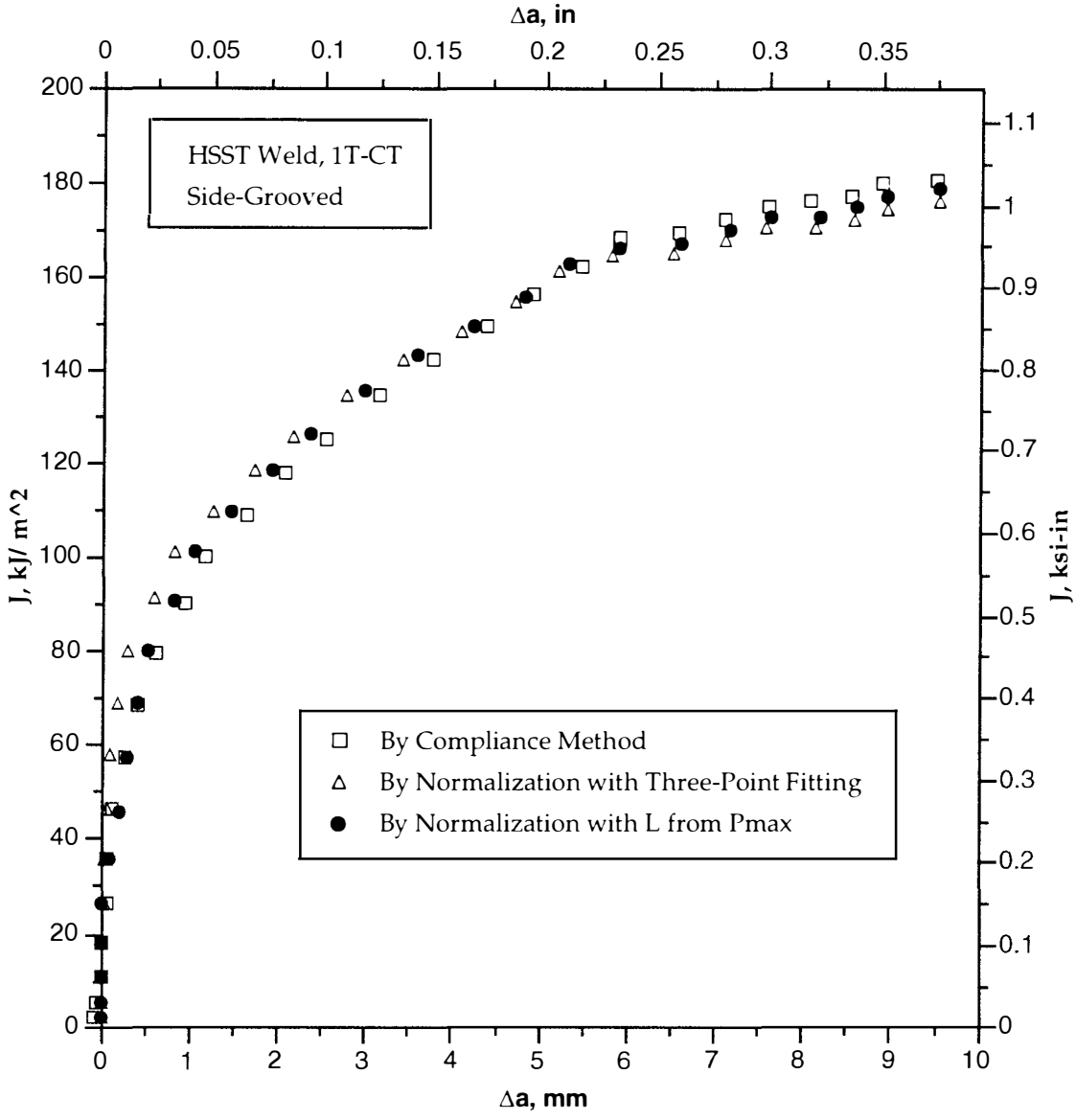

Fig. 3.8 - J-R Curve Developed by Method of Normalization Using L from P_{max} Compared with Results from Three-Point Fitting and Compliance Method, HSST Weld Material, Compact Specimen with Side-Grooving

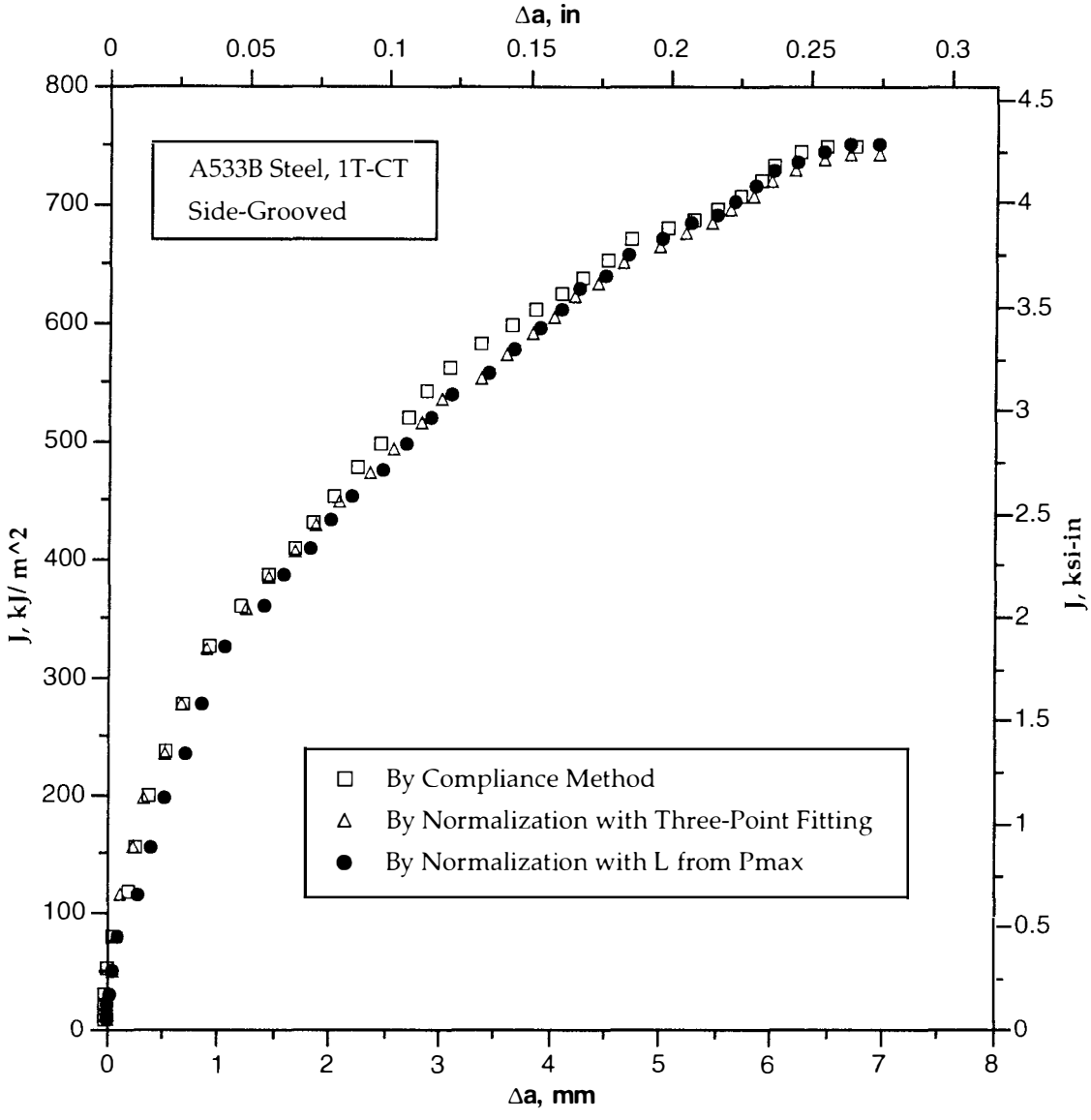

Fig. 3.9 - J-R Curve Developed by Method of Normalization Using L from P_{max} Compared with Results from Three-Point Fitting and Compliance Method, A533B Steel, Compact Specimen with Side-Grooving

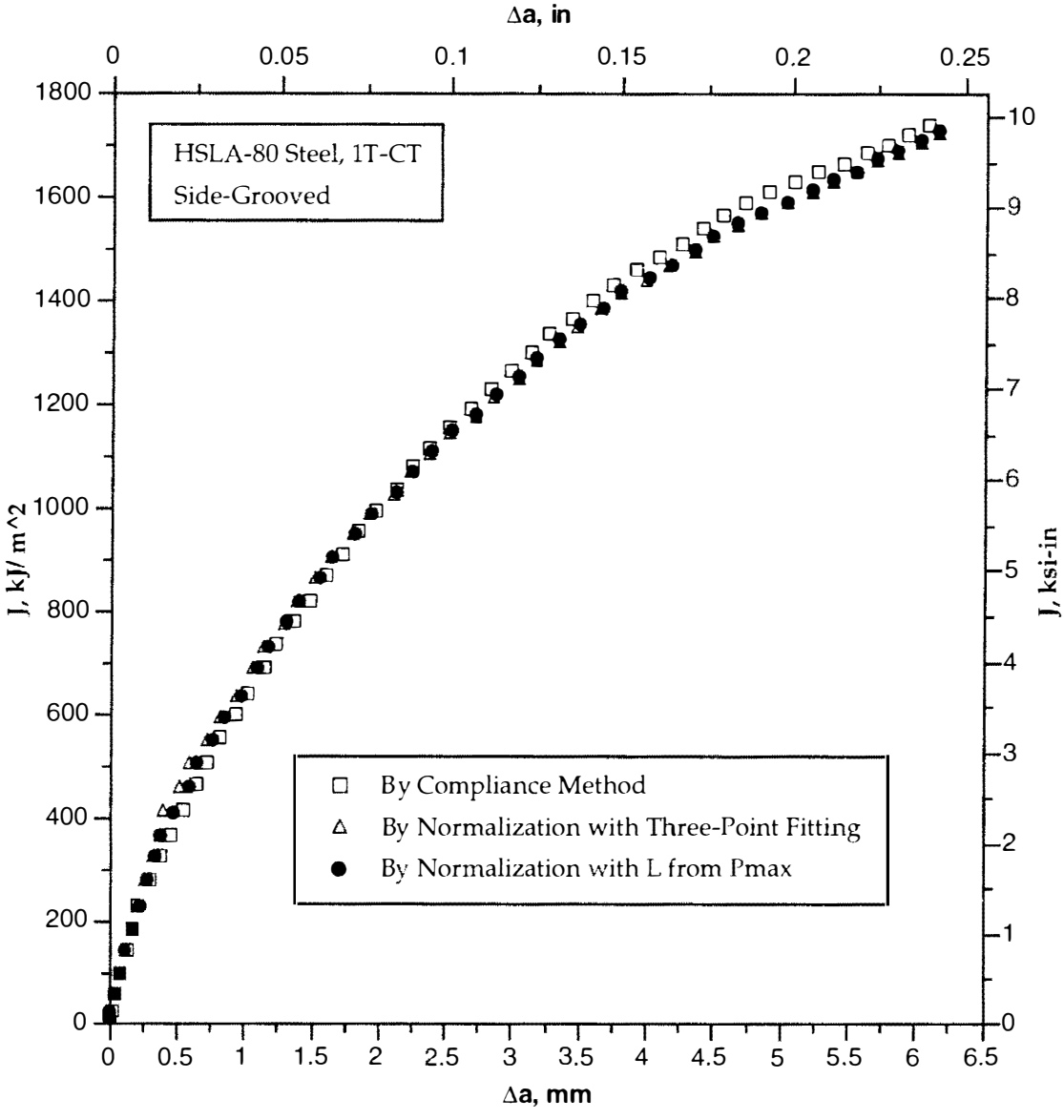

Fig. 3.10- J-R Curve Developed by Method of Normalization Using L from Pmax Compared with Results from Three-Point Fitting and Compliance Method, HSLA-80 Steel, Compact Specimen with Side-Grooving

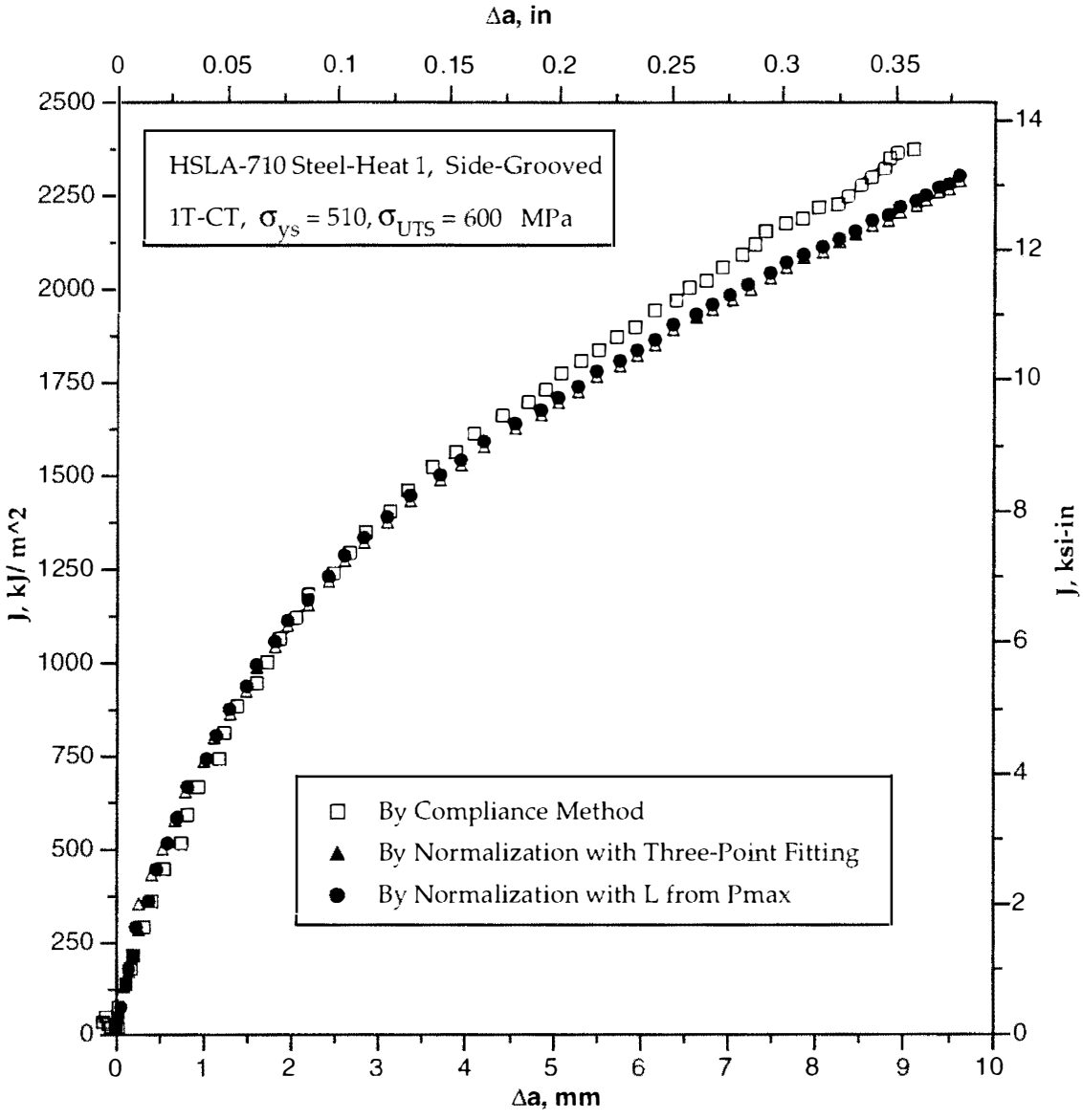

Fig. 3.11- J-R Curve Developed by Method of Normalization Using L from P_{max} Compared with Results from Three-Point Fitting and Compliance Method, HSLA-710 Steel-Heat 1, Side-Grooved Compact Specimen

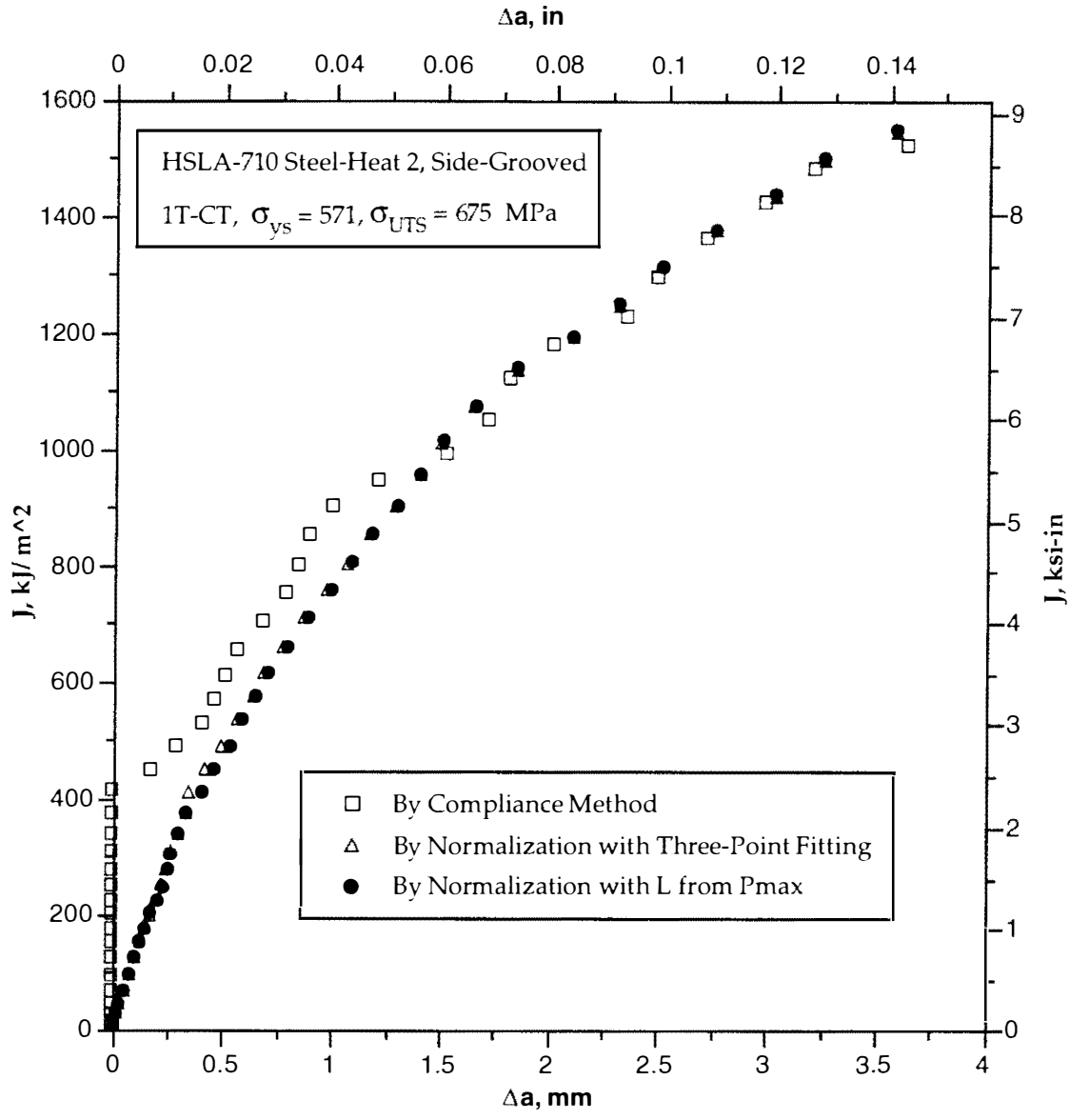

Fig. 3.12- J-R Curve Developed by Method of Normalization Using L from Pmax Compared with Results from Three-Point Fitting and Compliance Method, HSLA-710 Steel-Heat 2, Side-Grooved Compact Specimen

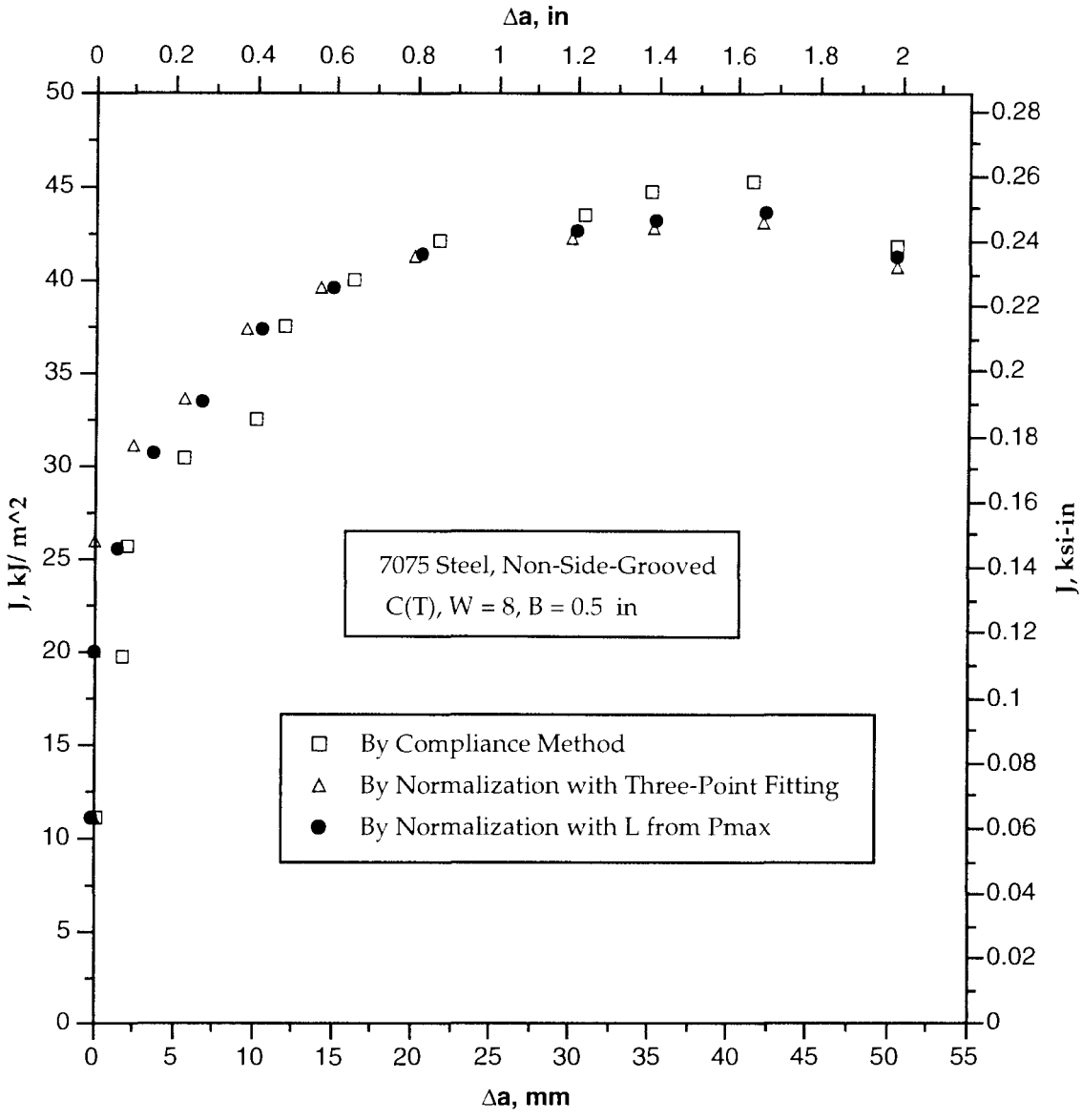

Fig. 3.13 - J-R Curve Developed by Method of Normalization Using L from P_{max} Compared with Results from Three-Point Fitting and Compliance Method, 7075 Steel, Compact Specimen without Side-Grooving

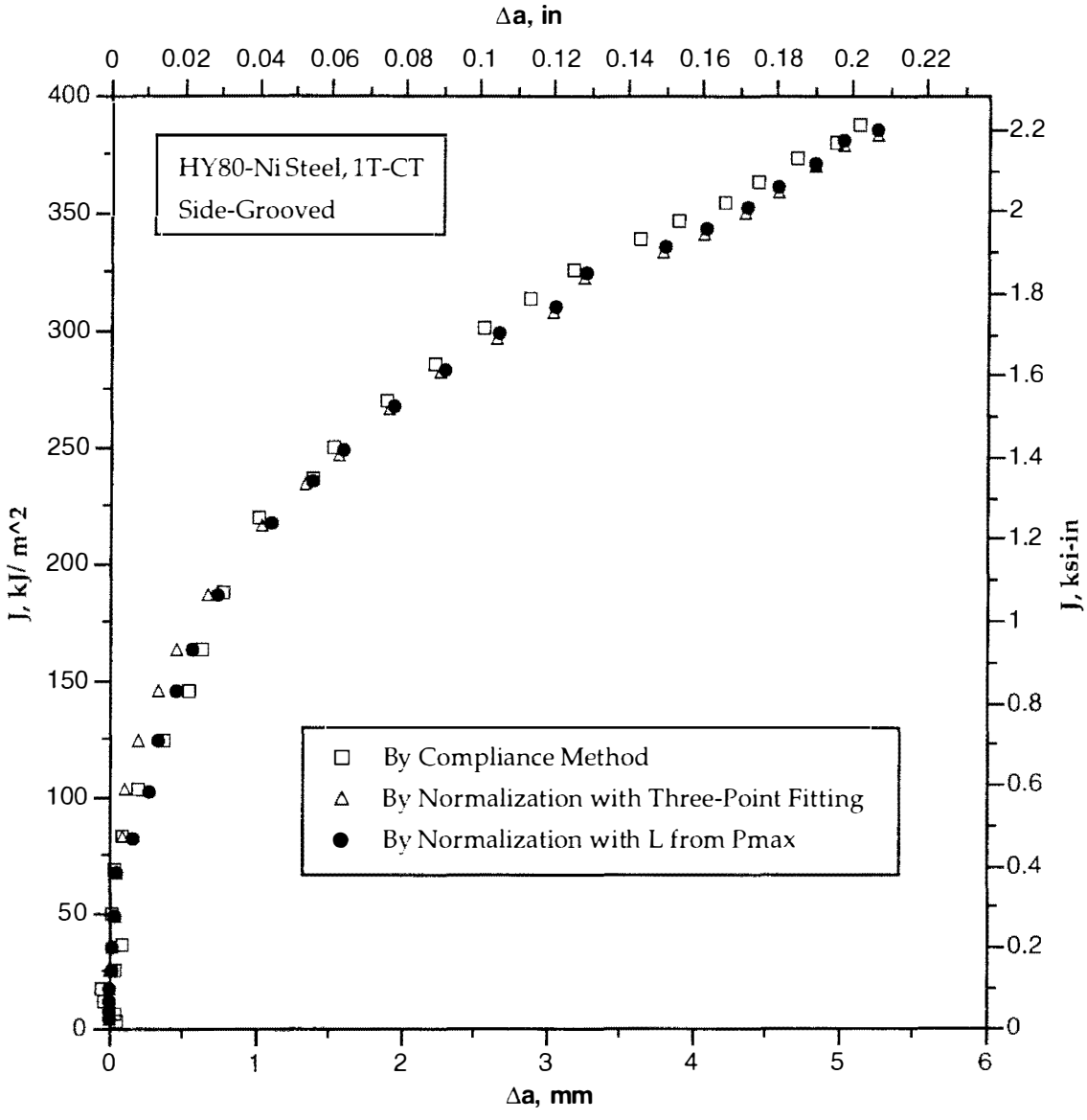

Fig. 3.14 - J-R Curve Developed by Method of Normalization Using L from P_{max} Compared with Results from Three-Point Fitting and Compliance Method, HY80-Ni Steel, Compact Specimen with Side-Grooving

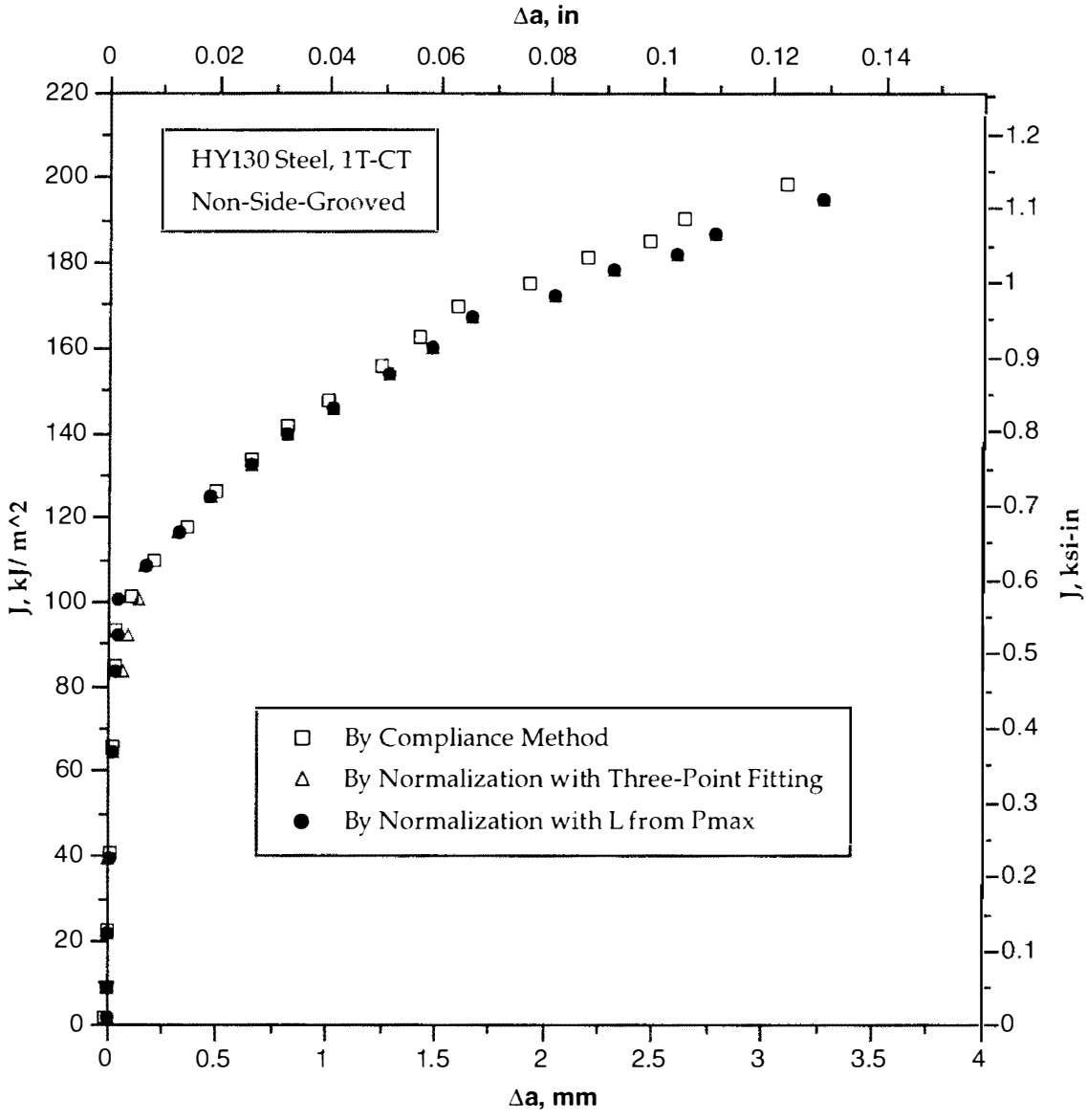

Fig. 3.15- J-R Curve Developed by Method of Normalization Using L from Pmax Compared with Results from Three-Point Fitting and Compliance Method, HY130 Steel, Compact Specimen without Side-Grooving

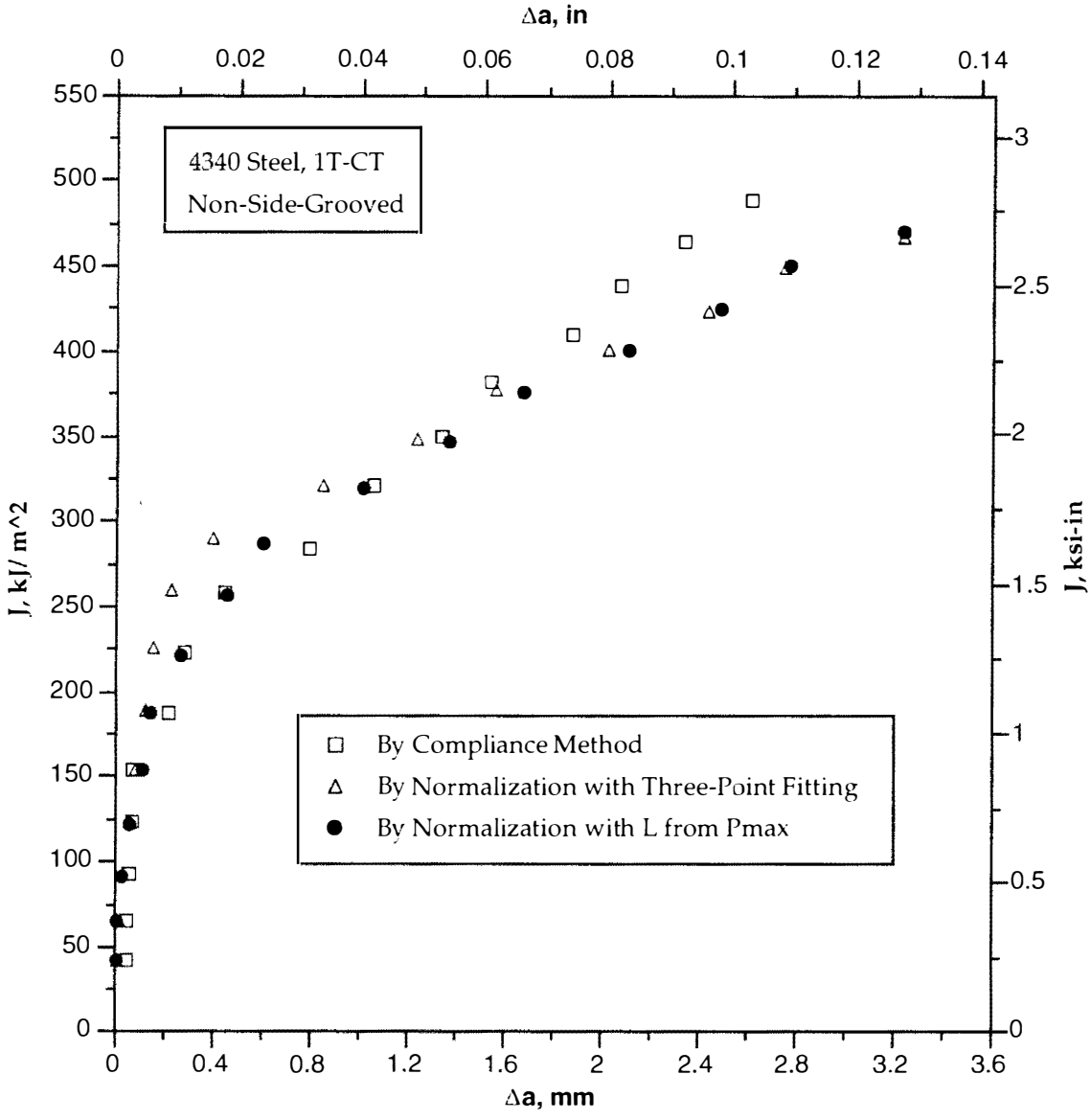

Fig. 3.16- J-R Curve Developed by Method of Normalization Using L from P_{max} Compared with Results from Three-Point Fitting and Compliance Method, 4340 Steel, Compact Specimen without Side-Grooving

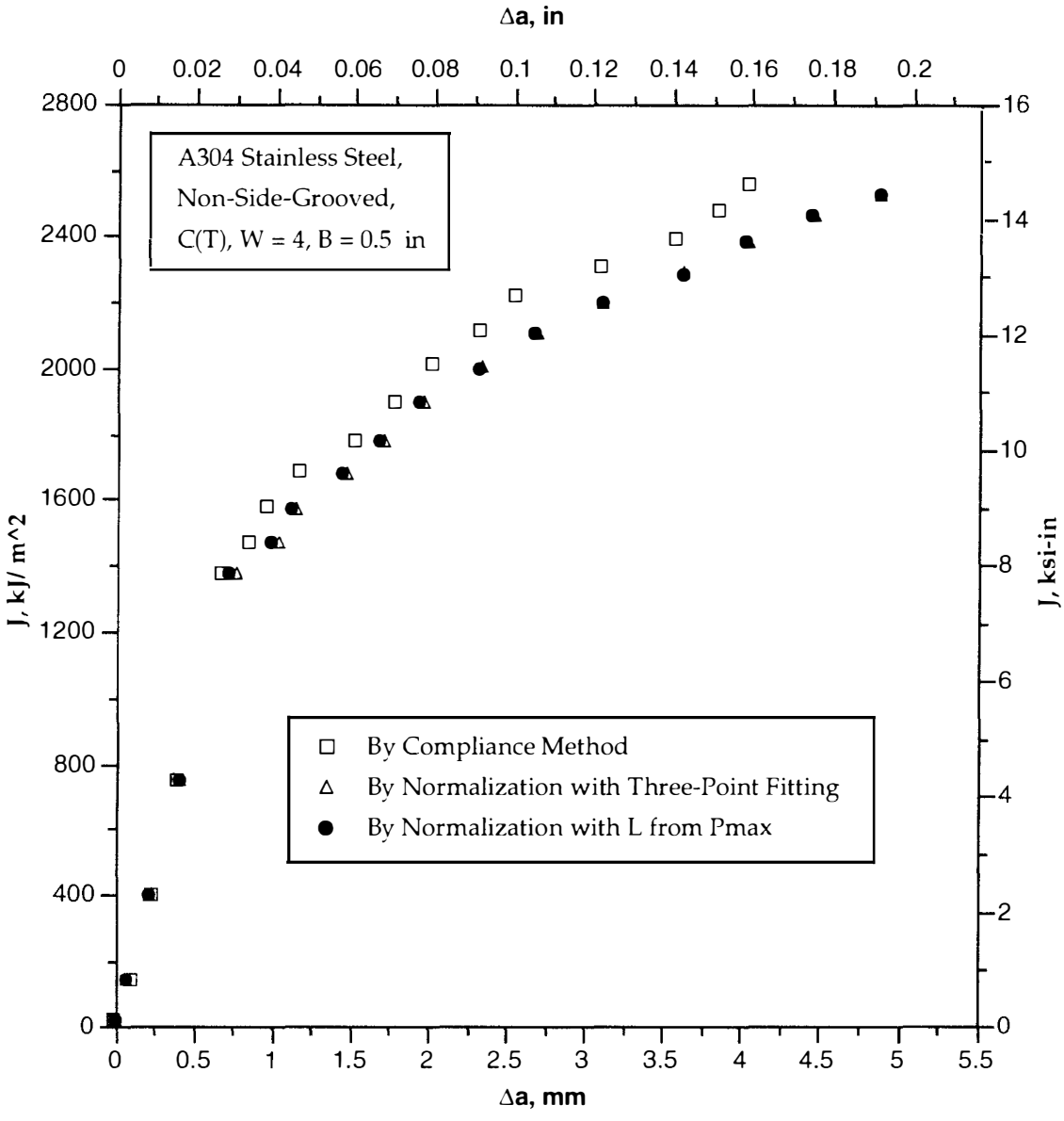

Fig. 3.17 - J-R Curve Developed by Method of Normalization Using L from Pmax Compared with Results from Three-Point Fitting and Compliance Method, A304 Stainless Steel, Compact Specimen without Side-Grooving

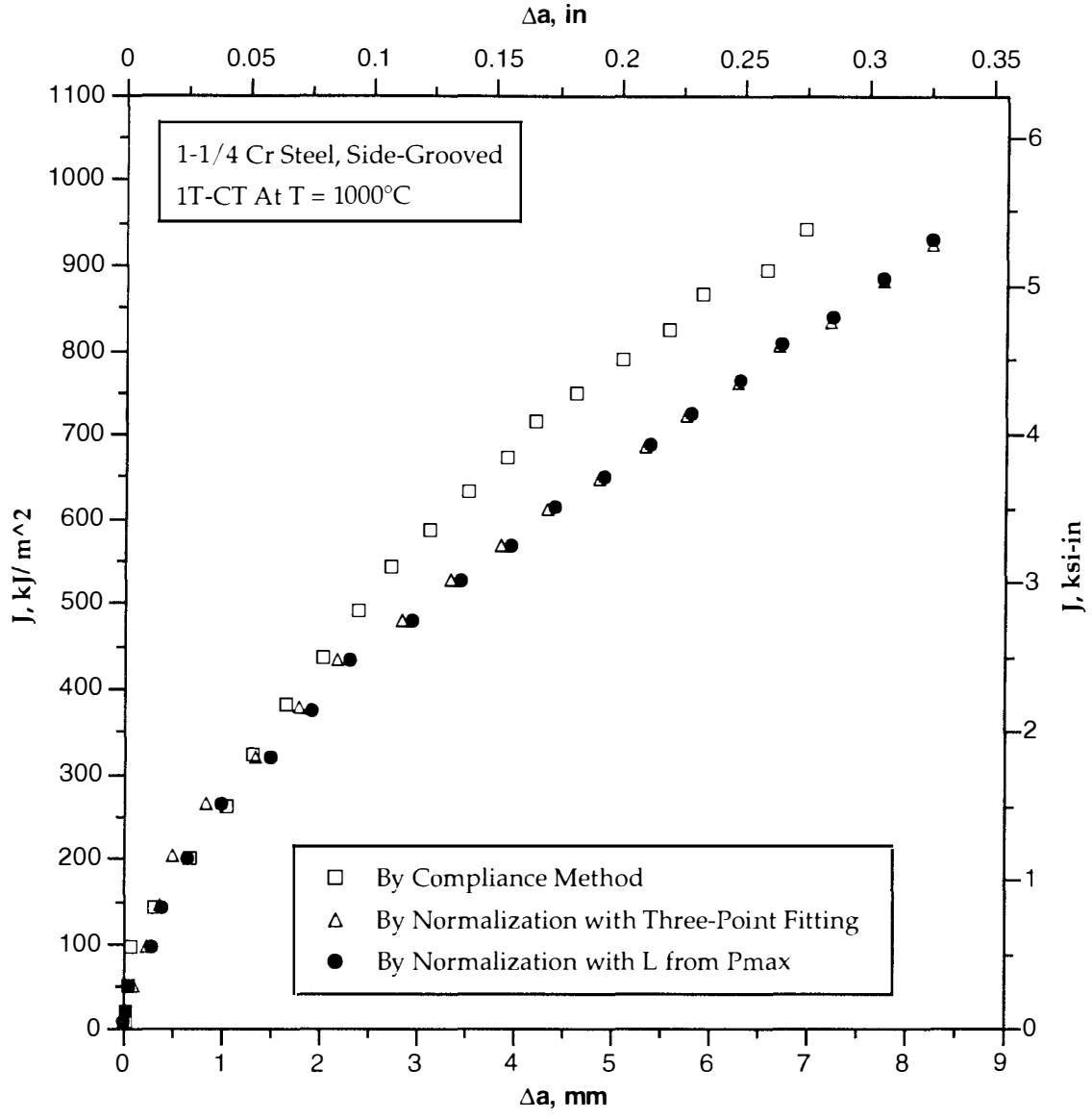

Fig. 3.18 - J-R Curve Developed by Method of Normalization Using L from P_{max} Compared with Results from Three-Point Fitting and Compliance Method, 1-1/4 Cr Steel at Temperature of 1000 °C, Compact Specimen with Side-Grooving

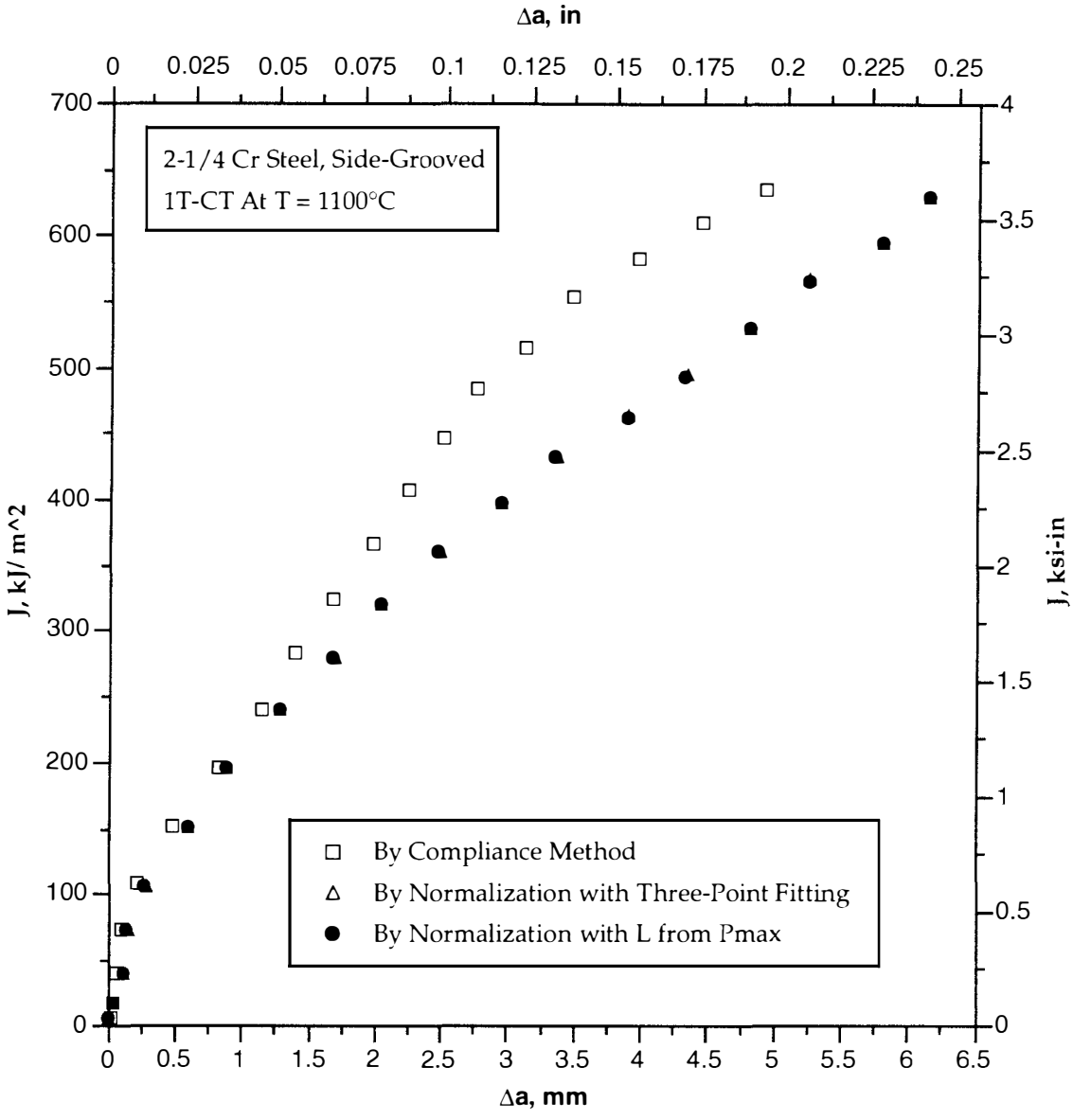

Fig. 3.19 - J-R Curve Developed by Method of Normalization Using L from Pmax Compared with Results from Three-Point Fitting and Compliance Method, 2-1/4 Cr Steel at Temperature of 1100 °C, Compact Specimen with Side-Grooving

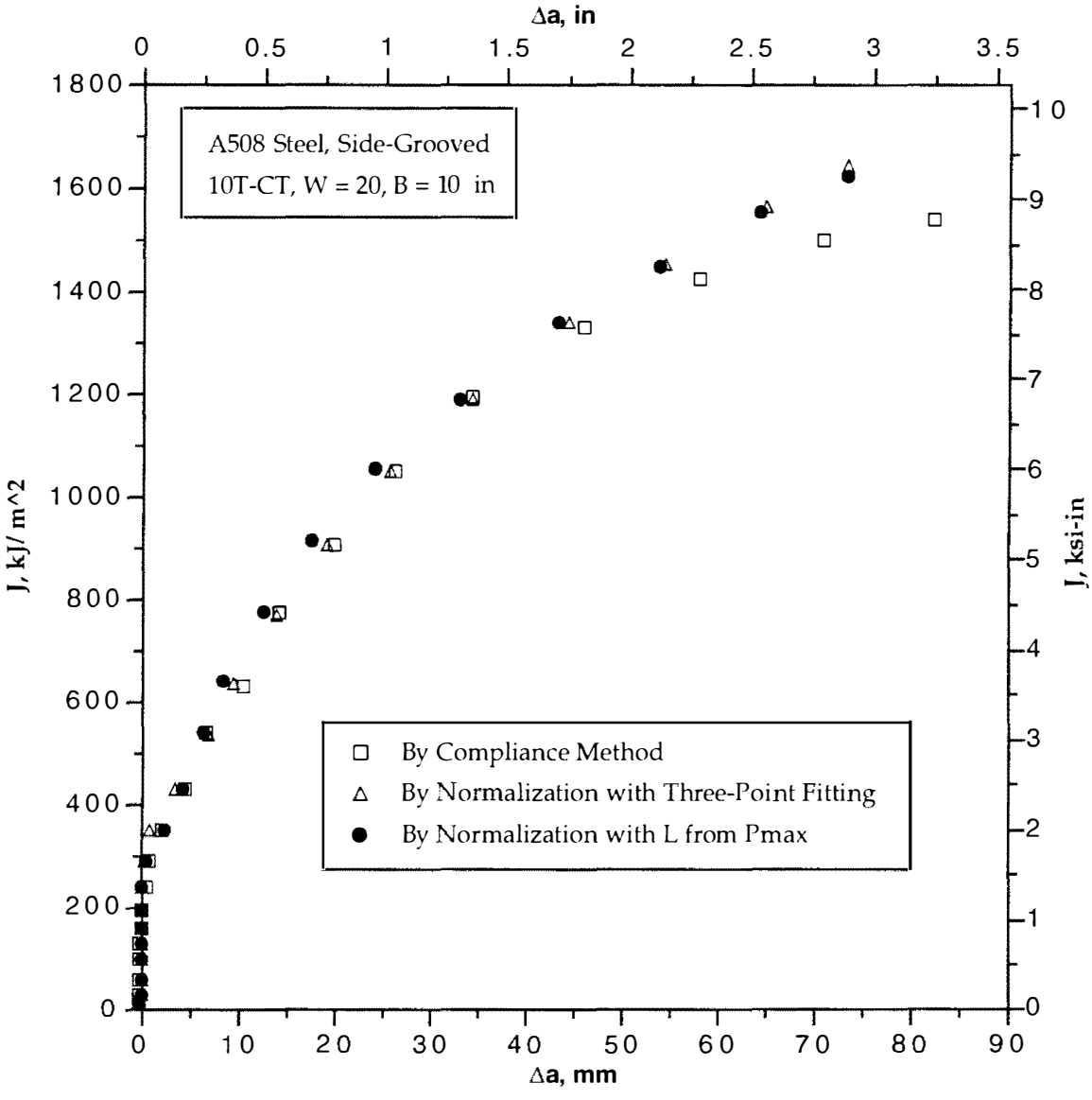

Fig. 3.20 - J-R Curve Developed by Method of Normalization Using L from Pmax Compared with Results from Three-Point Fitting and Compliance Method, A508 Steel, Side-Grooved Compact Specimen of W = 20, B = 10 in

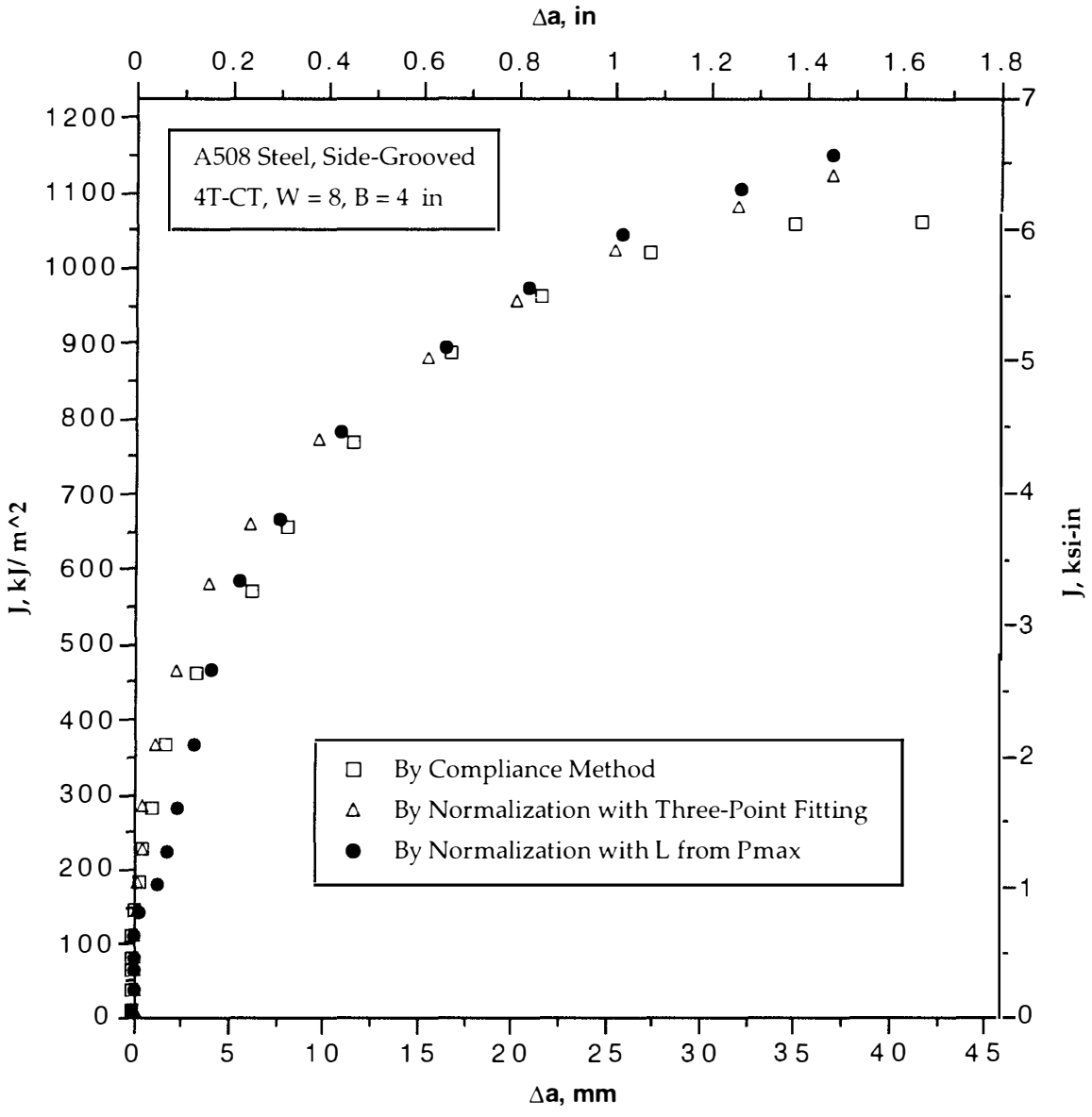

Fig. 3.21 - J-R Curve Developed by Method of Normalization Using L from P_{max} Compared with Results from Three-Point Fitting and Compliance Method, A508 Steel, Side-Grooved Compact Specimen of W = 8, B = 4 in

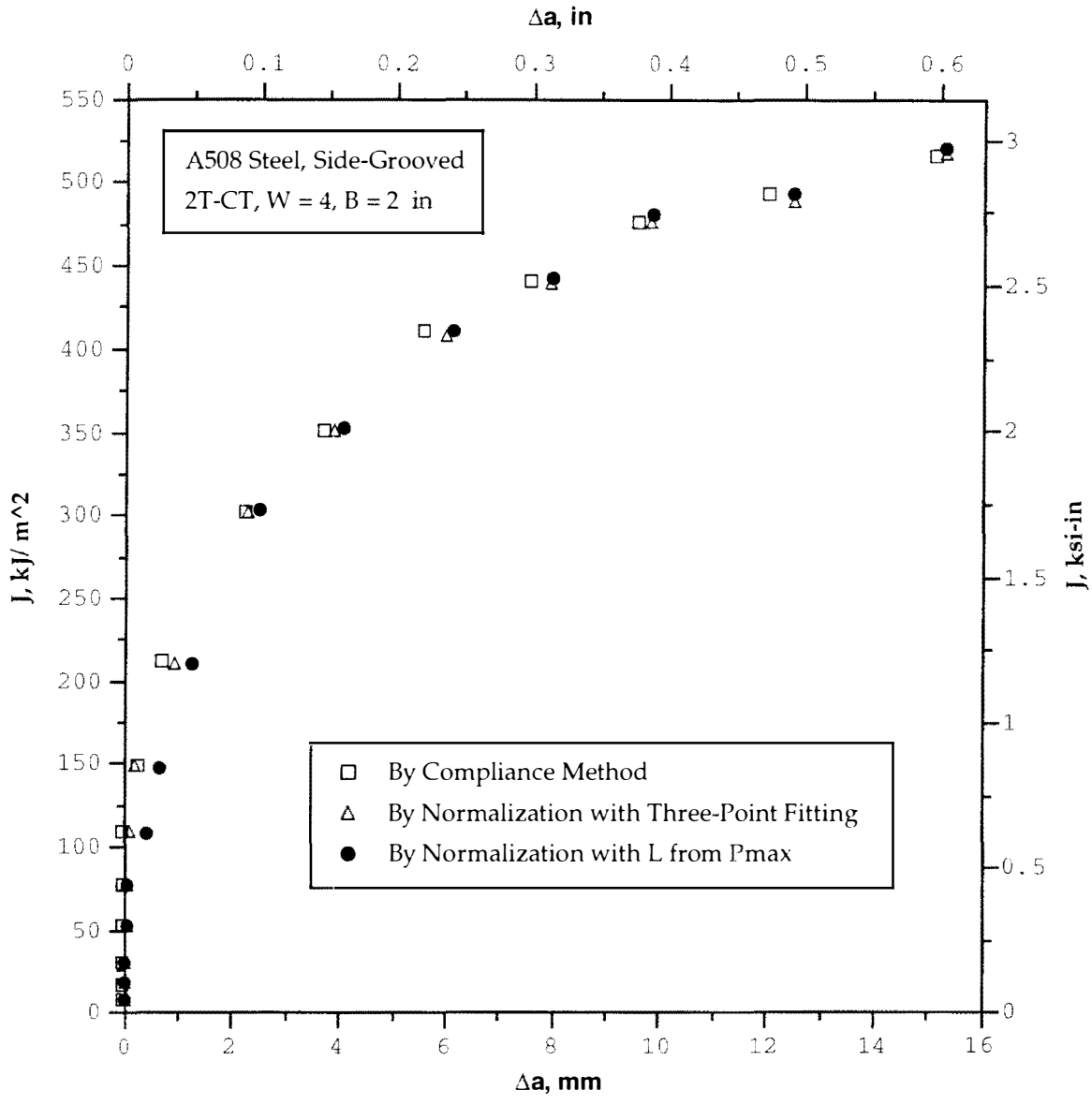

Fig. 3.22 - J-R Curve Developed by Method of Normalization Using L from Pmax Compared with Results from Three-Point Fitting and Compliance Method, A508 Steel, Side-Grooved Compact Specimen of W = 4, B = 2 in

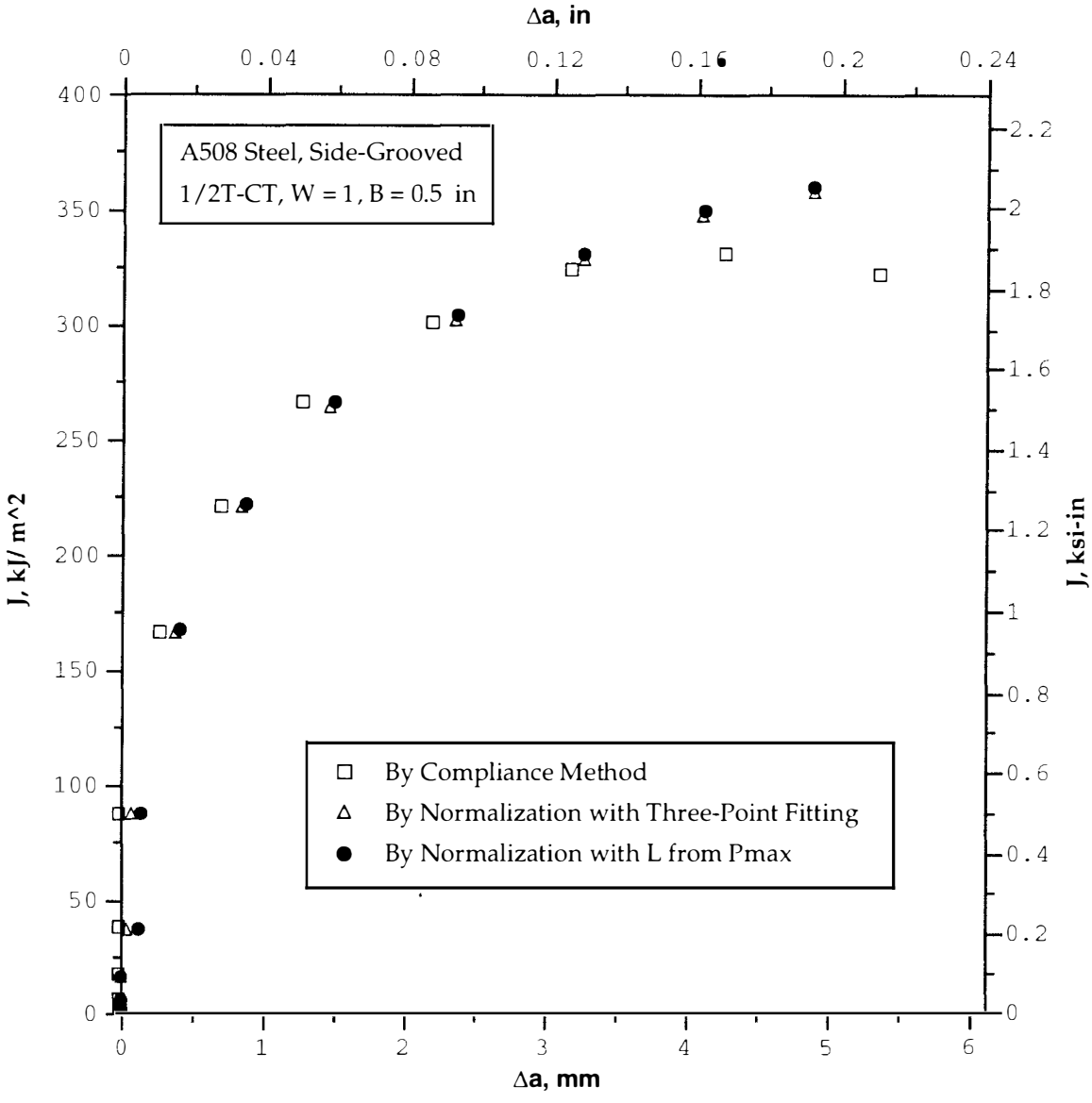

Fig. 3.23 - J-R Curve Developed by Method of Normalization Using L from Pmax Compared with Results from Three-Point Fitting and Compliance Method, A508 Steel, Side-Grooved Compact Specimen of W = 1, B = 0.5 in

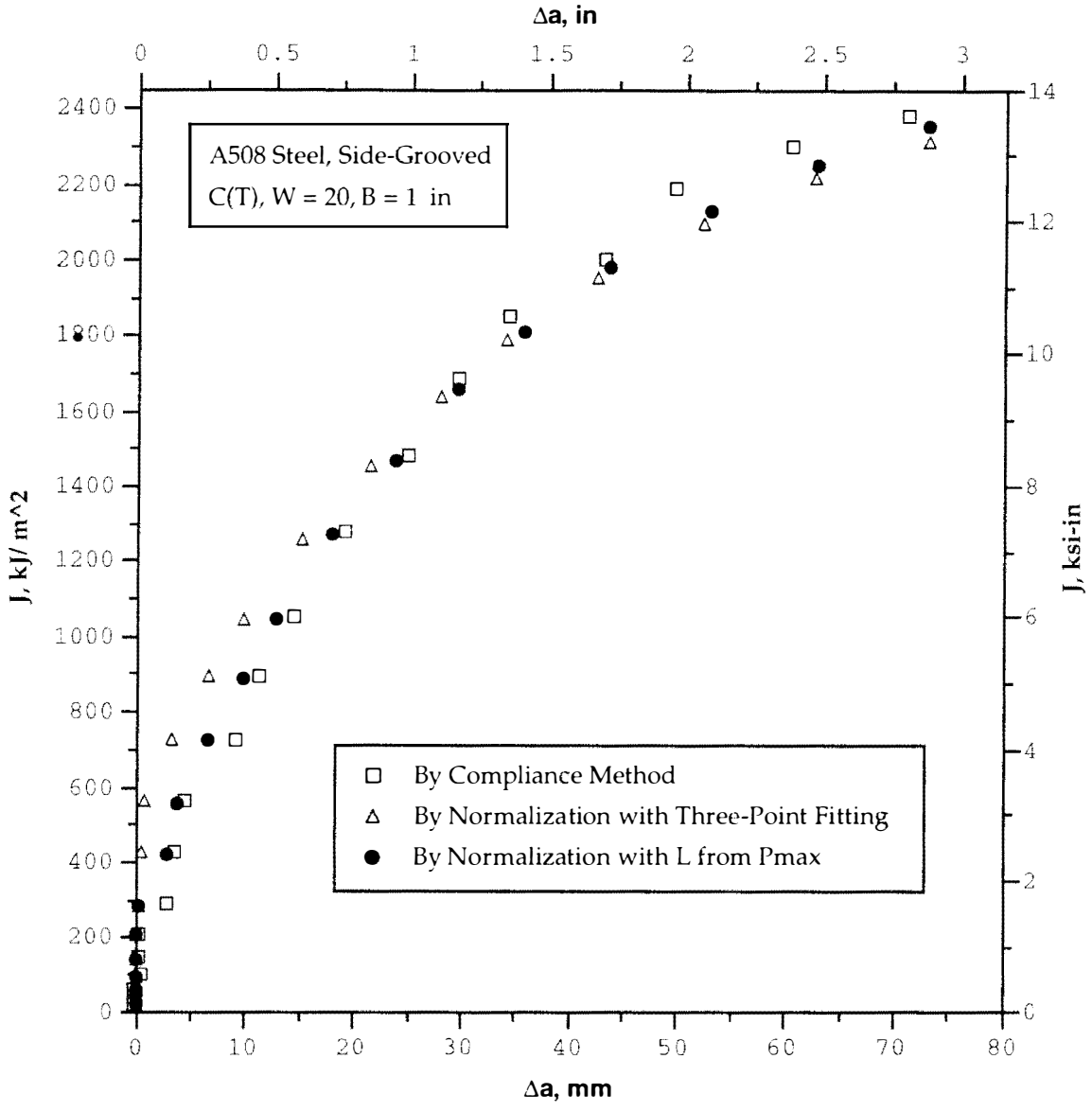

Fig. 3.24 - J-R Curve Developed by Method of Normalization Using L from Pmax Compared with Results from Three-Point Fitting and Compliance Method, A508 Steel, Side-Grooved Compact Specimen of W = 20, B = 1 in

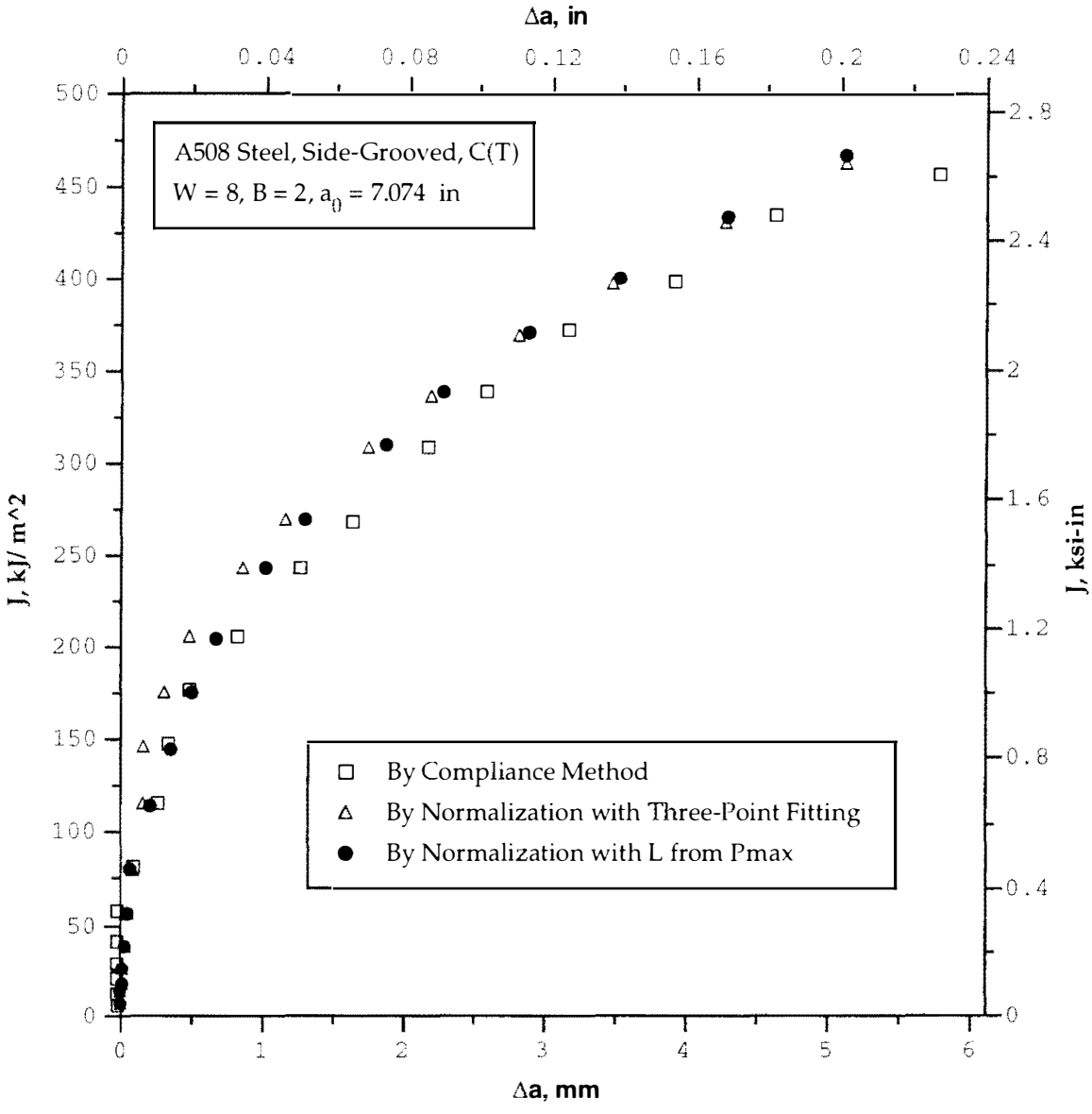

Fig. 3.25 - J-R Curve Developed by Method of Normalization Using L from Pmax Compared with Results from Three-Point Fitting and Compliance Method, A508 Steel, Side-Grooved Compact Specimen of W = 8, B = 2, a_0 = 7.074 in

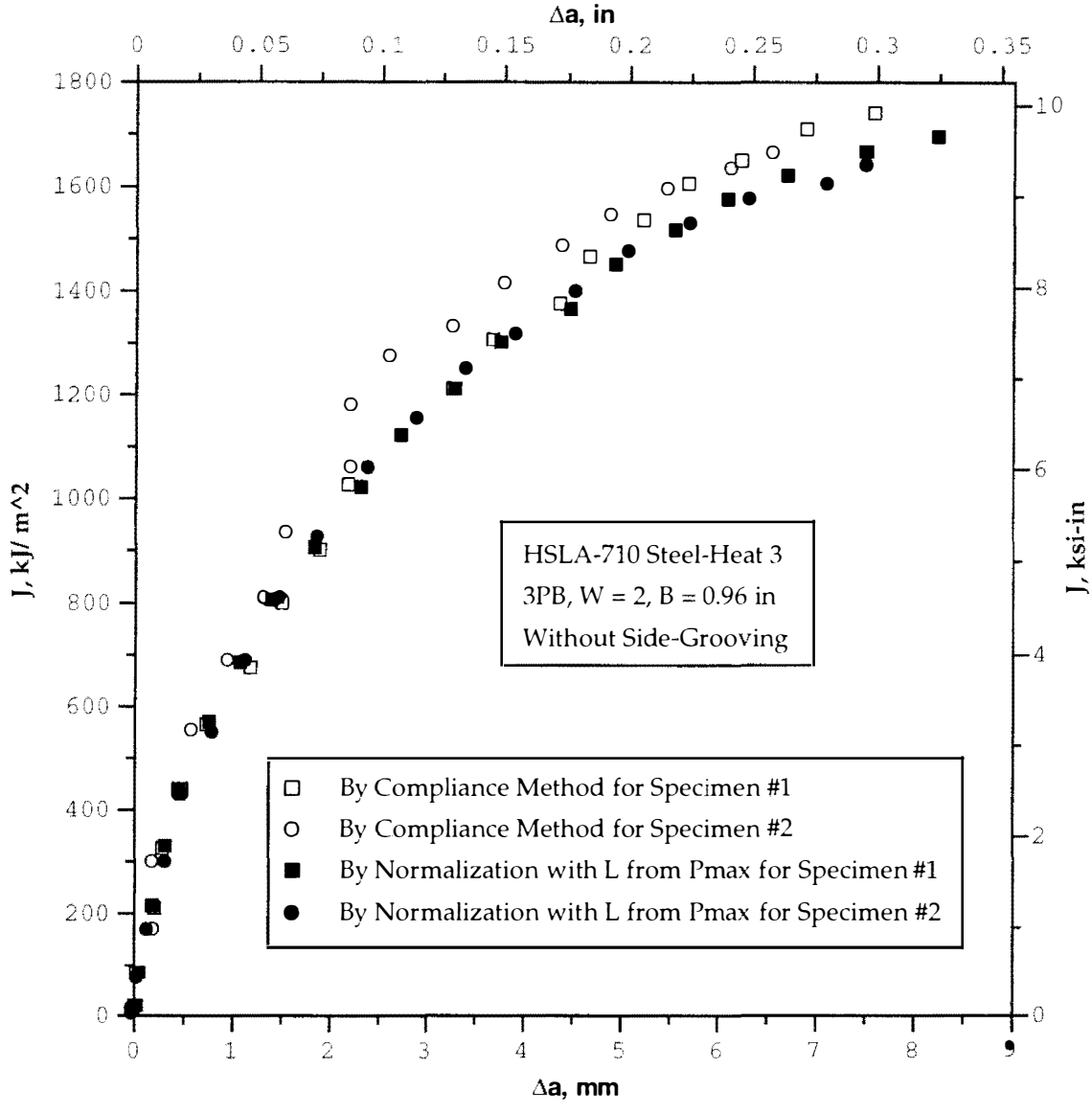

Fig. 3.26 - J-R Curve Developed by Method of Normalization Using L from P_{max} Compared with Result from Compliance Method for Non-Side-Grooved 3PB Specimens of HSLA-710 Steel-Heat 3

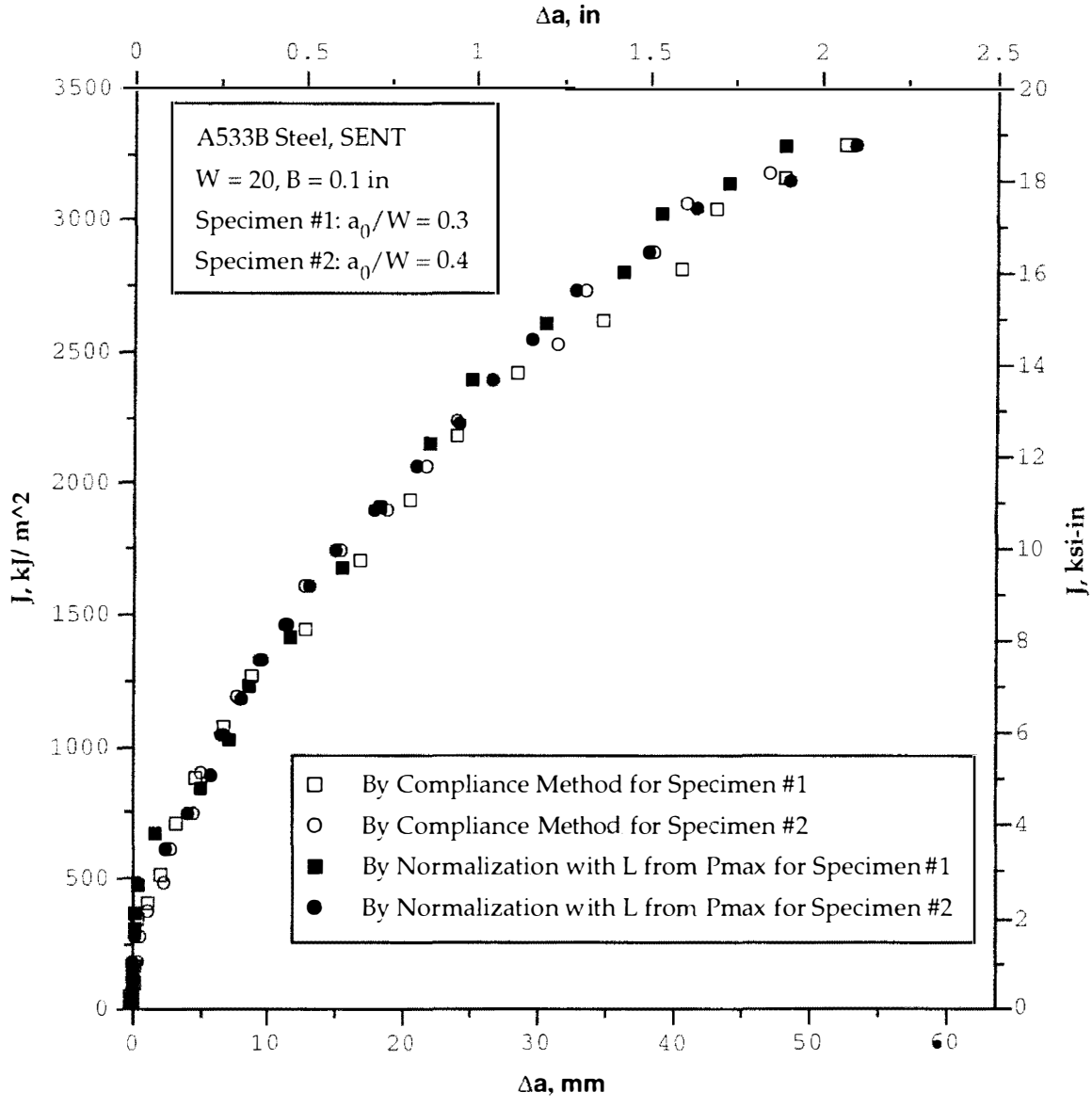

Fig. 3.27 - J-R Curve Developed by Method of Normalization Using L from Pmax Compared with Result from Compliance Method for Single Edge Notched Tension Specimens of A533B Steel

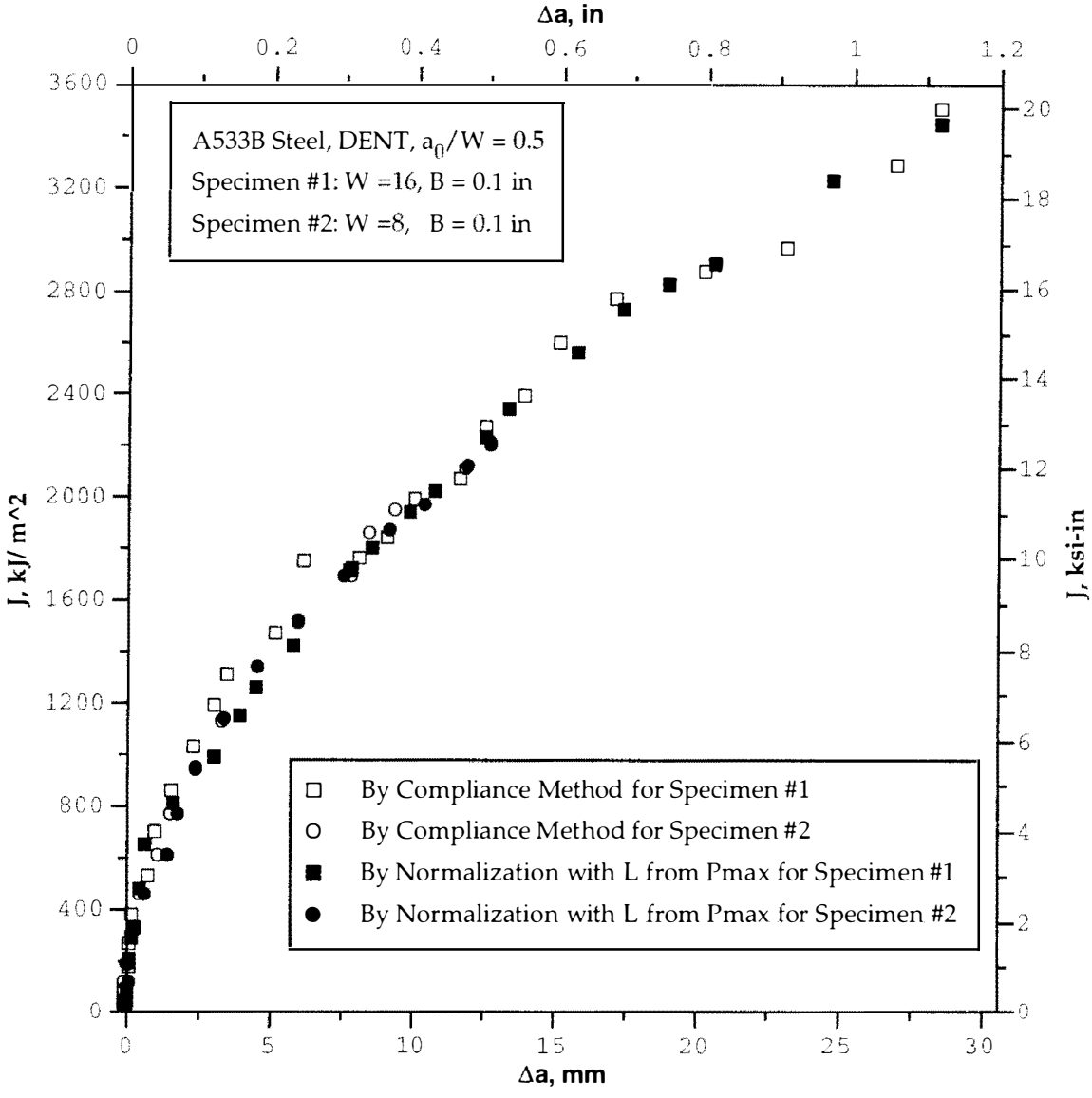

Fig. 3.28 - J-R Curve Developed by Method of Normalization Using L from Pmax Compared with Result from Compliance Method for Double Edge Notched Tension Specimens of A533B Steel

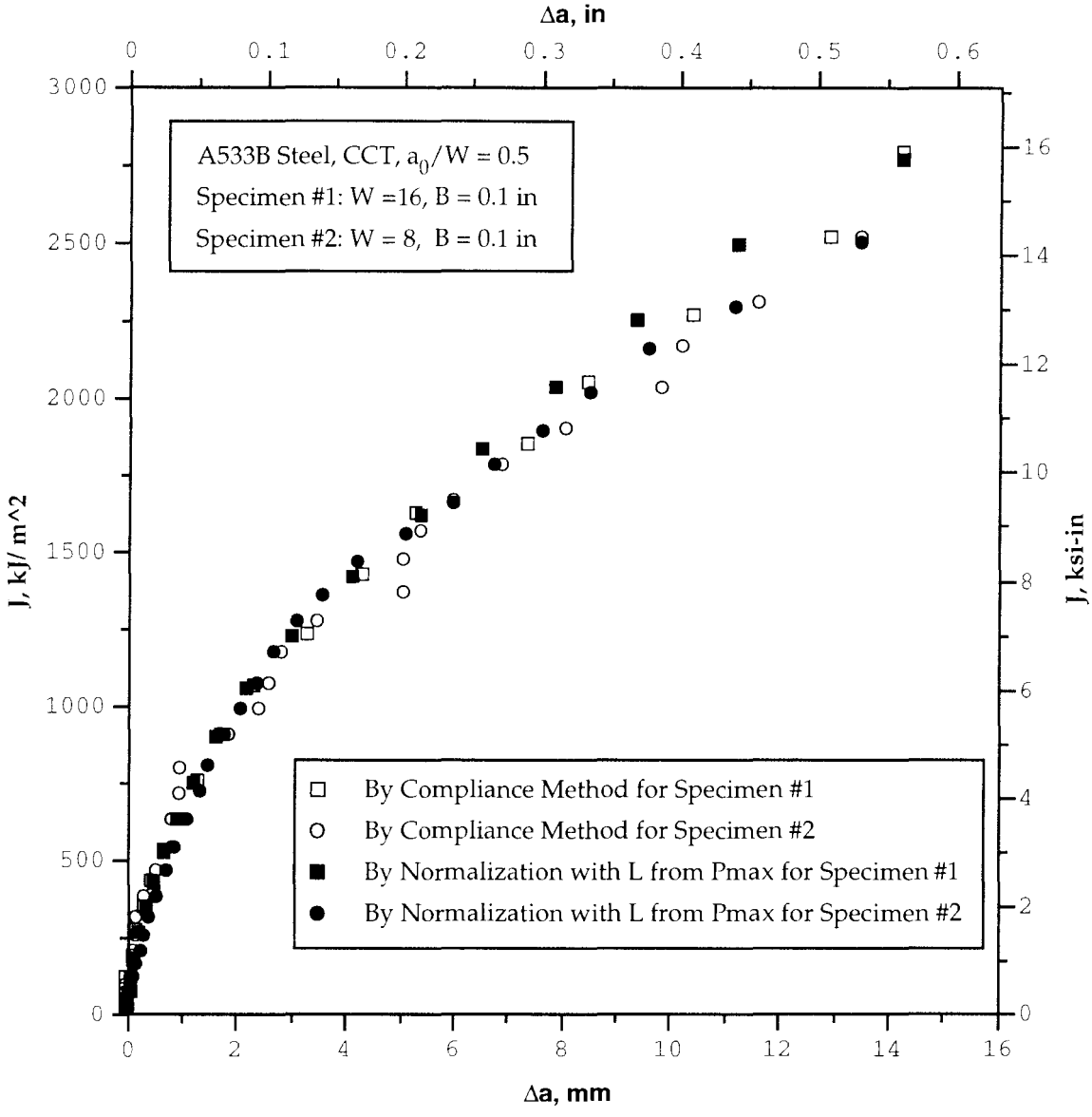

Fig. 3.29- J-R Curve Developed by Method of Normalization Using L from P_{max} Compared with Result from Compliance Method for Center Cracked Tension Specimens of A533B Steel

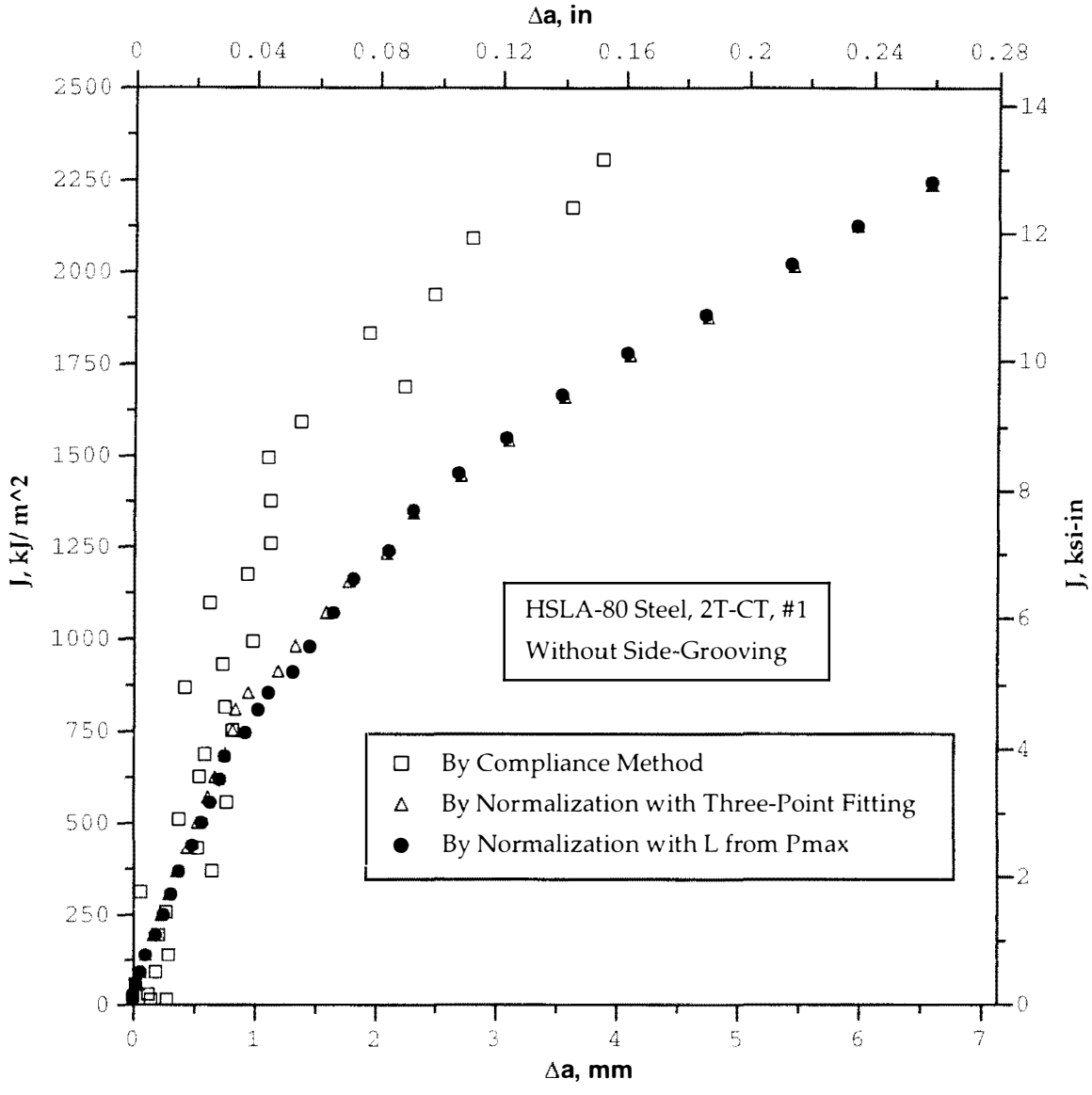

Fig. 3.30 - J-R Curve Developed by Method of Normalization Using L from P_{max} Compared with Results from Three-Point Fitting and Compliance Method, HSLA-80 Steel, Compact Specimen #1 of W = 4, B = 2 in. without Side-Grooving

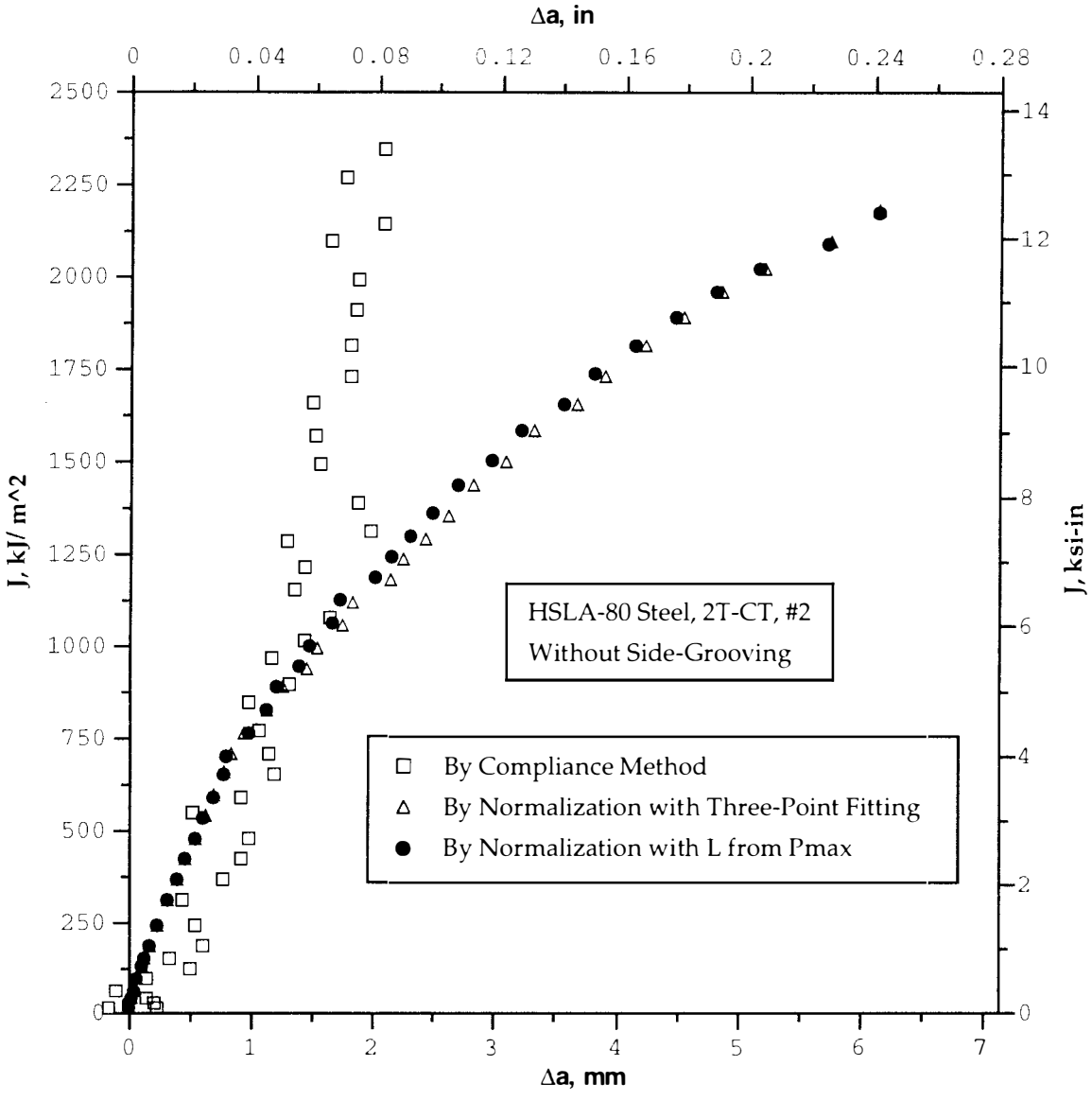

Fig. 3.31 - J-R Curve Developed by Method of Normalization Using L from P_{max} Compared with Results from Three-Point Fitting and Compliance Method, HSLA-80 Steel, Compact Specimen #2 of W = 4, B = 2 in. without Side-Grooving

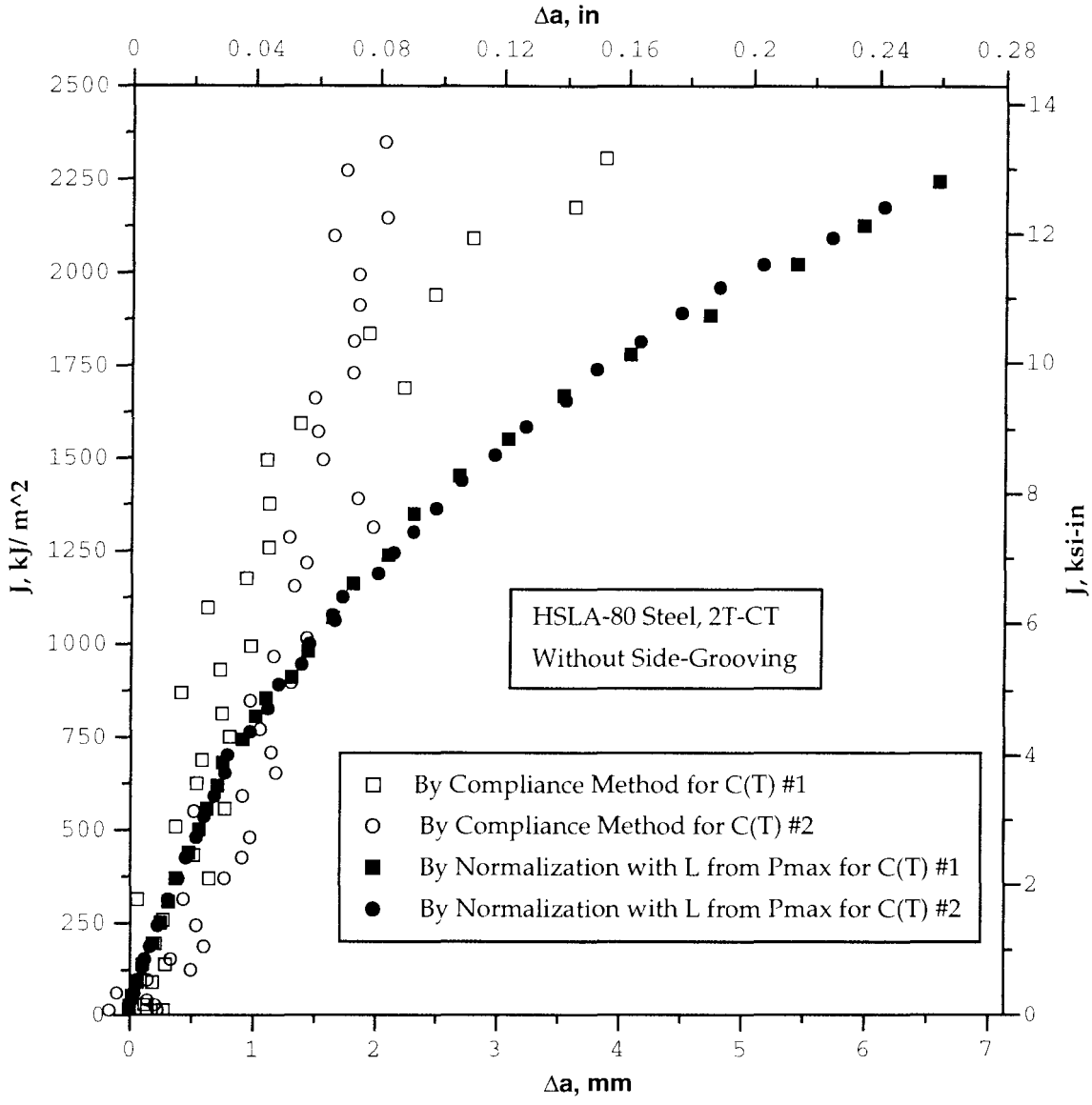

Fig. 3.32- J-R Curves Developed by Method of Normalization Using L from P_{max} Compared with Results from Compliance Method for Two Non-Side-Grooved Compact Specimens of HSLA-80 Steel

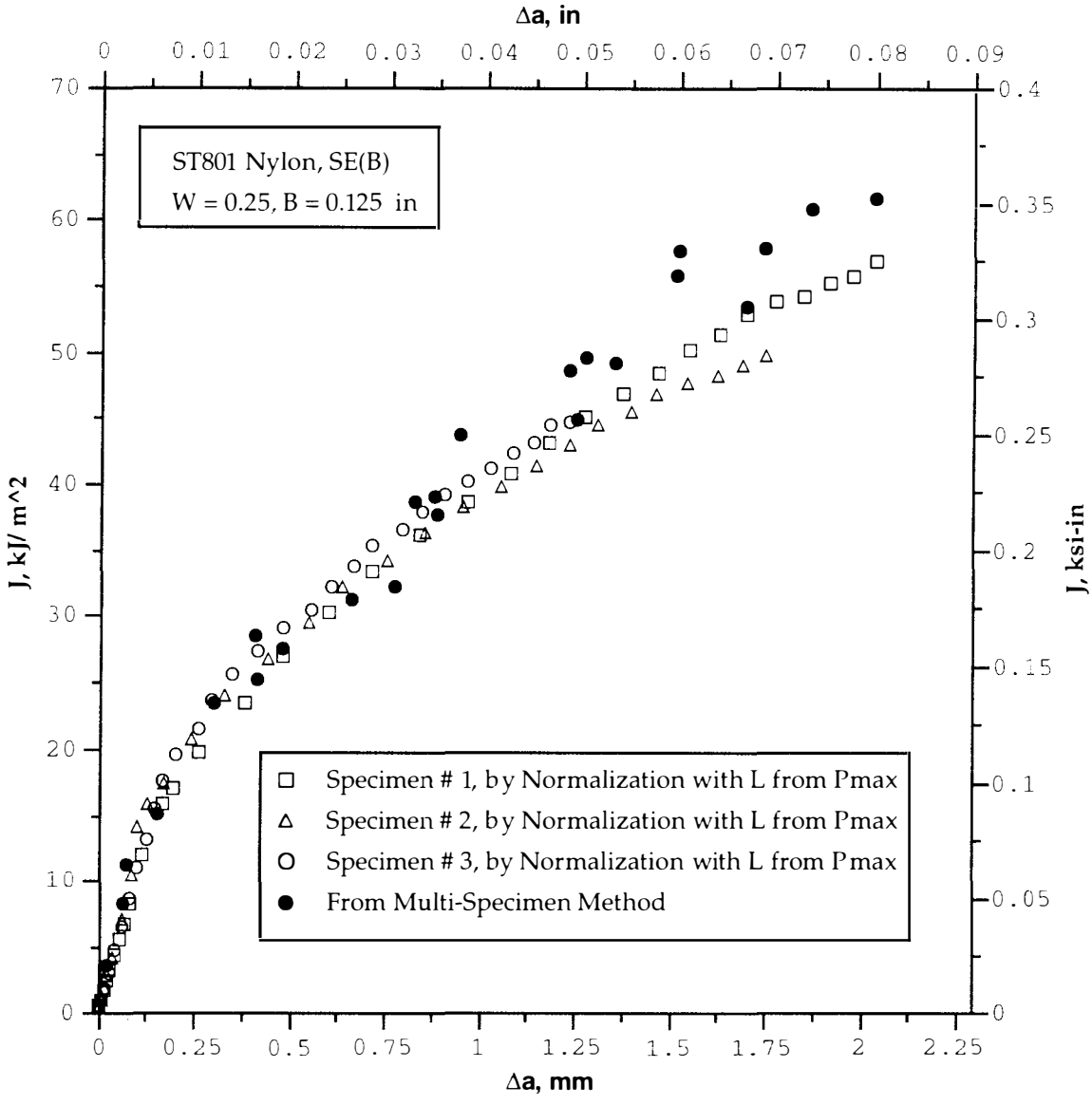

Fig. 3.33 - J-R Curves Developed by Method of Normalization Using L from P_{max} Compared with Results from Multiple Specimen Method, ST801 Nylon, Three-Point Bend Specimens of W = 0.25, B = 0.125 in

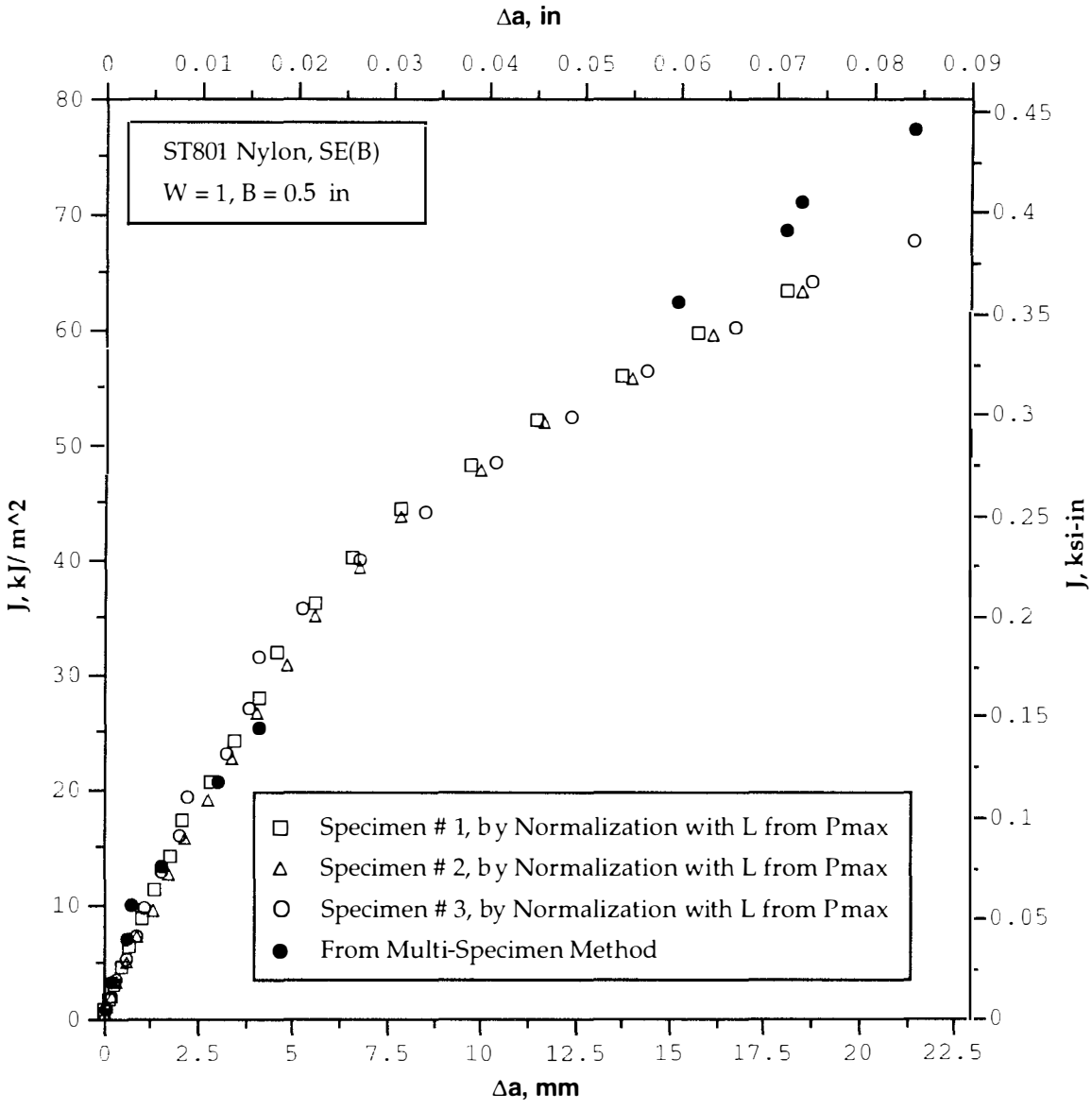

Fig. 3.34 - J-R Curves Developed by Method of Normalization Using L from P_{max} Compared with Results from Multiple Specimen Method, ST801 Nylon, Three-Point Bend Specimens of W = 1, B = 0.5 in

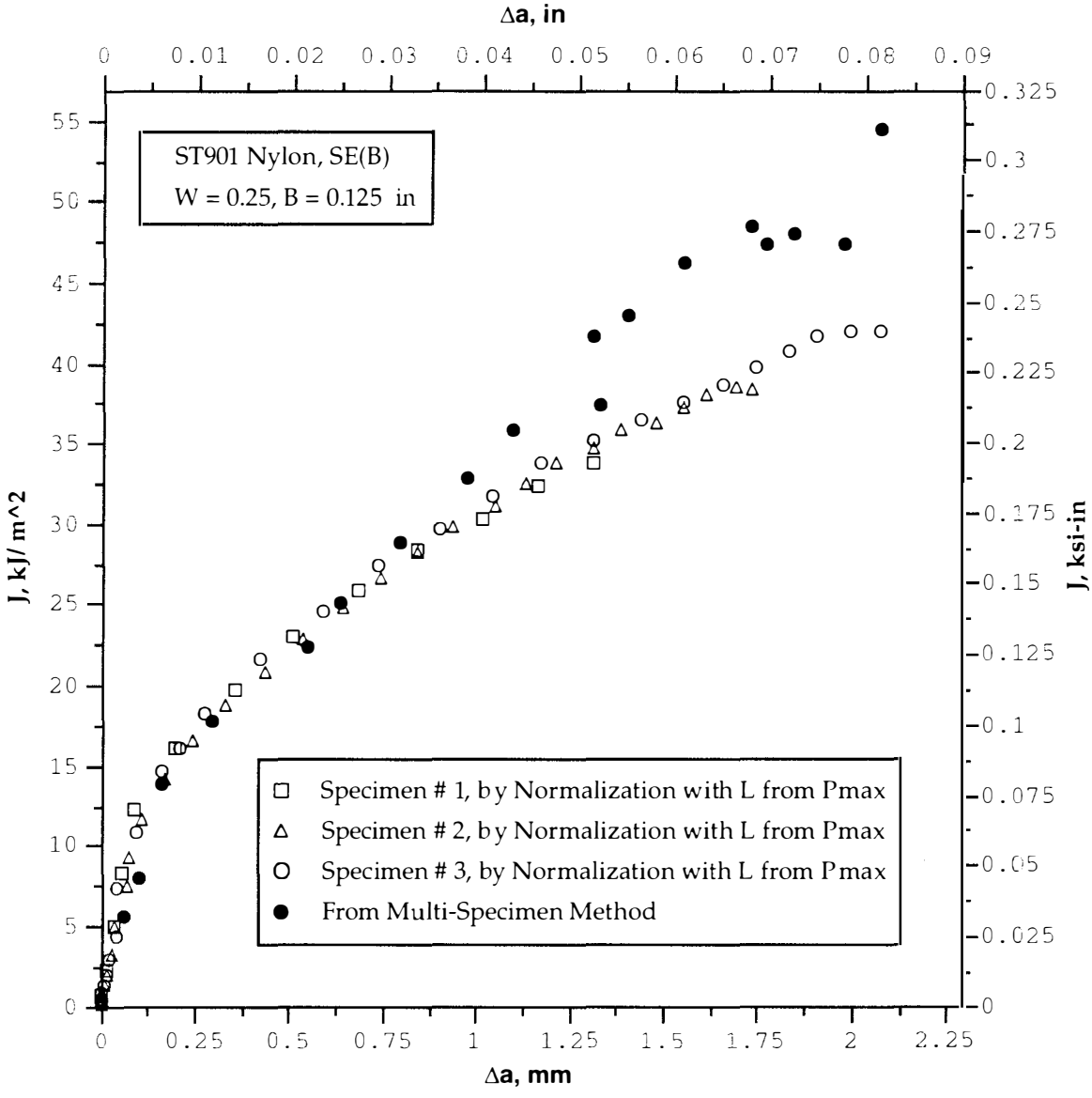

Fig. 3.35 - J-R Curves Developed by Method of Normalization Using L from Pmax Compared with Results from Multiple Specimen Method, ST901 Nylon, Three-Point Bend Specimens of W = 0.25, B = 0.125 in

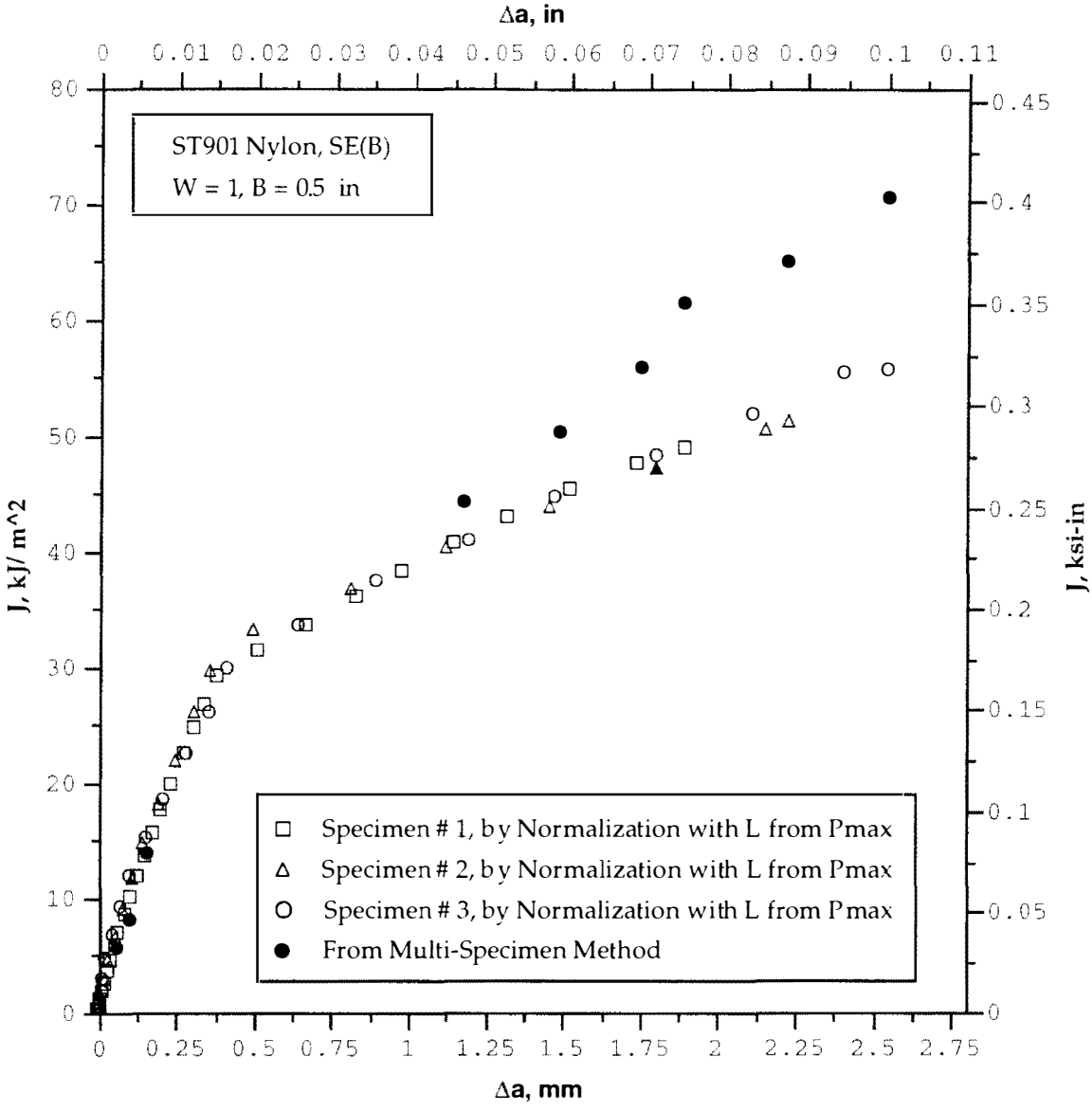

Fig. 3.36 - J-R Curves Developed by Method of Normalization Using L from Pmax Compared with Results from Multiple Specimen Method, ST901 Nylon, Three-Point Bend Specimens of W = 1, B = 0.5 in

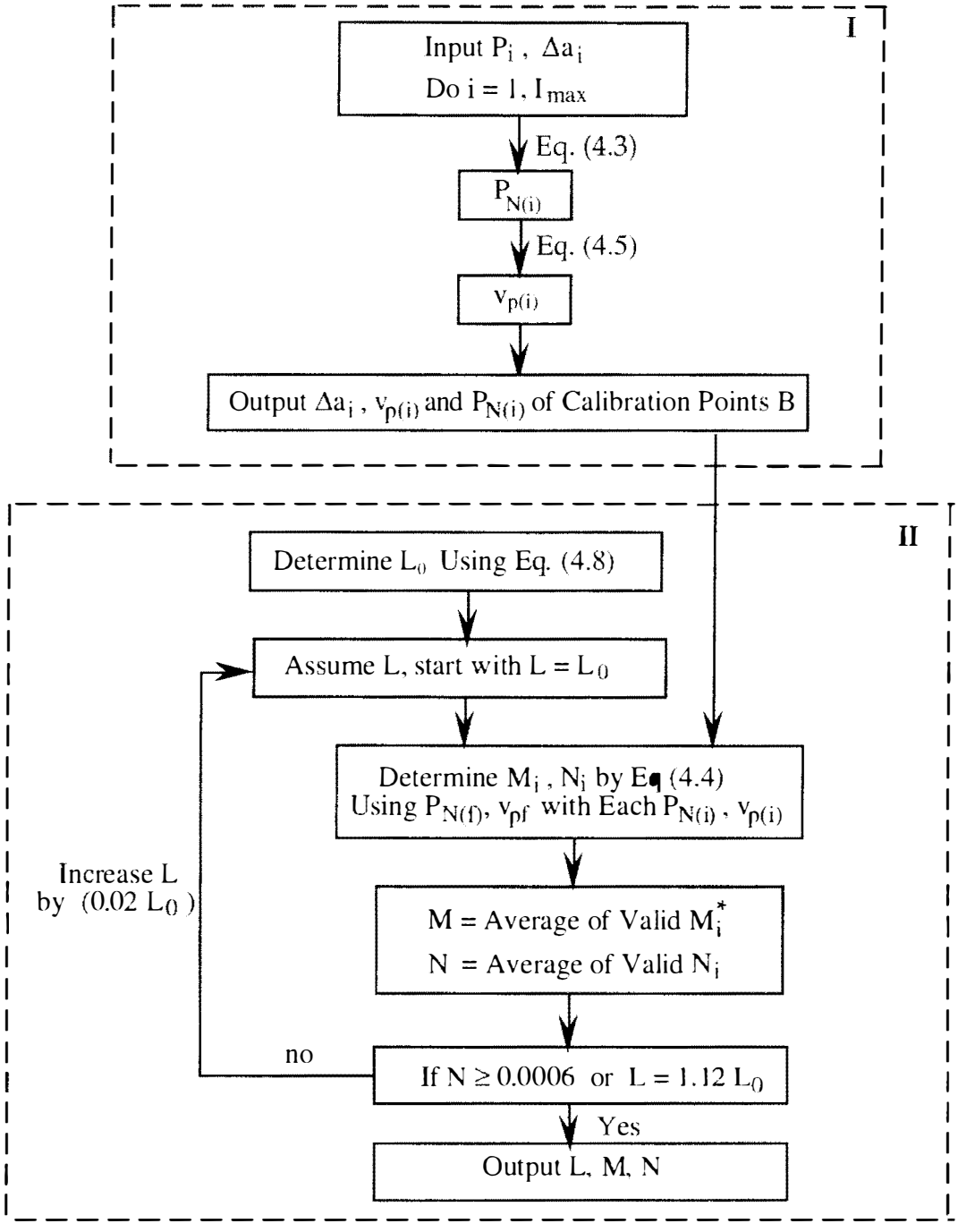

Note:

Part I: Calibration points B determination from a power law fit.

Part II: Constants L, M, N dtermination.

* : M_i and N_i determined are valid when $N_i > 0$

Fig. 4.1- A Flow Chart for LMN Function Determination from Maximum Load Point and a Power Law Fit When J-R Curves Are Determined from Load versus Displacement Pairs

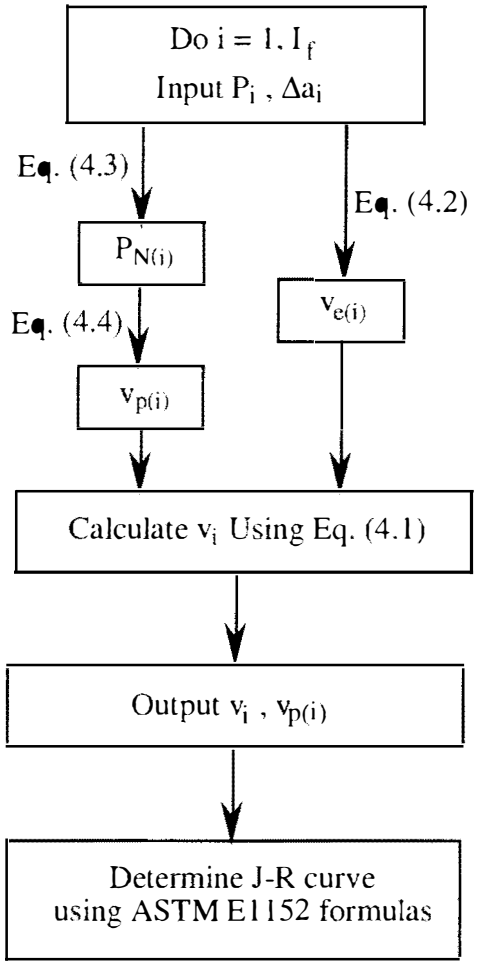

Fig. 4.2 - A Flow Chart for J-R Curve Determination from Load versus Crack Length Pairs by Predicting Displacement Using Method of Normalization with LMN Function

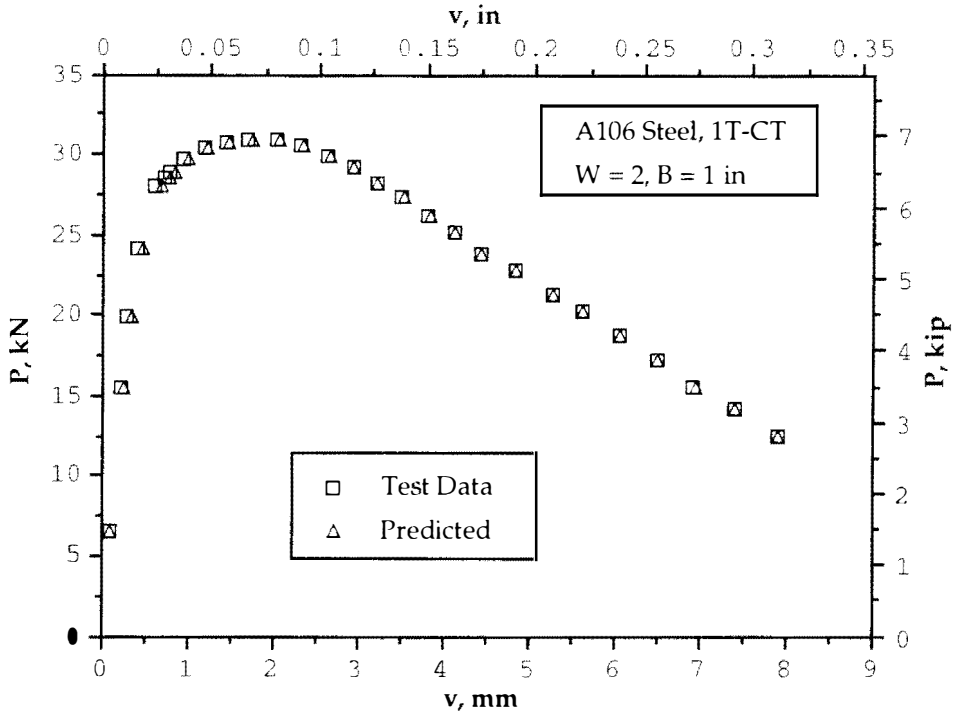

Fig. 4.3a Load versus Predicted Displacement by Normalization Method from P-Δa Compared with the Test Data, A106 Steel, Compact Specimen

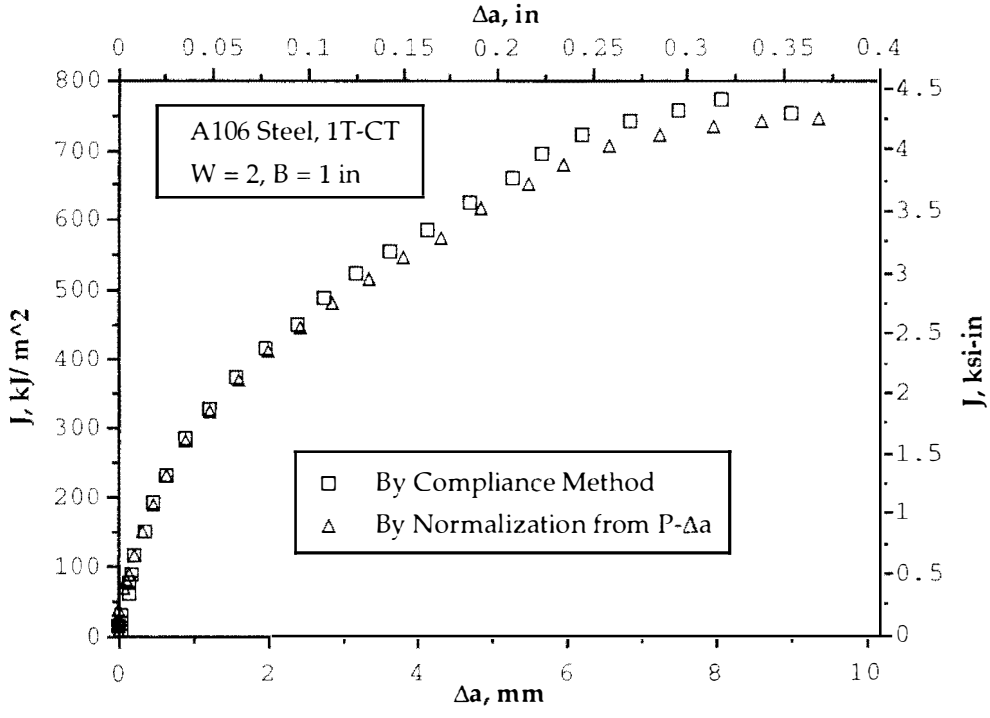

Fig. 4.3b J-R Curve Developed from P-Δa by Method of Normalization Using L from P_{max} Compared with Result from Compliance Method, A106 Steel, Compact Specimen

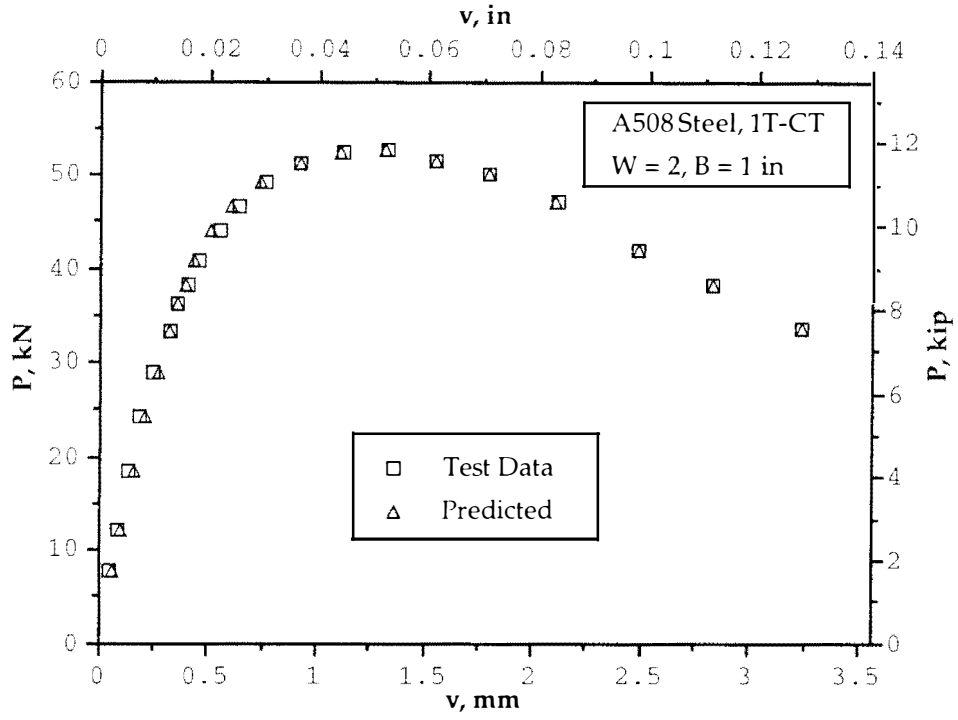

Fig. 4.4a Load versus Predicted Displacement by Normalization Method from P-Δa Compared with the Test Data, A508 Steel, Compact Specimen

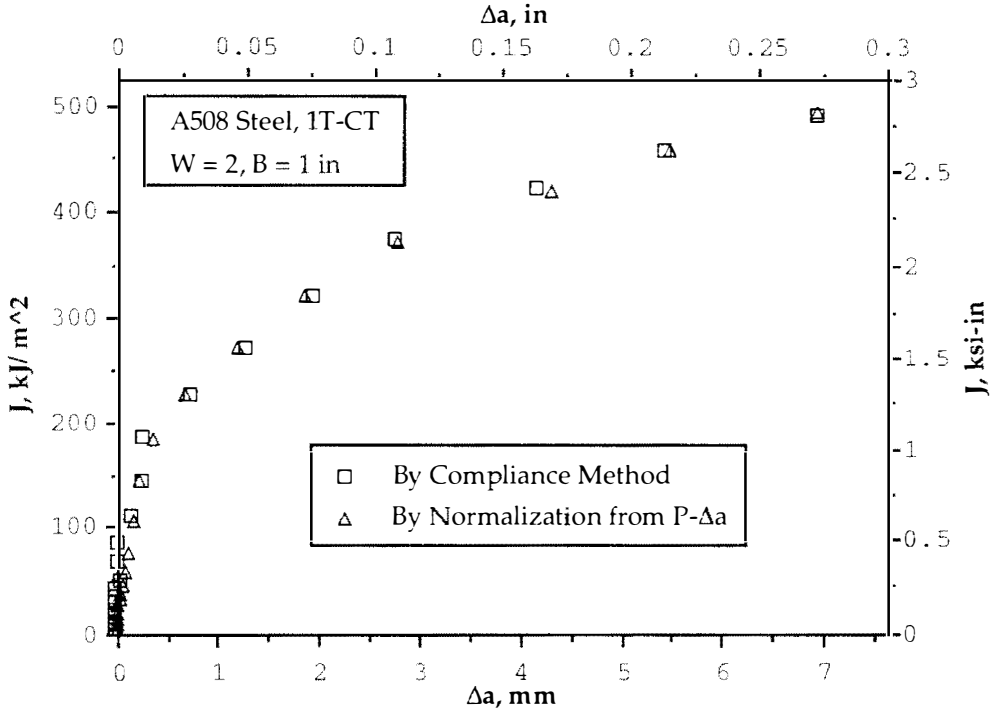

Fig. 4.4b J-R Curve Developed from P-Δa by Method of Normalization Using L from P_{max} Compared with Result from Compliance Method, A508 Steel, Compact Specimen

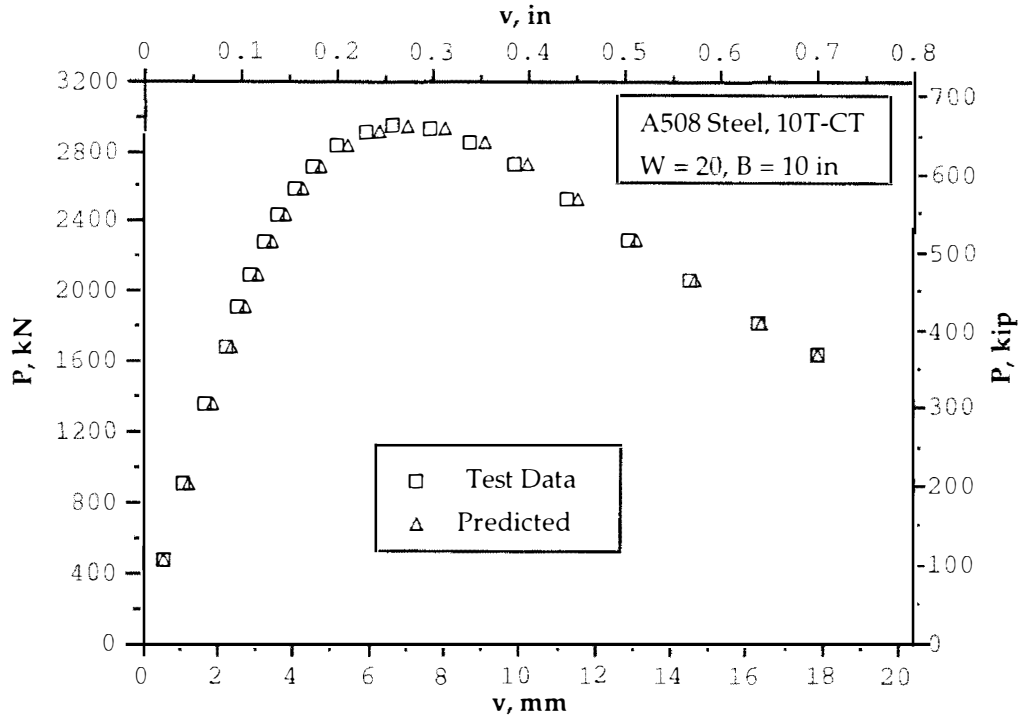

Fig. 4.5a Load versus Predicted Displacement by Normalization Method from P-Δa Compared with the Test Data, A508 Steel, 10T Compact Specimen

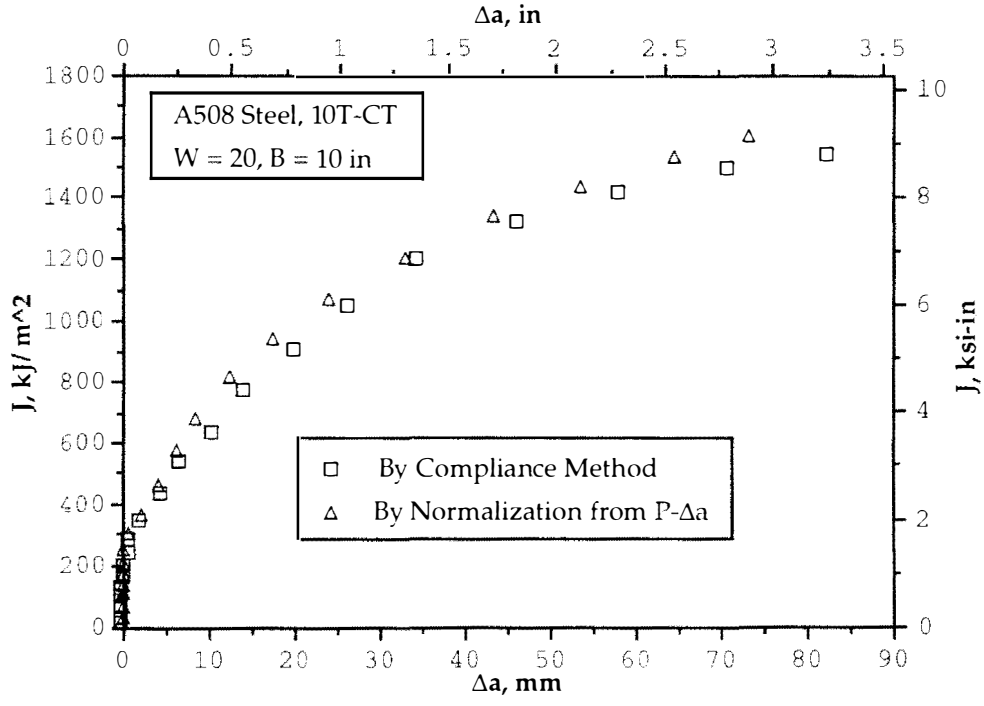

Fig. 4.5b J-R Curve Developed from P-Δa by Method of Normalization Using L from P_{max} Compared with Result from Compliance Method, A508 Steel, 10T Compact Specimen

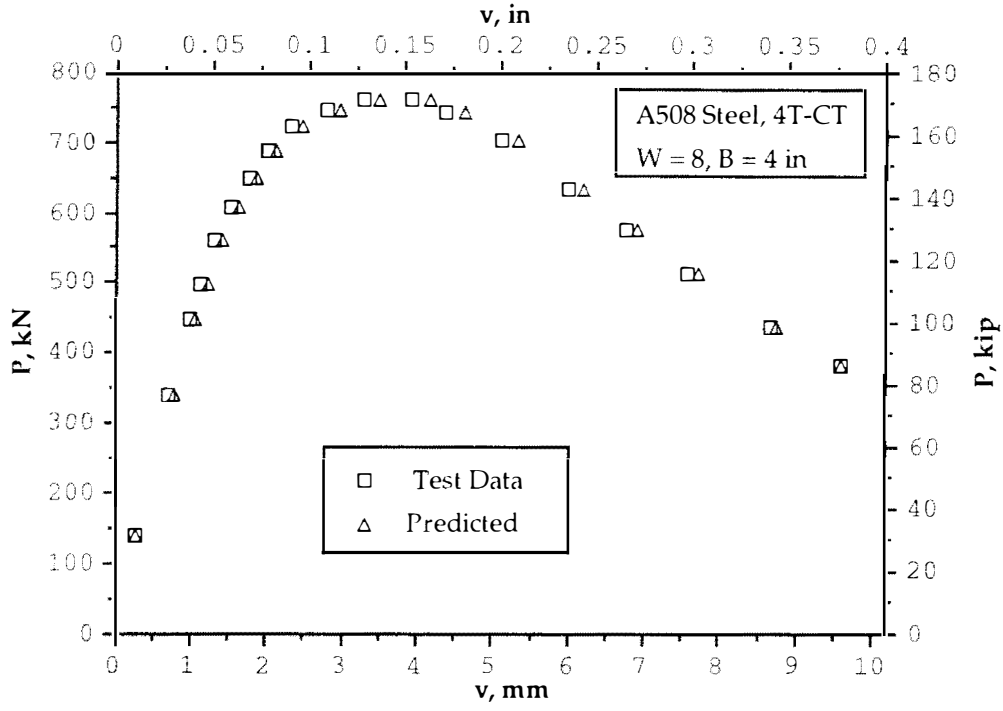

Fig. 4.6a Load versus Predicted Displacement by Normalization Method from P-Δa Compared with the Test Data, A508 Steel, 4T Compact Specimen

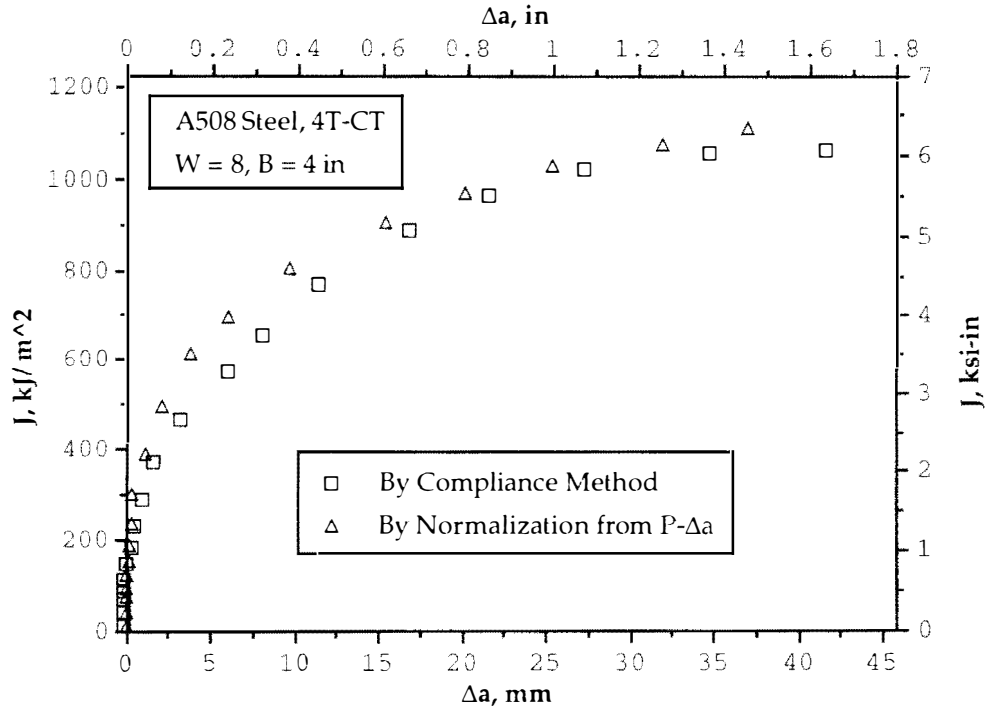

Fig. 4.6b J-R Curve Developed from P-Δa by Method of Normalization Using L from P_{max} Compared with Result from Compliance Method, A508 Steel, 4T Compact Specimen

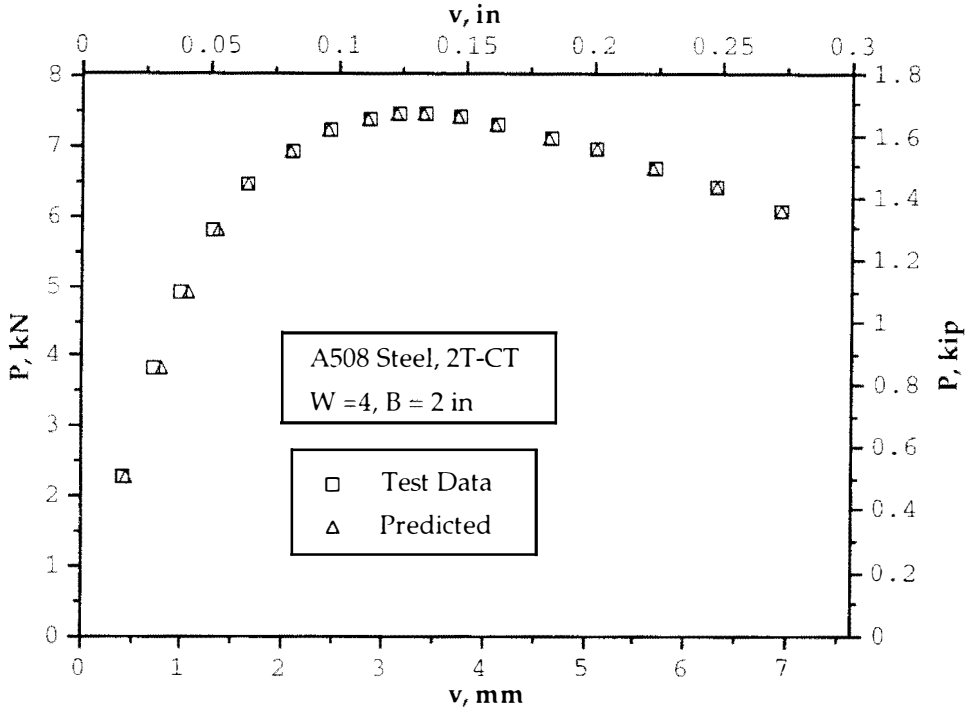

Fig. 4.7a Load versus Predicted Displacement by Normalization Method from P-Δa Compared with the Test Data, A508 Steel, 2T Compact Specimen

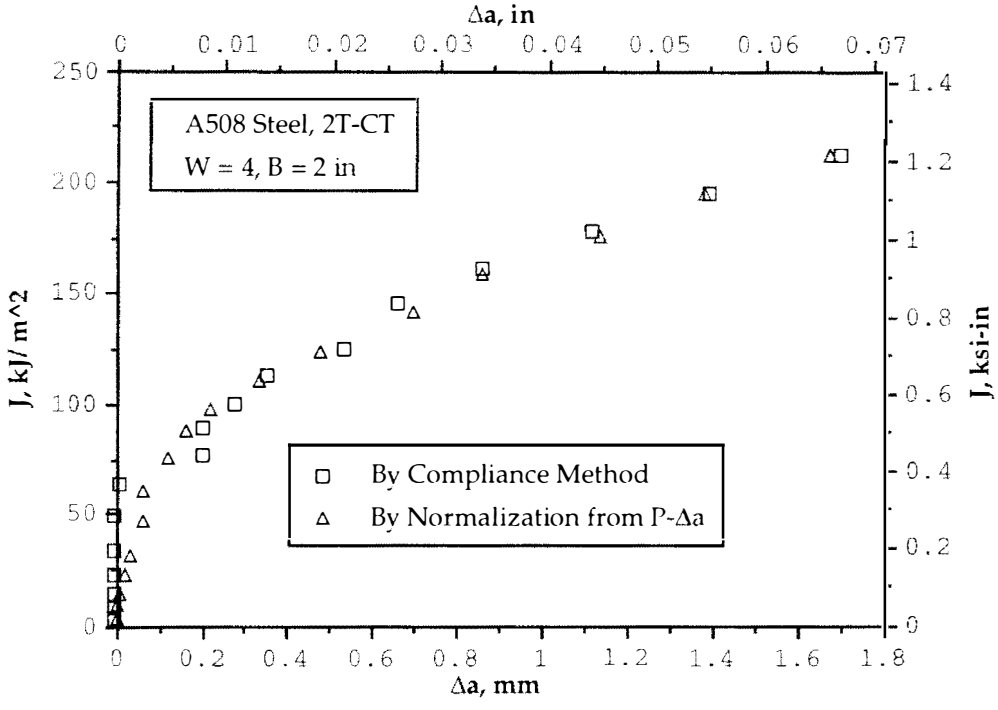

Fig. 4.7b J-R Curve Developed from P-Δa by Method of Normalization Using L from P_{max} Compared with Result from Compliance Method, A508 Steel, 2T Compact Specimen

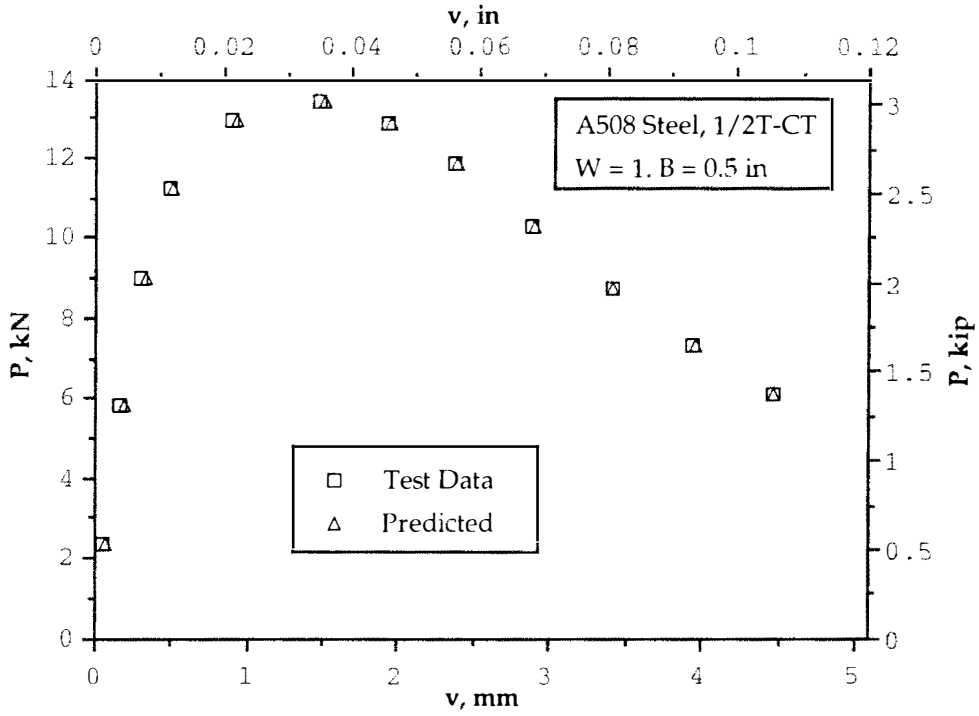

Fig. 4.8a Load versus Predicted Displacement by Normalization Method from P-Δa Compared with the Test Data, A508 Steel, 1/2T Compact Specimen

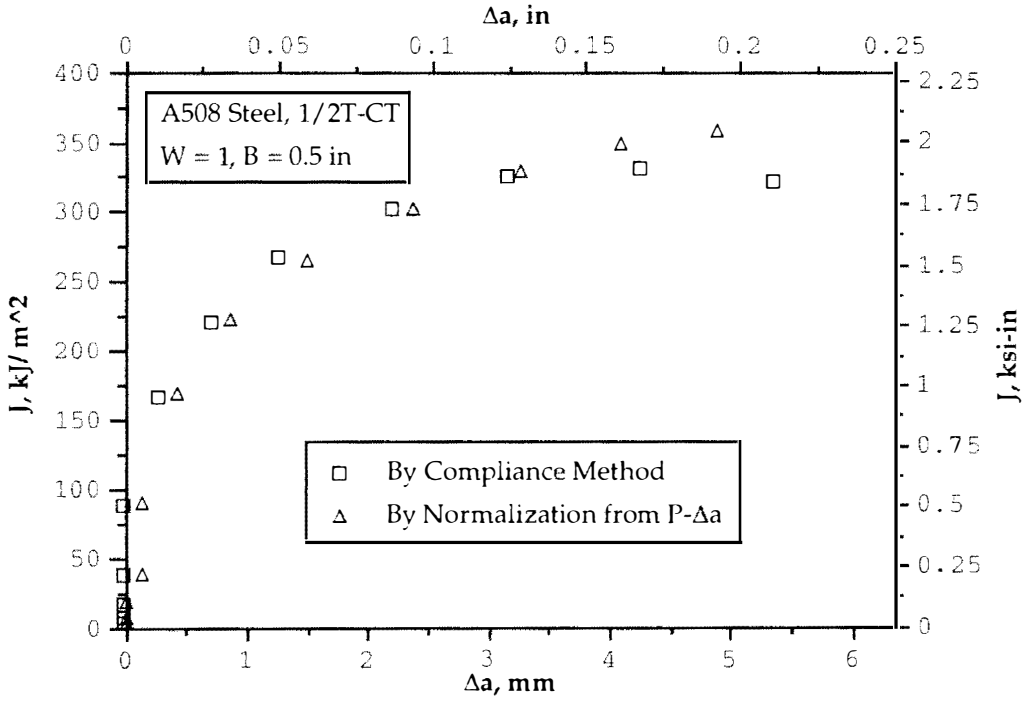

Fig. 4.8b J-R Curve Developed from P-Δa by Method of Normalization Using L from P_{max} Compared with Result from Compliance Method, A508 Steel, 1/2T Compact Specimen

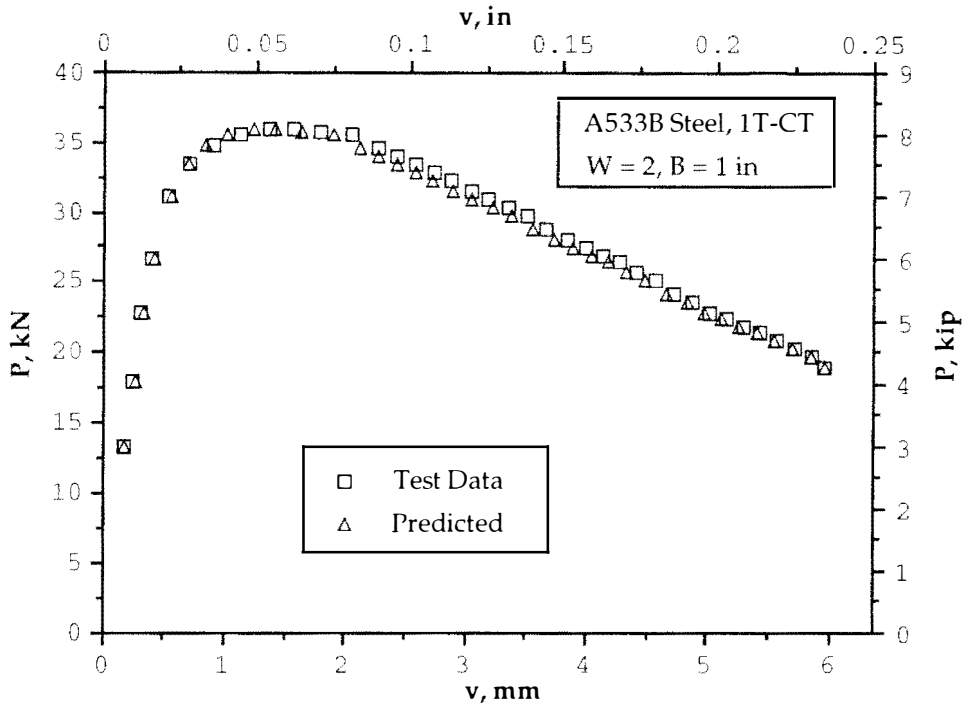

Fig. 4.9a Load versus Predicted Displacement by Normalization Method from P-Δa Compared with the Test Data, A533B Steel, Compact Specimen

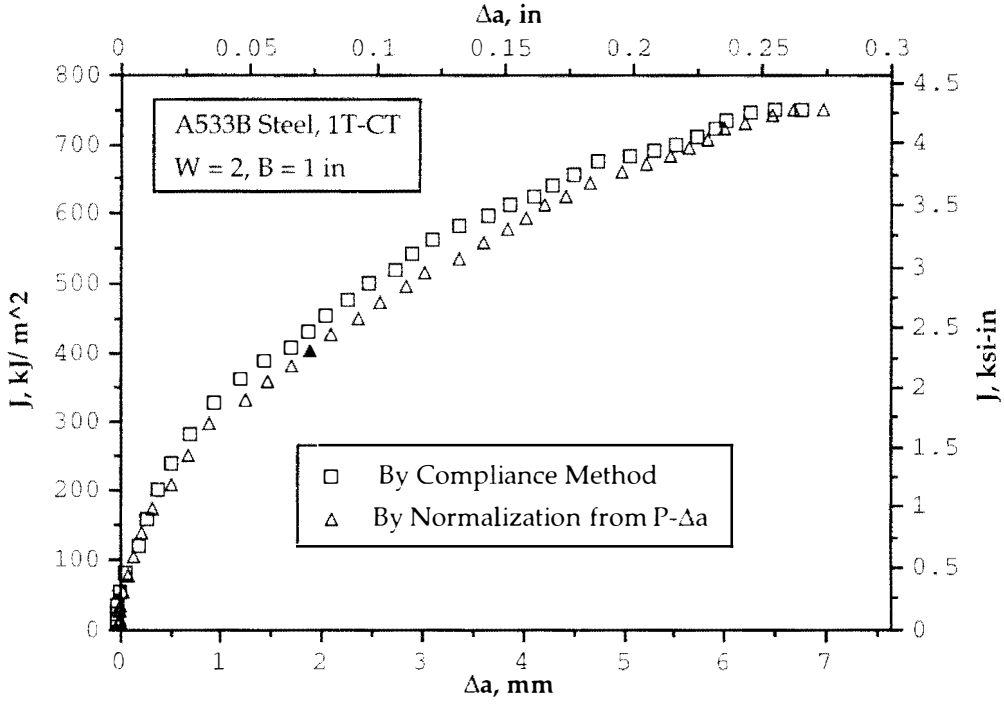

Fig. 4.9b J-R Curve Developed from P-Δa by Method of Normalization Using L from P_{max} Compared with Result from Compliance Method, A533B Steel, Compact Specimen

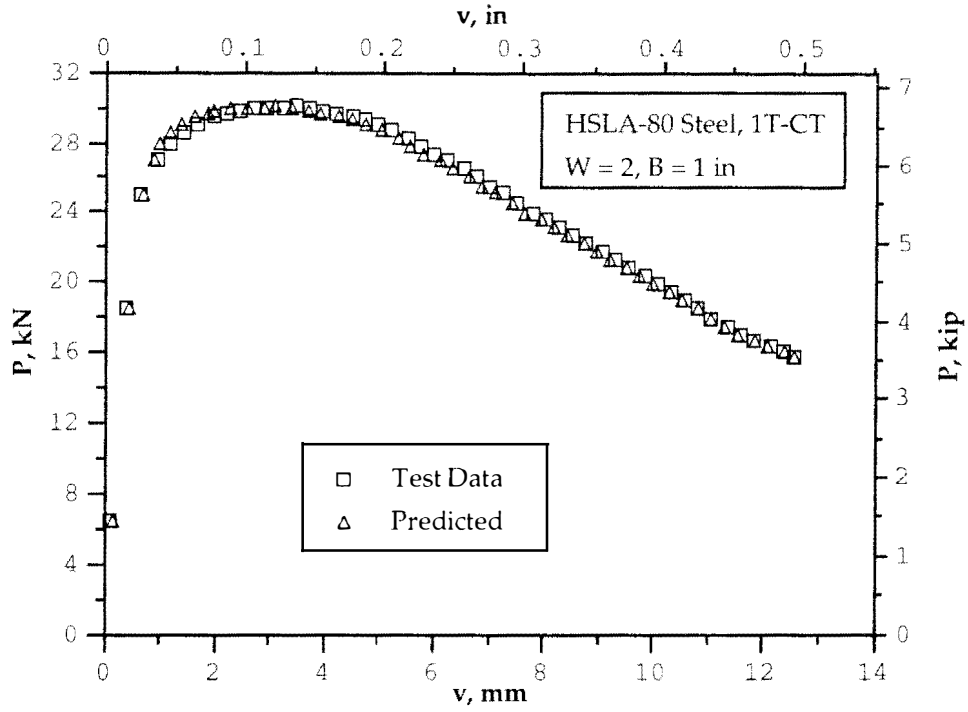

Fig. 4.10a Load versus Predicted Displacement by Normalization Method from P-Δa Compared with the Test Data, HSLA-80 Steel, Compact Specimen

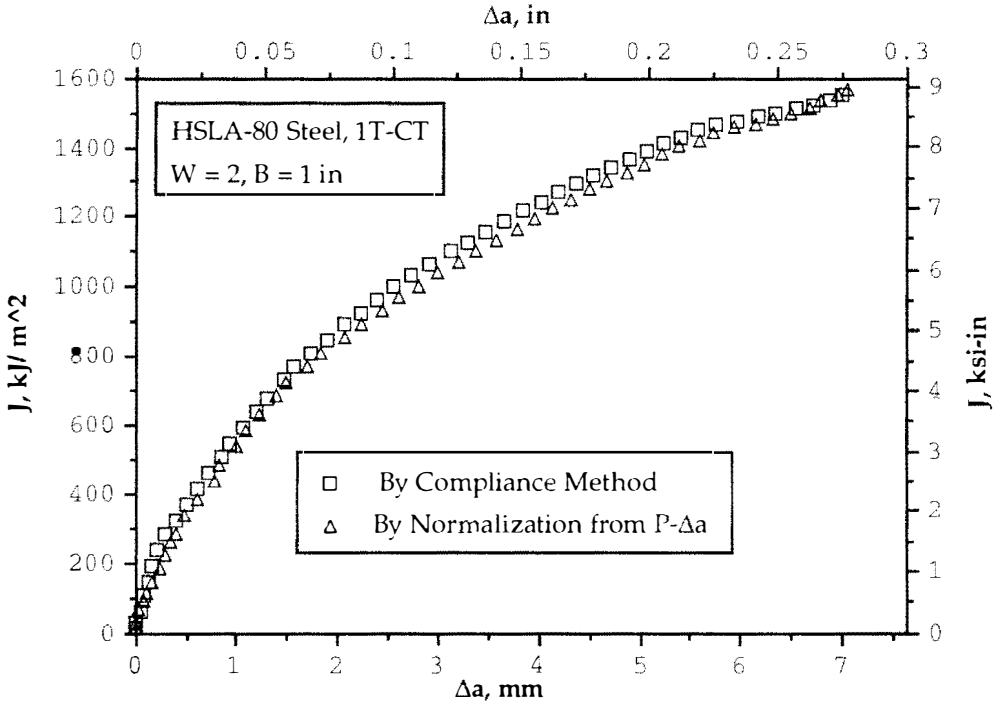

Fig. 4.10b J-R Curve Developed from P-Δa by Method of Normalization Using L from P_{max} Compared with Result from Compliance Method, HSLA-80 Steel, Compact Specimen

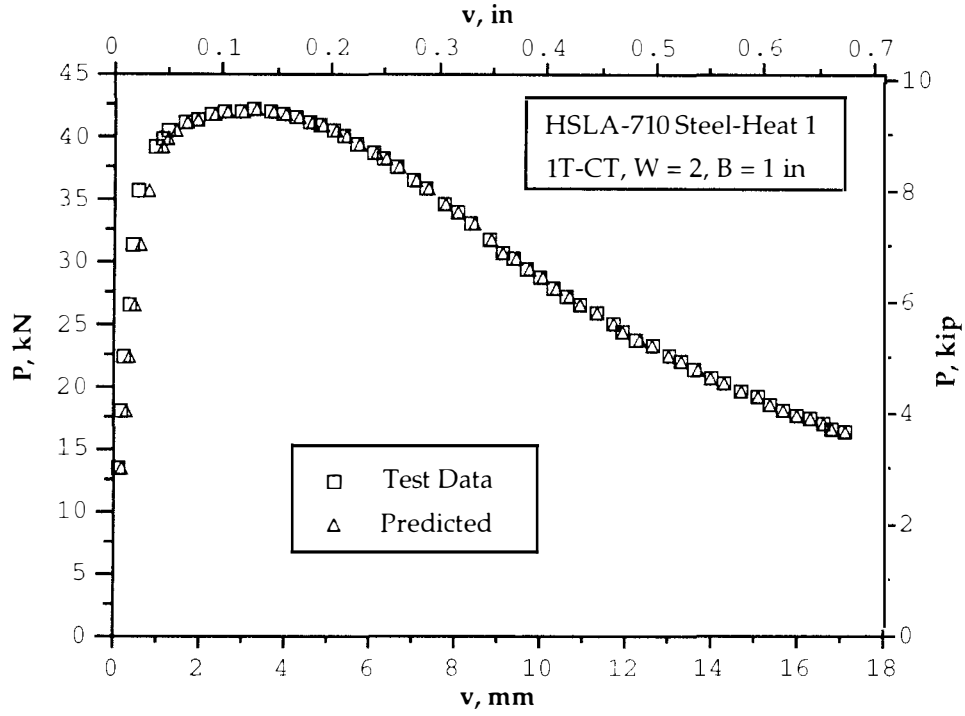

Fig. 4.11a Load versus Predicted Displacement by Normalization Method from P-Δa Compared with the Test Data, HSLA-710 Steel-Heat 1, CT Specimen

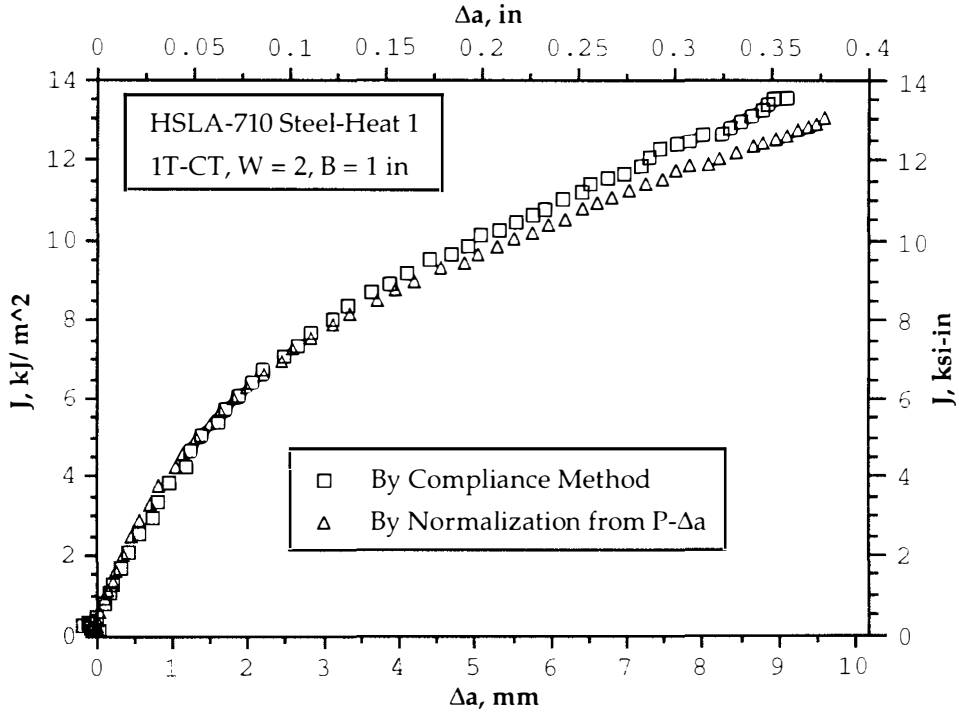

Fig. 4.11b J-R Curve Developed from P-Δa by Method of Normalization Using L from P_{max} Compared with Result from Compliance Method, HSLA-710 Steel-Heat 1, CT Specimen

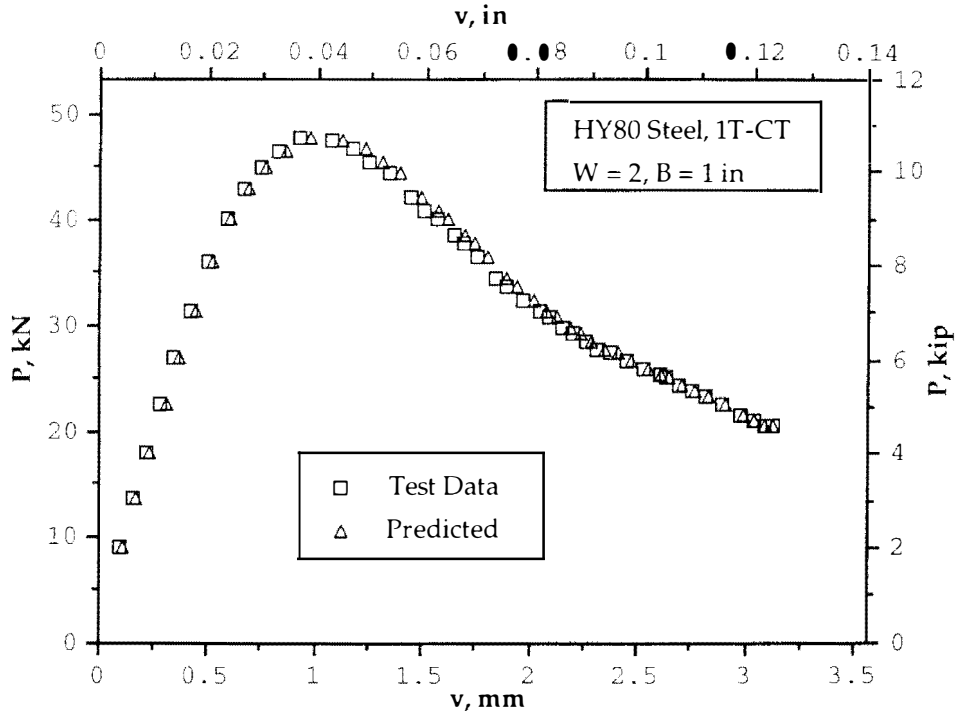

Fig. 4.12a Load versus Predicted Displacement by Normalization Method from P-Δa Compared with the Test Data, HY80 Steel, Compact Specimen

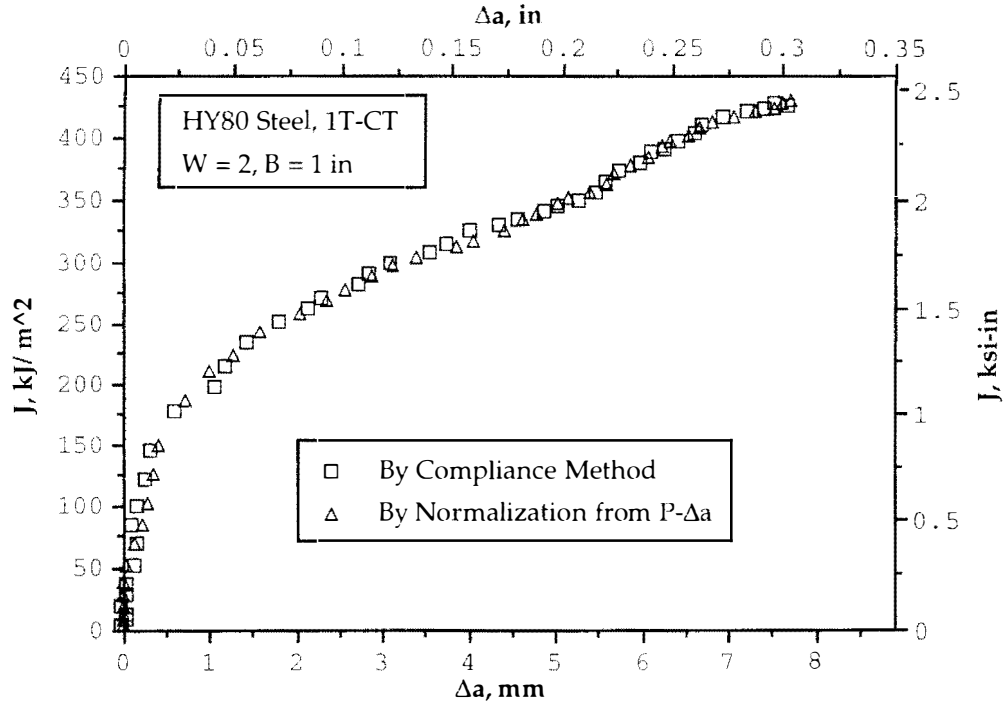

Fig. 4.12b J-R Curve Developed from P-Δa by Method of Normalization Using L from P_{max} Compared with Result from Compliance Method, HY80 Steel, Compact Specimen

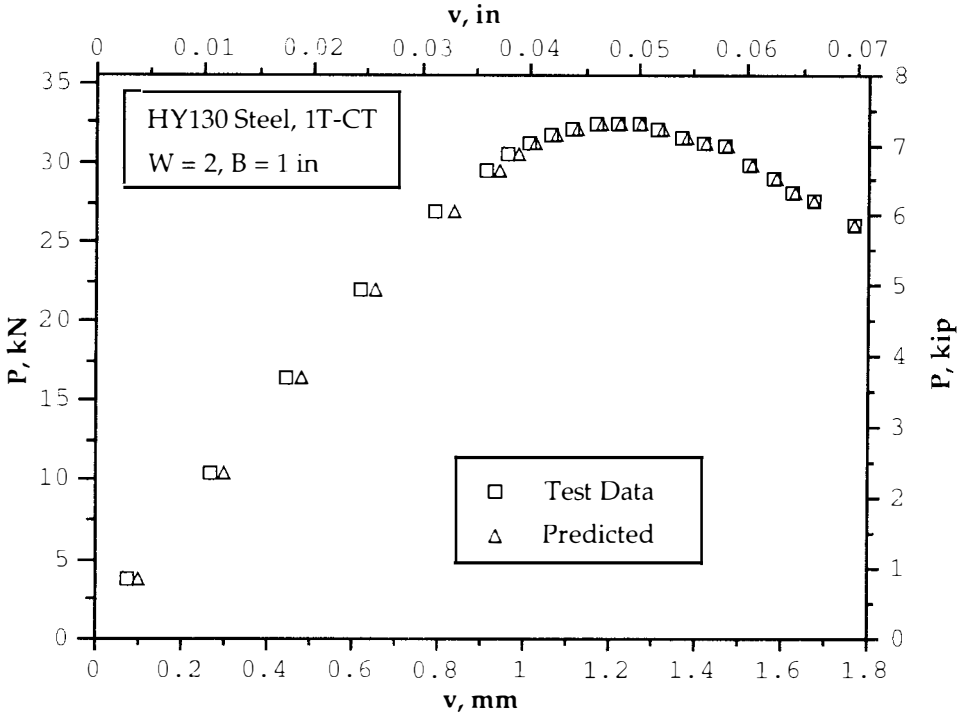

Fig. 4.13a Load versus Predicted Displacement by Normalization Method from P-Δa Compared with the Test Data, HY130 Steel, Compact Specimen

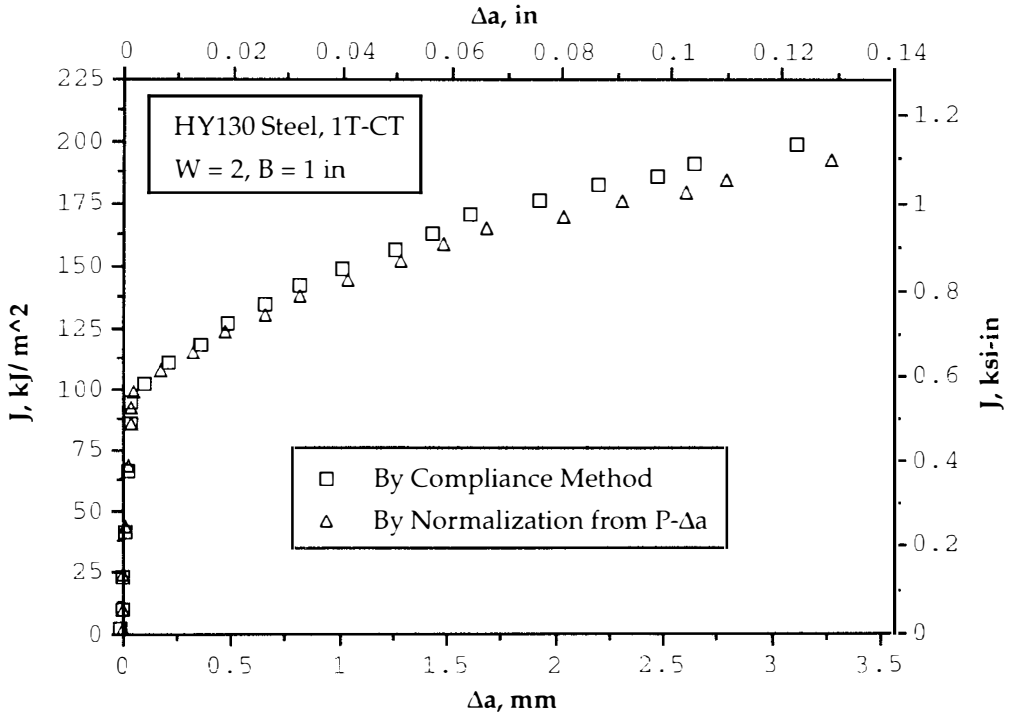

Fig. 4.13b J-R Curve Developed from P-Δa by Method of Normalization Using L from P_{max} Compared with Result from Compliance Method, HY130 Steel, Compact Specimen

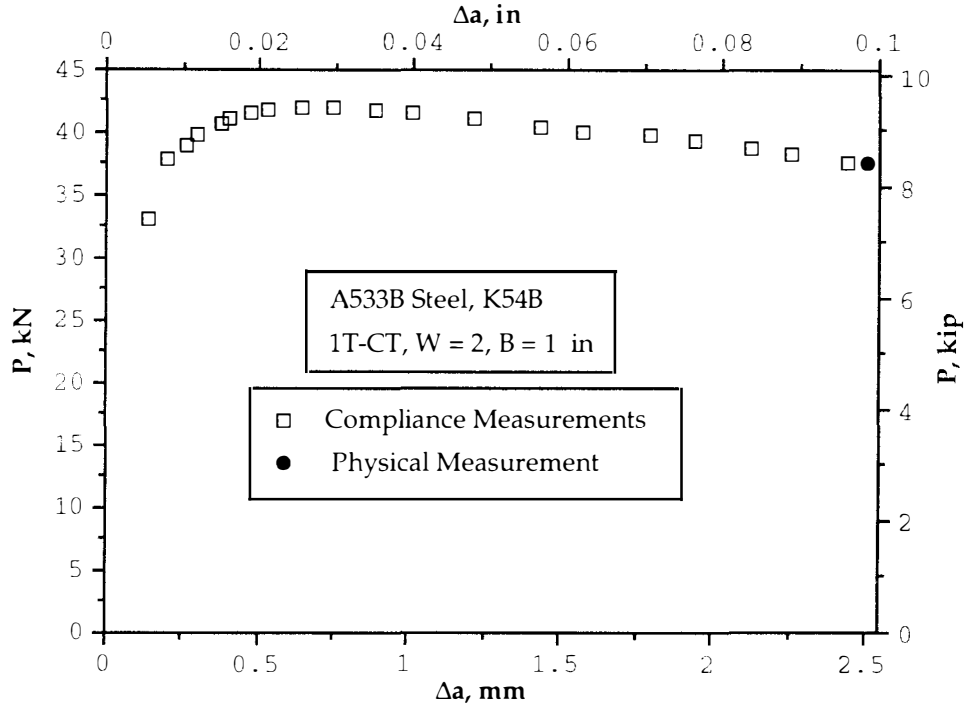

Fig. 4.14 - Load versus Crack Length for Specimen K54B, A533B Steel, Compact Specimen of W = 2, B = 1 in

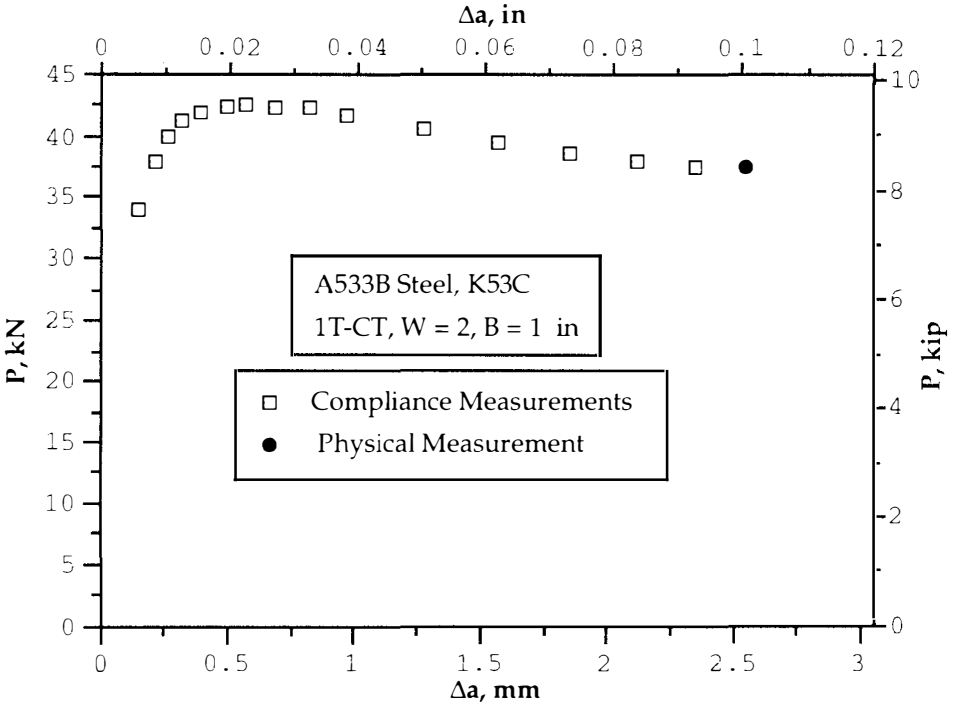

Fig. 4.15 - Load versus Crack Length for Specimen K53C, A533B Steel, Compact Specimen of W = 2, B = 1 in

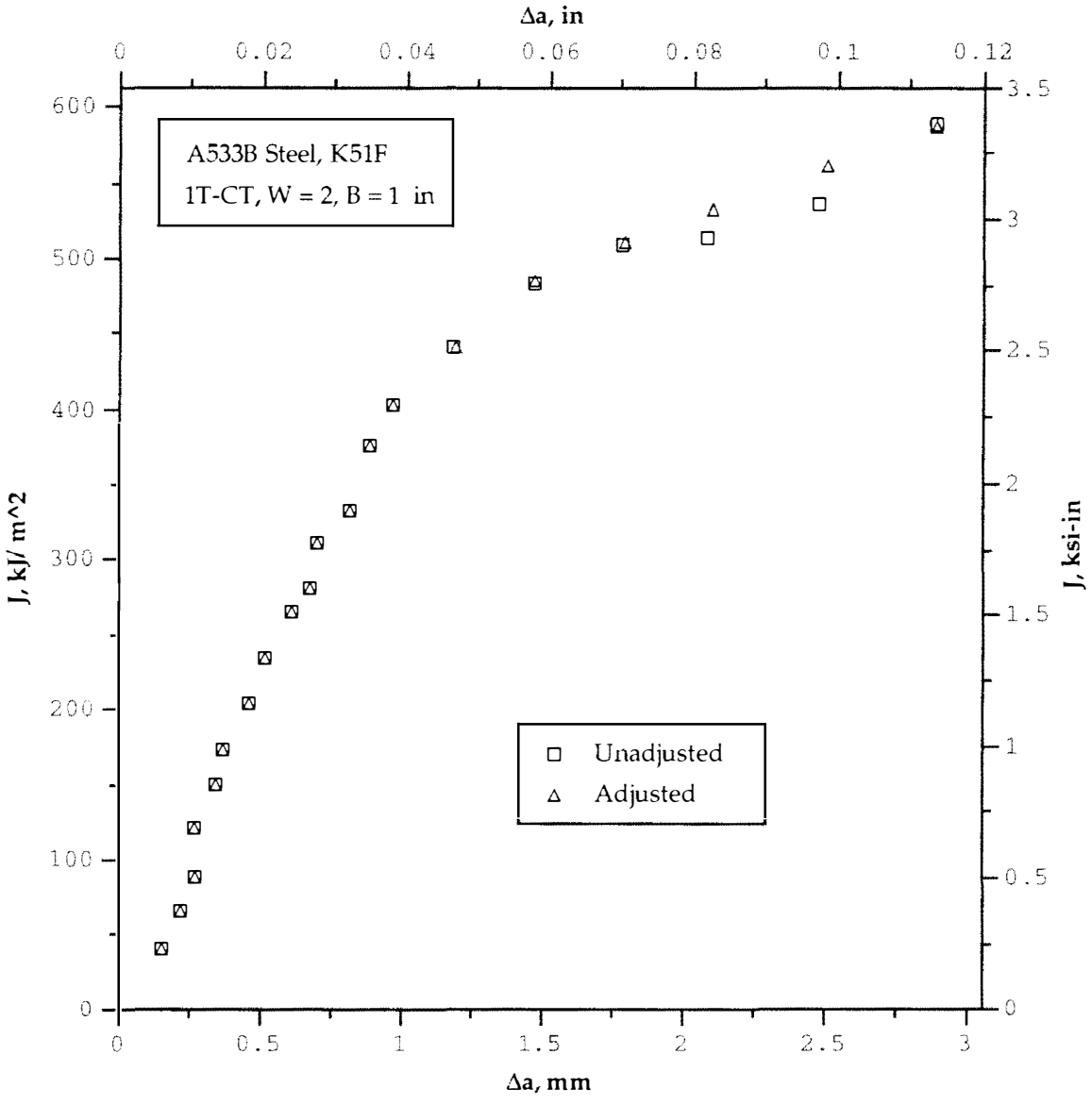

Fig. 4.16 - J-R Curves Developed from Load versus Crack Length by Method of Normalization Using L from P_{max}, Comparing Crack Length Adjusted versus Unadjusted, A533B Steel, Compact Specimen K51F of W = 2, B = 1 in

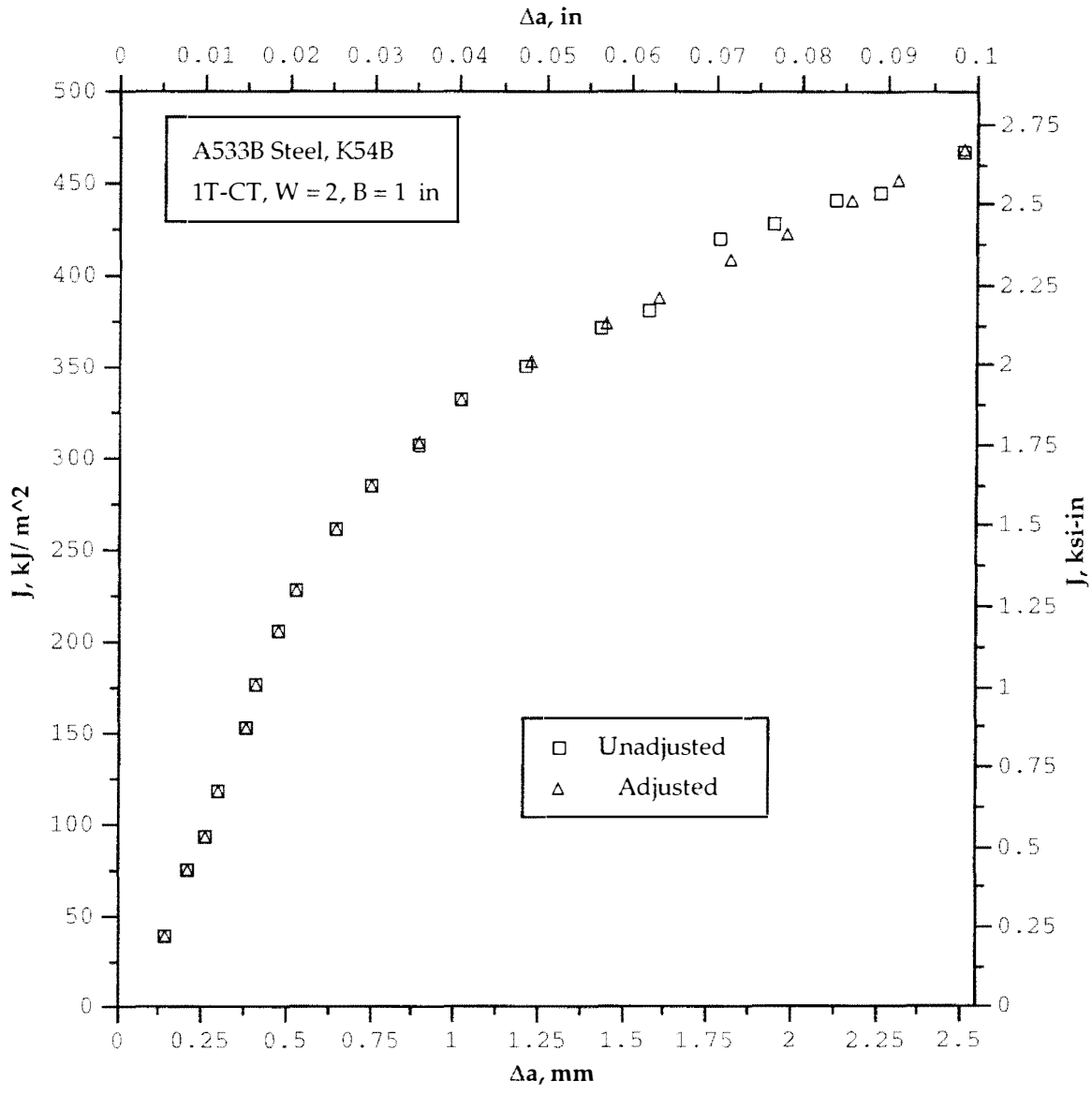

Fig. 4.17- J-R Curves Developed from Load versus Crack Length by Method of Normalization Using L from Pmax, Comparing Crack Length Adjusted versus Unadjusted, A533B Steel, Compact Specimen K54B of W = 2, B = 1 in

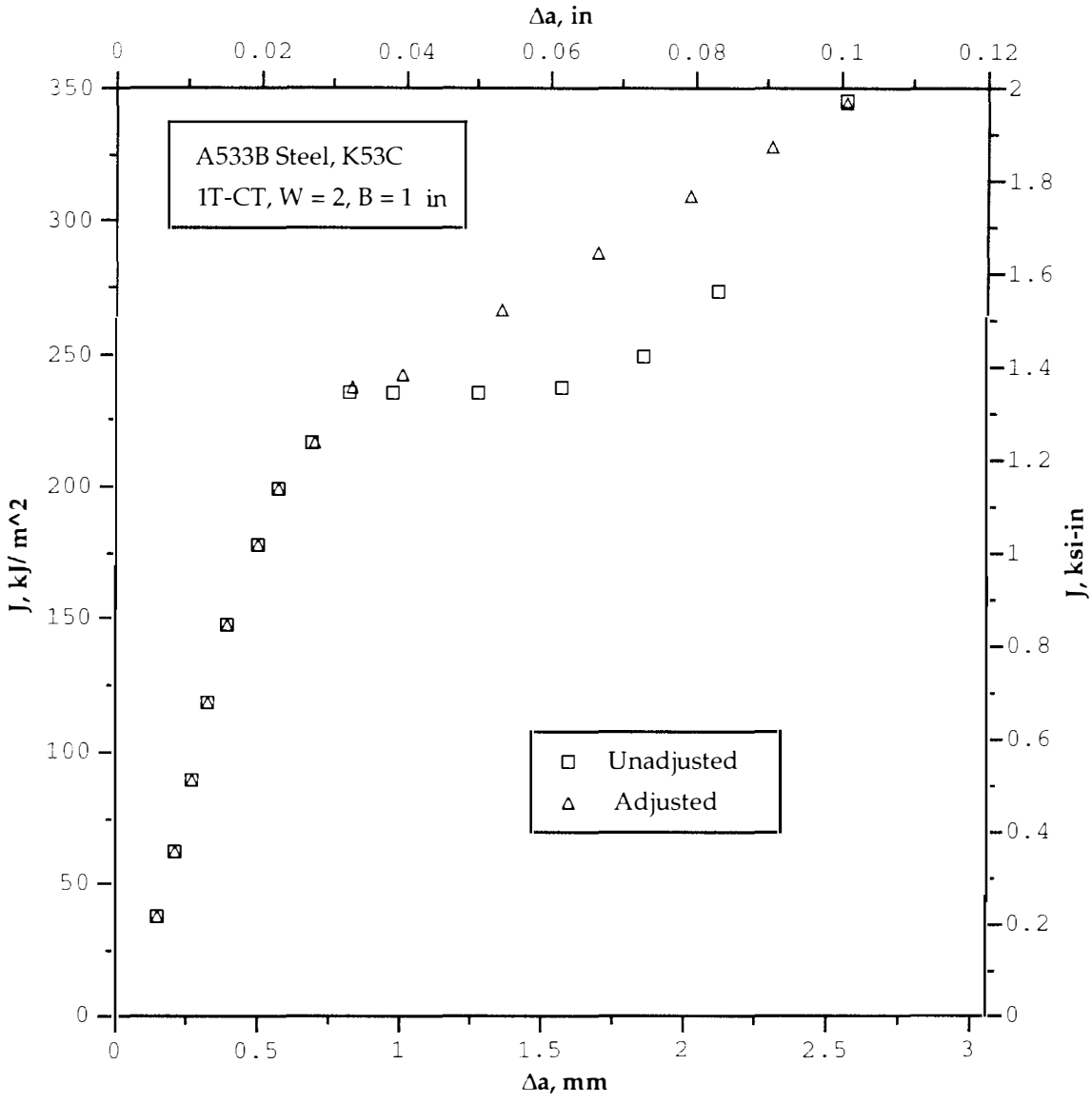

Fig. 4.18 - J-R Curves Developed from Load versus Crack Length by Method of Normalization Using L from P_{max}, Comparing Crack Length Adjusted versus Unadjusted, A533B Steel, Compact Specimen K53C of W = 2, B = 1 in

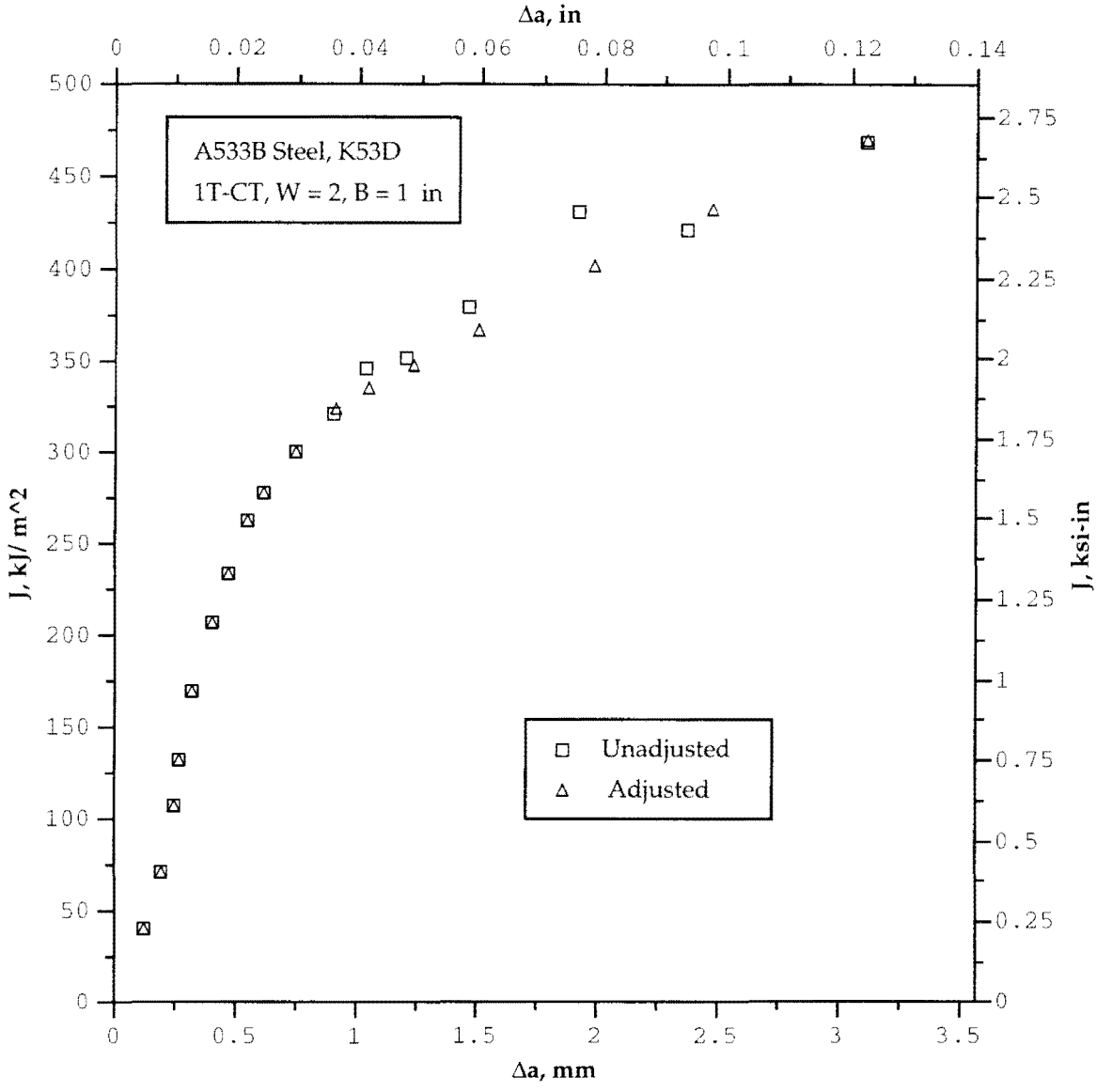

Fig. 4.19 - J-R Curves Developed from Load versus Crack Length by Method of Normalization Using L from P_{max}, Comparing Crack Length Adjusted versus Unadjusted, A533B Steel, Compact Specimen K53D of W = 2, B = 1 in

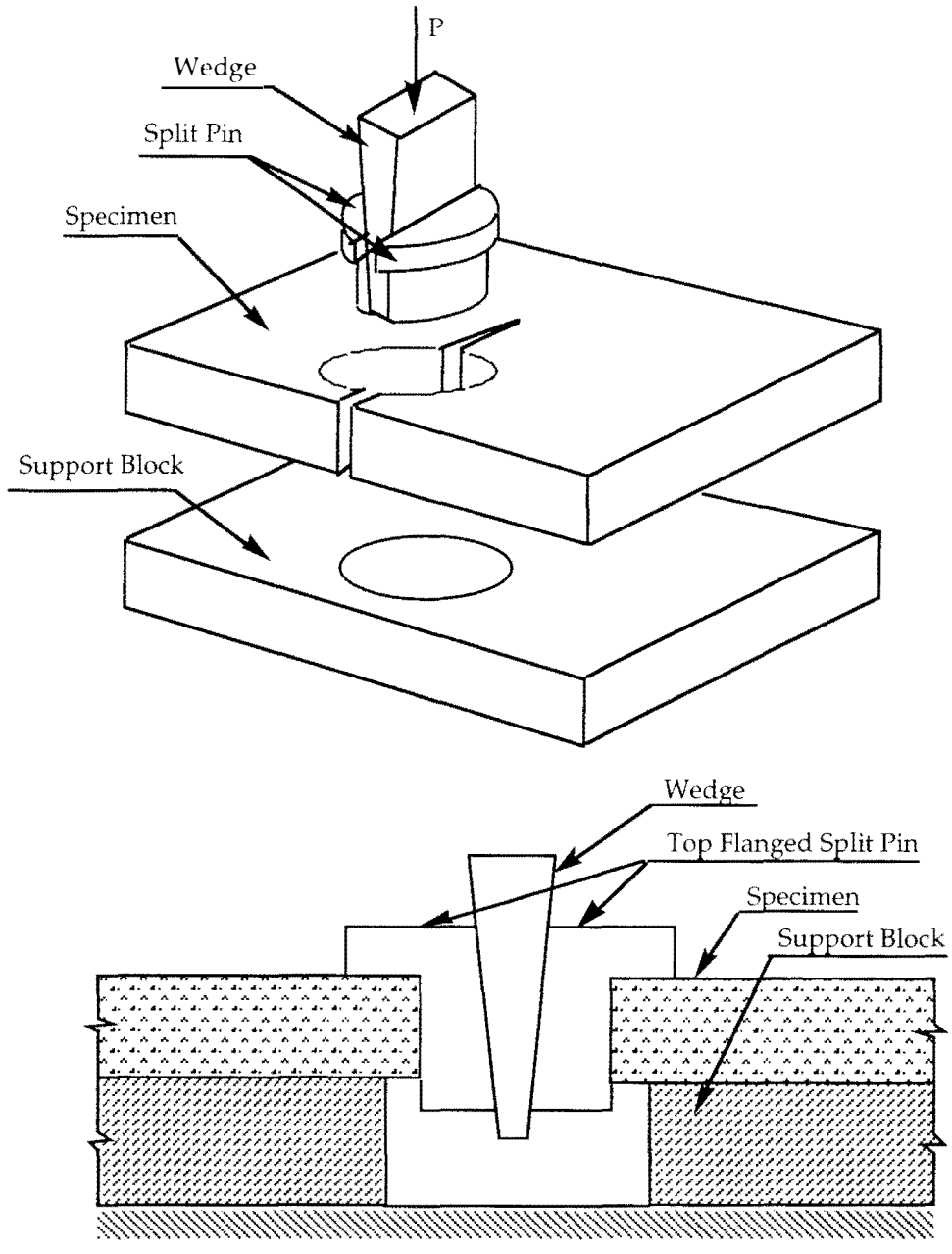

Fig. 5.1 Schematic of Pictorial and Sectional Views Showing The Arrangement of the Crack-Line-Wedge-Loaded Specimen Test

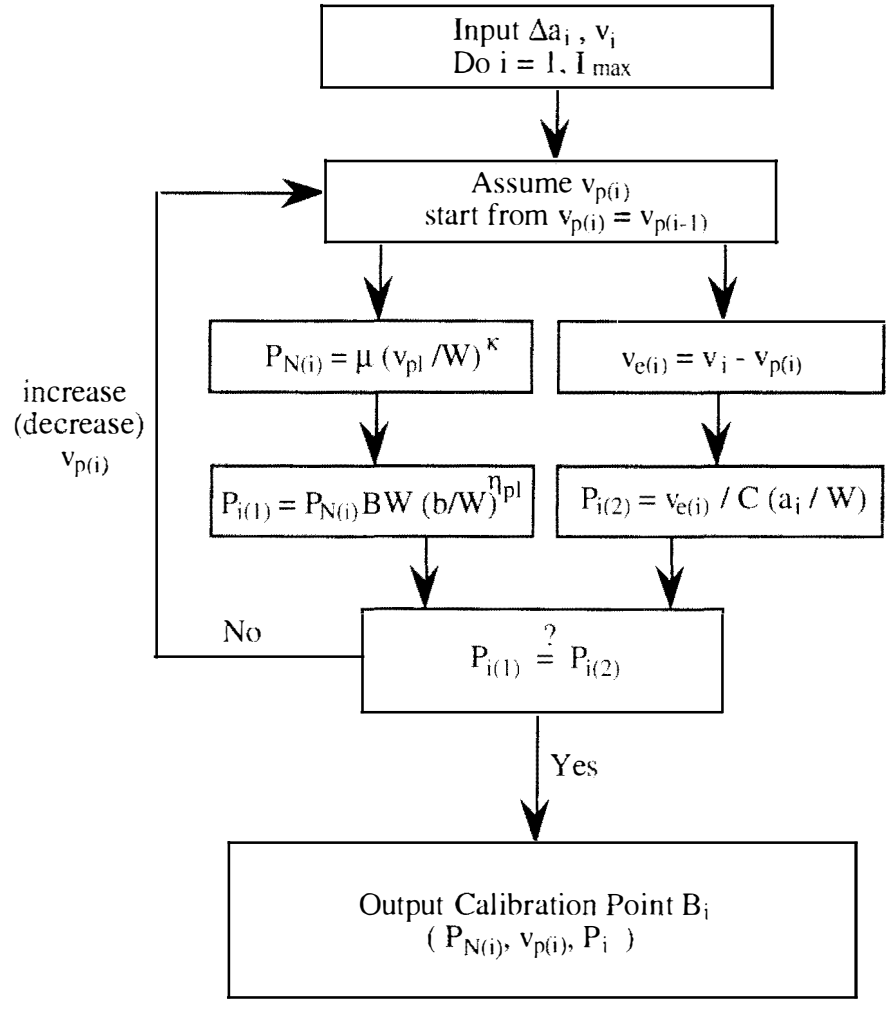

Fig. 5.2 - A Flow Chart for Solving Calibration Point Bi from Displacement versus Crack Length Using Power Law Assumption

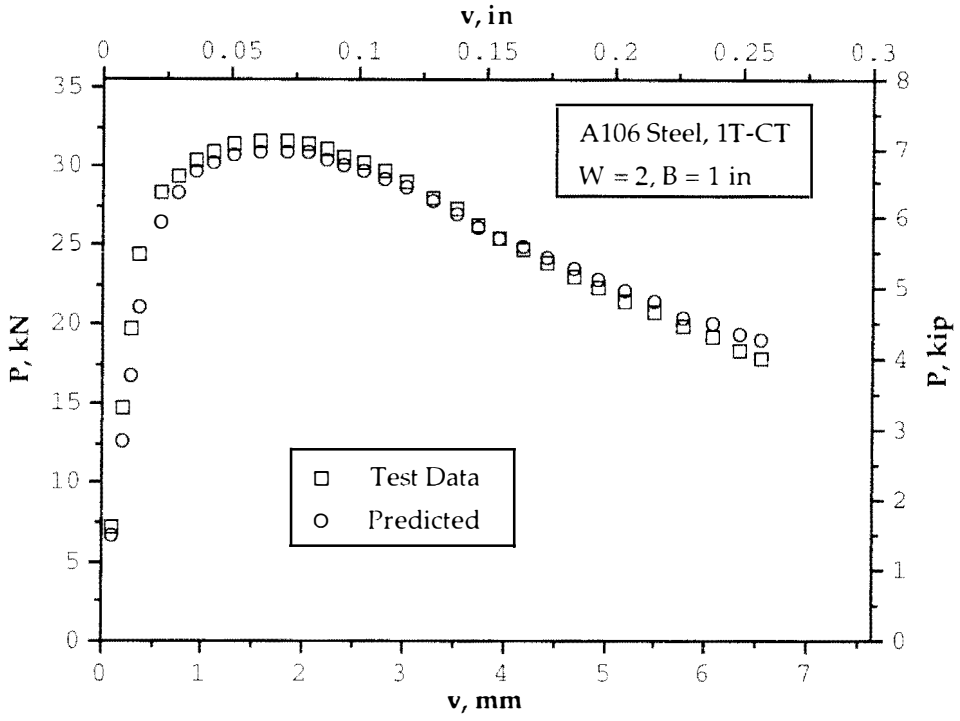

Fig. 5.3a Load versus Displacement Predicted by Normalization Method from v-Δa Compared with the Test Data, A106 Steel, Compact Specimen

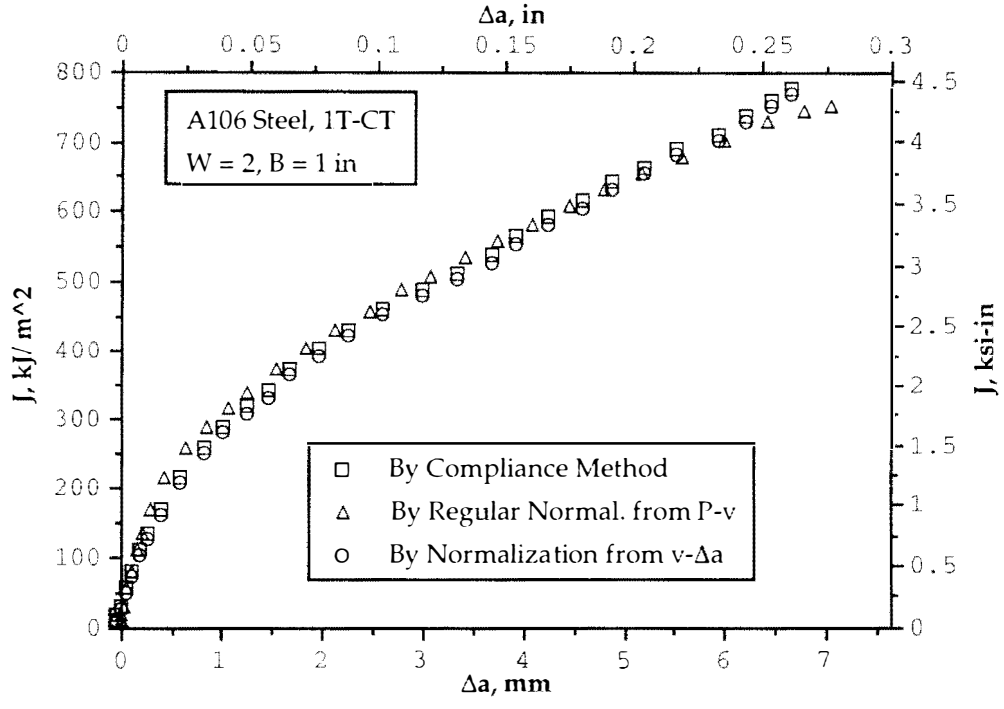

Fig. 5.3b J-R Curve Developed from v-Δa by Method of Normalization Compared with J-R Curve Results from Test Data and from Regular Normalization Method, A106 Steel, Compact Specimen

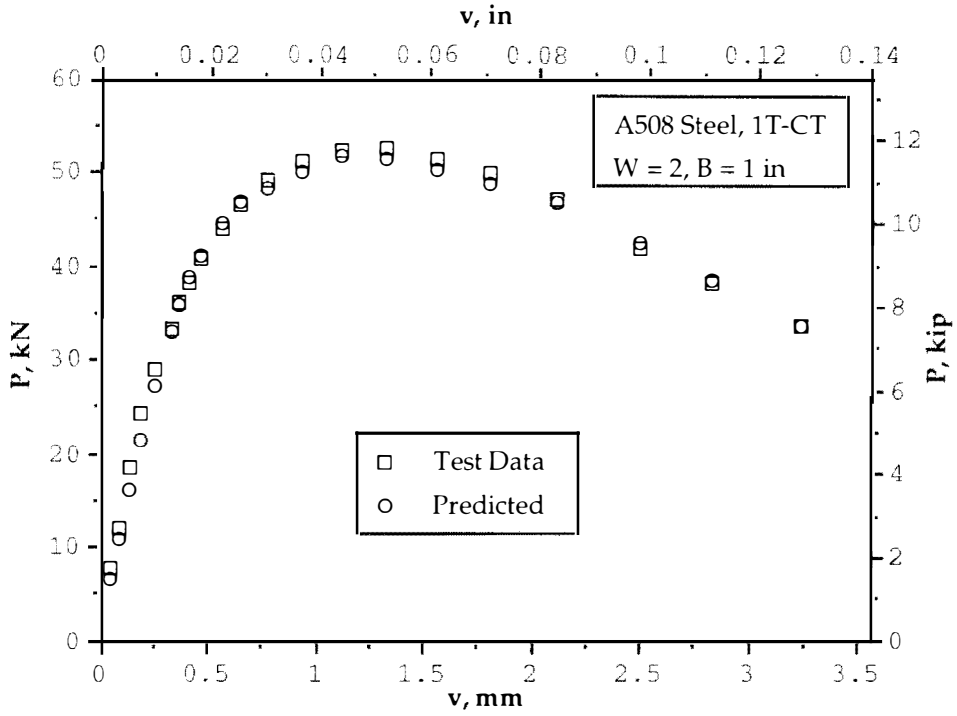

Fig. 5.4a Load versus Displacement Predicted by Normalization Method from v-Δa Compared with the Test Data, A508 Steel, Compact Specimen

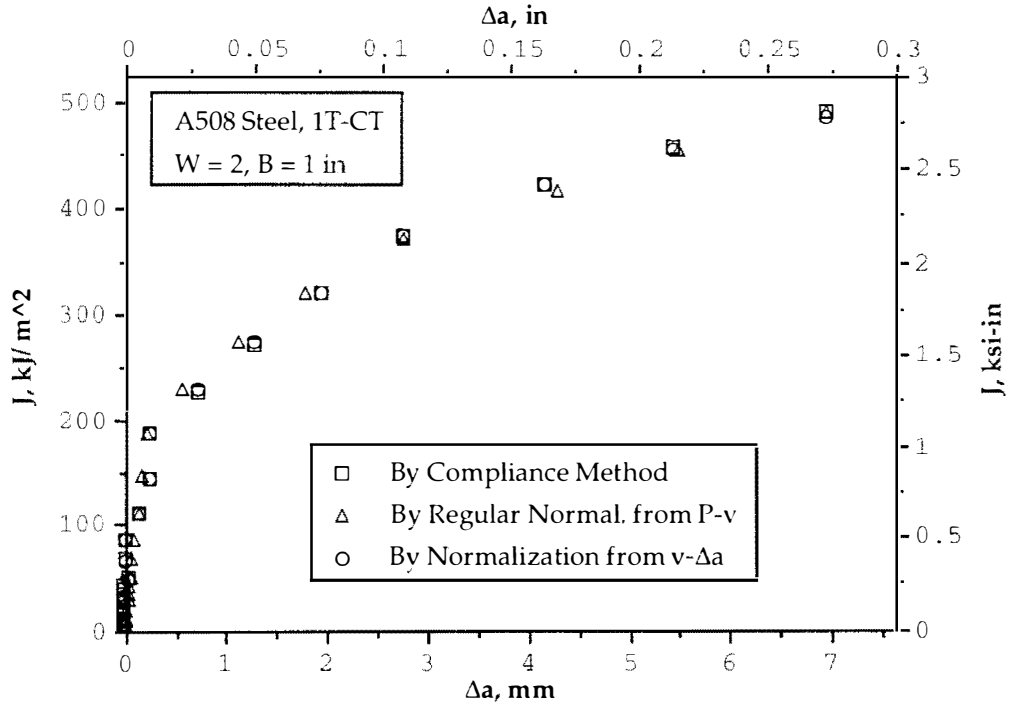

Fig. 5.4b J-R Curve Developed from v-Δa by Method of Normalization Compared with J-R Curve Results from Test Data and from Regular Normalization Method, A508 Steel, Compact Specimen

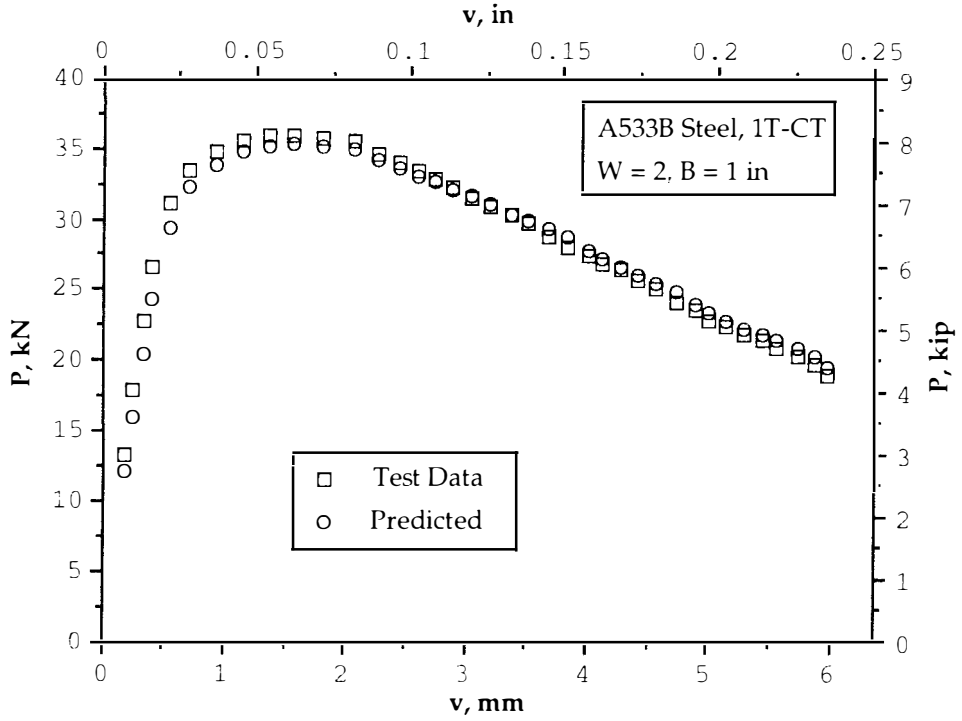

Fig. 5.5a Load versus Displacement Predicted by Normalization Method from v-Δa Compared with the Test Data, A533B Steel, Compact Specimen

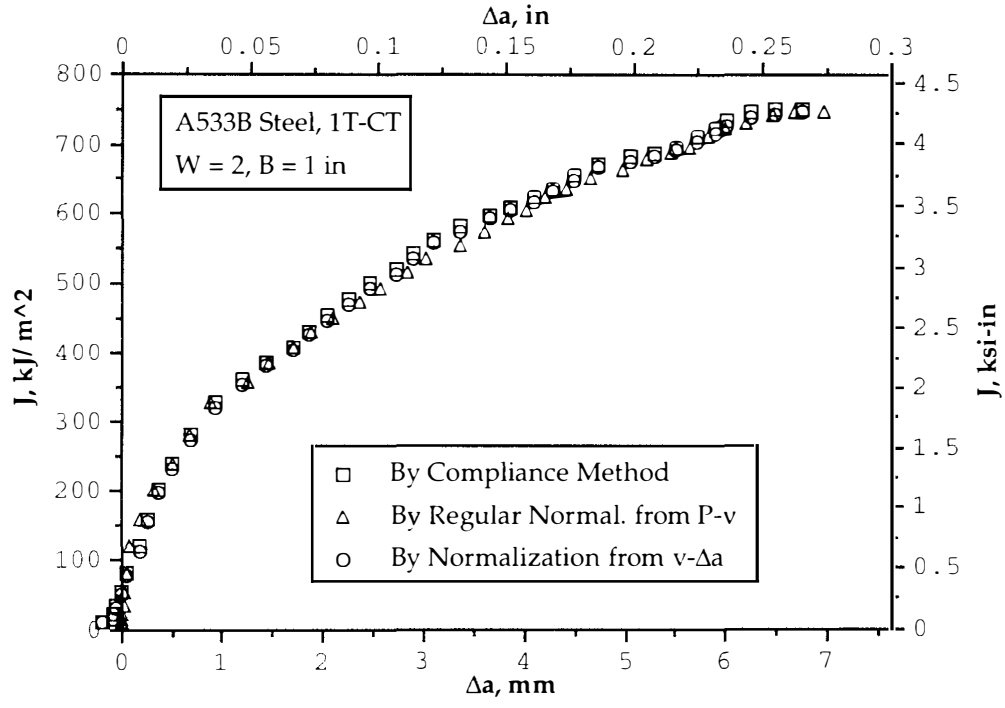

Fig. 5.5b J-R Curve Developed from v-Δa by Method of Normalization Compared with J-R Curve Results from Test Data and from Regular Normalization Method, A533B Steel, Compact Specimen

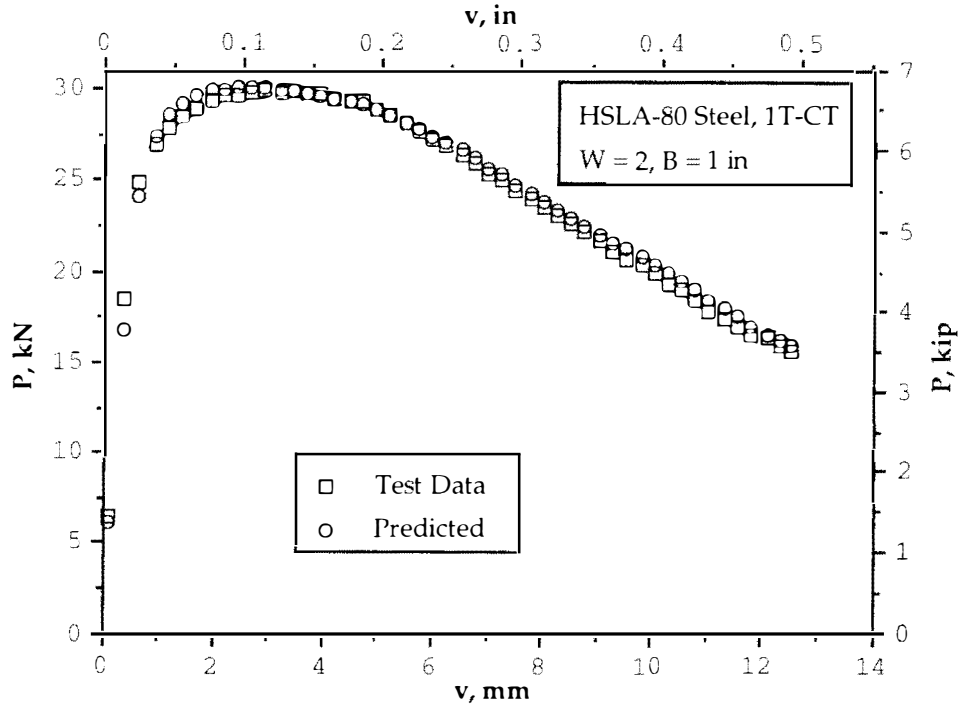

Fig. 5.6a Load versus Displacement Predicted by Normalization Method from v-Δa Compared with the Test Data, HSLA-80 Steel, Compact Specimen

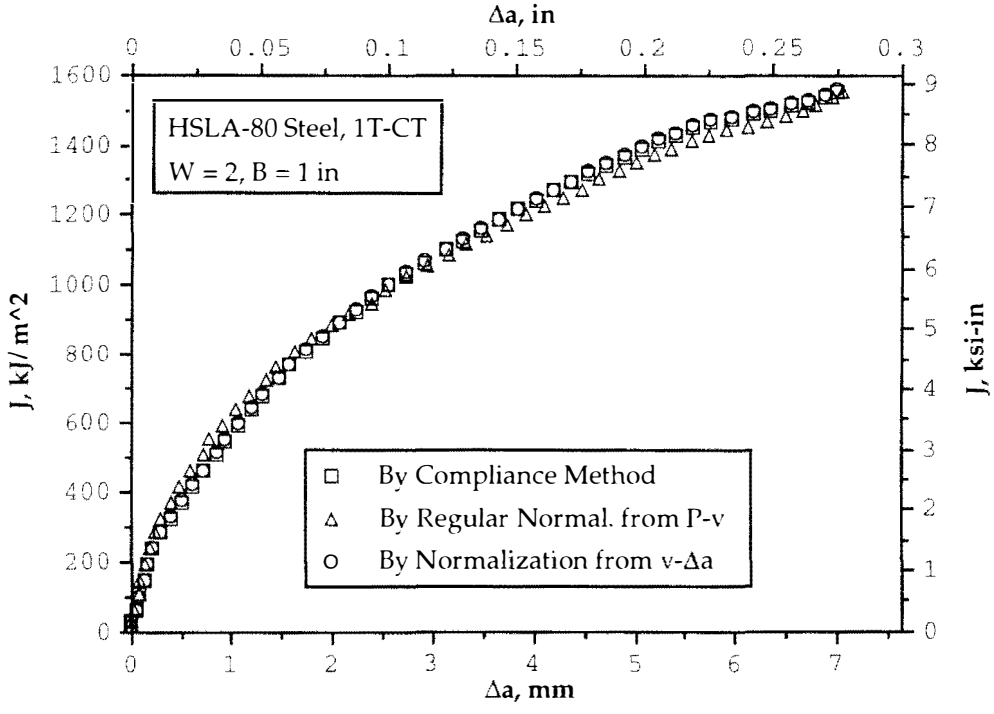

Fig. 5.6b J-R Curve Developed from v-Δa by Method of Normalization Compared with J-R Curve Results from Test Data and from Regular Normalization Method, HSLA-80 Steel, Compact Specimen

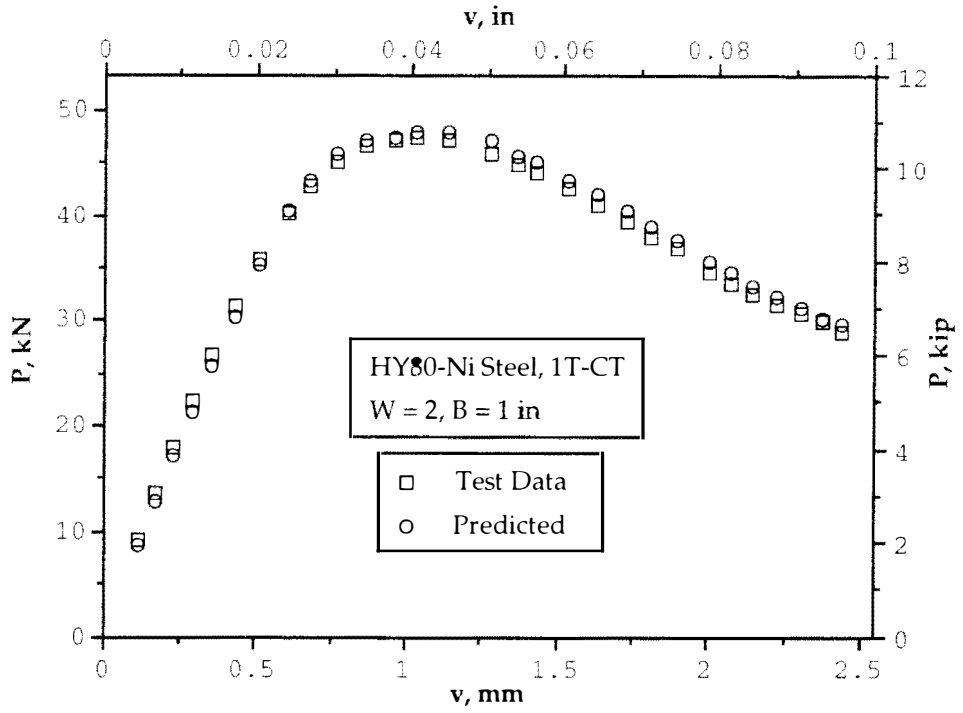

Fig. 5.7a Load versus Displacement Predicted by Normalization Method from v-Δa Compared with the Test Data, HY80-Ni Steel, Compact Specimen

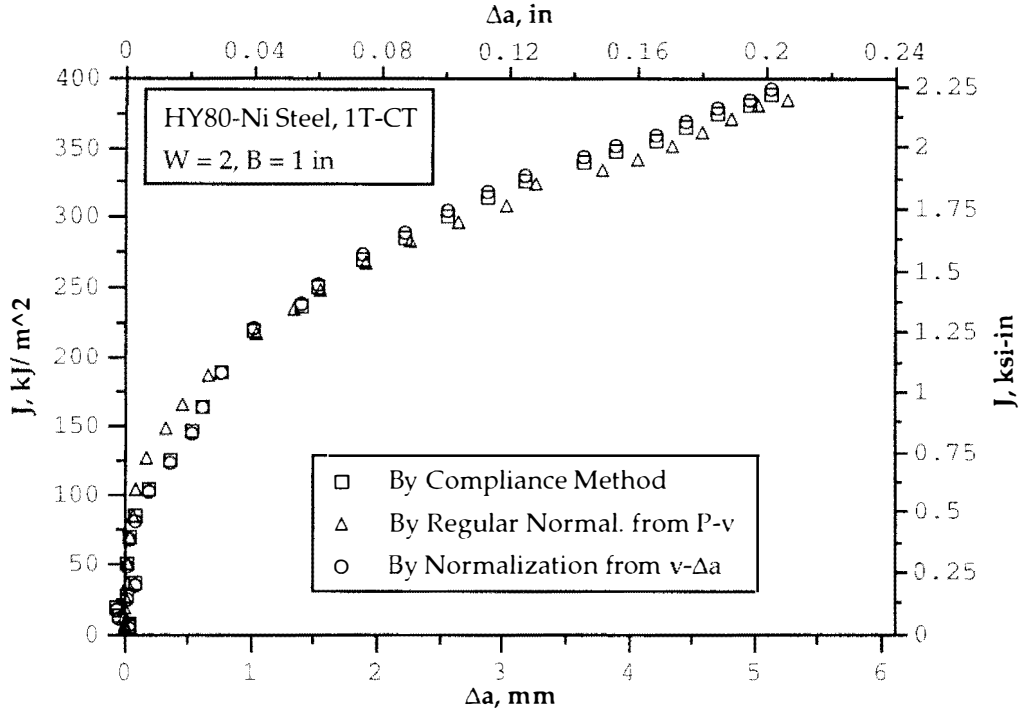

Fig. 5.7b J-R Curve Developed from v-Δa by Method of Normalization Compared with J-R Curve Results from Test Data and from Regular Normalization Method, HY80-Ni Steel, Compact Specimen

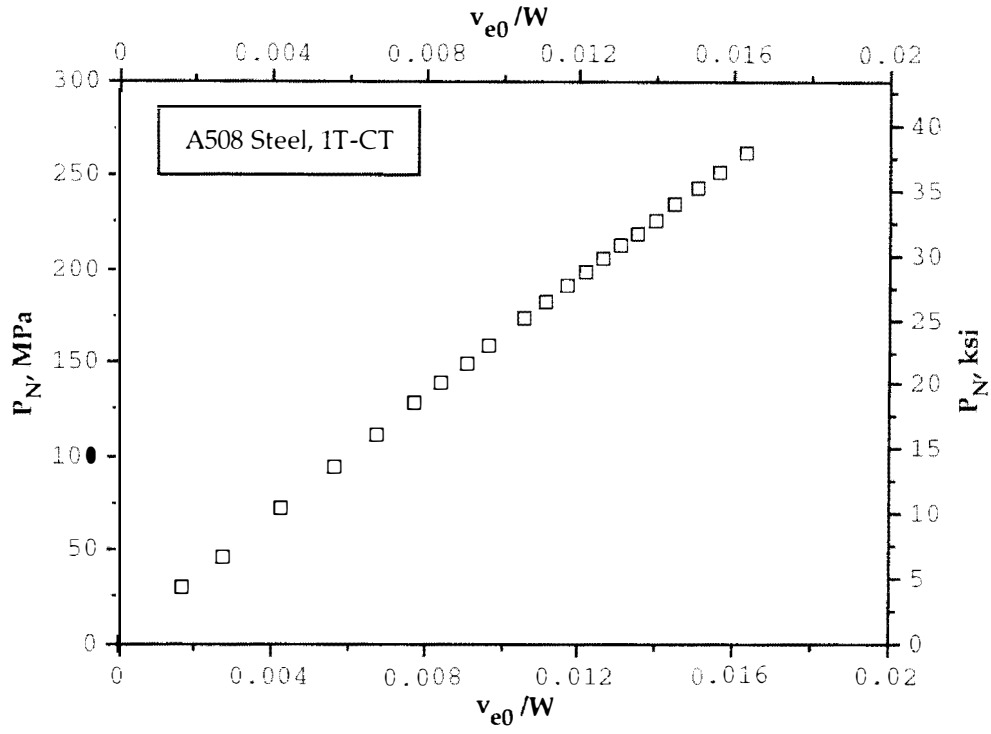

Fig. 5.8 - Normalized Load versus Front Face Elastic Displacement Showing a Linear Relationship, A508 Steel

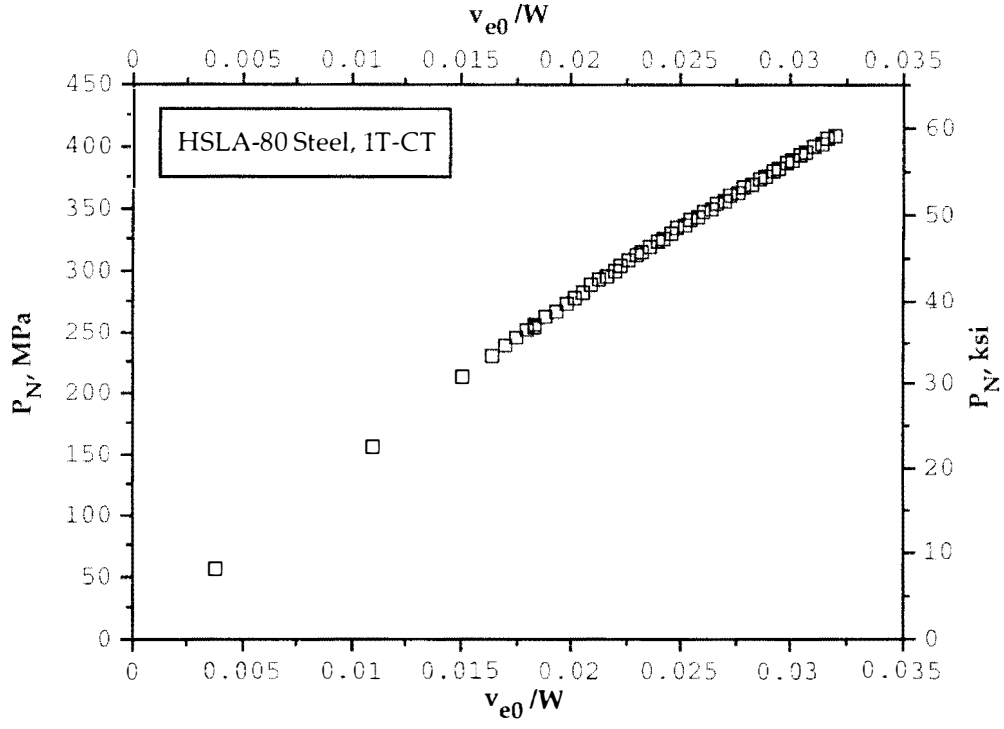

Fig. 5.9 - Normalized Load versus Front Face Elastic Displacement Showing a Linear Relationship, HSLA-80 Steel

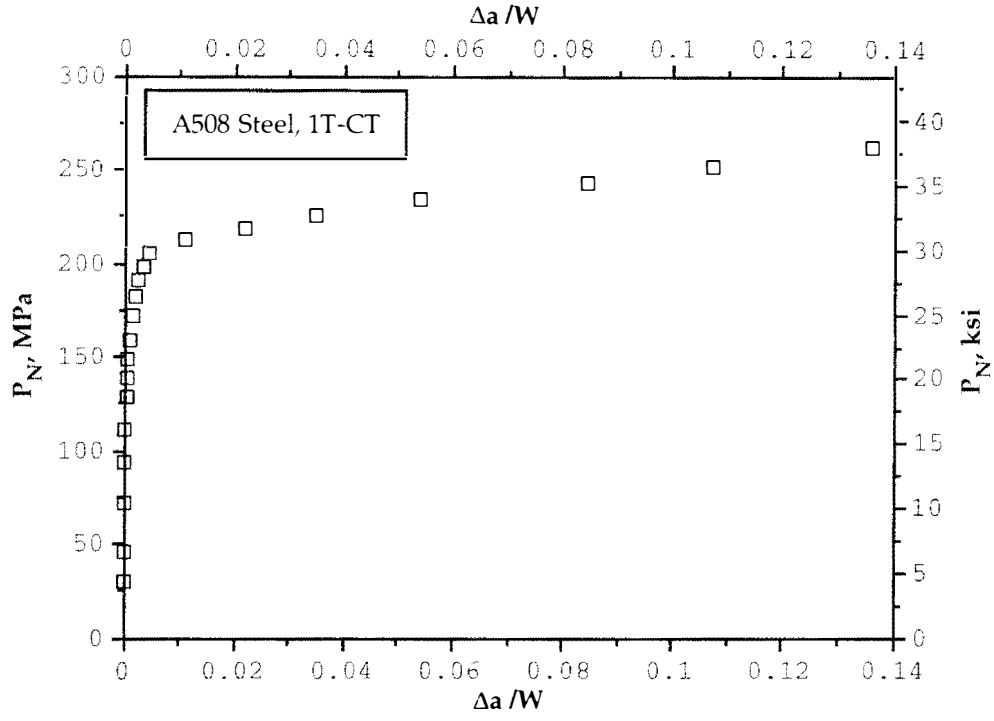

Fig. 5.10 - Normalized Load versus Normalized Crack Length for A508 Steel Showing a LMN Functional Relationship

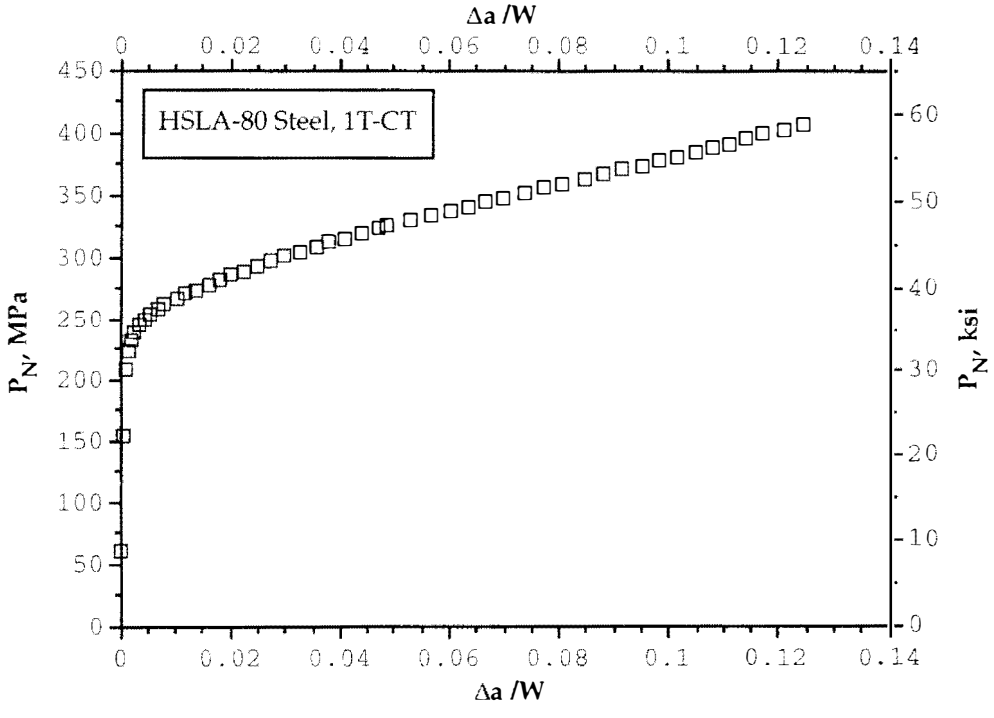

Fig. 5.11 - Normalized Load versus Normalized Crack Length for HSLA-80 Steel Showing a LMN Functional Relationship

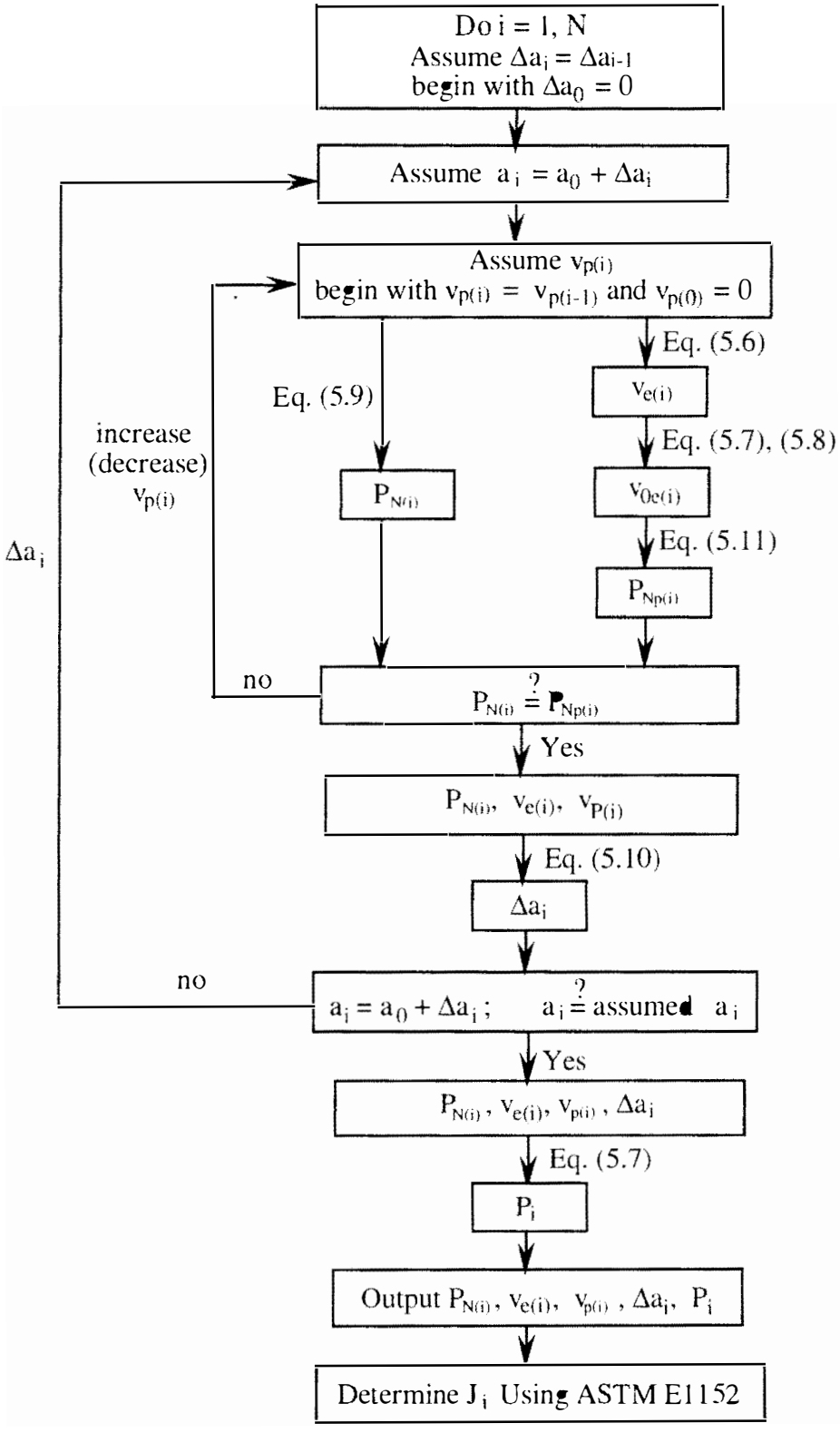

Fig. 5.12 - A Flow Chart for J-R Curve Determination from Only Displacement by Predicting Load and Crack Length Measurements

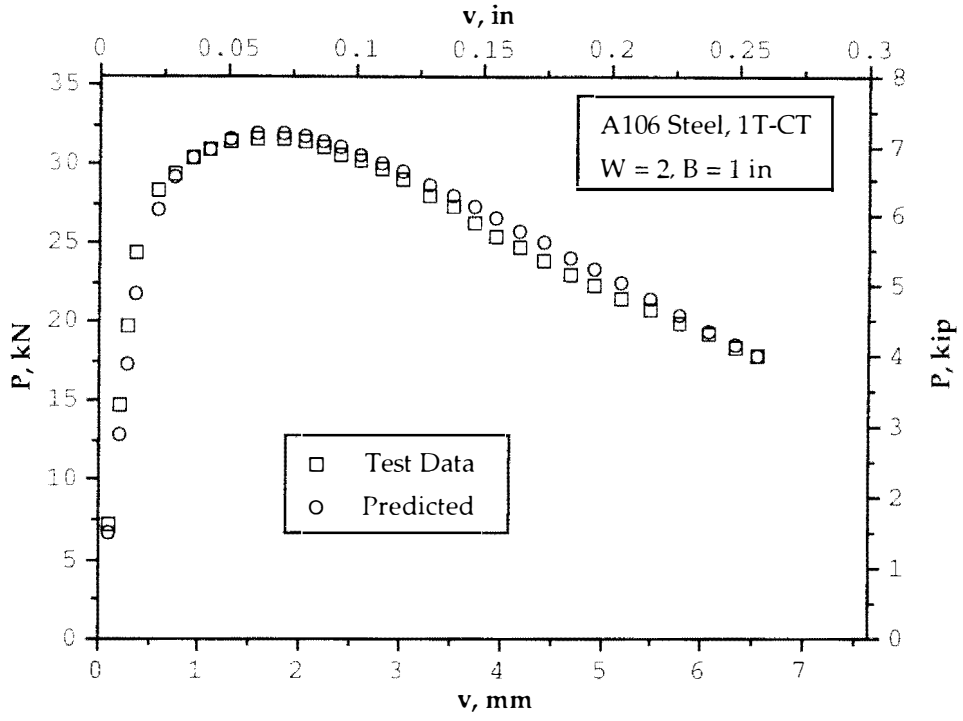

Fig. 5.13a Load versus Displacement Predicted by Normalization Method from Only v Compared with the Test Data, A106 Steel, Compact Specimen

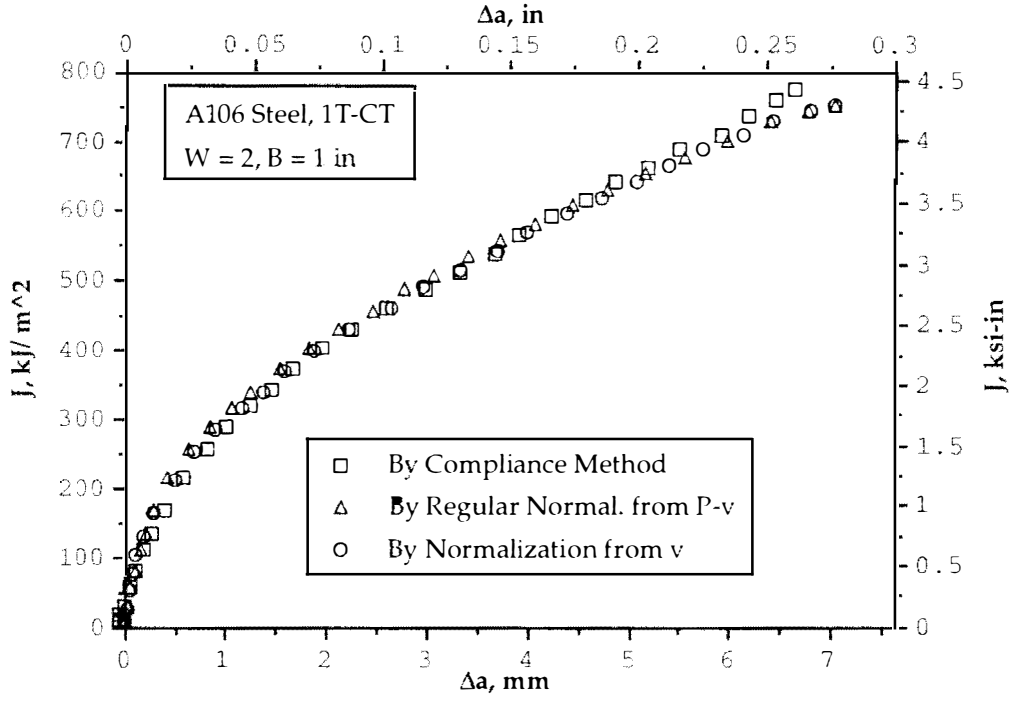

Fig. 5.13b J-R Curve Developed from Only v by Method of Normalization Compared with J-R Curve Results from Standard Test Method and from Regular Normalization Method, A106 Steel, Compact Specimen

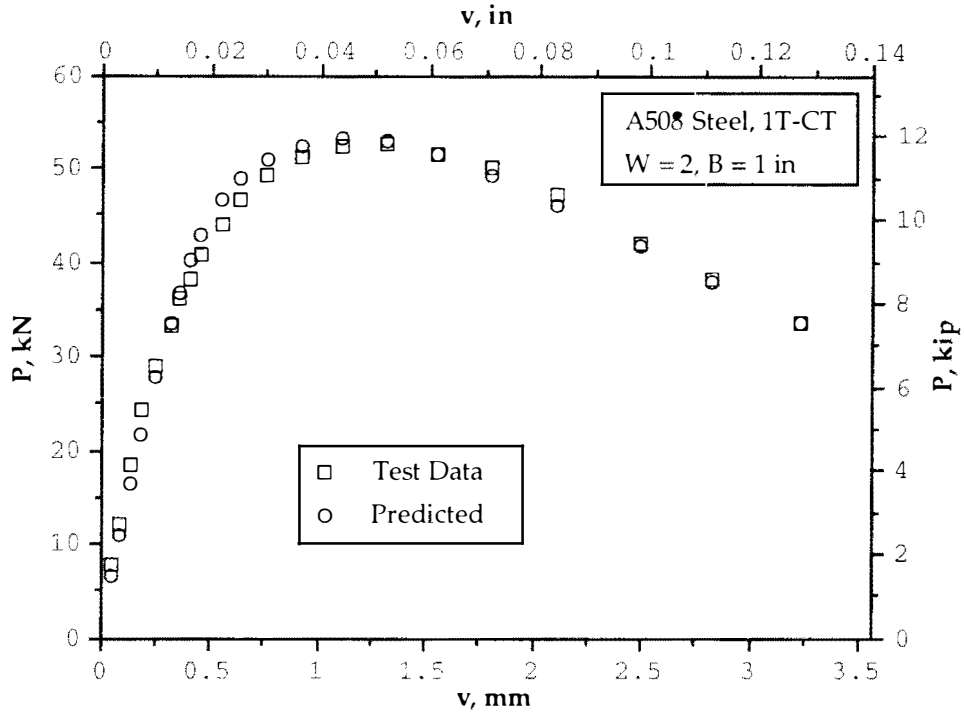

Fig. 5.14a Load versus Displacement Predicted by Normalization Method from Only v Compared with the Test Data, A508 Steel, Compact Specimen

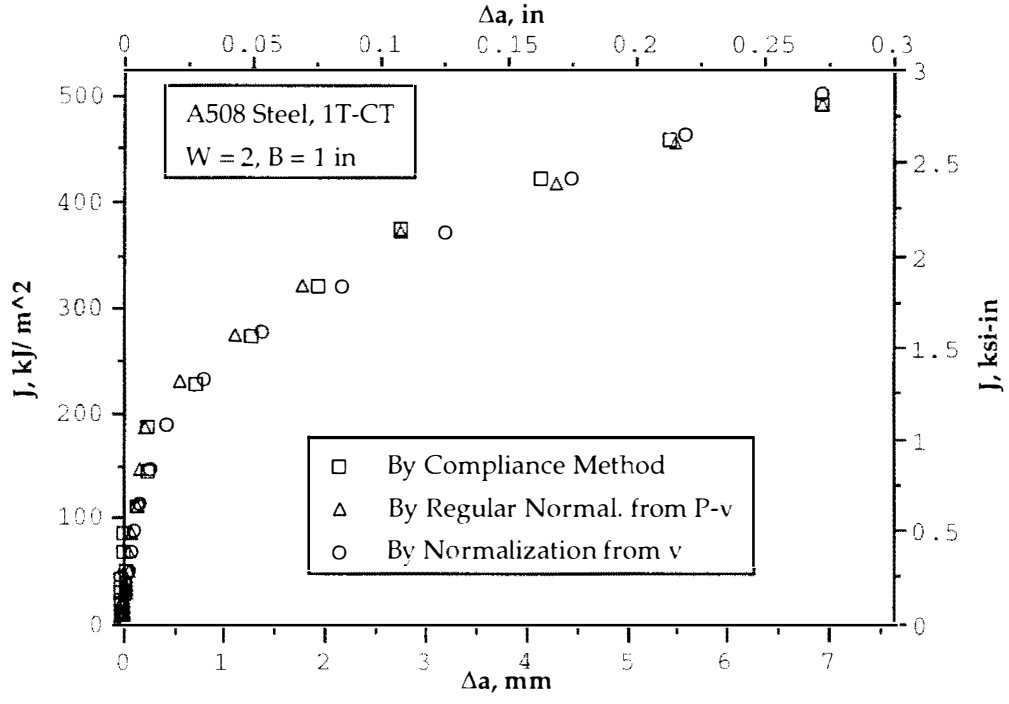

Fig. 5.14b J-R Curve Developed from Only v by Method of Normalization Compared with J-R Curve Results from Standard Test Method and from Regular Normalization Method, A508 Steel, Compact Specimen

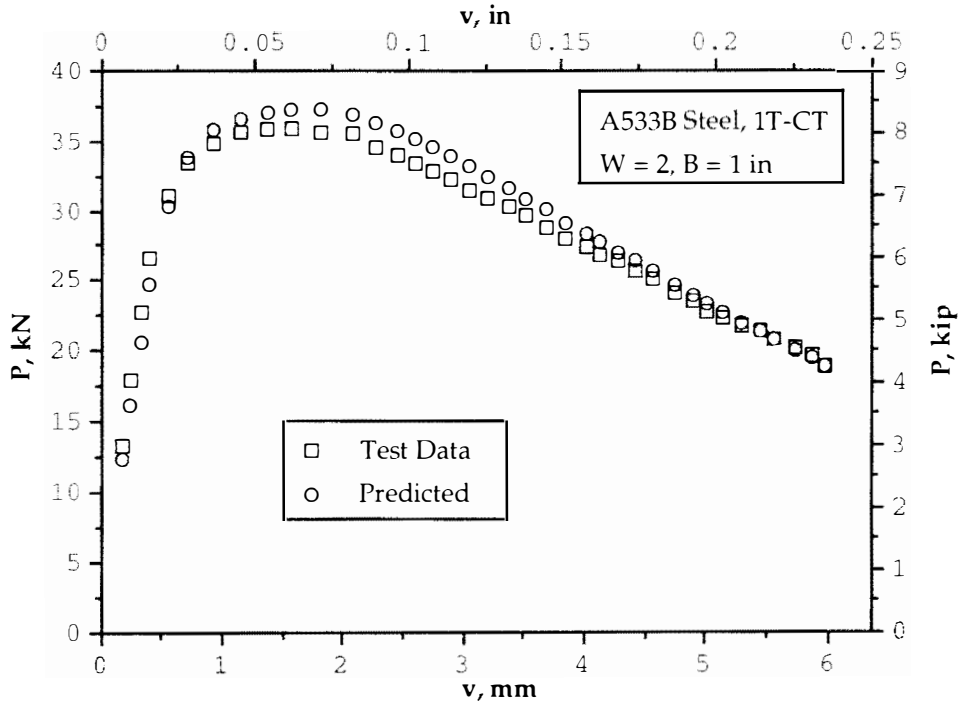

Fig. 5.15a Load versus Displacement Predicted by Normalization Method from Only v Compared with the Test Data, A533B Steel, Compact Specimen

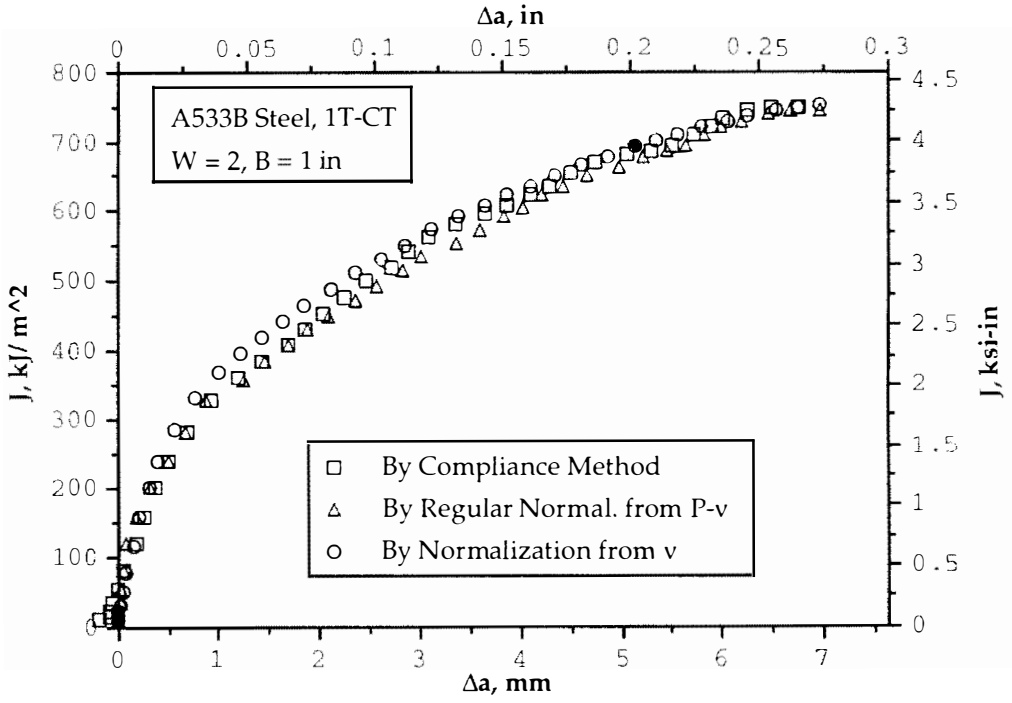

Fig. 5.15b J-R Curve Developed from Only v by Method of Normalization Compared with J-R Curve Results from Standard Test Method and from Regular Normalization Method, A533B Steel, Compact Specimen

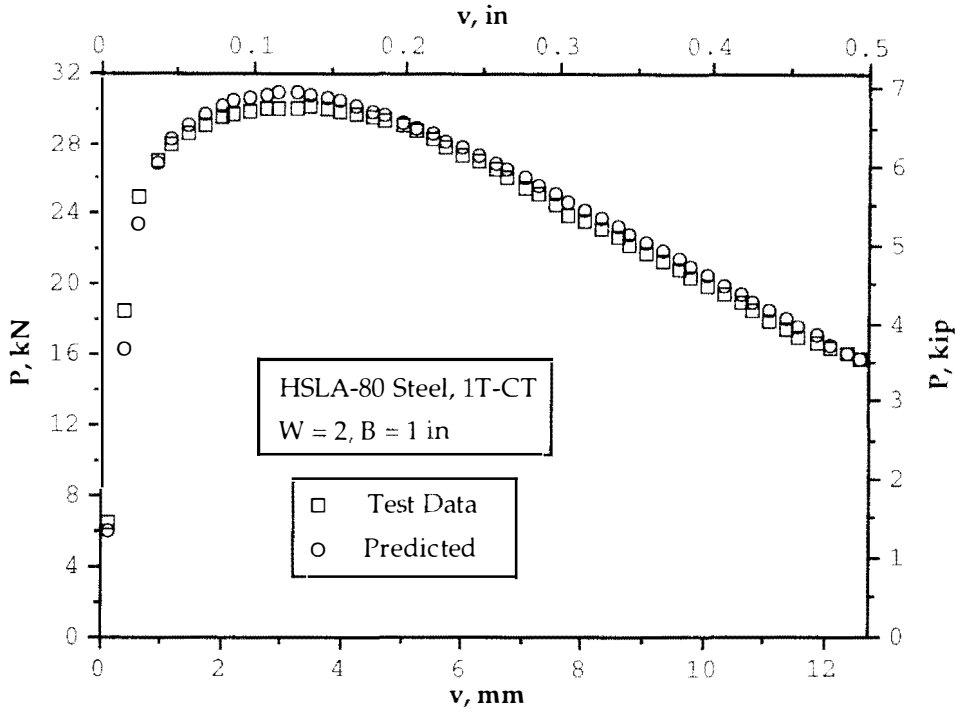

Fig. 5.16a Load versus Displacement Predicted by Normalization Method from Only v Compared with the Test Data, HSLA-80 Steel, Compact Specimen

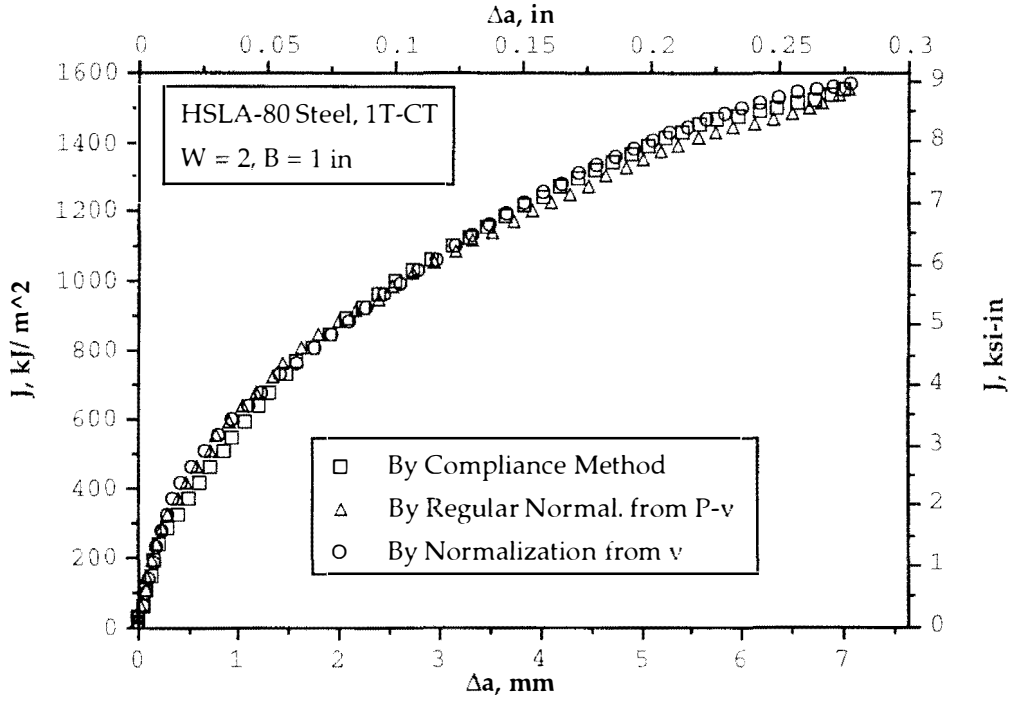

Fig. 5.16b J-R Curve Developed from Only v by Method of Normalization Compared with J-R Curve Results from Standard Test Method and from Regular Normalization Method, HSLA-80 Steel, Compact Specimen

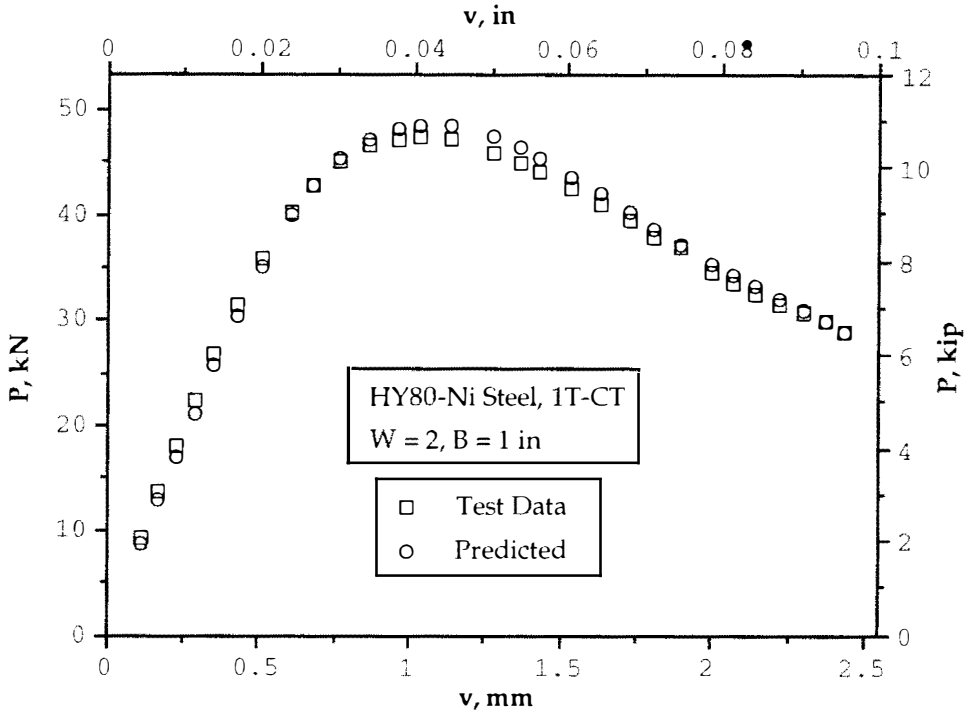

Fig. 5.17a Load versus Displacement Predicted by Normalization Method from Only v Compared with the Test Data, HY80-Ni Steel, Compact Specimen

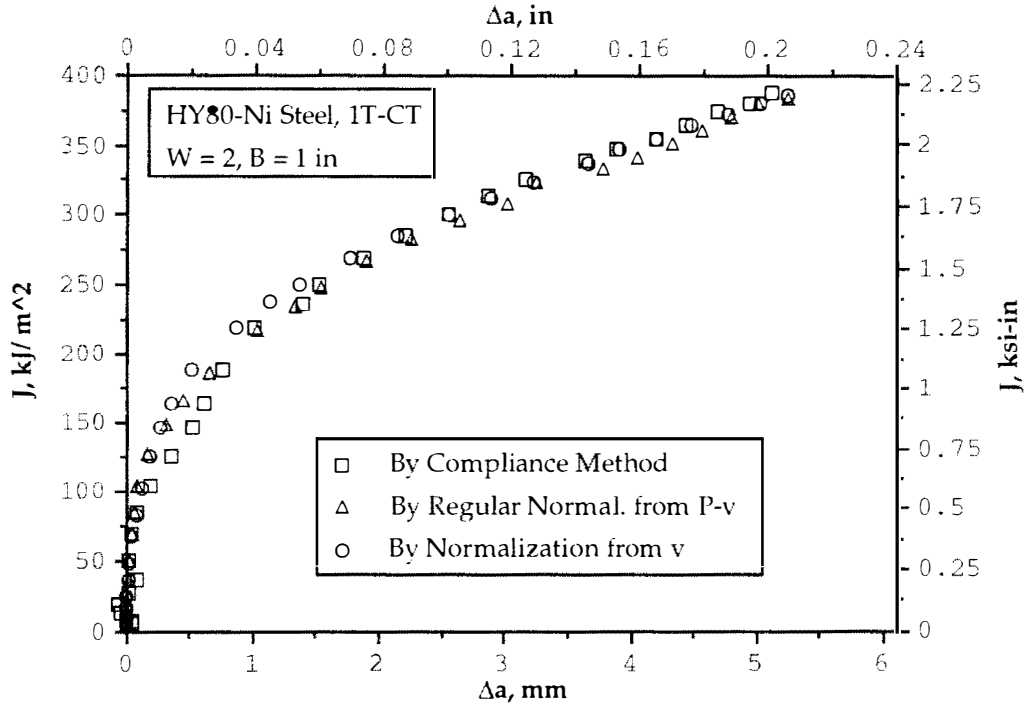

Fig. 5.17b J-R Curve Developed from Only v by Method of Normalization Compared with J-R Curve Results from Standard Test Method and from Regular Normalization Method, HY80-Ni Steel, Compact Specimen

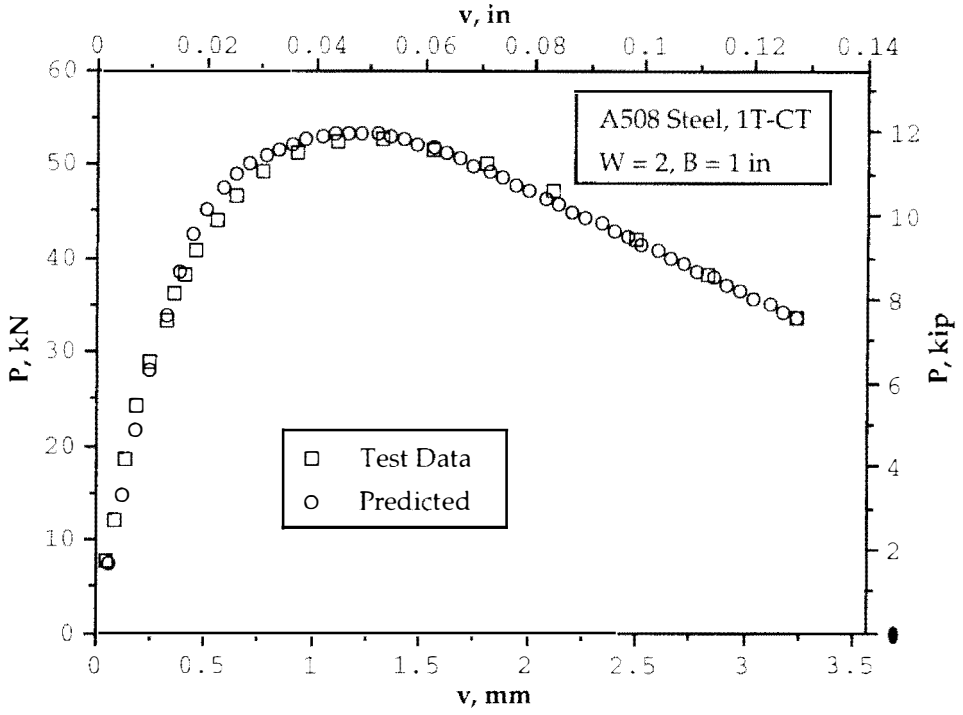

Fig. 5.18a Load versus Displacement Predicted by Normalization Method from Final Point Compared with the Test Data, A508 Steel, CT Specimen

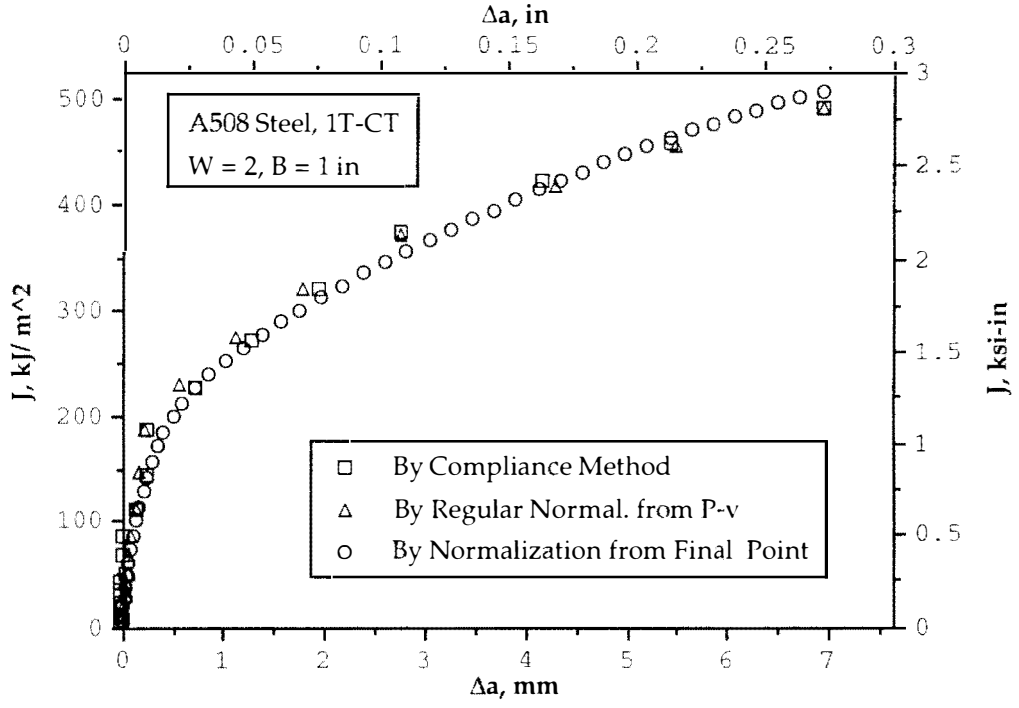

Fig. 5.18b J-R Curve Developed from Final Calibration Point by Method of Normalization Compared with J-R Curve Results from Standard Test Method and from Regular Normalization Method, A508 Steel, CT Specimen

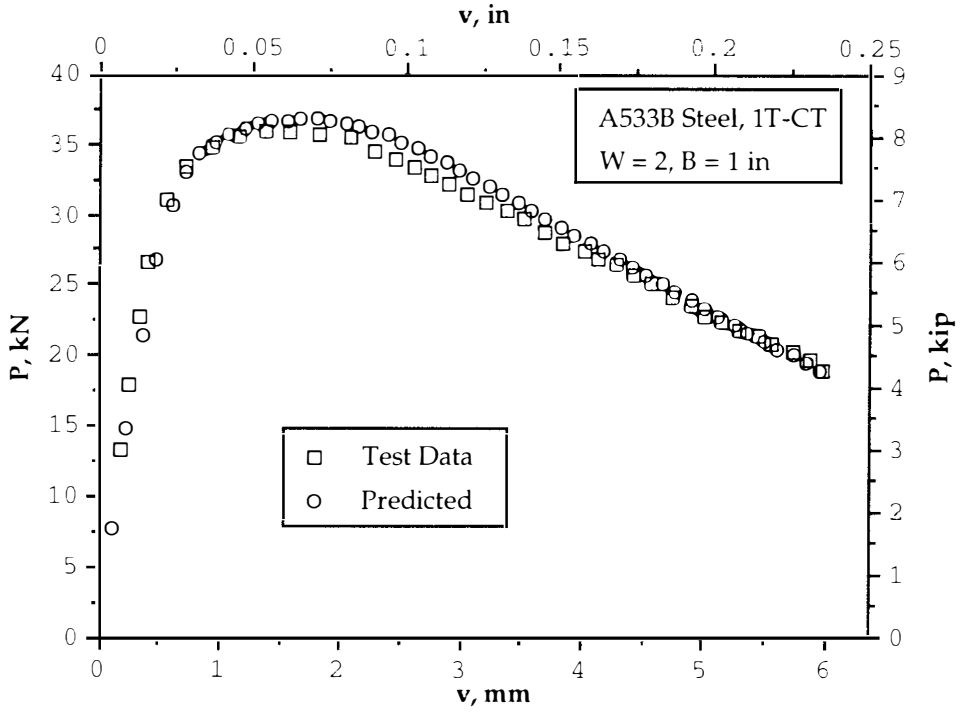

Fig. 5.19a Load versus Displacement Predicted by Normalization Method from Final Point Compared with the Test Data, A533B Steel, CT Specimen

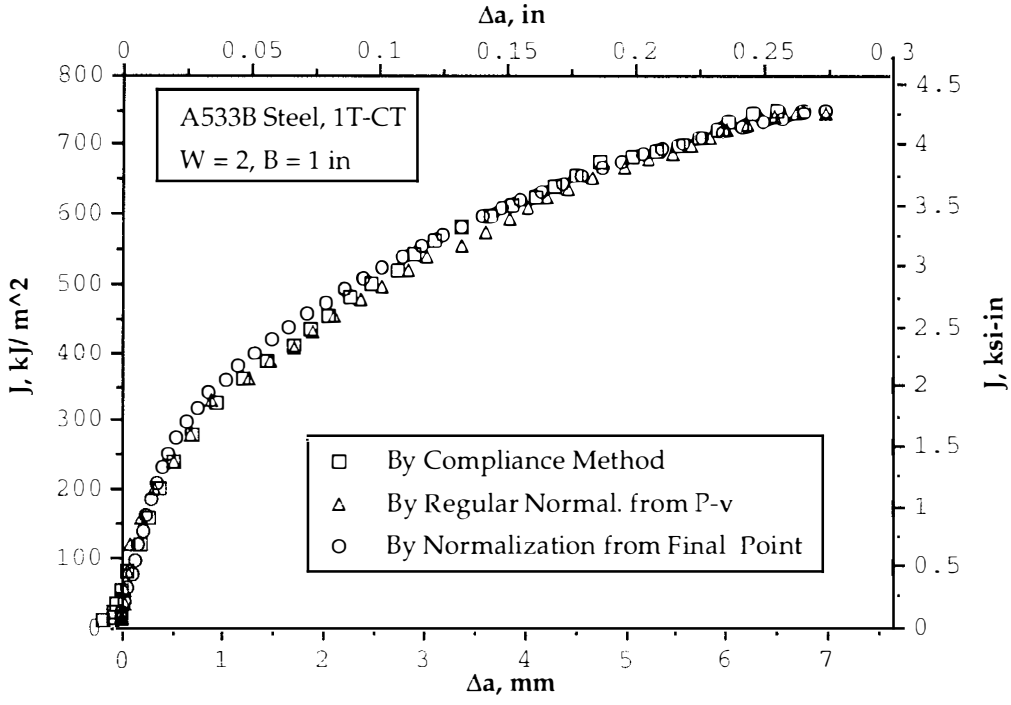

Fig. 5.19b J-R Curve Developed from Final Calibration Point by Method of Normalization Compared with J-R Curve Results from Standard Test Method and from Regular Normalization Method, A533B Steel, CT Specimen

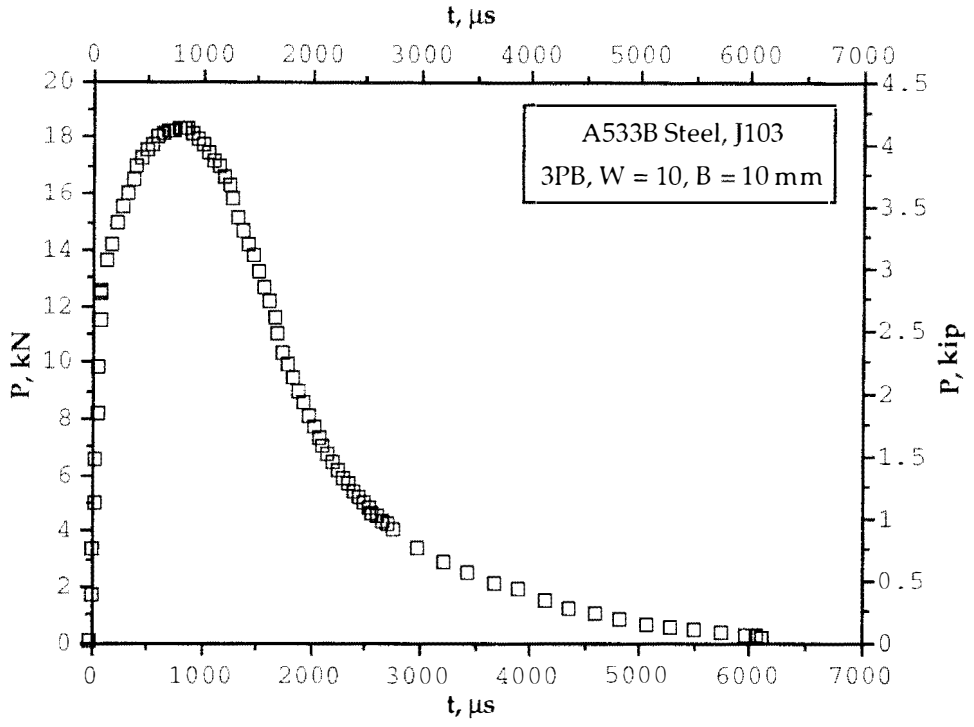

Fig. 6.1a Load versus Time Determined from Charpy Impact Test A533B Steel, Three-Point Bend Specimen J103, W = 10, B = 10 mm

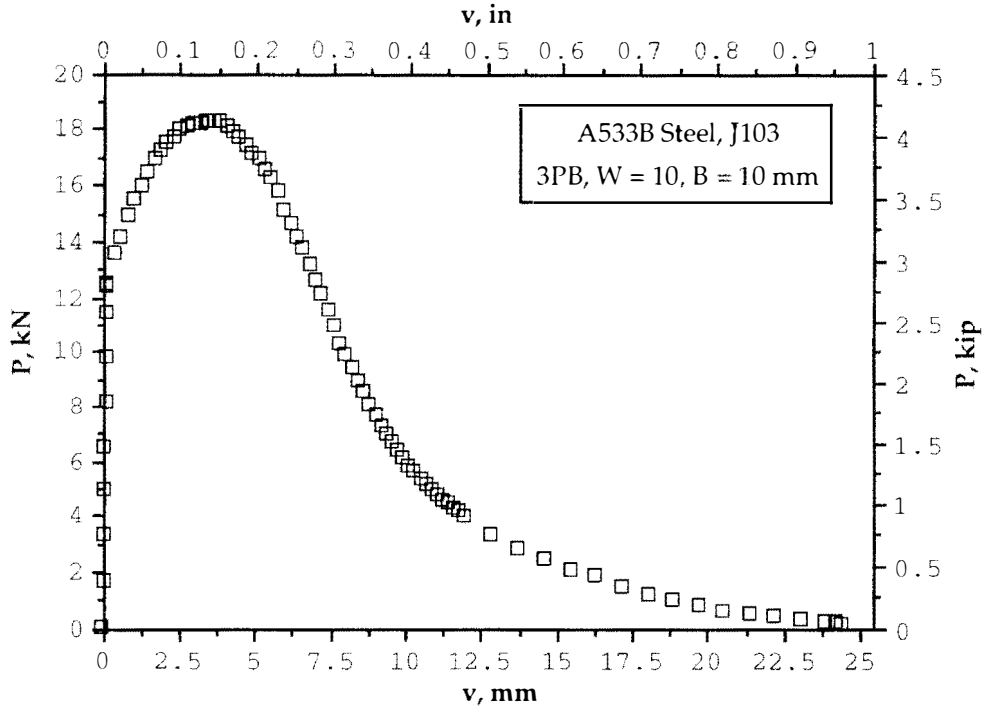

Fig. 6.1b Load versus Displacement Converted from Charpy Impact Test P-t Record, A533B Steel, Three-Point Bend Specimen J103, W = 10, B = 10 mm

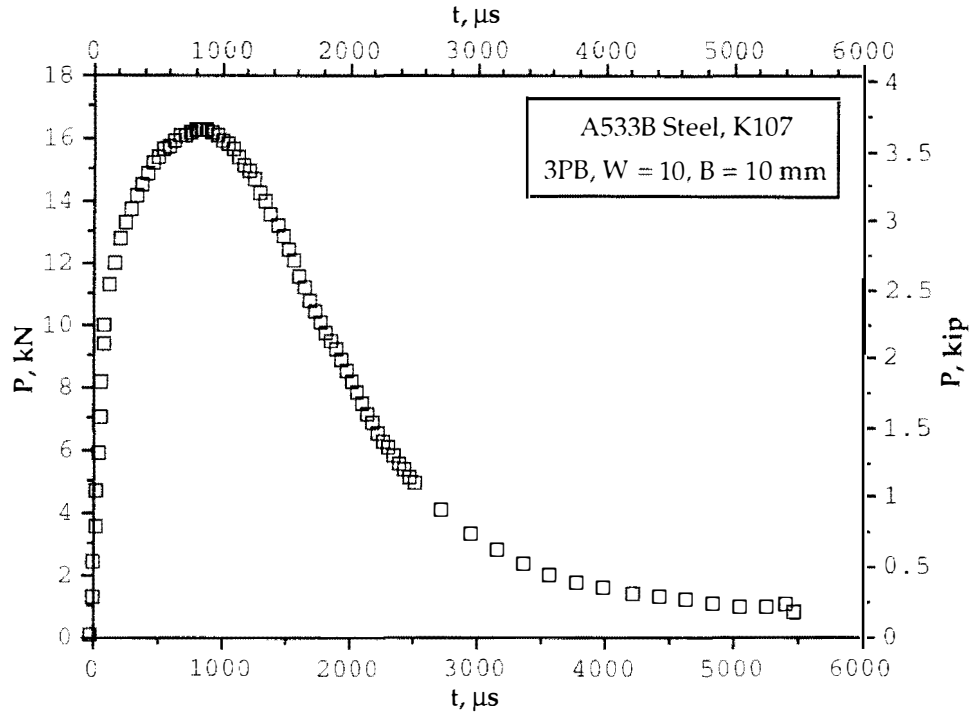

Fig. 6.2a Load versus Time Determined from Charpy Impact Test A533B Steel, Three-Point Bend Specimen K107, W = 10, B = 10 mm

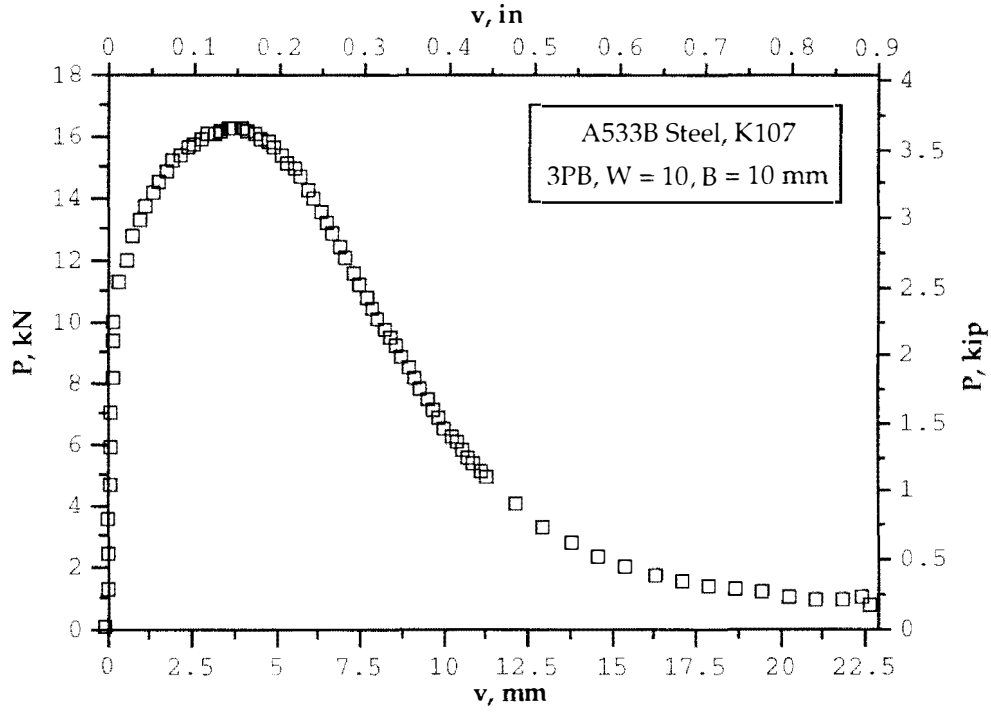

Fig. 6.2b Load versus Displacement Converted from Charpy Impact Test P-t Record, A533B Steel, Three-Point Bend Specimen K107, W = 10, B = 10 mm

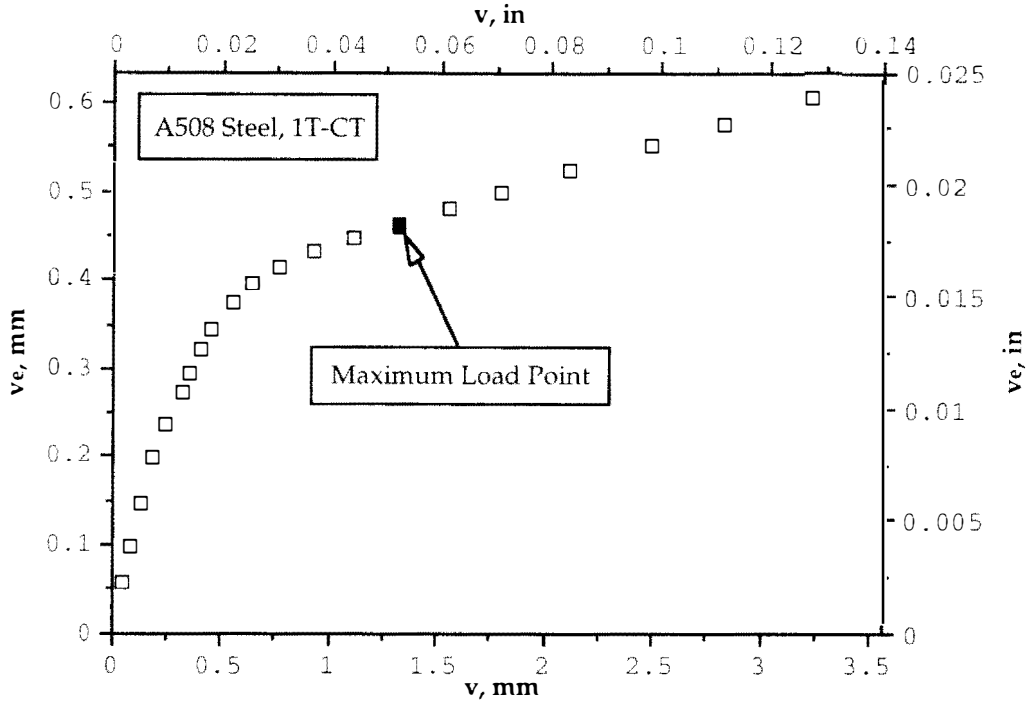

Fig. 6.3 Displacement versus Its Elastic Component Showing a Linear Relationship after the Maximum Load Point is Passed, A508 Steel, Compact Specimen, W = 2, B = 1 in

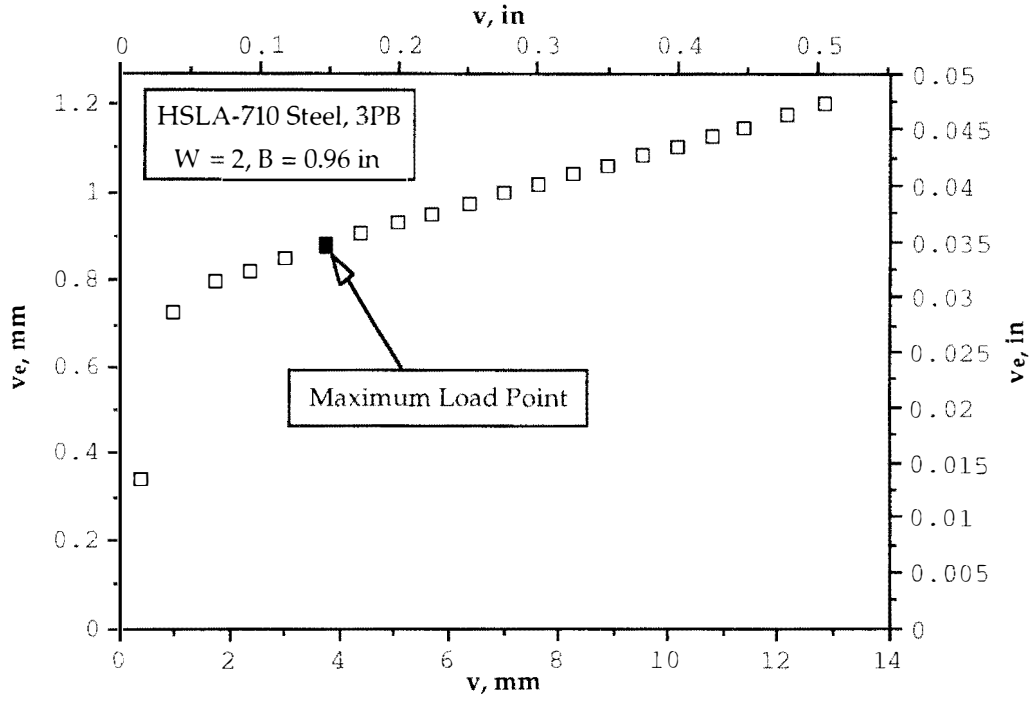

Fig. 6.4 Displacement versus Its Elastic Component Showing a Linear Relationship after the Maximum Load Point is Passed, HSLA-710 Steel, Tree-Point Bend Specimen, W = 2, B = 0.96 in

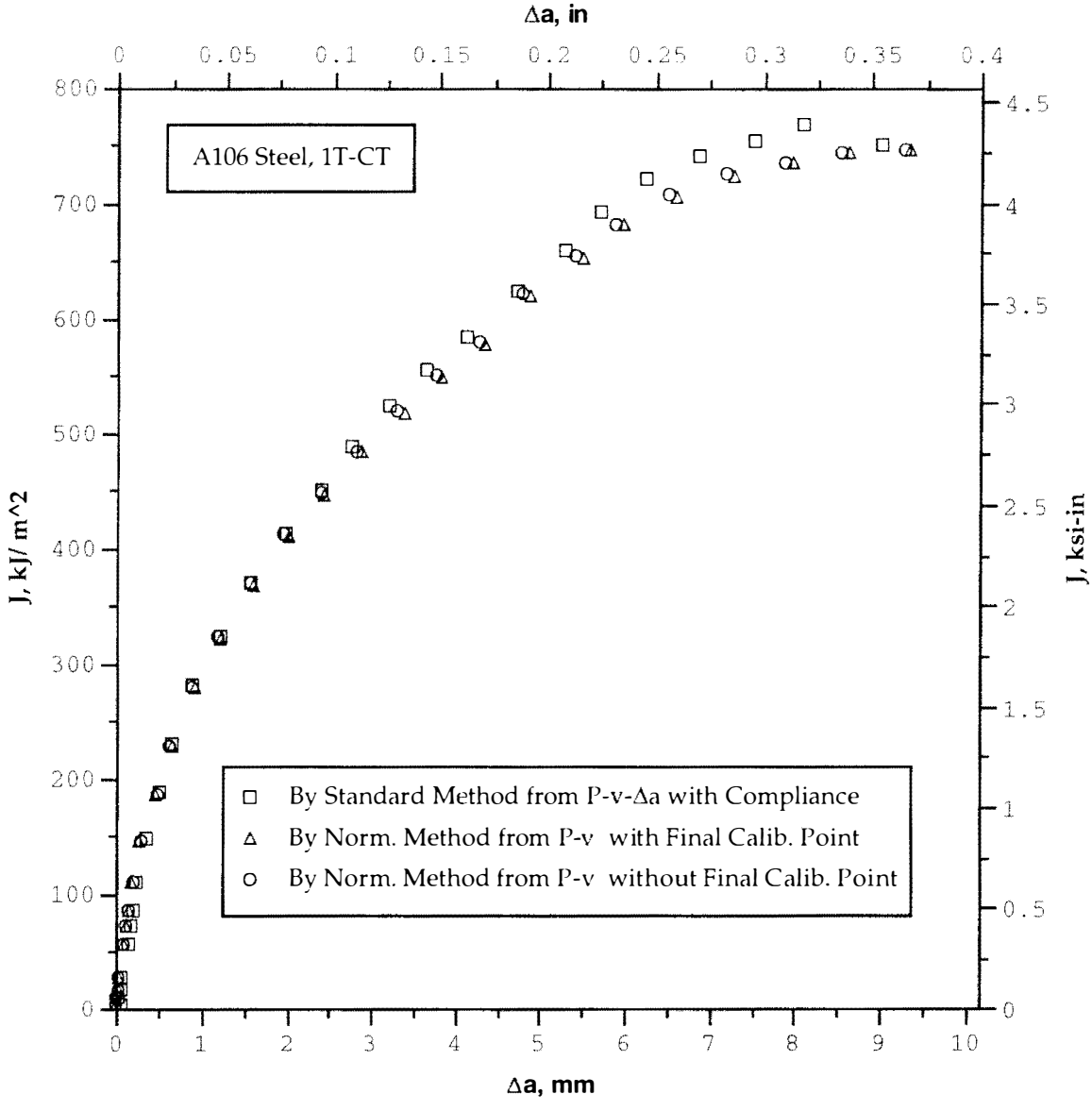

Fig. 6.5 - J-R Curve Developed by Method of Normalization from P-v without Final Calibration Point Compared with Results by Standard Method from P-v-Δa and by Regular Normalization Method from P-v with Final Calibration Point, A106 Steel, Compact Specimen

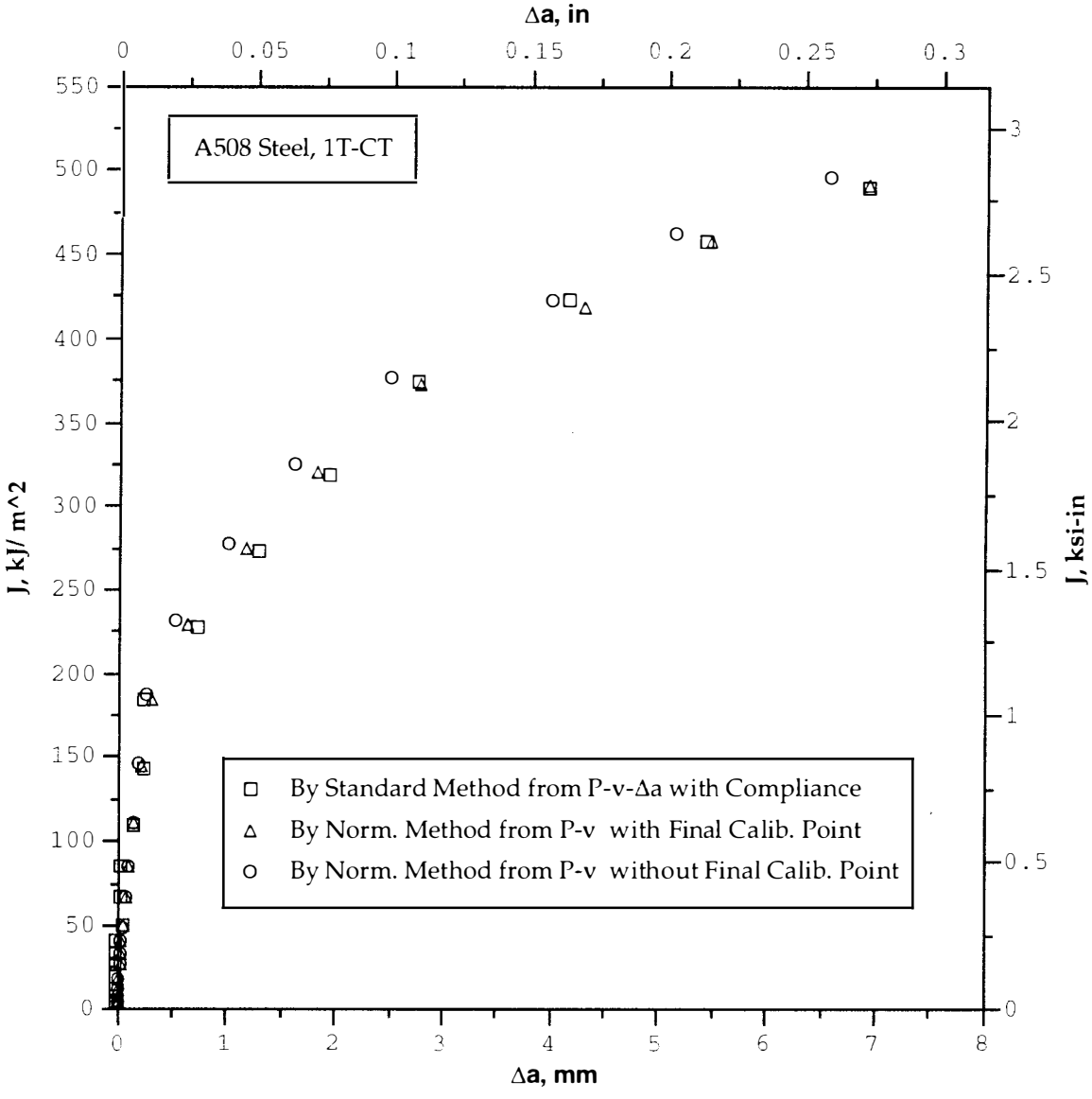

Fig. 6.6 - J-R Curve Developed by Method of Normalization from P-v without Final Calibration Point Compared with Results by Standard Method from P-v-Δa and by Regular Normalization Method from P-v with Final Calibration Point, A508 Steel, Compact Specimen

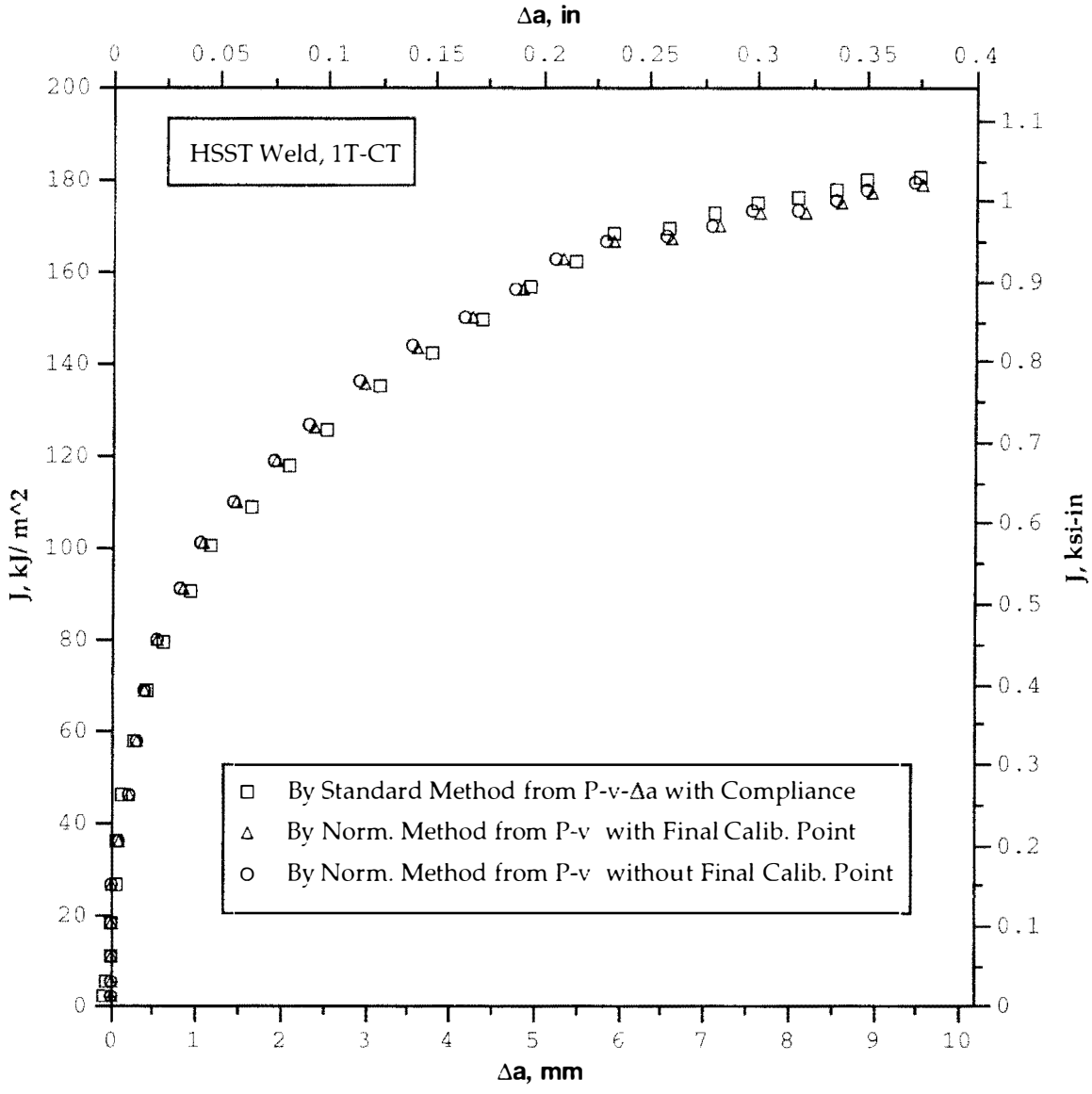

Fig. 6.7- J-R Curve Developed by Method of Normalization from P-v without Final Calibration Point Compared with Results by Standard Method from P-v-Δa and by Regular Normalization Method from P-v with Final Calibration Point, HSST Weld Material, Compact Specimen

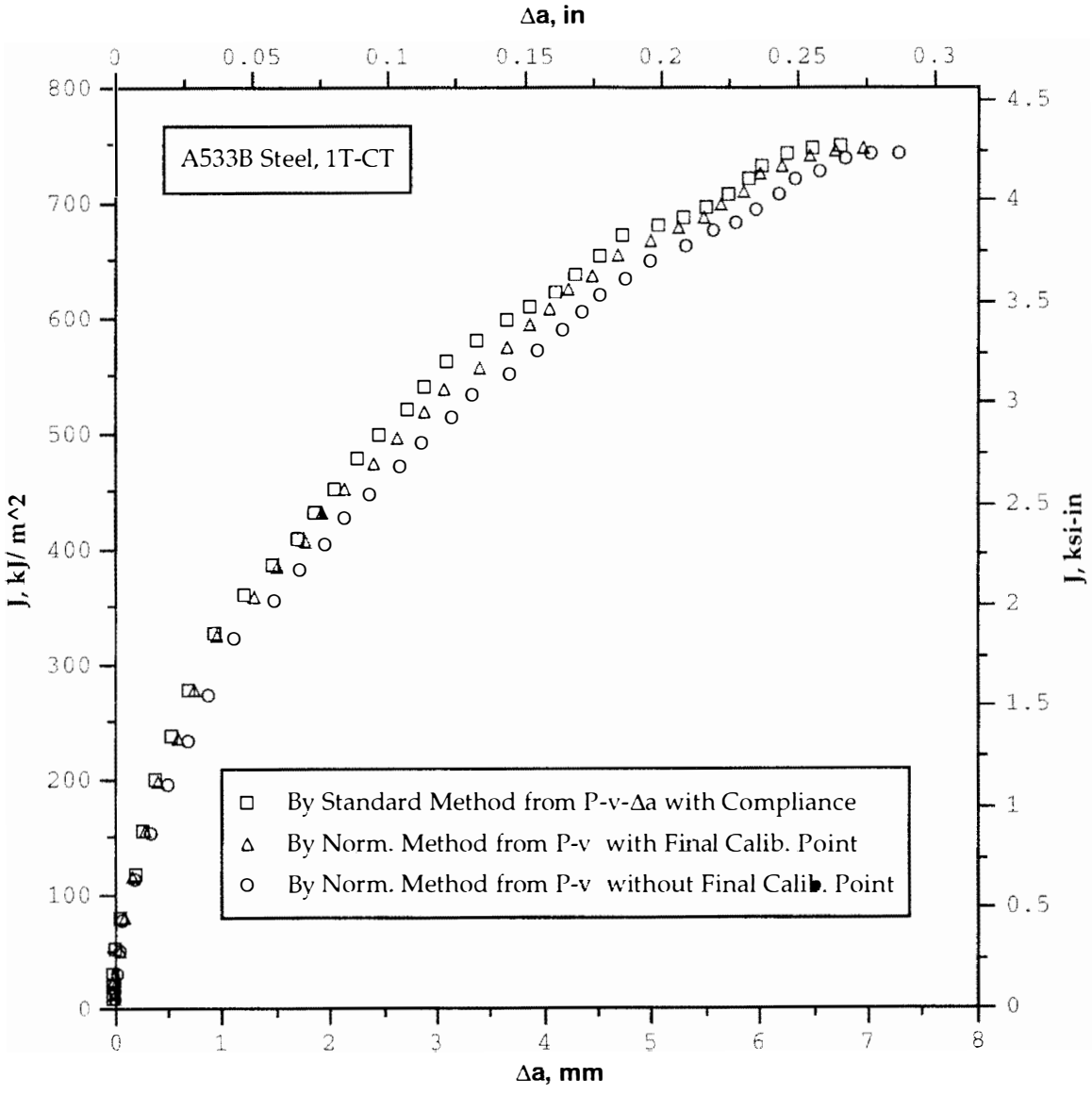

Fig. 6.8 - J-R Curve Developed by Method of Normalization from P-v without Final Calibration Point Compared with Results by Standard Method from P-v-Δa and by Regular Normalization Method from P-v with Final Calibration Point, A533B Steel, Compact Specimen

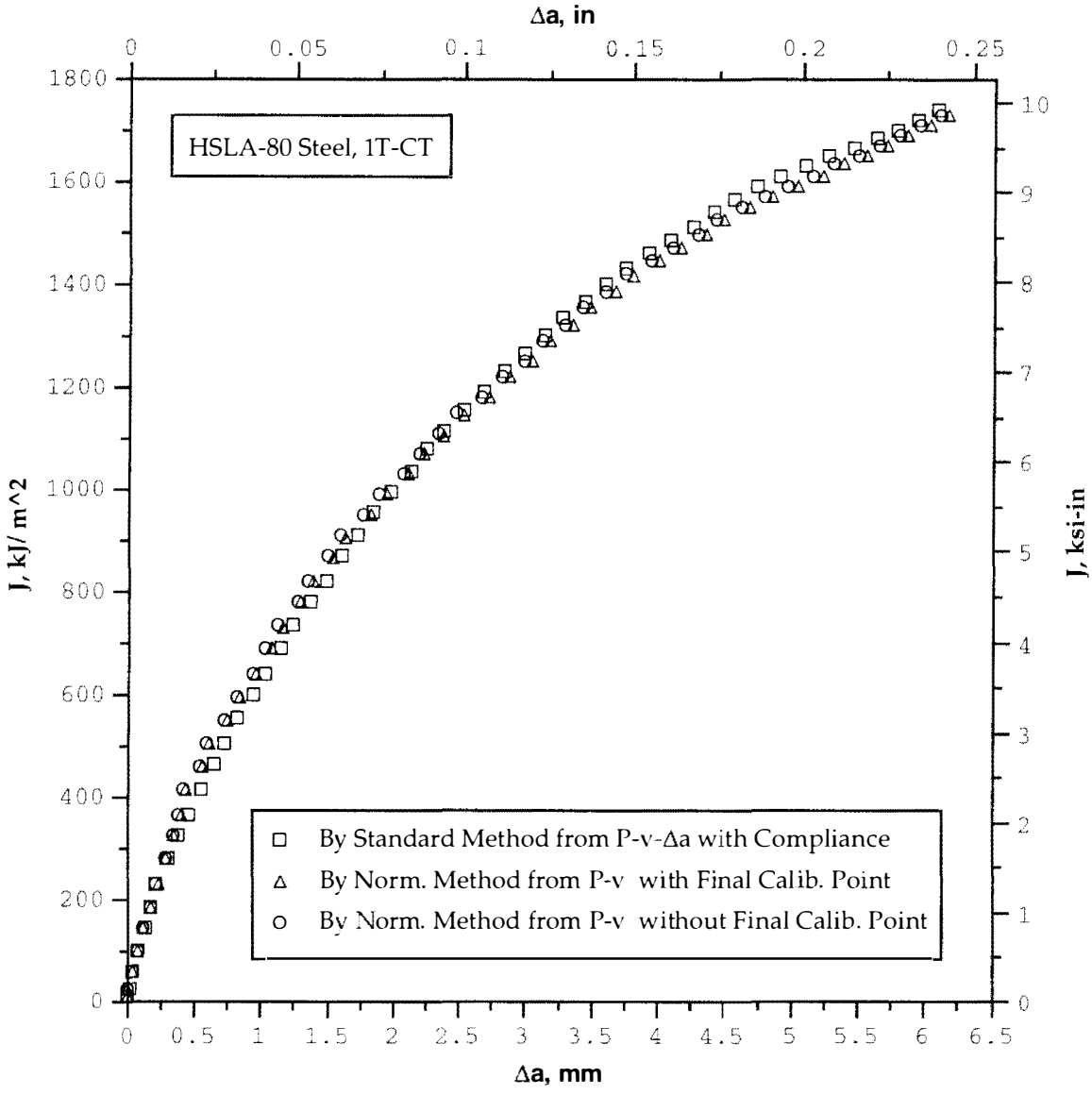

Fig. 6.9 - J-R Curve Developed by Method of Normalization from P-v without Final Calibration Point Compared with Results by Standard Method from P-v-Δa and by Regular Normalization Method from P-v with Final Calibration Point, HSLA-80 Steel, Compact Specimen

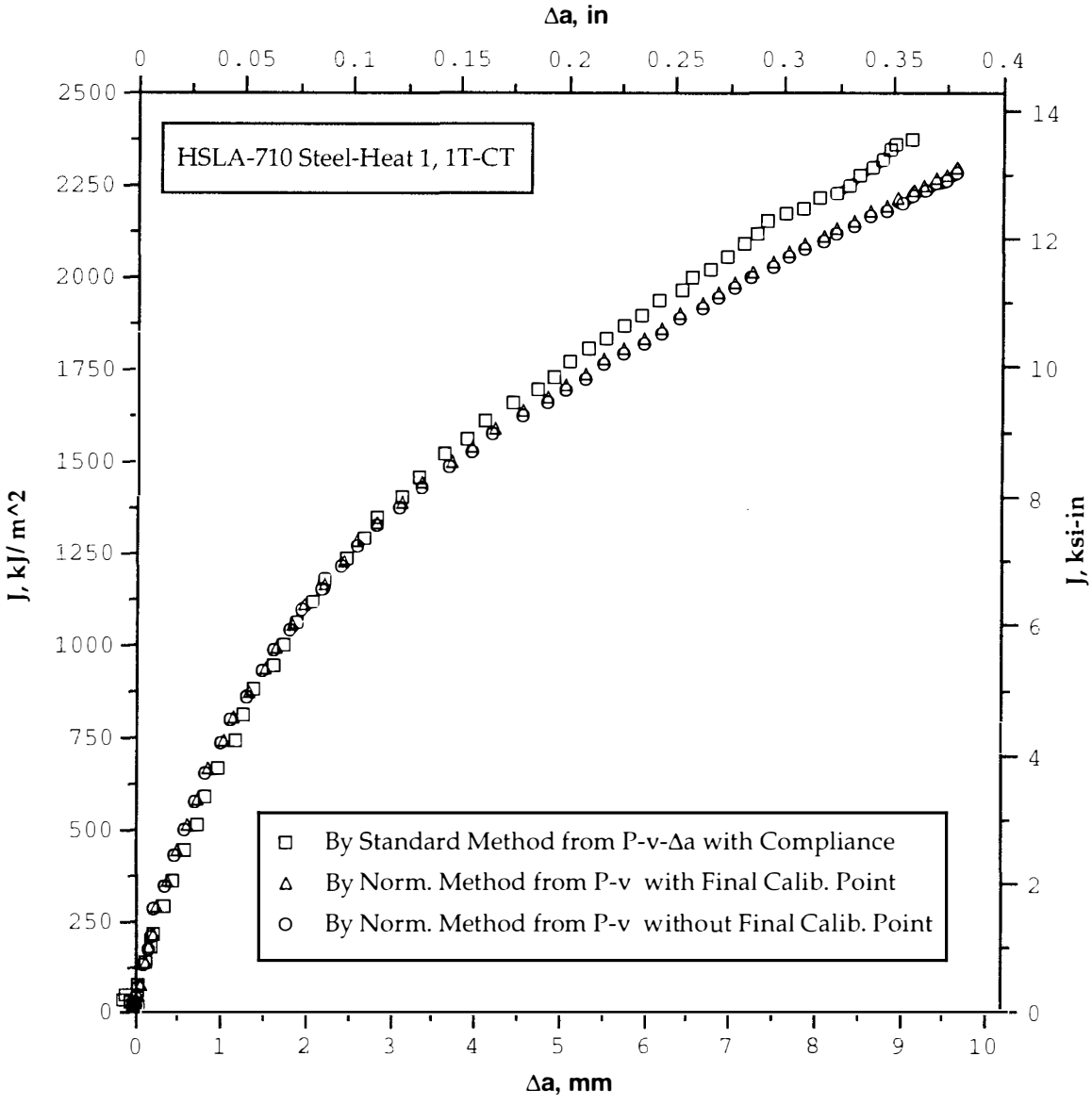

Fig. 6.10 - J-R Curve Developed by Method of Normalization from P-v without Final Calibration Point Compared with Results by Standard Method from P-v-Δa and by Regular Normalization Method from P-v with Final Calibration Point, HSLA-710 Steel-Heat 1, Compact Specimen

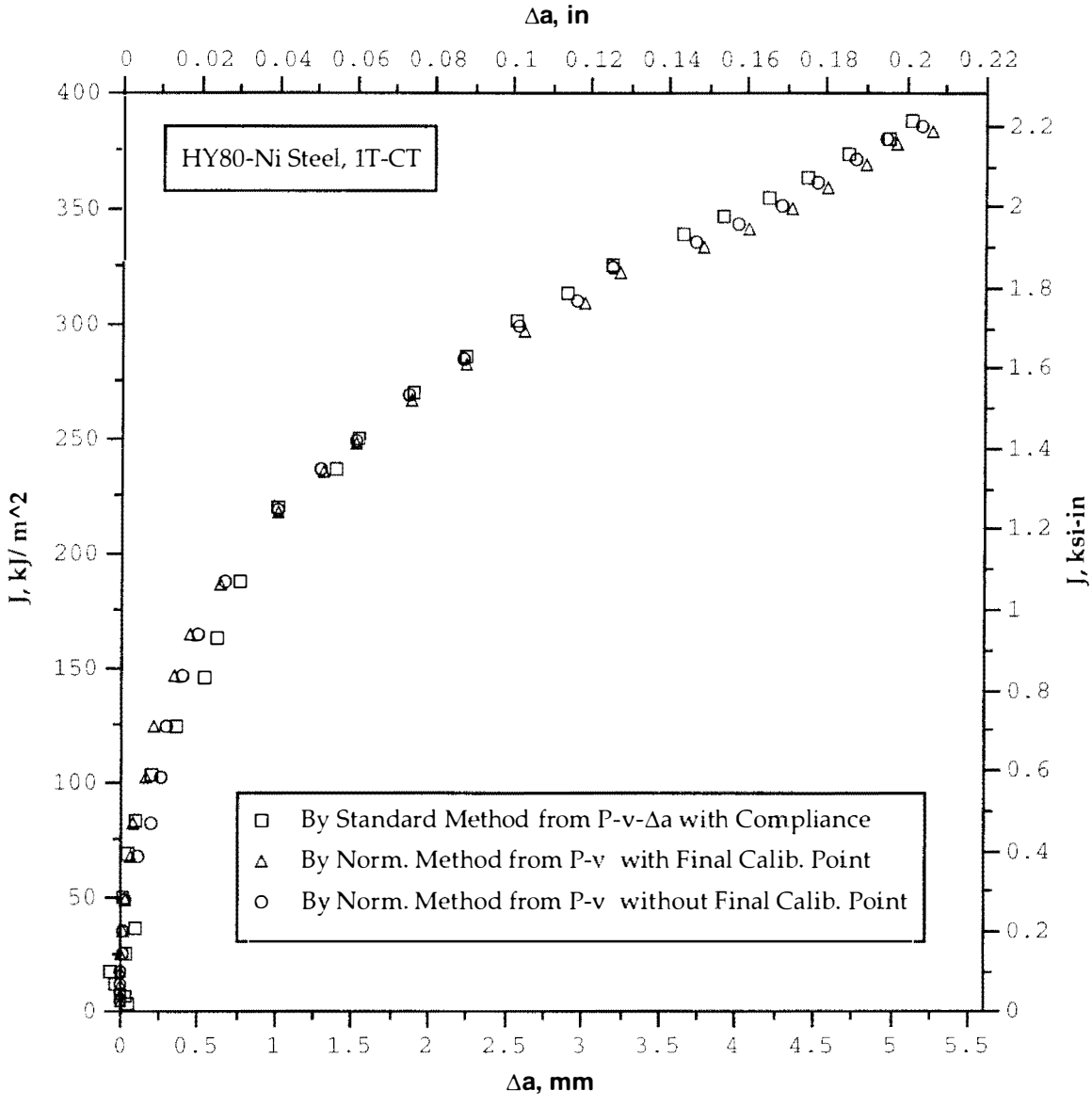

Fig. 6.11 - J-R Curve Developed by Method of Normalization from P-v without Final Calibration Point Compared with Results by Standard Method from P-v-Δa and by Regular Normalization Method from P-v with Final Calibration Point, HY80-Ni Steel, Compact Specimen

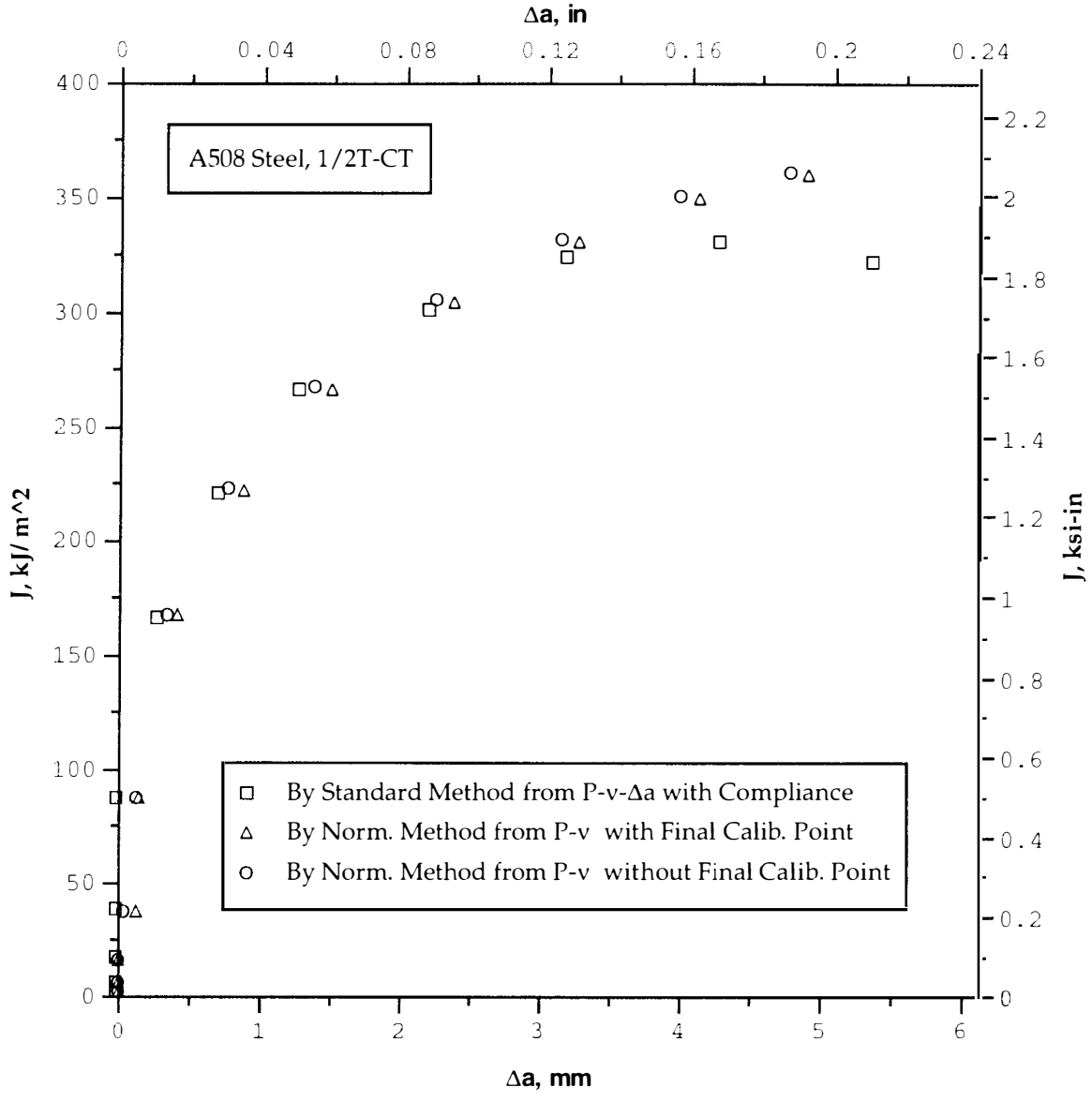

Fig. 6.12 - J-R Curve Developed by Method of Normalization from P-v without Final Calibration Point Compared with Results by Standard Method from P-v-Δa and by Regular Normalization Method from P-v with Final Calibration Point, A508 Steel, 1/2T Compact Specimen

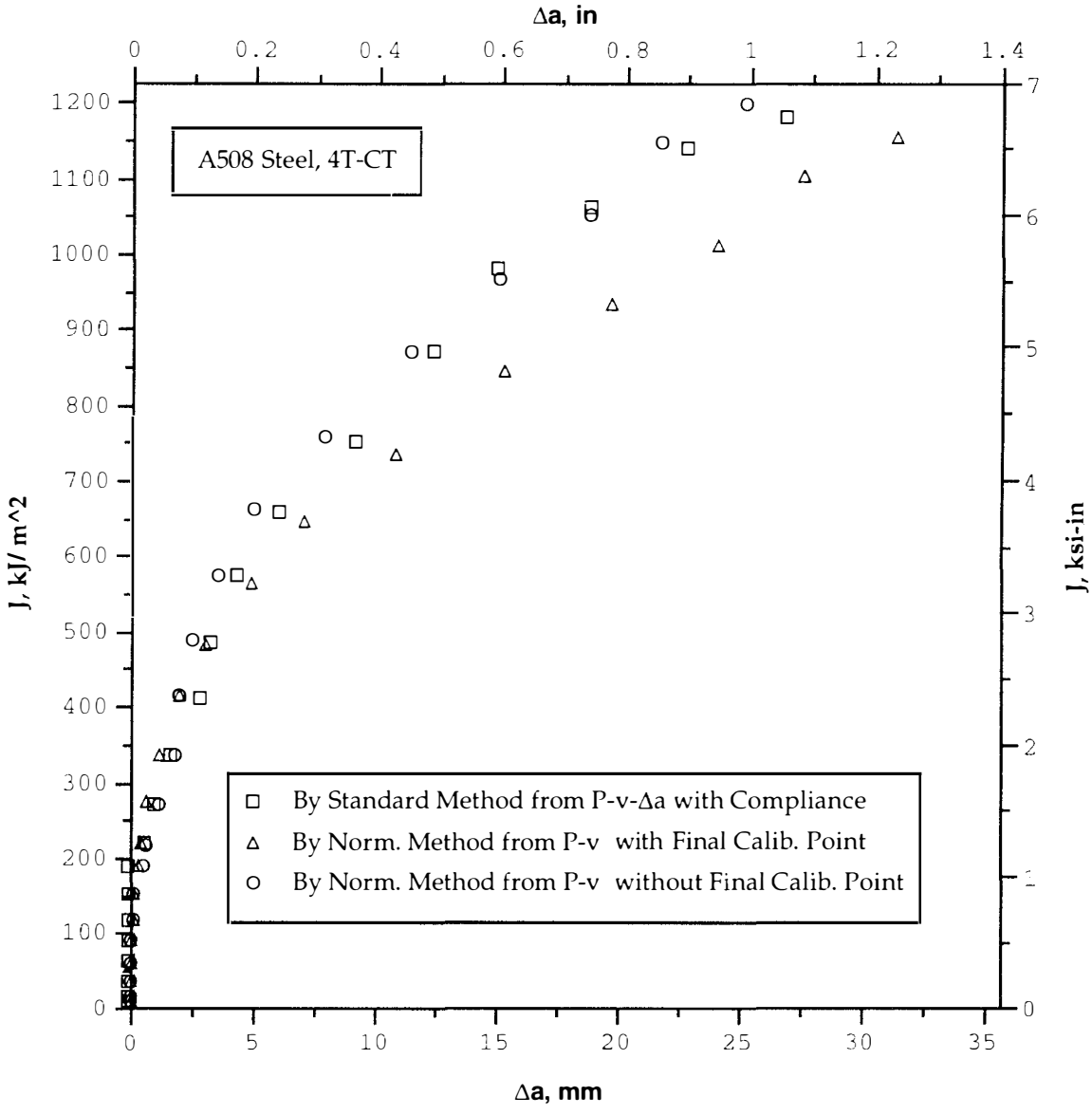

Fig. 6.13- J-R Curve Developed by Method of Normalization from P-v without Final Calibration Point Compared with Results by Standard Method from P-v-Δa and by Regular Normalization Method from P-v with Final Calibration Point, A508 Steel, 4T Compact Specimen

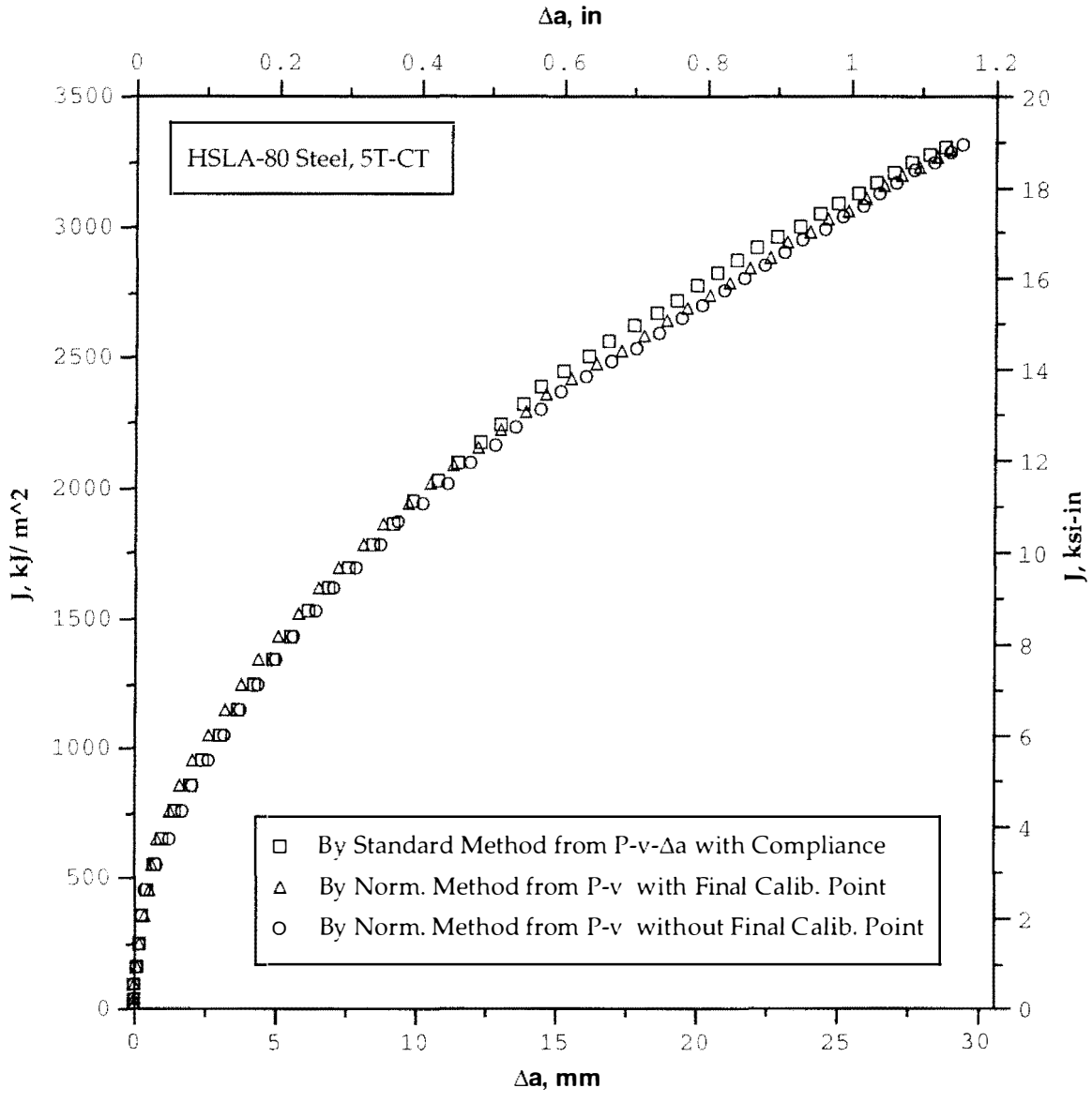

Fig. 6.14 - J-R Curve Developed by Method of Normalization from P-v without Final Calibration Point Compared with Results by Standard Method from P-v-Δa and by Regular Normalization Method from P-v with Final Calibration Point, HSLA-80 Steel, 5T Compact Specimen

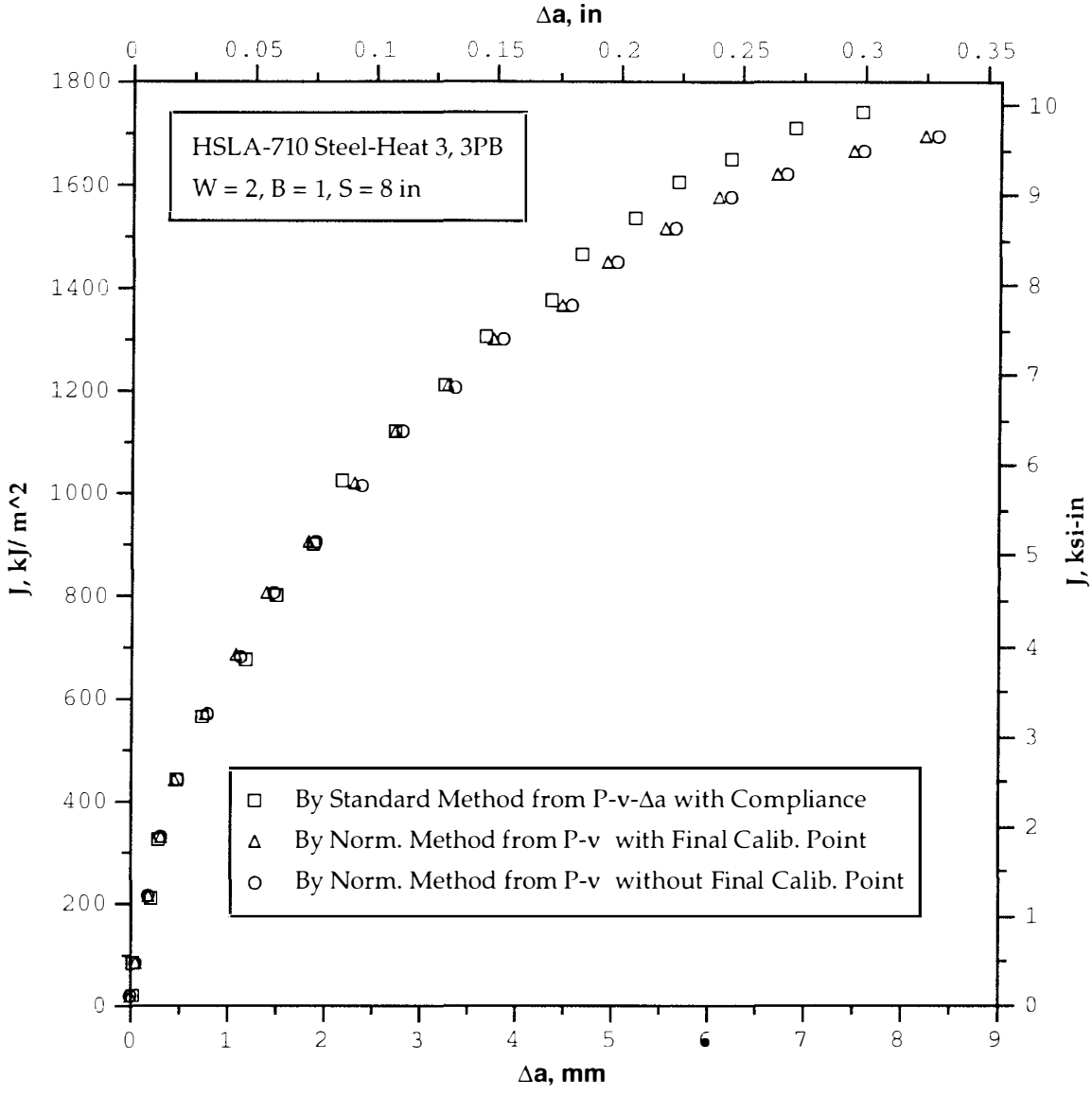

Fig. 6.15 - J-R Curve Developed by Method of Normalization from P-v without Final Calibration Point Compared with Results by Standard Method from P-v-Δa and by Regular Normalization Method from P-v with Final Calibration Point, HSLA-710 Steel-Heat 3, 3PB Specimen of W=2, B=1, S=8 in

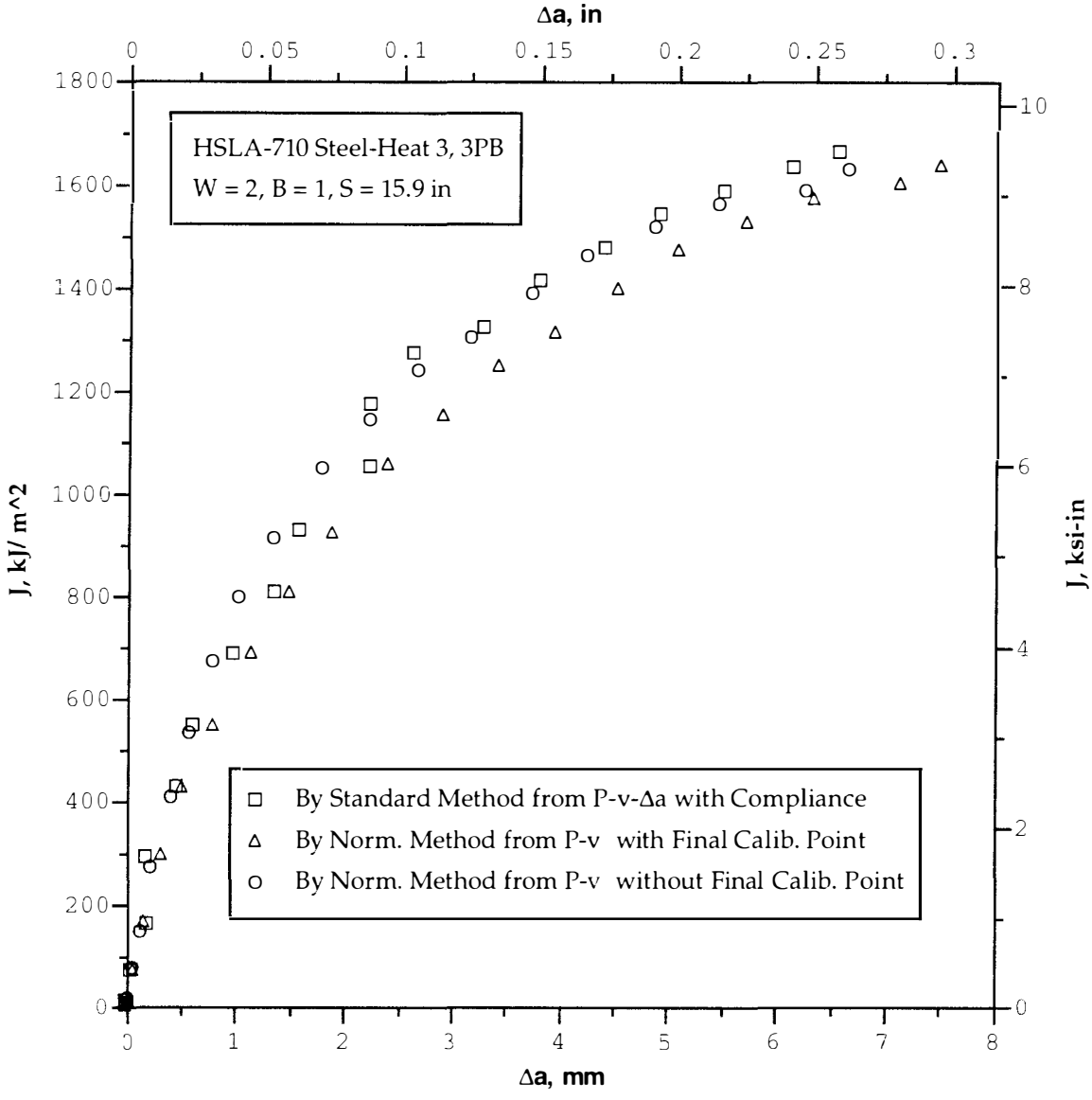

Fig. 6.16 - J-R Curve Developed by Method of Normalization from P-v without Final Calibration Point Compared with Results by Standard Method from P-v-Δa and by Regular Normalization Method from P-v with Final Calibration Point, HSLA-710 Steel-Heat 3, 3PB Specimen of W=2, B=1, S=16 in

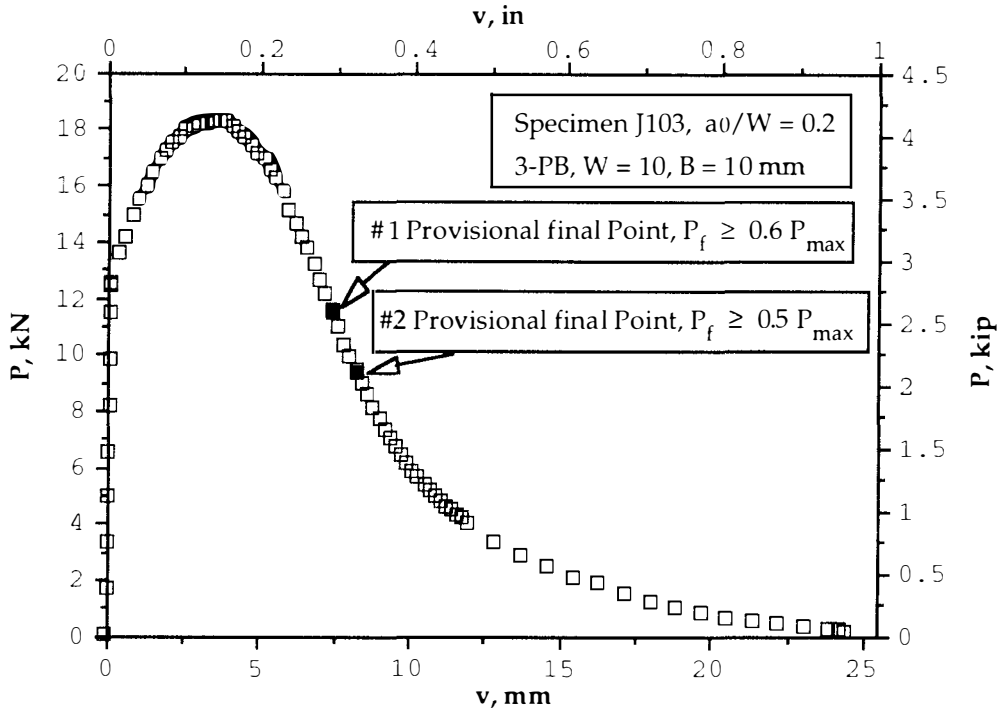

Fig. 6.17a Load versus Displacement Determined from Charpy Impact Test Record, A533B Steel, Three-Point Bend Specimen J103

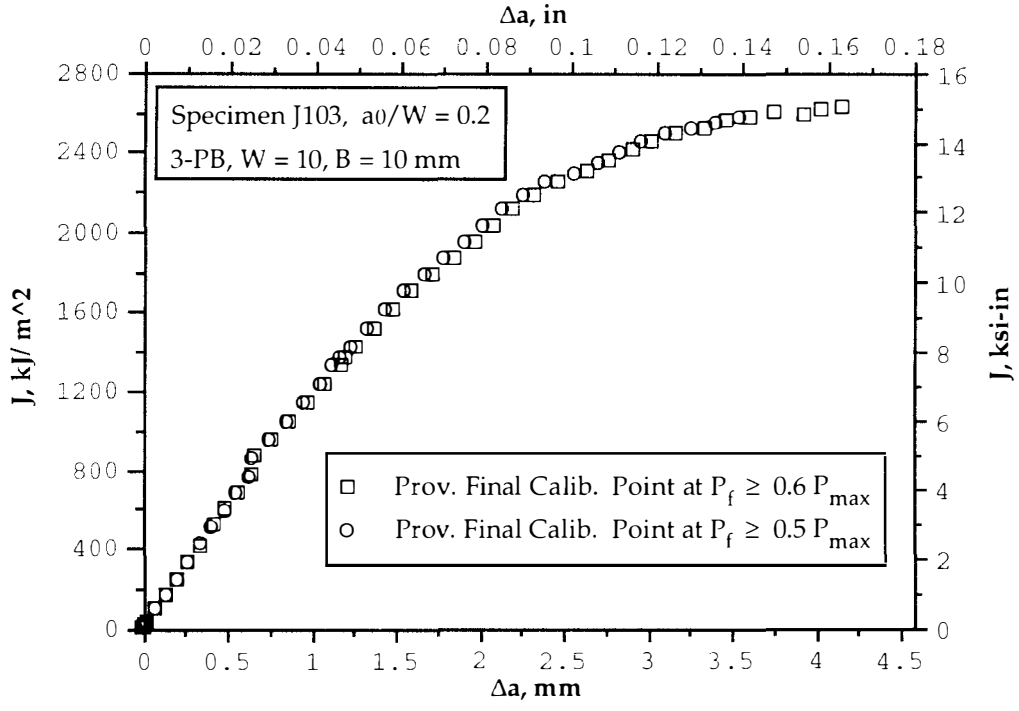

Fig. 6.17b J-R Curves for Charpy Impact Specimen J103 with the Provisional Final Calibration Points at $P_f \geq 0.6\ P_{max}$ and $P_f \geq 0.5\ P_{max}$ A533B Steel, Three-Point Bend Specimen, $a_0/W = 0.2$, W = 10, B = 10 mm

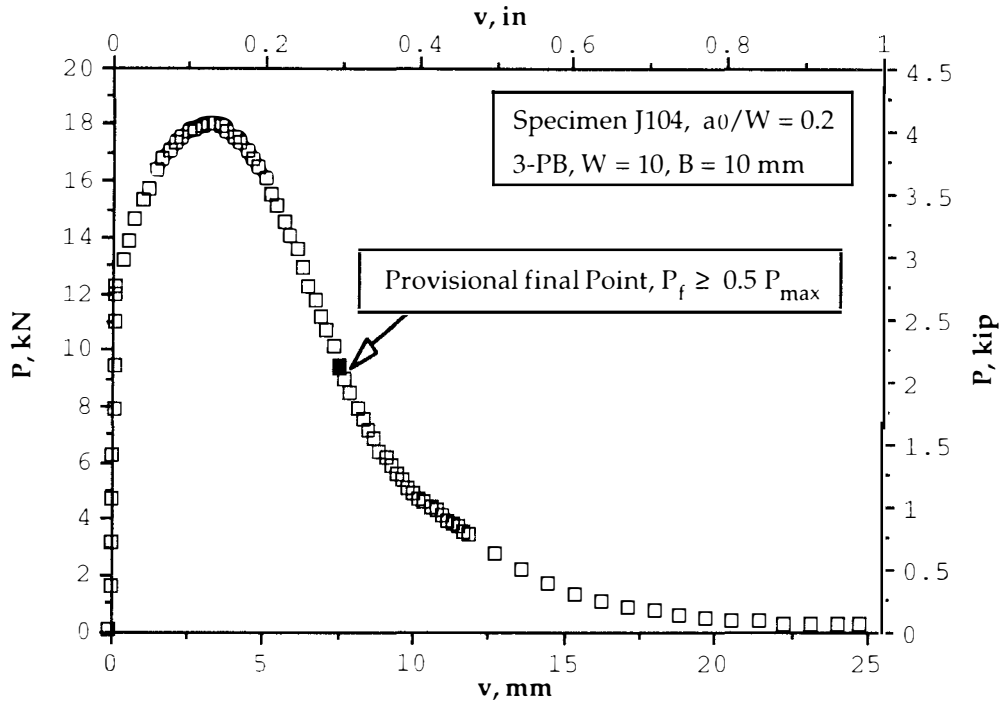

Fig. 6.18a Load versus Displacement Determined from Charpy Impact Test Record, A533B Steel, Three-Point Bend Specimen J104

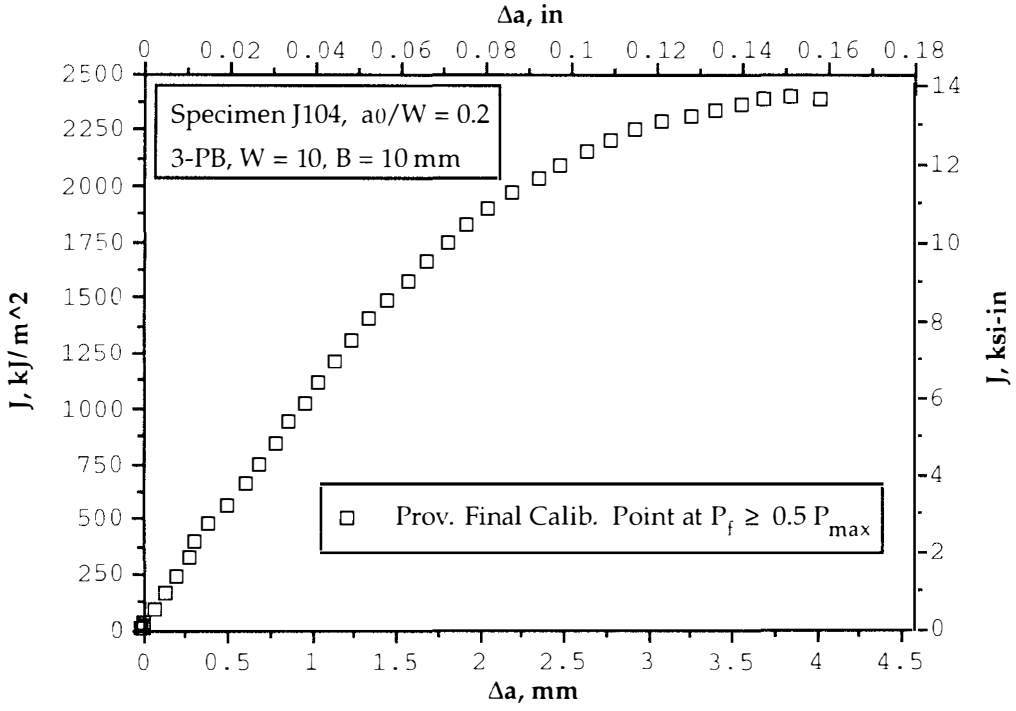

Fig. 6.18b J-R Curve for Charpy Impact Specimen J104 with the Provisional Final Calibration Point at $P_f \geq 0.5\ P_{max}$, A533B Steel, Three-Point Bend Specimen, $a_0/W = 0.2$, W = 10, B = 10 mm

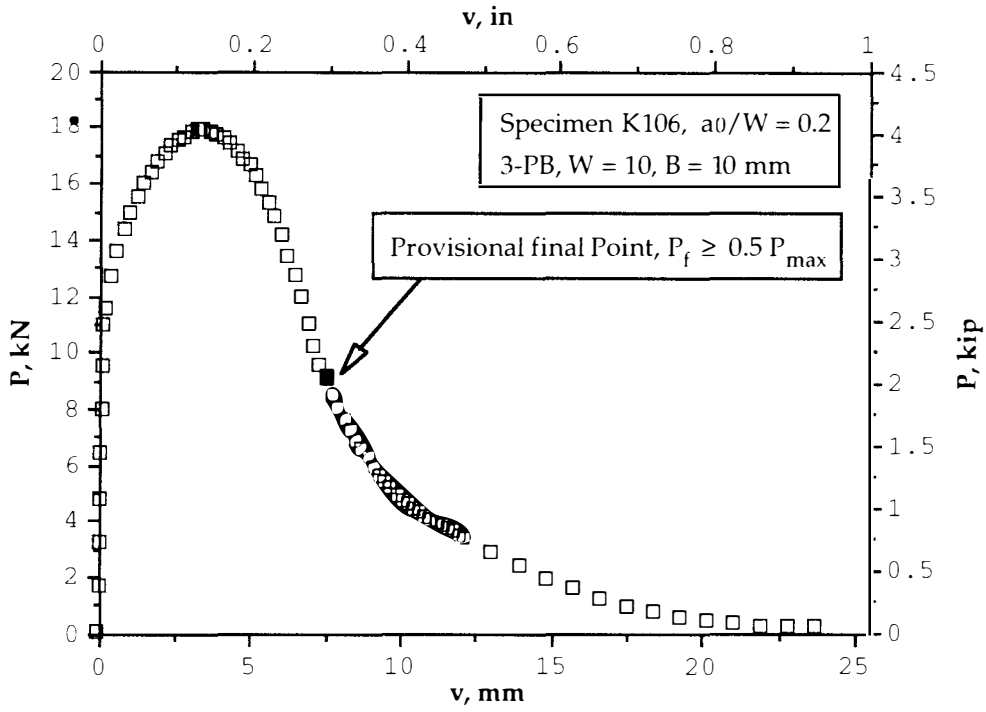

Fig. 6.19a Load versus Displacement Determined from Charpy Impact Test Record, A533B Steel, Three-Point Bend Specimen K106

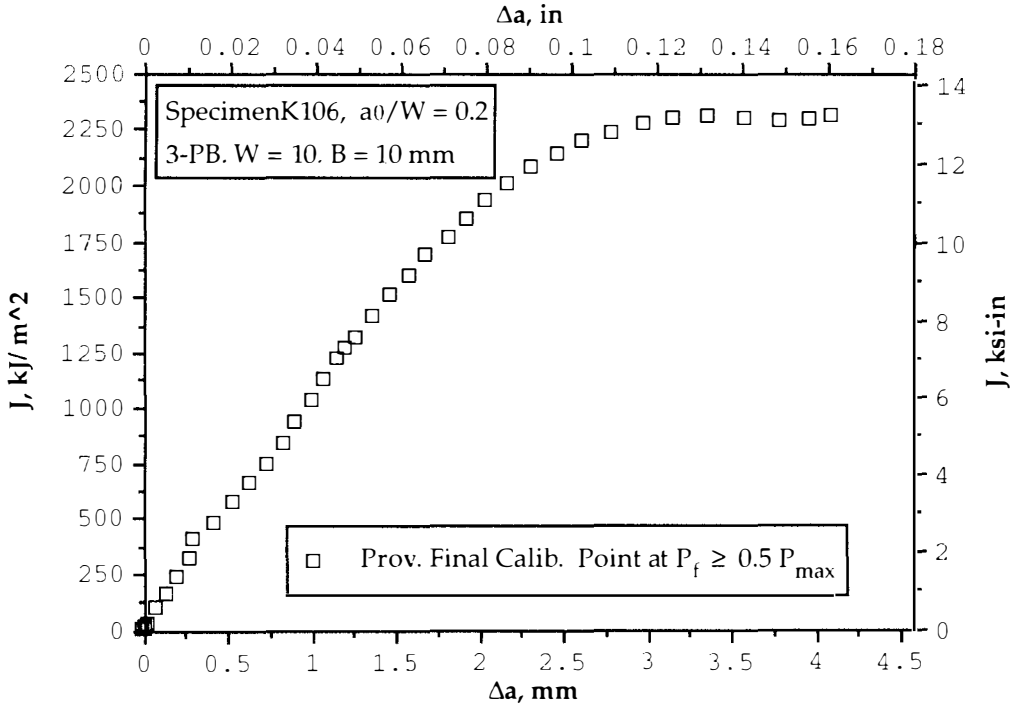

Fig. 6.19b J-R Curve for Charpy Impact Specimen K106 with the Provisional Final Calibration Point at $P_f \geq 0.5\ P_{max}$, A533B Steel, Three-Point Bend Specimen, $a_0/W = 0.2$, W = 10, B = 10 mm

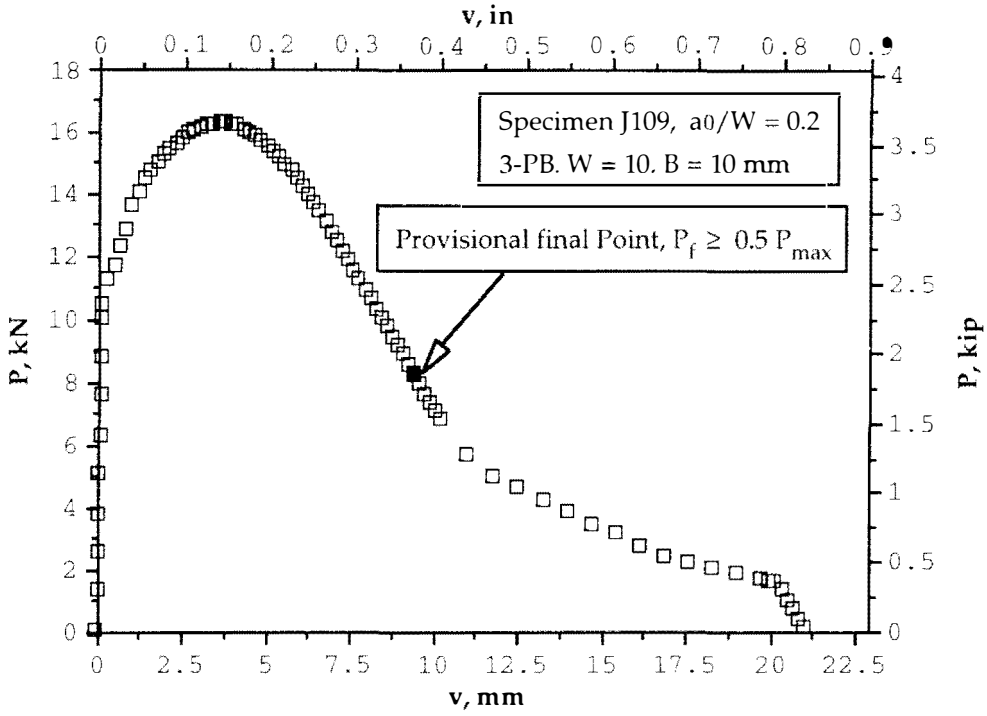

Fig. 6.20a Load versus Displacement Determined from Charpy Impact Test Record, A533B Steel, Three-Point Bend Specimen J109

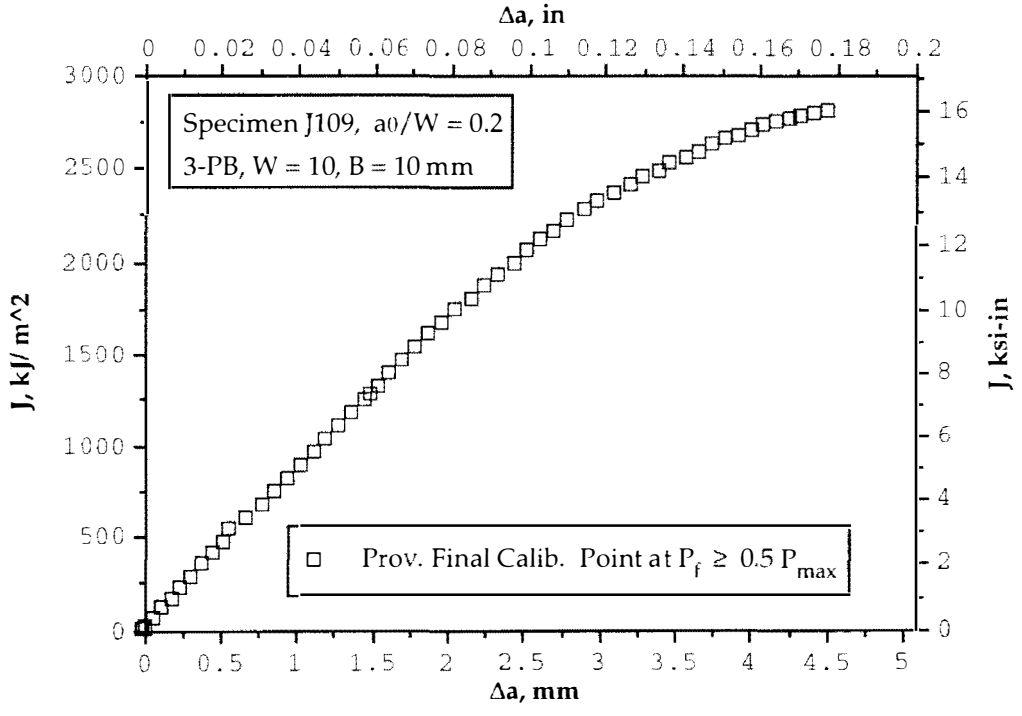

Fig. 6.20b J-R Curve for Charpy Impact Specimen J109 with the Provisional Final Calibration Point at $P_f \geq 0.5\ P_{max}$, A533B Steel, Three-Point Bend Specimen, $a_0/W = 0.2$, W = 10, B = 10 mm

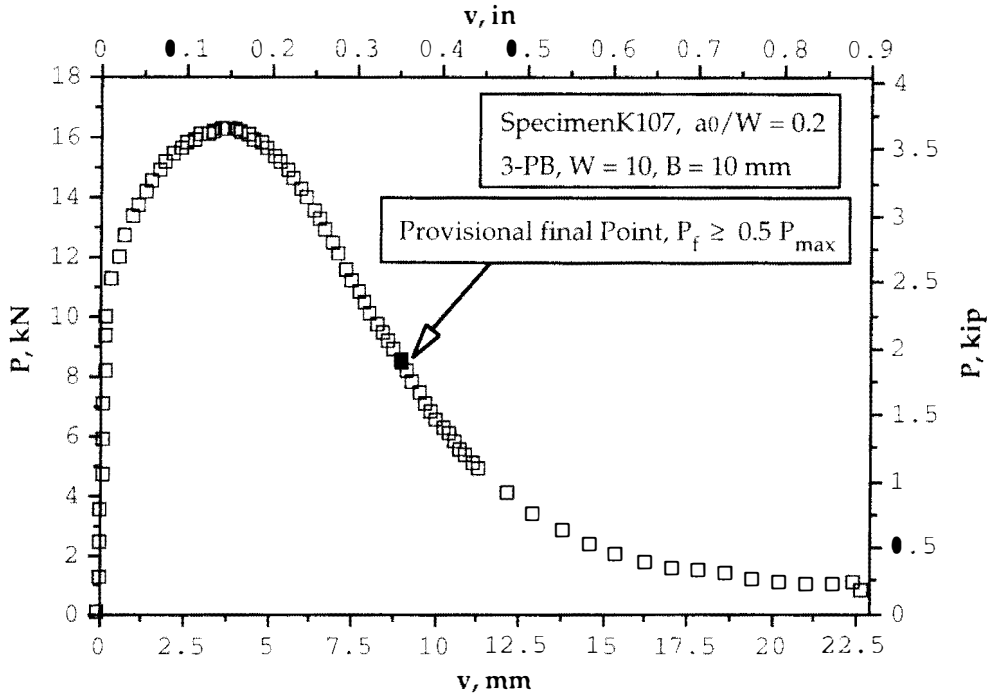

Fig. 6.21a Load versus Displacement Determined from Charpy Impact Test Record, A533B Steel, Three-Point Bend Specimen K107

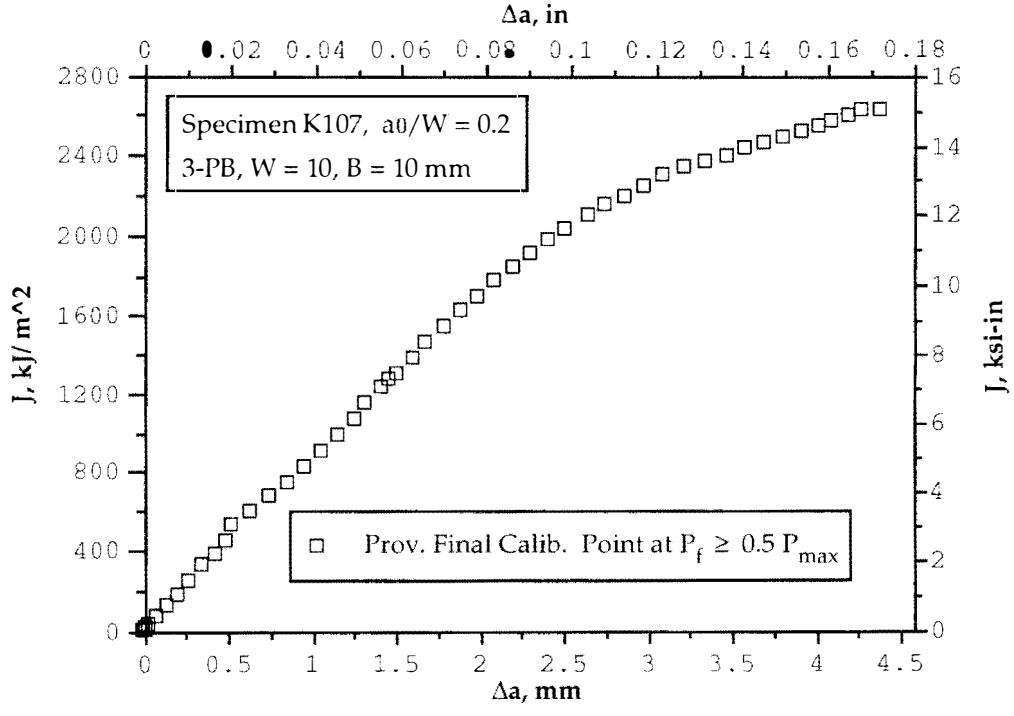

Fig. 6.21b J-R Curve for Charpy Impact Specimen K107 with the Provisional Final Calibration Point at $P_f \geq 0.5\ P_{max}$, A533B Steel, Three-Point Bend Specimen, $a_0/W = 0.2$, W = 10, B = 10 mm

APPENDIX B

APPENDIX B

A Program for J-R Curve Determination from Load versus Displacement Using the Method of Normalization

```
C     PROGRAM JRPV1
C-------------------------------------------------------------------------*
C     THIS PROGRAM COMPUTES THE J-R CURVE FROM P-V TEST RECORD BY        *
C     PREDICTING CRACK LENGTH USING NORMALIZATION METHOD WITH LMN        *
C     FUNCTION WHERE L IS DETERMINED FROM Pmax FOR COMPACT SPECIMEN      *
C                                                                        *
C     Δa ADJUSTMENT IS USED AT THE INITIAL PART BEFORE Pmax IS REACHED   *
C     IF NECESSARY                                                       *
C                                                                        *
C     FOR COMPARISON, THE J-R CURVE IS ALSO DETERMINED FROM P-V-Δa       *
C     WHERE THE CRACK LENGTH WAS MEASURED BY THE ELASTIC COMPLIANCE      *
C     METHOD                                                             *
C                                                                        *
C************************************************************************
C      A0:      INITIAL CRACK LENGTH                                     *
C      AF:      FINAL CRACK LENGTH                                       *
C      B:       SPECIMEN THICKNESS                                       *
C      BN:      NET SPECIMEN THICKNESS                                   *
C      BE:      EFFECTIVE SPECIMEN THICKNESS                             *
C      W:       SPECIMEN WIDTH                                           *
C      EEF:     EFFECTIVE MODULUS                                        *
C      NU:      POISON RATIO                                             *
C      NJ:      TOTAL MEASURED POINTS                                    *
C      YS:      YIELD STRESS                                             *
C      UTS:     ULTIMATE STRESS                                          *
C      SIG0:    FLOW STRESS                                              *
C      P(I):    LOAD                                                     *
C      V(I):    LOAD LANE DISPLACEMENT                                   *
C      VE(I):   ELASTIC COMPONENT OF DISPLACEMENT FROM NORMALIZATION     *
C               METHOD                                                   *
C      VP(I):   PLASTIC COMPONENT OF DISPLACEMENT FROM NORMALIZATION     *
C               METHOD                                                   *
C      A(I):    CRACK LENGTH FROM NORMALIZATION METHOD                   *
C      DA(I):   CRACK GROWTH FROM NORMALIZATION METHOD                   *
C      RB(I):   UNCRACKED LIGAMENT BASED ON A(I)                         *
C      C(I):    COMPLIANCE BASED ON A(I)                                 *
C      AY(I):   CRACK GROWTH CORRECTION BASED ON ENFORCED BLUNTING       *
C      PN(I):   NORMALIZED LOAD FROM NORMALIZATION METHOD                *
C      K(I):    STRESS INTENSITY FACTOR FROM NORMALIZATION METHOD        *
C      J(I):    J INTEGRAL FROM NORMALIZATION METHOD                     *
C      JE(I):   ELASTIC COMPONENT OF J(I)                                *
C      JP(I):   PLASTIC COMPONENT OF J(I)                                *
C      VVE(I):  ELASTIC COMPONENT OF DISPLACEMENT FROM COMPLIANCE METHOD *
C      VVP(I):  PLASTIC COMPONENT OF DISPLACEMENT FROM COMPLIANCE METHOD *
C      AV(I):   CRACK LENGTH FROM COMPLIANCE METHOD                      *
C      DAV(I):  CRACK GROWTH FROM COMPLIANCE METHOD                      *
C      RBV(I):  UNCRACKED LIGAMENT BASED ON AV(I)                        *
C      CV(I):   COMPLIANCE BASED ON AV(I)                                *
```

```
C       PNV(I): NORMALIZED LOAD FROM COMPLIANCE METHOD                        *
C       KV(I):  STRESS INTENSITY FACTOR FROM COMPLIANCE METHOD                *
C       JV(I):  J INTEGRAL FROM COMPLIANCE METHOD                             *
C       JEV(I): ELASTIC COMPONENT OF JV(I)                                    *
C       JPV(I): PLASTIC COMPONENT OF JV(I)                                    *
C-------------------------------------------------------------------------*
        INTEGER I,NJ,N,IMAX,NX,KK
        PARAMETER (N=100)
        REAL V(N),PN(N),PNV(N),DA(0:N),DAV(N),VE(N),VVE(N),JE(N),JEV(N)
        REAL VP(0:N),P(0:N),A(0:N),AV(0:N),JP(0:N),VVP(0:N),JPV(0:N)
        REAL J(N),JV(N),AY(N),C(N),CV(N),RB(N),RBV(N),K(N),KV(N)
        REAL AA2(N),AA3(N)
        REAL A0,B,BN,BE,W,EEF,NU,AF,YS,UTS,PMAX,SIG0,A1,A2
        REAL ETAP,GAMA,HH,HL,SUM2,SUM3,L,L0,DET,AAA,BBB,CCC
        CHARACTER*14 IFIL,OFIL1,OFIL2
        CHARACTER YN1*2,YN2*2,OFM*2,YN3*2
C
C-------------------------------------------------------------------------*
C       INPUT THE TEST DATA                                                 *
C-------------------------------------------------------------------------*
C
5       WRITE (*,*) 'INPUT THE NAME OF THE INPUT FILE?'
        READ 10, IFIL
        WRITE (*,*) 'NEED ROTATION CORRECTION? [Y/N]'
        READ 10, YN1
10      FORMAT (A)
        OPEN (7, FILE=IFIL,STATUS='OLD')
        READ (7,*) A0,B,BN,BE,W,EEF,NU,AF,NJ,YS,UTS
        PMAX=0
        DO I=1,NJ
          READ (7,*) P(I),V(I),DAV(I)
C         READ (7,*) P(I),V(I)
          IF (P(I) .GT. PMAX) THEN
            PMAX=P(I)
            IMAX=I
          END IF
C         WRITE (*,*) I,P(I),V(I),DAV(I),V0,V2
        END DO
        CLOSE (7)
C-------------------------------------------------------------------------*
C       DETERMINE THE CALIBRATION POINT B USING THE FORCED BLUNTING         *
C       ASSUMPTION                                                          *
C-------------------------------------------------------------------------*
        SIG0=(YS+UTS)/2
        WRITE (*,11) 'SPECIMEN NAME:',IFIL
        WRITE (*,12) 'INITIAL CRACK LENGTH:',A0,'FINAL CRACK LENGTH:',AF
        WRITE (*,13) 'SPECIMEN THICKNESS:',B,'SPECIMEN WIDTH:',W
        WRITE (*,14) 'FLOW STRESS:',SIG0,'EFFECTIVE MODULUS:',EEF
        WRITE (*,*) ('=',I=1,78)
        WRITE (*,15) 'I','DAV(I)','AY(I)','VP(I)','VVP(I)','PN(I)',
     1  'PNV(I)'
        WRITE (*,*) ('-',I=1,78)
11      FORMAT (///20X,A15,X,A12)
12      FORMAT (2X,A22,X,F6.3,14X,A22,X,F6.3)
13      FORMAT (2X,A22,2X,F5.2,14X,A22,2X,F5.2)
14      FORMAT (2X,A22,2X,F7.3,12X,A22,2X,F9.2)
```

```
15     FORMAT (2X,A3,6(5X,A6))
       ETAP=2.15
       GAMA=1.15
       A(0)=A0
       AV(0)=A0
       VP(0)=0
       VVP(0)=0
       NX=0
       DO I=1,IMAX
         AV(I)=A0+DAV(I)
         RBV(I)=W-AV(I)
         PNV(I)=P(I)/(W*BE*(RBV(I)/W)**ETAP)
         CALL FINDC(I,AV,V,CV,BE,W,EEF,YN1)
         VVP(I)=V(I)-P(I)*CV(I)
         A1=A0
         A2=AF
         F0=-1
21       A(I)=(A1+A2)/2
         AW=A(I)/W
         CALL FINDC(I,A,V,C,BE,W,EEF,YN1)
C        WRITE (*,*) I,'   CV(I)=',CV(I)
         VP(I)=V(I)-P(I)*C(I)
         CALL FINDK(I,P,K,AW,B,BN,W)
C        WRITE (*,*) I,'   K(I)=',K(I)
         CALL FINDJ(I,P,K,A,W,BN,NU,EEF,ETAP,GAMA,VP,JE,JP,J)
         BJ=2.0*SIG0*(A(I)-A0)
         F=BJ-J(I)
C        WRITE (*,*) I,' F=',F,' BJ=',BJ,' J(I)=',J(I),' A(I)=',A(I)
         IF (ABS(F) .LT. .0001) GO TO 22
         IF (F .GT. 0) THEN
            A2=A(I)
            GO TO 21
         ELSE
            A1=A(I)
            GO TO 21
         END IF
22       AY(I)=A(I)-A0
         B0=W-A(I)
         G0=EXP(.522*B0/W)
         PN(I)=P(I)/(W*BE*(B0/W)**ETAP)
         IF (VP(I) .LE. 0) NX=I
         WRITE (*,25) I,DAV(I),AY(I),VP(I),VVP(I),PN(I),PNV(I)
       END DO
       DO I=1,IMAX
         VP(I)=VP(I)/W
       END DO
       IF (NJ .EQ.IMAX) GO TO 23
C------------------------------------------------------------------------*
C      THE FINAL CALIBRATION POINT DETERMINATION                         *
C------------------------------------------------------------------------*
       I=NJ
       A(I)=AF
       DA(I)=A(I)-A0
       CALL FINDC(I,A,V,C,BE,W,EEF,YN1)
       VP(I)=V(I)-P(I)*C(I)
       RB(I)=W-A(I)
```

```
      PN(I)=P(I)/(W*BE*(RB(I)/W)**ETAP)
      WRITE (*,25) I,DAV(I),DA(I),VP(I),VVP(I),PN(I),PNV(I)
      VP(I)=VP(I)/W
23    WRITE (*,*) ('-',I=1,78)
      WRITE (*,26)
25    FORMAT (2X,I3,4(4X,F7.5),2(4X,F7.4))
26    FORMAT (///)
28    FORMAT (4X,A3,X,F8.5)
C-----------------------------------------------------------------------*
C     LMN FUNCTION DETERMINATION                                        *
C-----------------------------------------------------------------------*
      L=1.0*PMAX/(W*BE*((W-A0)/W)**ETAP)
      L0=L
      HL=L/50
      WRITE (*,28) 'L =',L
30    SUM2=0
      SUM3=0
      KK=0
      DO I=NX+1,IMAX
        IF (I .EQ. IMAX) GO TO 35
        DET=PN(I)*VP(NJ)**2-PN(NJ)*VP(I)**2
        AA3(I)=(L-PN(I))*VP(I)*VP(NJ)**2-(L-PN(NJ))*VP(NJ)*VP(I)**2
        AA3(I)=AA3(I)/DET
        AA2(I)=PN(NJ)*(L-PN(I))*VP(I)-PN(I)*(L-PN(NJ))*VP(NJ)
        AA2(I)=AA2(I)/DET
        WRITE (*,36) I,'AA2(I) = ',AA2(I),'AA3(I) = ',AA3(I)
C       IF (AA2(I) .LE. 0) GO TO 35
        IF (AA3(I) .LE. 0) GO TO 35
        KK=KK+1
        SUM2=SUM2+AA2(I)
        SUM3=SUM3+AA3(I)
35    END DO
      WRITE (*,37)
36    FORMAT(5X,I3,5X,A9,F9.3,5X,A9,F9.7)
37    FORMAT (/)
38    FORMAT (/5X,A4,X,F8.4,8X,A4,X,F9.3,8X,A4,X,F9.7/)
      AAA=L
      BBB=SUM2/KK
      CCC=SUM3/KK
      IF ( L .GE. 1.115*L0) GO TO 40
      IF (CCC .GT. .0006) GO TO 40
      IF (CCC .EQ. 1.14*L0) THEN
        L=L+HL/2
        GO TO 30
      ELSE
        L=L+HL
        GO TO 30
      END IF
40    WRITE(*,*) ' THE SUGGEST L,M,N ARE:'
      WRITE(*,38) 'L = ',AAA,'M = ',BBB,'N = ',CCC
      WRITE(*,*) ' DO YOU WANT TO CHANGE THE L,M,N VALUES ?? [Y/N]'
      READ (*,'(A)') YN3
      IF (YN3 .EQ. 'Y') THEN
        WRITE(*,*) 'INPUT THE NEW VALUES OF L, M & N'
        READ (*,*) AAA,BBB,CCC
      END IF
```

```
C
C-----------------------------------------------------------------------*
C     THE J-R CURVE DETERMINATION, ASTM STANDARD TEST METHOD E1152 IS   *
C     USED                                                              *
C-----------------------------------------------------------------------*
      WRITE (*,41) '***** J-R CURVE CALCULATION RESULT FOR SPECIMEN:'
     1  ,IFIL,'*****'
      WRITE (*,12) 'INITIAL CRACK LENGTH:',A0,'FINAL CRACK LENGTH:',AF
      WRITE (*,13) 'SPECIMEN THICKNESS:',B,'SPECIMEN WIDTH:',W
      WRITE (*,14) 'FLOW STRESS:',SIG0,'EFFECTIVE MODULUS:',EEF
      WRITE (*,42) 'PN= [',AAA,' + ',BBB,'(VPL/W)] (VPL/W) / [',
     1  CCC,' + (VPL/W)]'
      WRITE (*,*) ('=',I=1,78)
      WRITE (*,43) 'I','P(I)','V(I)','DAV(I)','DA(I)','JV(I)',
     1  'J(I)','PN(I)','VP(I)/W','VVP(I)/W'
      WRITE (*,*) ('-',I=1,78)
41    FORMAT (///2X,A52,X,A12,X,A5/)
42    FORMAT (8X,A5,X,F8.4,A3,F10.4,X,A20,X,F8.7,A11)
43    FORMAT (2X,A2,8(X,A7),2X,A8)
      DO I=1,NJ
        HH=(AF-A0)/10
        AV(I)=A0+DAV(I)
        RBV(I)=W-AV(I)
        CALL FINDC(I,AV,V,CV,BE,W,EEF,YN1)
        VVE(I)=P(I)*CV(I)
        VVP(I)=V(I)-VVE(I)
        PNV(I)=P(I)/(W*BE*(RBV(I)/W)**ETAP)
        CALL FINDA(I,P,A0,A,DA,AY,RB,V,VE,VP,PN,W,BE,EEF,YN1,
     1       ETAP,AAA,BBB,CCC,HH,IMAX)
C       WRITE(*,*) DAV(I),DA(I),VVP(I),VP(I)
        AW=AV(I)/W
        CALL FINDK(I,P,KV,AW,B,BN,W)
        CALL FINDJ(I,P,KV,AV,W,BN,NU,EEF,ETAP,GAMA,VVP,JEV,JPV,JV)
        AW=A(I)/W
        CALL FINDK(I,P,K,AW,B,BN,W)
        CALL FINDJ(I,P,K,A,W,BN,NU,EEF,ETAP,GAMA,VP,JE,JP,J)
        WRITE(*,44) I,P(I),V(I),DAV(I),DA(I),JV(I),J(I),PN(I),
     1  VP(I)/W,VVP(I)/W
      END DO
      WRITE (*,*) ('-',I=1,78)
      WRITE (*,26)
      CALL ADJA(NX,IMAX,J,DA,AY)
      WRITE (*,*) 'INPUT THE NAME OF THE OUTPUT FILE?'
      READ 10, OFM
      OFIL1='JR'//OFM//'.DAT1'
      OFIL2='JR'//OFM//'.OUT1'
      WRITE (*,*) 'OUTPUT FILE NAME IS :',OFIL1
      OPEN (8, FILE= OFIL2)
      WRITE (8,41) '***** J-R CURVE CALCULATION RESULT FOR SPECIMEN:'
     1  ,IFIL,'*****'
      WRITE (8,12) 'INITIAL CRACK LENGTH:',A0,'FINAL CRACK LENGTH:',AF
      WRITE (8,13) 'SPECIMEN THICKNESS:',B,'SPECIMEN WIDTH:',W
      WRITE (8,14) 'FLOW STRESS:',SIG0,'EFFECTIVE MODULUS:',EEF
      WRITE (8,42) 'PN= [',AAA,' + ',BBB,'(VPL/W)] (VPL/W) / [',
     1  CCC,' + (VPL/W)]'
      WRITE (8,48) '=============================================',
```

```
     1  '========================================'
        WRITE (8,46) 'I','P(I)','V(I)','DAV(I)','DA(I)','JV(I)',
     1  'J(I)','PNV(I)','PN(I)','VP(I)/W','VVP(I)/W'
         WRITE (8,48) '-----------------------------------------------',
     1  '----------------------------------------'
         DO I=1,NJ
           WRITE(8,47) I,P(I),V(I),DAV(I),DA(I),JV(I),J(I),PNV(I),
     1   PN(I),VP(I)/W,VVP(I)/W
         END DO
         WRITE (8,48) '-----------------------------------------------',
     1  '----------------------------------------'
         CLOSE (8)
         OPEN (9, FILE= OFIL1)
C         WRITE (9,43) 'I','P(I)','V(I)','DAV(I)','DA(I)','J(I)',
C    1  'JV(I)','PN(I)','VP(I)/W','VVP(I)/W'
         DO I=1,NJ
           WRITE(9,45) I,P(I),V(I),DAV(I),DA(I),JV(I),J(I),PNV(I),
     1    PN(I),VVP(I)/W,VP(I)/W
         END DO
         CLOSE (9)
        WRITE (*,*) 'DO YOU NEED TO CONTINUE? [Y/N]'
        READ 10, YN2
        WRITE (*,49)
        IF (YN2 .EQ.'Y') GOTO 5
44      FORMAT (2X,I2,X,F7.3,3(X,F7.5),3(X,F7.4),2(X,F7.5))
45      FORMAT (2X,I2,'    ',2X,F7.3,' ',3(2X,F7.5,'      '),
     1  4(2X,F7.4,'       '),2X,F7.5,'       ',2X,F7.5)
46      FORMAT (2X,A2,9(X,A7),2X,A8)
47      FORMAT (2X,I2,X,F7.3,3(X,F7.5),2(X,F7.4),2(X,F7.3)
     1  2(X,F7.5))
48      FORMAT (X,A45,A40)
49      FORMAT (//)
        STOP
        END
C
C
        SUBROUTINE FINDK(I,P,K,AW,B,BN,W)
C-------------------------------------------------------------------------------*
C       THIS SUBROUTINE DETERMINE K(I) FOR COMPACT SPECIMEN                     *
C-------------------------------------------------------------------------------*
        INTEGER I
        PARAMETER (N=100)
        REAL P(0:N),K(N),K1,K2,AW,B,BN,W
C
        K1=(2+AW)/(1-AW)**1.5
        K1=K1*(.886+4.64*AW-13.32*AW**2+14.72*AW**3-5.6*AW**4)
        K(I)=K1*P(I)/(B*BN*W)**.5
C       WRITE (*,*) K1,K(I),P(I),B,BN,W
        RETURN
        END
C
C
```

```
      SUBROUTINE FINDC(I,A,V,C,BE,W,EEF,YN1)
C-----------------------------------------------------------------------*
C     THIS SUBROUTINE DETERMINE THE ELASTIC COMPLIANCE C(I) FOR         *
C     COMPACT SPECIMEN                                                  *
C-----------------------------------------------------------------------*
      INTEGER I
      PARAMETER (N=100)
      REAL A(0:N),V(N),C(N),BE,W,EEF,AW,H,D,R,C1,C2,C3,C4
      REAL X1,X2,SITA
      CHARACTER YN1*2
C
      C1=(1/(EEF*BE))*((W+A(I))/(W-A(I)))**2
      AW=A(I)/W
      C2=2.163+12.219*AW-20.065*AW**2-.9925*AW**3+20.609*AW**4
      C2=C2-9.9314*AW**5
      C(I)=C1*C2
C     WRITE (*,*) YN1,C(I)
      IF (YN1 .EQ.'N') THEN
        GO TO 100
      END IF
      H=.355*W
      D=.05*W
      R=(W+A(I))/2
      X1=(V(I)/2+D)/(D*D+R*R)**.5
      X2=D/R
      SITA=ASIN(X1)-ATAN(X2)
      C3=H*SIN(SITA)/R-COS(SITA)
      C4=D*SIN(SITA)/R-COS(SITA)
      C(I)=C(I)/(C3*C4)
C     WRITE (*,*) '****','  AW=',AW,' C(I)=',C(I),' A(I)=',A(I)
100   RETURN
      END
C
C
      SUBROUTINE FINDJ(I,P,K,A,W,BN,NU,EEF,ETAP,GAMA,VP,JE,JP,J)
C-----------------------------------------------------------------------*
C     THIS SUBROUTINE DETERMINE J(I)                                    *
C-----------------------------------------------------------------------*
      INTEGER I
      PARAMETER (N=100)
C     DIMENSION VP(0:N),P(0:N),A(0:N),JP(0:N)
      REAL JE(N),J(N),K(N),VP(0:N),P(0:N),A(0:N),JP(0:N)
      REAL ETAP,GAMA,NU,EEF,BN,W
C
      JP(0)=0
      JE(I)=K(I)**2*(1-NU**2)/EEF
      JP(I)=.5*ETAP*(P(I)+P(I-1))*(VP(I)-VP(I-1))/((W-A(I))*BN)
      JP(I)=(JP(I-1)+JP(I))*(1-GAMA*(A(I)-A(I-1))/(W-A(I)))
      J(I)=JE(I)+JP(I)
C     WRITE (*,*) I,K(I),JE(I),JP(I),J(I),A(I),VP(I)
      RETURN
      END
C
C
```

```
      SUBROUTINE FINDA(I,P,A0,A,DA,AY,RB,V,VE,VP,PN,W,BE,EEF,YN1,
     1  ETAP,AAA,BBB,CCC,HH,IMAX)
C-----------------------------------------------------------------------*
C       THIS SUBROUTINE DETERMINE A(I) AND VP(I) VIA LMN FUNCTION       *
C   PN=P(I)/(W*BE*(b(I)/W)**ETAP)=[L+M*(VP(I)/W)](VP(I)/W)/[N+(VP(I)/W] *
C-----------------------------------------------------------------------*
      INTEGER I,IMAX
      PARAMETER (N=100)
C     DIMENSION VP(0:N),P(0:N),A(0:N)
      REAL VP(0:N),P(0:N),A(0:N),RB(N),DA(0:N),VE(N),V(N),PN(N),C(N)
      REAL AY(N)
      REAL ETAP,EEF,BE,W,AAA,BBB,CCC,PNIA,PNIB,DFPN,VP1,HH
      CHARACTER*5 YN1
C
      A(I)=A0
121   RB(I)=W-A(I)
      CALL FINDC(I,A,V,C,BE,W,EEF,YN1)
      VE(I)=P(I)*C(I)
      VP1=(V(I)-VE(I))/W
      PNIA=P(I)/(W*BE*(RB(I)/W)**ETAP)
      PNIB=(AAA+BBB*VP1)*VP1/(CCC+VP1)
      DFPN=PNIB-PNIA
      IF (ABS(DFPN) .LT. .001) THEN
        GO TO 122
      ELSE IF (DFPN .GT. 0) THEN
        A(I)=A(I)+HH
        GO TO 121
      ELSE IF (A(I) .LE. A0) THEN
        GO TO 122
      ELSE
        A(I)=A(I)-HH
        HH=HH/10
        A(I)=A(I)+HH
        GO TO 121
      END IF
122   VP(I)=VP1*W
      DA(I)=A(I)-A0
      PN(I)=PNIA
      IF (VP(I) .LT. 0) THEN
        VP(I)=0
        DA(I)=AY(I)
        A(I)=A0+DA(I)
      END IF
      IF (I .GT. IMAX) THEN
        GO TO 123
      ELSE IF (DA(I) .GT. 0) THEN
        GO TO 123
      ELSE
        DA(I)=AY(I)
        A(I)=A0+DA(I)
        RB(I)=W-A(I)
        CALL  FINDC(I,A,V,C,BE,W,EEF,YN1)
        VE(I)=P(I)*C(I)
        VP(I)=V(I)-VE(I)
        PN(I)=P(I)/(W*BE*(RB(I)/W)**ETAP)
      END IF
```

```
123   RETURN
      END
C
C
      SUBROUTINE ADJA(NX,IMAX,J,DA,AY)
C-----------------------------------------------------------------------*
C     THIS SUBROUTINE ADJUSTS DA(I) USING ENFORCED BLUNTING ASSUMPTION  *
C     FOR THE SEGMENT BEFORE PMAX IS REACHED WHEN NECESSARY             *
C-----------------------------------------------------------------------*
      INTEGER I,JJ,NX,IMAX,KK1,IDACH
      PARAMETER (N=100)
      REAL MM,LBATA,BATA,SUMP,SUMX,SUMXX,SUMY,SUMXY
      REAL J(N),DA(0:N),AY(N),LJ(40),LDA(40)
C
      KK1=1
      IDACH=1
131   DO I=NX+1,IMAX
        IF (DA(I) .LT. DA(I-1)) IDACH=I
      END DO
      WRITE(*,*) '   NX=',NX,'   IDACH=',IDACH
      IF (IDACH .EQ. KK1) GO TO 132
      DO I=1,IDACH
        DA(I)=AY(I)
      END DO
      KK1=IDACH
      GO TO 131
132   SUMP=0
      SUMX=0
      SUMXX=0
      SUMY=0
      SUMXY=0
      DO I=NX+1,IMAX
        LJ(I)=LOG(J(I))
        LDA(I)=LOG(DA(I))
        SUMP=SUMP+1
        SUMX=SUMX+LDA(I)
        SUMXX=SUMXX+LDA(I)*LDA(I)
        SUMY=SUMY+LJ(I)
        SUMXY=SUMXY+LDA(I)*LJ(I)
      END DO
      MM=(SUMP*SUMXY-SUMX*SUMY)/(SUMP*SUMXX-SUMX**2)
      LBATA=(SUMXX*SUMY-SUMXY*SUMX)/(SUMP*SUMXX-SUMX**2)
      BATA=EXP(LBATA)
133   DO I=NX+1,KK1
        DA(I)=(J(I)/BATA)**(1/MM)
      END DO
      IF (DA(KK1+1) .LT. DA(KK1)) THEN
        KK1=KK1+1
        GO TO 133
      END IF
134   RETURN
      END
```

VITA

Kang Lee was born on May 2, 1946, in Kunming, P. R. China. He got elementary education in that city and was graduated from a high school in September 1965. At that time, "The Cultural Revolution of China" had begun and all universities were closed in China. He cannot continue to get college education and was employed by the Third Machine Manufacturing Company of Kunming. He worked for that company for fourteen years, began as a machine tool operator and then promoted to an assistant mechanical engineer. In January 1979, he got an opportunity to enter the Central Radio-Television University of China. He received a Bachelor of Science degree in Mechanical Engineering in June 1982. After that he returned to the same company and served as a mechanical engineer and the Head of the Department of Design and Technology.

In November 1984, he came to the United States and studied as a visiting scholar in the Department of Engineering Science and Mechanics, University of Tennessee. In Spring 1988, he received a graduated assistantship and began his graduated study in the same department. He received the Master of Science in Engineering Science and Mechanics in August 1990. He continued to work toward a doctoral degree in the same area. This degree will be awarded in August 1995.